December 2019

Application of Survival Analysis Techniques to Probabilistic Assessment of Fatigue in Steel Bridges

Azam Nabizadehdarabi
University of Wisconsin-Milwaukee

APPLICATION OF SURVIVAL ANALYSIS TECHNIQUES TO PROBABILISTIC ASSESSMENT OF FATIGUE IN STEEL BRIDGES

by

Azam Nabizadeh

A Dissertation Submitted in

Partial Fulfilment of the

Requirements for the Degree of

Doctor of Philosophy

in Engineering

at

The University of Wisconsin-Milwaukee

December 2019

ABSTRACT

RELIABILITY OF BRIDGE SUPERSTRUCTURES IN WISCONSIN

by

Azam Nabizadeh

The University of Wisconsin-Milwaukee, 2019
Under the Supervision of Professor Habib Tabatabai

Abstract (Summary)

The fatigue of engineering materials under repetitive loading is a significant issue affecting the design and durability of components and systems in a variety of engineering-related applications including civil, mechanical, aerospace, automotive, and electronics. Many factors can affect the service life of a component or system under repetitive loading, such as the type of structure, loading, connection details, stress state, peak stress or stress range, surface condition, temperature, and environmental exposure. Currently, there is no comprehensive probabilistic approach that can systematically address all the factors that contribute to fatigue on a single mathematical platform. However, advanced analysis techniques developed for and used in various medical research applications may hold some answers. In such research, probabilistic assessments of time to reach a milestone (e.g., time to recurrence of a disease) is considered under the influence of a range of numerical and/or categorical parameters. The experimental data obtained from observations during research is used to generate the analysis models. Such “survival analysis” involves comprehensive, multi-parameter nonlinear regression techniques that incorporate various baseline statistical distributions.

This research aims to develop, apply, and verify long-standing survival analysis techniques, widely used in medical research, to the engineering fatigue problem. This research will also use conditional survival analysis techniques derived from the conditional probability theory to address the remaining service life and load sequence effects in a probabilistic manner. A comprehensive literature review, theoretical development of fatigue survival models for various engineering applications, and verification of these models using existing or new experiments, and synthesis of results constitute the scope of this research.

To
my parents

TABLE OF CONTENTS

LIST OF FIGURES

LIST OF TABLES

Chapter 1. Introduction

1.1. Research Background

Metal fatigue is a form of progressive damage resulting from crack propagation under repetitive fluctuating stress. Fatigue damage can lead to failure of civil, mechanical and electrical systems and components due to cyclic loading. During past decades, the challenge of developing new approaches for assessment of various mechanical systems' reliability and remaining useful life under fatigue damage has been a focus of much research worldwide. Many factors can affect the service life and sustainability of a component or system under repetitive loading. These include the type of structure, loading, connection details, stress state, peak stress or stress range, surface condition, temperature, and environmental exposure. Although, fatigue has been widely investigated from a micromechanical viewpoint, stochastic processes inherent in fatigue failure make it a random phenomenon, and thus probabilistic methods are suitable for fatigue life prediction.

For some engineers, the relative simplicity and probabilistic nature of the phenomenological approach make it a generally more attractive fatigue analysis option when compared to the micromechanical models. Although both approaches can be complimentary to each other, the phenomenological approach can empower the micromechanical constitutive models, especially when using advanced statistical tools (Pyttel et al., 2016).

In phenomenological fatigue analysis, data on the number of cycles to failure are typically plotted versus stress (or strain) as S-N diagram, also known as Wohler diagram. The stress range or peak stress is commonly considered as an independent variable, and the number of cycles to failure is viewed as a dependent variable. Material engineers have been using statistical analyses to interpret the S-N (or Ɛ-N) data assuming that the test specimens are a random sample of the subject structure/material under a certain set of test conditions. Therefore, the characterized fatigue properties of the structure/material could be used to predict performance of any other sample of the same structure/material (under the same test conditions) (ASTM E739-10).

Typically, multiple tests are performed on a component or structure to assess fatigue life under several constant-amplitude stress cycles (or stress range cycles). The results are usually displayed on a log-log scale, and a linear or multilinear S-N curve is drawn to collectively represent the data. There are a variety of ways to arrive at the S-N curve. ASTM E739-10 assumes that the data at each stress level are lognormally distributed and the distributions at different stress levels have the same variance. Based on this, ASTM E739-10 provides equations for the two parameters of the linear S-N curve using the maximum likelihood estimation. Others may fit distributions to the results from each stress range tested and fit a straight line through the mean of the distributions. In other cases, a line may be drawn at a specific distance away from the mean. A constant variance is again assumed in such cases.

The National Cooperative Highway Research Program (NCHRP) sponsored extensive studies on experimental fatigue behavior of steel bridge members during the 1960s to 1980s. As a result, current standard AASHTO design S-N curves were established as a deterministic approach to fatigue life estimation of different categories of steel bridge details. The current AASHTO Bridge Design Specifications (AASHTO 2018) assume a linear relationship between the log of stress range and the log of the number of cycles to failure. The slope of this linear relationship is taken as a constant (-3), and the intercept is determined from a linear regression analysis of the test data. The intercept is set at 1.96 standard deviations below the mean value of the intercept (representing 97.5% probability of exceedance assuming a lognormal distribution for the values of the intercept)

(NCHRP Report 102 by Fisher et al., 1970; NCHRP Report 147 by Fisher et al., 1974; and NCHRP Report 286 by Keating and Fisher, 1986).

The stochastic nature of fatigue damage is due to variability of fatigue resistance (uncertainties inherent in the material properties and component geometry) and loading (Shen et al., 2000). Probabilistic assessments of fatigue service life in bridges has received widespread attention during the past decades. Despite extensive studies on fatigue reliability analysis, fatigue life prediction analyses and procedures are not well-established at the present time. There is a need for a comprehensive set of tools for probabilistic assessment of fatigue resistance based on test data. The survival analysis techniques have the potential to provide a well-established platform for such analyses in various areas of engineering including bridge engineering.

Large-scale data related to various diseases, treatments, and drugs have long been obtained from a wide range of medical and biomedical studies. In such research, probabilistic assessments of time to reach a milestone is frequently considered under the influence of a range of numerical and/or categorical parameters, in which the covariates used must be uncorrelated (i.e., independent of each other). The time-to-event parameter may include the patient's age when a disease appears, time to death of a cancer patient since diagnosis, time to recurrence of a disease after treatment, or time for a disease, tumor, or condition to reach a critical stage. The experimental data obtained from observations during research is used to generate the analysis models. Over the last 40-50 years, a powerful set of mathematical/statistical tools have been developed that collectively form the "survival analysis" platform for analysis of time-to-event data (Hosmer et al., 2008; Liu, 2012). Survival analyses include comprehensive, multi-parameter nonlinear regression techniques that can incorporate various baseline statistical distributions. Although survival analyses are mostly used in medical and biomedical research, they have also found growing applications in engineering, economics, finance, and other fields. A number of studies have applied survival analysis techniques to bridge structures (Tabatabai et al., 2011; Tabatabai et al., 2015; Tabatabai et al., 2016, Nabizadeh et al., 2018) and medical applications, including development of new survival models (Tabatabai et al, 2007; Tabatabai et al., 2008). This study develops survival analysis techniques for probabilistic analyses of fatigue resistance in steel bridges by considering the number of stress cycles as a fictitious "time-to-event" parameter, and stress range and detail category as covariates.

1.2. Problem Statement

It is estimated that the annual cost associated with fatigue failures in the U.S. is more than US$100 billion (Safarian, 2014). Optimum design, maintenance, and management of systems and components that are subject to fatigue can result in significant economic benefits. A comprehensive methodology and tools for probabilistic fatigue assessments, including remaining service life estimates, can lead to improved design and maintenance strategies. This research aims to develop and verify a methodology for data-based probabilistic assessment of fatigue resistance of steel bridges using the survival analysis techniques. The proposed concept has the potential to bring nearly all computational aspects of probabilistic fatigue analysis onto a single analytical platform.

Bridge fatigue deterioration is inevitable despite applying best practices for bridge prevention such as cathodic protection, electrochemical chloride extraction, epoxy and metal alloy coating, and inhibitors (Kordijazi, 2014; Kordijazi, 2019). Therefore, there is a growing need to develop field performance-based tools that could help to evaluate bridge fatigue life (Nabizadeh et al., 2019).

There are several important issues with the current approach to probabilistic assessment of fatigue resistance and remaining service life in a broad range of engineering applications (not limited to bridges). Although there are works that address one or more of the items listed below, currently there is no comprehensive approach that can systematically address all of the following issues on a single mathematical/statistical platform.

1. The current approach typically considers the number of cycles to failure as a dependent variable and the stress as the independent variable. In fact, the number of cycles applied, and the stress range, can both be considered independent variables that influence the probability of fatigue failure.

2. The effect of potential contributing parameters (covariates) on fatigue resistance, other than stress range (or stress), is typically not considered within a single probabilistic analysis. When deemed important, data associated with the covariates are typically considered in separate analyses. Covariates may include structure type (detail type), temperature, mean stress, existence of corrosion, environmental exposure/chemical exposure, and differing surface conditions.

3. The types of data considered in the analyses are generally not comprehensive. In some cases, data on run-outs or suspended tests are not included in the statistical analyses, even though they contain valuable information and should be systematically considered in the mathematical model. Furthermore, non-numerical (or categorical) data are typically not considered except as separate analyses. For example, if a component were to be subjected to either high, medium, or low temperatures during cyclic load testing, a parameter to be considered could be a categorical temperature parameter with possible outcomes of L (low), M (medium), or H (high).

4. The points along the linear S-N curve (on a log-log scale) are not associated with a uniform probability of fatigue failure. In fact, points along the AASHTO S-N design curves for bridges could have a wide range of probabilities of failure (Pytell et al., 2016; Albrecht, 1983).

5. The current procedures do not typically consider *conditional* service life probabilities. For example, if a detail or component has already sustained 1.2 million cycles of loading at a stress range of 10 ksi, what is the probability that it could sustain 500,000 more cycles at the same stress range? The knowledge that survival was achieved at 1.2 million cycles alters the original probability of failure at 1.7 million cycles. Furthermore, what is the probability of survival if the additional 500,000 cycles were applied at a different stress range?

6. The current procedures do not systematically consider the statistical significance of covariates on service life. If a parameter is considered in the fatigue analyses, there should be an objective measure to decide the statistical significance of that parameter and whether it can be omitted from further consideration.

1.3. Objectives and Scopes

The objective of this research is to develop, apply, and verify long-standing survival analysis techniques that are widely used in medical research to the fatigue resistance problem in bridge engineering applications. This study will also use conditional survival analysis techniques derived from the conditional probability theory to assess the change in the probability of exceeding fatigue resistance during the service life (as the number of cycles increase). This work includes development of theoretical survival models of fatigue resistance for bridge engineering applications using experimental data from the 1970s and 1980s (NCHRP Report 102 by Fisher et al., 1970; NCHRP Report 147 by Fisher et al., 1974; and NCHRP Report 286 by Keating and Fisher, 1986). These data form the basis for the current fatigue design provisions in the building and bridge design codes in the U.S. Although the focus of this work is on fatigue resistance in bridges, the proposed approach can be used to develop probabilistic fatigue resistance models in other civil engineering disciplines as well as aerospace, mechanical, materials, electrical, and industrial engineering applications. Effective probabilistic assessments can lead to important economic benefits in the design and maintenance of fatigue-prone components and systems made using a wide variety of materials.

Chapter 2. Literature Review

2.1. Deterministic fatigue damage models

The mechanisms of metal fatigue failure have been discussed and characterized extensively over the last few decades. Examples include works by Schijve (1967), Ritchie (1986), Miller (1987) [a, b], Shang et al. (1998), and Cui (2002). Fatigue failure has been mainly characterized as a three-stage phenomenon (Corten and Dolan, 1956). In the first stage, slip and fragmentation of lamella results in localized damage in some regions. Second stage involves nucleation of microcracks (crack formation) around the localized slip lines, especially when closely spaced. The third stage includes crack growth (crack propagation) that can potentially evolve into failure (Craig, 1952; Love, 1952; and Forsyth, 1952, Corten and Dolan, 1956). At the crack propagation stage, sub-microcracks enlarge and may join and form larger cracks and voids, contributing to failure. Each of these stages can occur at different locations and can affect the fatigue life of a component. Therefore, fatigue life includes the effect of all localized defects. It has been reported that 50 to 99 percent of a metal fatigue life is accompanied by second (crack formation) and third (crack propagation) stages, depending on the stress level, material properties, surface condition, and other environmental effects (Demer, 1955; Weibull, 1954; Martin, 1955).

Structures and mechanical components are also subject to random fluctuating stress during their service life. However, fatigue tests conditions cannot simulate all the fluctuations in loading history of a component, and thus the tests are typically conducted under constant amplitude conditions.

Fatigue damage is cumulative with respect to applied cyclic stresses. Cumulative fatigue damage theory has long been investigated (Freudenthal and Heller, 1959; Stallmeyer and Walker, 1968; Tanaka and Akita, 1975; Shimokawa and Tanaka, 1980; Tanaka et al., 1980; Manson and Halford, 1981). Many fatigue damage models have been developed, which were mostly phenomenological before 1970s and progressed into micromechanical models after the 1970s (Fatemi and Yang, 1998).

The linear damage rule (LDR) was first proposed by Palmgren (1924). A similar theory was introduced by Langer (1937) while studying fatigue in steel pressure vessels and piping components. In 1945, Miner formulated cumulative fatigue as linear summation of cycle ratios (Equation 2.1) and applied it to axial tension fatigue in aluminum alloy aircraft skin.

$$D = \sum_{i=1}^{n} r_i = \sum_{i=1}^{n} \frac{n_i}{N_i} \qquad \text{Equation 2.1}$$

Where D is an indicator of cumulative damage, n is the number of different levels of stress cycle, r_i is the i^{th} cycle ratio, n_i is the number of stress cycles applied at the i^{th} stress level, and N_i is the total number of cycles to failure under the i^{th} stress level. It is assumed that fatigue failure would occurs when D reaches 1.0. This damage model would result in a diagonal straight line on a damage versus cycle ratio (D-r) diagram (Figure 2.1).

The linear damage rule has long been used for its simplicity and agreement with special cases of experimental data. However, LDR is not accurate under all cases as evidenced by several experimental results. For example, Newmark (1950) reviewed cumulative fatigue damage models and reported that, based on experimental data by Dolan et al. (1949), the cumulative damage value can be much larger than D=1. Kibbey (1949) tested rotating beam specimen under multiple stress levels under increasing and decreasing stress amplitudes, and reported LDR damage values of 1.49 and 0.78 for ascending and descending stress sequences, respectively.

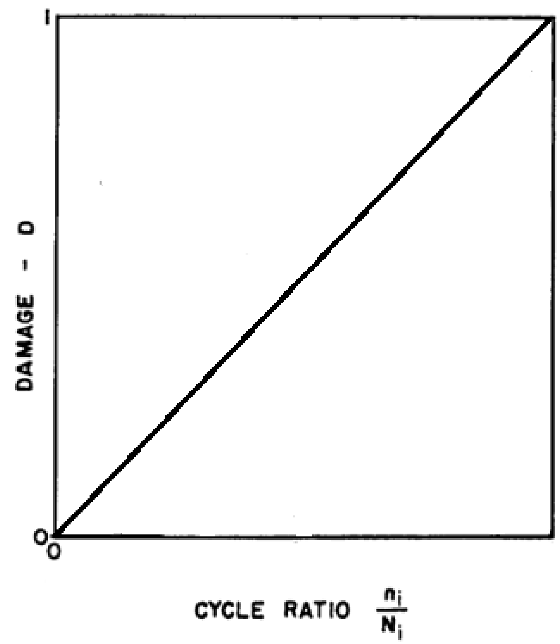

Figure 2.1. Miner's cumulative damage rule, (Miner, 1945)

LDR assumes that under any stress level σ_1, the fraction of fatigue life α (equal to $\frac{n_1}{N_1}$) is consumed and the remaining fatigue life fraction under stress level σ_2 is $(1\text{-}\alpha)$, regardless of the stress level (Marco and Starkey, 1954). Primary deficiencies inherent in LDR are lack of consideration of the effect of load level, load sequence, or load interactions. Experimental results for load sequences of low to high (L-H) loading, and from high to low (H-L) loading, resulted in cumulative damage levels above and below 1, respectively (Marco and Starkey, 1954).

Over time, many modifications to LDR have been proposed including the damage curve approach (DCA), endurance limit approach, S-N curve modification, two-stage damage approach, and crack growth-based approach (Fatemi and Yang, 1998). Some of these theories and modifications to LDR are briefly discussed below.

Richard and Newmark (1948) introduced the damage curve approach (D-r curve) to address the deficiencies associated with LDR and reported that the damage curve should be different at various stress levels. Marko and Starkey (1954) tested fatigue specimens fabricated of aluminum and steel alloys under sequential loads. The authors proposed a fatigue damage model as a function of cycle ratio and suggested a power function for cumulative damage as follows:

$$D = f\left({}^{n_i}/_{N_i}\right) = \sum \left({}^{n_i}/_{N_i}\right)^{x_i} = \sum {r_i}^{x_i} \qquad \text{Equation 2.2}$$

Where, r_i and x_i represent cycle ratio $({}^{n_i}/_{N_i})$ and loading variable at stress level i, respectively.

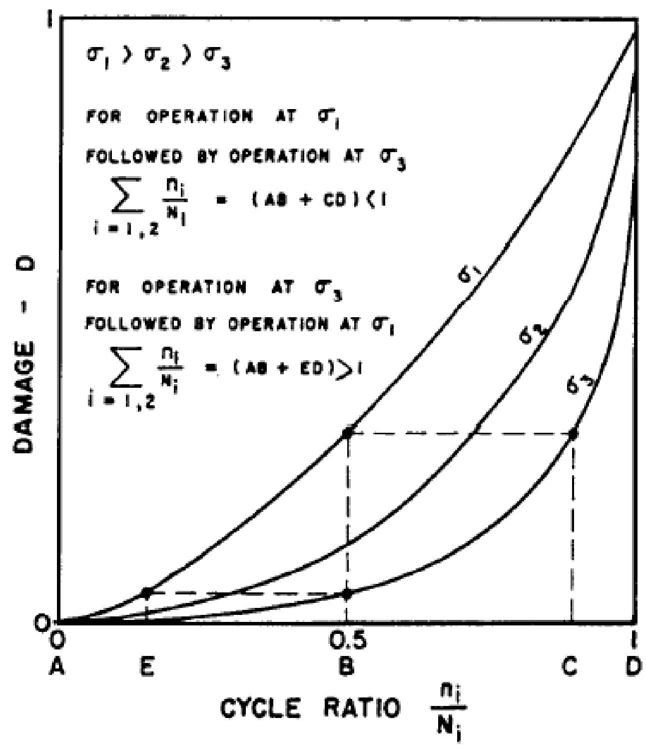

Figure 2.2. Damage vs cycle ratio curve, $D = \sum \left({}^{n_i}/_{N_i}\right)^{x_i}$ (Marco and Starkey, 1954)

Figure 2.2 illustrates a graphical representation of D-r curves with different stress levels. It is obvious that Miner's rule is a special case of D-r approach when $x_i = 1$. As shown in Figure 2.2, damage accumulation with power law results in $D < 1$ when stress amplitudes follow descending pattern (high to low load sequence, σ_1 to σ_3) and $D > 1$ when the load pattern is ascending (L-H load sequence, σ_3 to σ_1) (Marco and Starkey, 1954). The transition between different damage curves occurs through a horizontal line indicating damage equivalency. It is evident that at a lower stress level, fatigue damage propagates slowly at the early age of loading, and as cracks develops, damage grows more rapidly. On the contrary, at a higher stress level, growth of fatigue damage starts rapidly at early cycles.

A damage model was presented by Grover (1960), considering load interaction and load sequence effects in accumulated fatigue damage. The crack initiation (Equation 2.3) and crack growth (Equation 2.4) conditions were considered as the main damage phases. In this approach, α, the proportion of life during crack initiation phase, should be determined for different stress levels.

$$\sum_{i=1}^{n} \frac{n_i}{\alpha N_i} = 1 \qquad \text{Equation 2.3}$$

$$\sum_{i=1}^{n} \frac{n_i}{(1-\alpha) N_i} = 1 \qquad \text{Equation 2.4}$$

Kaechele (1963) examined Grover's theory for a variable stress spectrum (Figure 2.3). Grover's theory is more conservative than Miner's rule, thus predicting fewer number of cycles to failure.

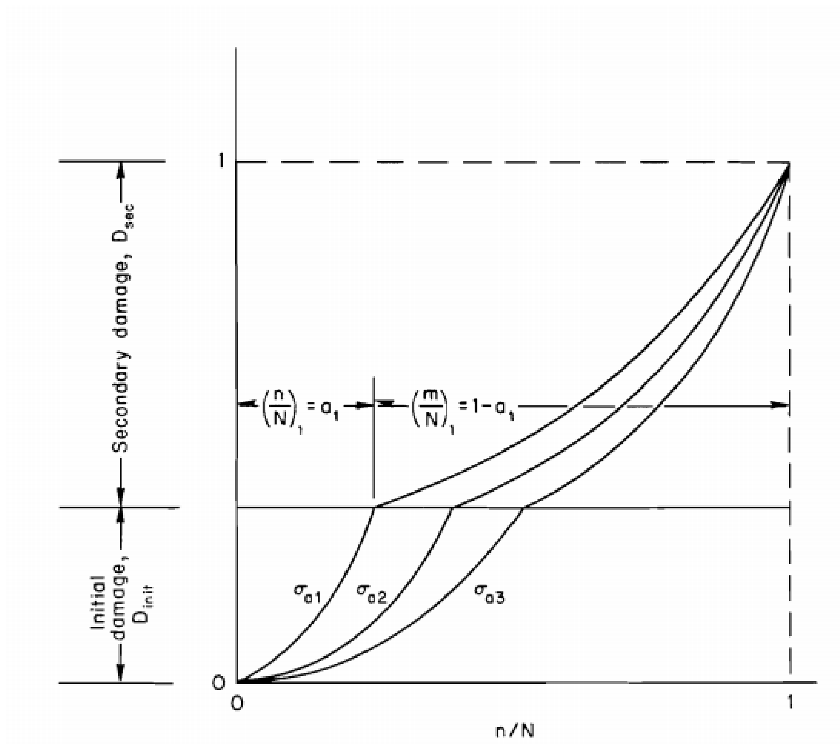

Figure 2.3. Two-stage damage cycle relationship considering stress level effect (Grover, 1960).

Manson et al. (1961) proposed a double linear damage rule (DLDR) to model the fatigue crack initiation and propagation stages. In this approach, the crack initiation period *(N_0)* and the crack propagation period *($\Delta N)_f$* are presented in terms of the total fatigue life N_f, as follows:

$$(\Delta N)_f = P.N_f^{0.6} \qquad \text{Equation 2.5}$$

$$N_0 = N_f - (\Delta N)_f = N_f - P.N_f^{0.6} \qquad \text{Equation 2.6}$$

A "P" value of 14 was determined based on experimental test data performed on 1/4-inch-diameter (6.35-mm) specimens of notched ductile materials (Manson, 1966; Manson and Hirschberg, 1966; Manson et al., 1967). Figure 2.3 shows a schematic representation of DLDR for a fatigue test involving two different stress levels (high and low, H-L). Figure 2.4. shows residual cycle ratio

($^{n_2}/_{N_{f,2}}$) at a second stress level versus the cycle ratio ($^{n_1}/_{N_{f,1}}$) applied at an initial stress level (Manson et al., 1961).

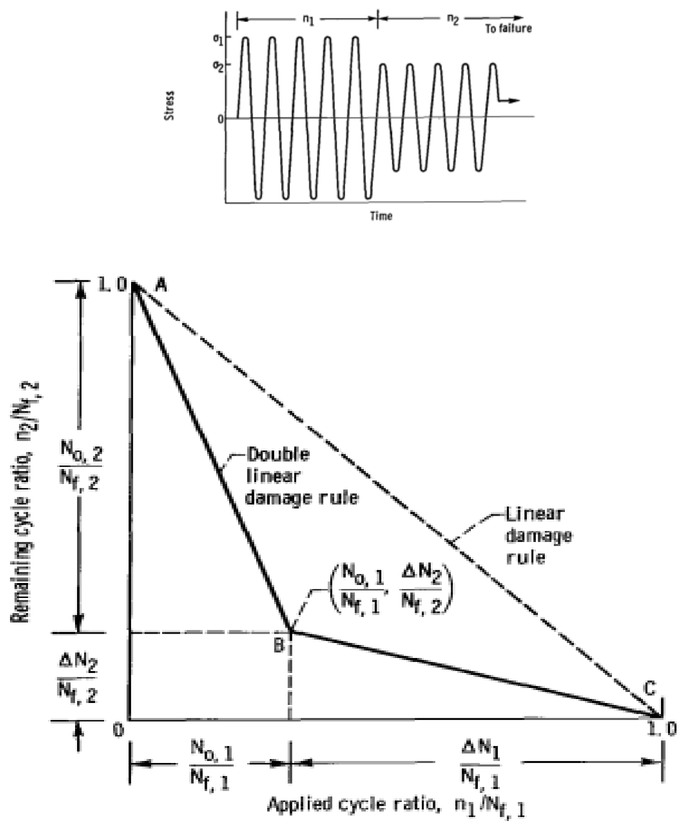

Figure 2.4. Double linear damage rule for fatigue test involving two stress levels (H-L) (Manson et al., 1961).

The authors further investigated the validity of the proposed model for two types of steel (SAE 4130 and an 18-percent nickel maraging steel). Experimental investigation was carried out on specimens under two-level-cyclic tests in rotating bending as well as two-strain level tests in axial reversed strain cycling (Manson et al., 1967). Bilir (1991) also applied the two-level stress approach on notched 1100 aluminum fatigue test specimens. They reported that test data was in good agreement with the remaining life predicted through DLDR.

Crack growth theory is another approach employed in fatigue damage models. In this approach, damage can be measured using the crack growth rate, which is a function of stress and material properties (Equation 2.7).

$$\frac{da}{dN} = C.f(\sigma).a \qquad \text{Equation 2.7}$$

In Equation 2.7, C is a constant related to material properties, "a" indicates crack length, $f(\sigma)$ is a function of loading pattern, and N is number of cycles to failure. Examples of studies considering crack growth as a measure of damage include works by Shanley (1952), Valluri (1961a, 1961b), and Scharton and Crandall (1966).

Corten and Donald (1956) tested 721 steel wire samples under constant- and variable-amplitude fluctuating stress levels and analyzed the experimental results. They modeled the cumulative damage using the power function and investigated the effect of constant- and variable-amplitude stresses on crack initiation, crack propagation and damage level. The authors used a power function (Equation 2.8) to represent damage at each damage nucleus.

$$D' = rN^a \qquad \text{Equation 2.8}$$

Therefore, for "m" damage nuclei, cumulative damage can be expressed as:

$$D = mrN^a \qquad \text{Equation 2.9}$$

Where, m is umber of damage nuclei, r is coefficient of rate of damage propagation, N is number of cycles to failure, and a is exponent on N in damage propagation process. Failure at a constant stress level (S_i) was presumed at $D_f = m_i r_i {N_i}^{a_i}$. Cumulative damage ($D$) as a function of the number of cycles to failure (N_f) at each constant-amplitude stress level is shown as in Figure 2.5.

The authors expressed cumulative damage under fluctuating stress levels as $D = \sum \Delta D$ as shown in Figure 2.6. Several other nonlinear damage accumulation models have also been proposed (Gatts, 1961; Manson and Halford, 1981). Fatemi and Yang (1998) reviewed proposed phenomenological and analytical methods on fatigue damage assessments (Fatemi and Yang, 1998).

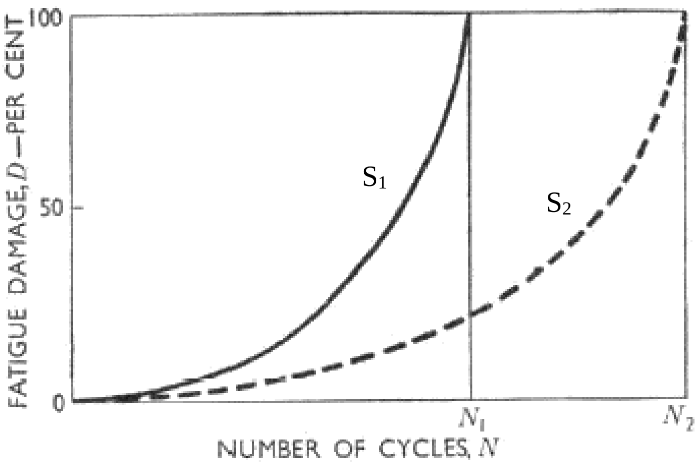

Figure 2.5. Theory of cumulative fatigue damage under constant amplitude stress ($S_1 > S_2$) (Corten and Donald, 1956).

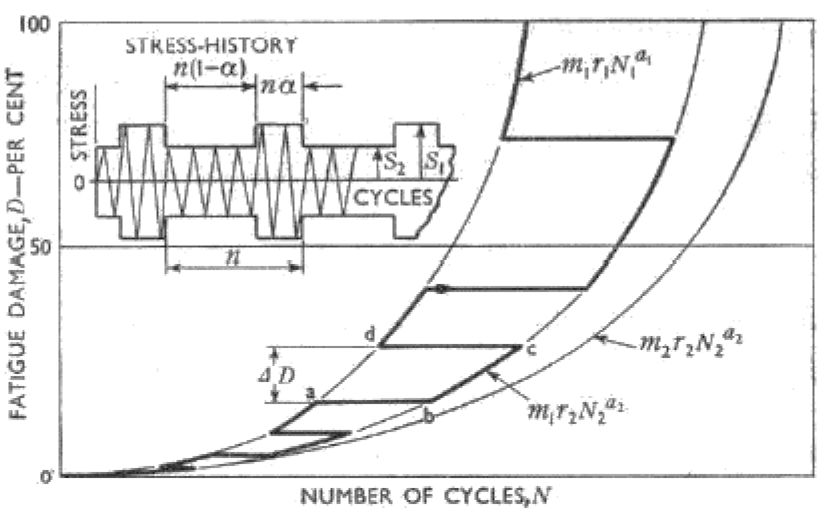

Figure 2.6. Theory of cumulative damage under variable stress amplitudes (Corten and Donald, 1956).

2.2 Reliability Index

Due to uncertainties in design, loading, construction procedures, material properties and strength parameters, there is always a slight risk of failure in any structure. Although absolute safety is not realistic, an acceptable risk level consistent with safety and economic considerations is inherent in the design provisions for bridges (AASHTO), steel buildings (AISC), and offshore platforms (API) (Frangopol, 1999).

Developments in probability theory and risk analysis along with available statistical data on load and resistance have changed the traditional approach for structural design. In the early design methods, a single safety factor was used to determine allowable stresses. The traditional allowable stress design, however, generally resulted in non-uniform levels of reliability across various elements of a structure. The reliability-based approaches aim for a more uniform level of reliability cross all elements and components of the bridge (Frangopol, 1999).

For strength-based reliability models, the basic random variables are resistance (R) and load or load effect (S). Each of these two parameters may be dependent on other random variables. Live load has uncertainties related to magnitude of truck loads and positions of those loads on a bridge. A function representing each random variable can be expressed based on available statistical information (Frangopol, 1999).

In general, a limit state failure function g is defined as follows (Frangopol, 1999):

$$g = R - S \qquad \text{Equation 2.10}$$

If $g > 0$, resistance of the element under consideration exceeds the corresponding load effect, and thus failure would not occur. When $g < 0$, the applied load exceeds the resistance of the element under consideration and the element would fail. The probability of failure may be written as (P_f):

$$P_f = P[g < 0] \quad \text{Equation 2.11}$$

Strength-based reliability assessment involves evaluating the risk associated with load exceeding resistance considering the variability of both parameters (Figure 2.7). The probability of failure can be controlled through the choice of load and resistance factors in the design specifications. Risks are measured based on a comparison of demand and capacity and the uncertainties related to these parameters (Frangopol, 1999). This approach is not intended to eliminate the risk of failure, but to realize an "acceptable" level of risk.

Strength-based reliability in structures including bridges is usually calculated through an assumption of normal (or log-normal) distributions for random variables. The reliability index, β, can be determined using the following equation (Nowak, 2000):

$$\beta = \overline{g}/\sigma_g \quad \text{Equation 2.12}$$

Where, $\overline{g}$ is the mean of the failure function g and σ_g is the standard deviation of g. The reliability index β indicates the number of standard deviations that the mean of the failure function is distanced from $g=0$ (failure). A larger β value is representative of higher reliability.

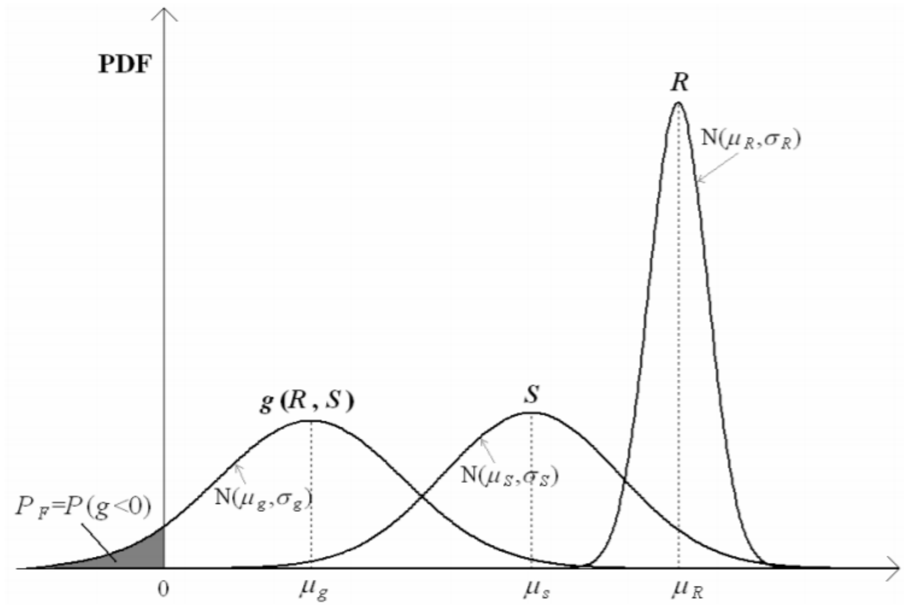

Figure 2.7. Schematic view of load and resistance concept (Chung, 2004).

Evaluation of the reliability index is another approach that has been widely used in reliability analysis of fatigue life. Limit state functions have been defined considering variability of load and resistance through commonly used (normal and lognormal) probability density functions (Wirsching and Chen, 1987; Albrecht, 1983; Wu et al., 1997), and to a lesser extent, through the Weibull distribution (Zaccone, 2001; Munse et al., 1983).

Wirsching (1984) defined a limit state function for fatigue failure considering stochasticity in cumulative damage range:

$$D - \Delta \geq 0 \qquad \text{Equation 2.13}$$

The author used fatigue test data from Miner's study (Miner, 1945) and assumed a lognormal distribution to the reported cumulative damage at failure (Δ), with a mean of 1.0 ($\mu = 1$ in agreement with Miner's rule) and a coefficient of variation of 0.3.

Hirose (1993) used reliability analyses to estimate the mean fatigue life corresponding to the service stress and threshold stress. He used the inverse power law for the stress-fatigue life relationship and incorporated the threshold stress into the model. Experimental right-censored data from an accelerated life-test on polyethylene terephthalate (PET) was used to develop failure time models at different stress levels. The reliability model was based on the Weibull distribution. Using actual accelerated test data, the author showed that there was a threshold stress below which the service life was indefinite (Figure 2.8).

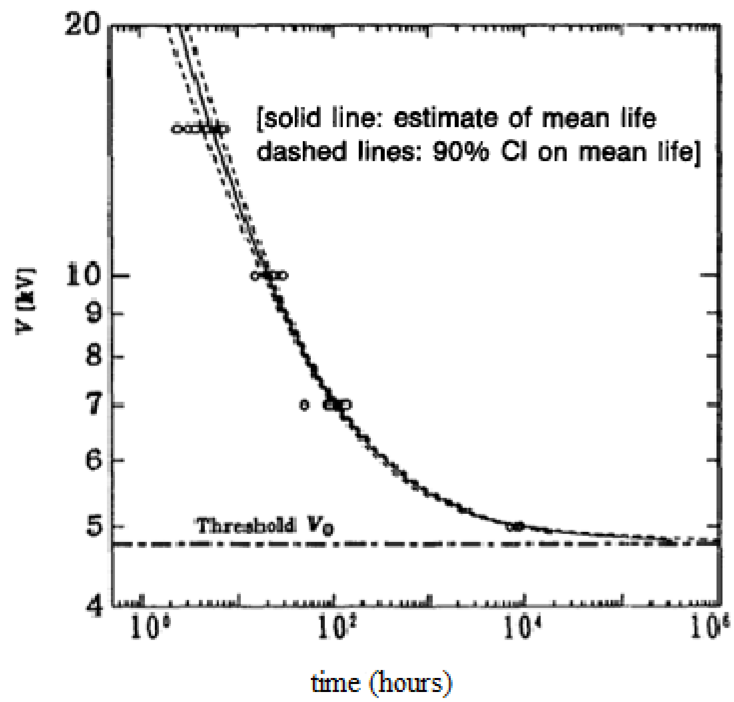

Figure 2.8. Accelerated Fatigue life, (Hirose, 1993).

As damage accumulates in a component, the cumulative damage distribution may change over time as shown in Figure 2.9 (Rathod et al., 2011). Rathod et al. (2011) developed a "nonstationary" fatigue cumulative damage model and calculated a reliability index based on the accumulated damage criteria. In their model, accumulated damage (D) was considered to be a function of fatigue life (N_f). A normal distribution was assumed for fatigue life at each stress level (Figure 2.10), and a PDF of damage accumulation was calculated at each stress level (Figure 2.11).

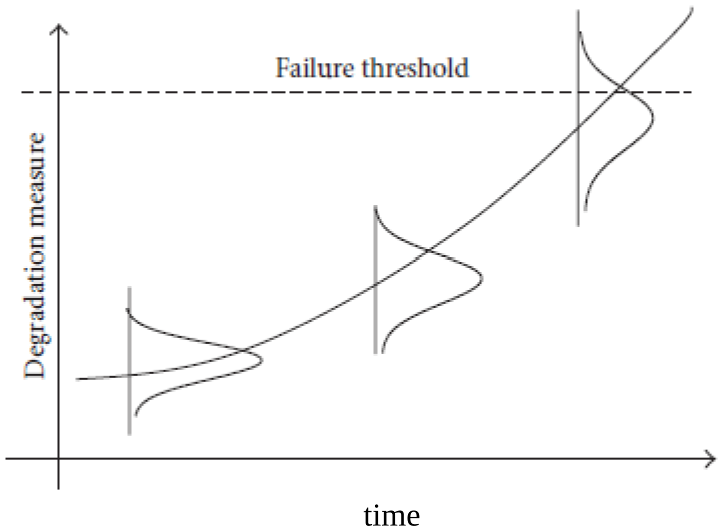

Figure 2.9. Degradation change pattern over time, (Rathod et al., 2011).

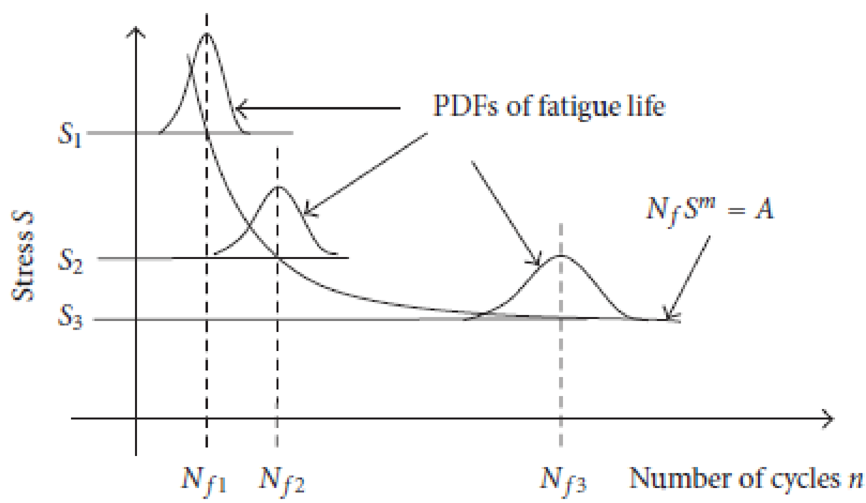

Figure 2.10. Probability Based S-N Curve, (Rathod, et al., 2011).

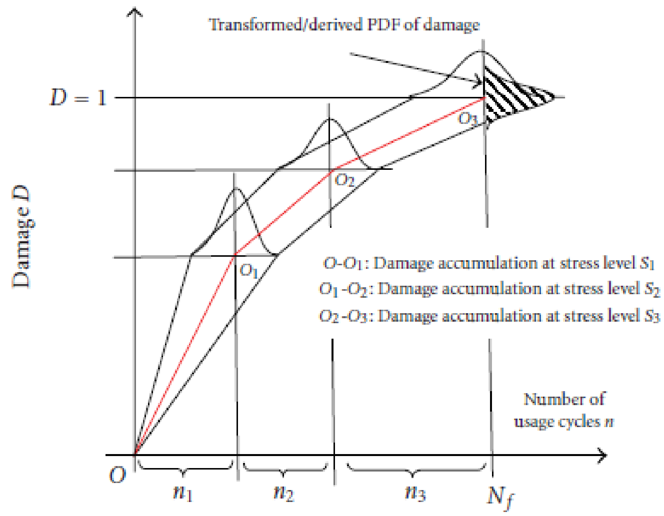

Figure 2.11. Probability distributions of accumulated damage under variable stress amplitude, (Rathod, et al., 2011).

2.3. Probabilistic Damage Accumulation Models

The Miner's rule has been commonly used in fatigue life estimation due to its simplicity. However, experimental results from constant and variable amplitude tests have shown widely scattered fatigue life (Marko and Starkey, 1945; Dolan et al., 1949; Kibbey, 1949). Therefore, interest in probabilistic assessment of cumulative fatigue damage has increased, and many studies have applied reliability-based analyses of fatigue data.

As discussed earlier, the LDR deterministic approach (Miner, 1945) assumes that fatigue failure would occur at D = 1. However, experimental data indicate that the actual value of D may range from 0.5 to 2.0 (Miner, 1945; Sobczyk and Spencer, 1992).

The Miner's rule for fatigue life under the application of two sets of constant amplitude cyclic stresses applications (1 and 2) would be:

$$\frac{n_1}{N_1} + \frac{n_2}{N_2} = 1 \qquad \text{Equation 2.14}$$

Where $\frac{n1}{N1}$ and $\frac{n_2}{N_2}$ are cycle ratios corresponding to stress amplitudes σ_1 and σ_2, respectively. However, there is scatter in measured values of N_1 and N_2, fatigue resistance (number of cycles to fatigue failure), under both stress amplitudes. Therefore, using the mean life ($\bar{N}$) of the individual test specimen, the Miner's rule could be restated as (Tanaka and Akita, 1975):

$$\frac{n_1}{\bar{N}_1} + \frac{n_2}{\bar{N}_2} = 1 \qquad \text{Equation 2.15}$$

Tanaka and Akita (1975) reported that Equation 2.14 would not be valid for individual samples and modified it as:

$$\frac{n_1}{\bar{N}_1} + \frac{n_2}{\bar{N}_2} = \frac{n_1}{N_1}.\frac{N_1}{\bar{N}_1} + \frac{n_2}{N_2}.\frac{N_2}{\bar{N}_2} = \alpha\left(\frac{n_1}{N_1} + \frac{n_2}{N_2}\right) \qquad \text{Equation 2.16}$$

Where $\frac{N_1}{\bar{N}_1}$ and $\frac{N_2}{\bar{N}_2}$, "relative strength" of specimens under stress σ_1 and σ_2, respectively, were introduced as the ratio of life of a specimen to its corresponding mean life ($\frac{N}{\bar{N}} = \alpha$). It was assumed that the relative strength ratio is independent of the stress level. According to the Miner's rule ($\frac{n_1}{N_1} + \frac{n_2}{N_2} = 1$), cumulative damage is independent of stress levels and stress interaction. Therefore, Equation 2.16 could be revised as:

$$\frac{n_1}{\bar{N}_1} + \frac{n_2}{\bar{N}_2} = \alpha \qquad \text{Equation 2.17}$$

Based on materials, testing procedures, stress ranges and the specimen affect the range of α. According to available fatigue life data from several studies (Yokobori, 1965; Dolan and Brown, 1952; Siclair and Dolan, 1953; Levy, 1955; Konishi and Shinozuka, 1956; Matolcsy, 1969; Tanaka and Akita, 1972), Tanaka and Akita (1975) assumed a normal distribution for fatigue life (*x*), (with mean of μ and variance σ^2) and used a coefficient of variance $V = {}^{\sigma}/_{\mu}$ of 0.2. The authors considered that the probability of fatigue life being one standard deviation from the mean ($\mu - \sigma \leq x \leq \mu + \sigma$), therefore, range of α=0.8-1.2. The resulting probability of survival (or reliability, R) for specimens under two different stress levels is shown in Figure 2.12. However, the authors stated that the probability of survival with respect to fatigue life ratio ($\frac{N}{\bar{N}}$) is almost equivalent for different stress levels (σ_1 and σ_2) (Figure 2.13). A plot of the probability of survival with respect to the normalized fatigue life ($\frac{N}{\bar{N}}$) was considered to be a normalized reliability curve.

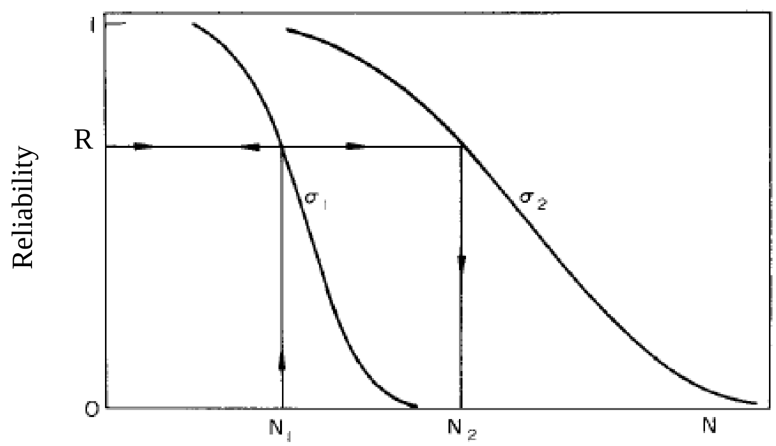

Figure 2.12. Probability of survival (reliability) versus number of cycles to failure (N) (Tanaka and Akita, 1975).

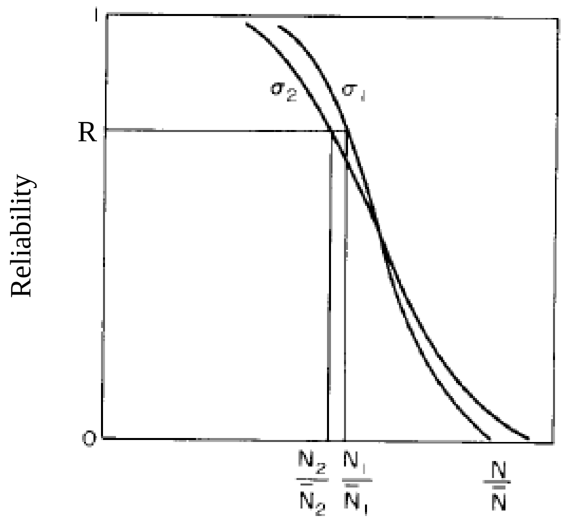

Figure 2.13. Probability of survival (reliability) versus normalized fatigue life ($\frac{N}{\bar{N}}$) (Tanaka and Akita, 1975).

Tanaka et al. (1980) first introduced the Transfer Law of Reliability Curve (TLRC) for prediction of fatigue life under variable stress amplitudes from reliability curves under constant amplitude stress. The TLRC assumes that if a specimen undergoes n_1 cycles under stress level σ_1, it would follow its respective reliability curve (corresponding to stress level σ_1). After switching to stress level σ_2, fatigue life transfers to the reliability curve corresponding to stress level σ_2 along a horizontal line of equal reliability from point B to E, as shown in Figure 2.14.

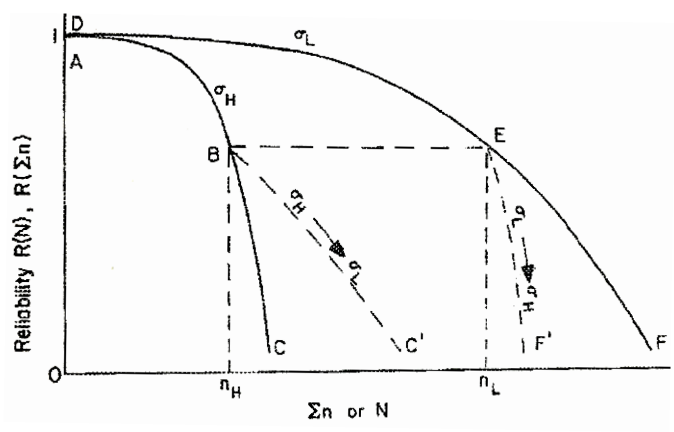

Figure 2.14. Schematic representation of TLRC (Tanaka et al., 1980).

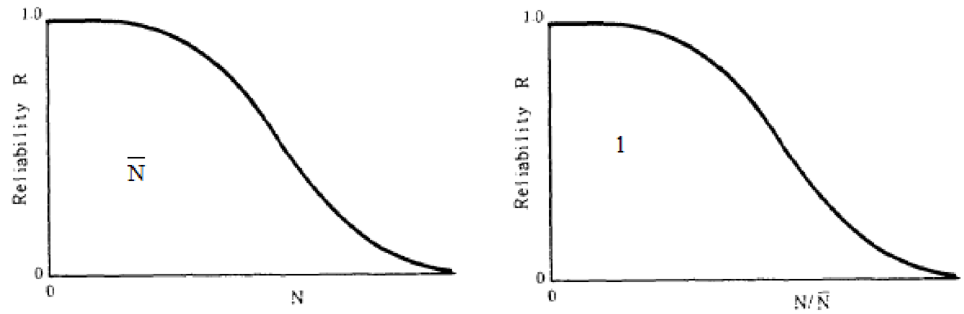

a b

Figure 2.15. Reliability curves a) versus (N) and b) versus ($\frac{N}{\overline{N}}$) or normalized, (Tanaka et al., 1980).

The authors tested 1000 nickel-silver test specimens under constant and variable amplitude loading and summarized the results as follows (Tanaka et al., 1980):

- From the experimental data, it was shown that the distribution of normalized failure life ($\frac{N}{\overline{N}}$) under constant amplitude loading was almost equivalent to the distribution of $\sum \frac{n}{\overline{N}}$ under variable amplitude loading.
- It was also noted that the expected value of damage was equal to 1 ($E\left(\sum \frac{n}{\overline{N}}\right) = 1$) and the standard deviation of $\sum \frac{n}{\overline{N}}$ under variable amplitude tests was equal to the coefficient of variation of fatigue life (N) under constant amplitude tests.
- The area under the reliability (R) versus fatigue life (N) curve for a specific constant amplitude stress is equal to mean fatigue life under that stress level (Figure 2.15a).
- The area under the reliability (R) versus normalized fatigue life ($\frac{N}{\overline{N}}$) is equal to unity and independent of stress level (Figure 2.15b).
- When the constant amplitude stress levels change, at number of cycles n_1^* (point B), to either a lower (path ABC′) or higher (path ABC″) stress level, the area under the normalized reliability curve for the two consequent-amplitude stress levels would be either

larger or smaller than unity, as shown in Figure 2.16.

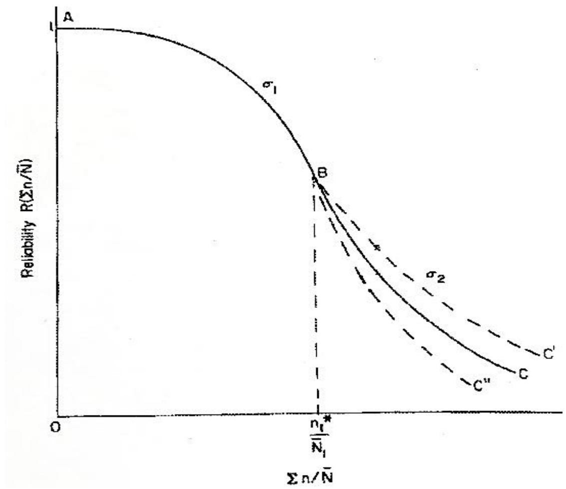

Figure 2.16. Reliability curve for two-level stress transformation (Tanaka et al., 1980).

2.4. AASHTO Fatigue Curves

The main limit states for welded connections in steel bridges can be generally categorized as strength, serviceability, and fatigue limit states. Although, 80-90% of steel structure failures are related to fatigue and fracture issues (ASCE Committee on Fatigue and Fracture Reliability, 1982; Zhao et al., 1994).

AASHTO fatigue design specifications (AASHTO, 2018) provide relationships for fatigue life as a function of cyclic stress range for various design categories as shown below:

$N_C = AS_r^{-B}$ Equation 2.18

Where, N_C is total number of stress cycle to failure; S_r represents constant-amplitude stress range; and A and B are constants that are provided for various fatigue categories. The S-N curve is normally plotted as a log-log scale. Taking log of Equation 2.18:

$logN_C = logA - B\ logS_r$ Equation 2.19

The coefficient ($logA$) is the intercept, and the exponent B is the slope of the code-specified S-N curve on a log-log scale plot.

The National Cooperative Highway Research Program (NCHRP) sponsored several studies related to fatigue evaluation of steel bridges (NCHRP Report 102, NCHRP Report 147, NCHRP Report 227, NCHRP Report 267, NCHRP Report 286, NCHRP Report 354, NCHRP Report 417) during the 1960's to 1980's. Researchers conducted several experimental fatigue studies on steel beams and plate girders with a variety of details. Several different design categories were defined (A, B, C, D, E, and E′). Using linear regression analysis of experimental test results (log N_C and log S_r) for each different design category, the best fit B and $logA$ values were first determined (NCHRP Report 102 by Fisher et al., 1970; NCHRP Report 147 by Fisher et al., 1974; NCHRP Report 286 by Keating and Fisher, 1986) for the data associated with each design category. Using these two parameters, the $logA$ values for all experimental data sets were determined and the standard deviation of $logA$ values was determined. The authors assumed that the $logA$ values were lognormally distributed and used the mean value of $logA$ minus two standard deviations to come up with the recommended intercept to be used for the design equation. Therefore, the value of B from the linear regression analysis and the $logA$ value associated with two standard deviations below its corresponding mean were recommended as design values to be used in conjunction with Equation 2.18 or 2.19 (NCHRP Report 286 by Keating and Fisher, 1986). In a later study (NCHRP Report 286 by Keating and Fisher, 1986), it was recommended that the B values for different design categories (values ranging from 3.000 to 3.372) be unified and made equal to a constant equal to 3.0 for all design categories (NCHRP Report 286 by Keating and Fisher, 1986). $logA$, which is equal to the y-intercept of fatigue S-N curve, is different for each category. According to NCHRP Report 286 (Keating and Fisher, 1986) this recommendation is the basis of the current

AASHTO Design Specifications (AASHTO 2018) (Figure 2.17). The AASHTO standard S-N curves are reported by some to correspond to a 95% probability of exceedance (Albrecht, 1983; NCHRP Report 286 by Keating and Fisher, 1986; Chung, 2004), or two standard deviations below the mean of a lognormally distributed pdf at each stress level (i.e. a horizontal distribution as shown in Figure 2.18) (Zhao et al., 1994, Chung, 2004). The design curves were reported by the authors to represent a probability of failure of 5% at any specified detail (category) and stress range (Zhao et al., 1994, Chung, 2004). In fact, the developed design relationships were not based on an assumption of a horizontal lognormal distribution at each stress range. The variability assumed in the development of the AASHTO S-N curves was associated with the intercept parameter alone (NCHRP Report 286 by Keating and Fisher, 1986). Furthermore, the 95% confidence interval presumed in the development of the design recommendations was based on two standard deviations below the mean of the intercept, indicating 2.5% probability of exceedance (of the intercept) for a lognormal distribution of $logA$.

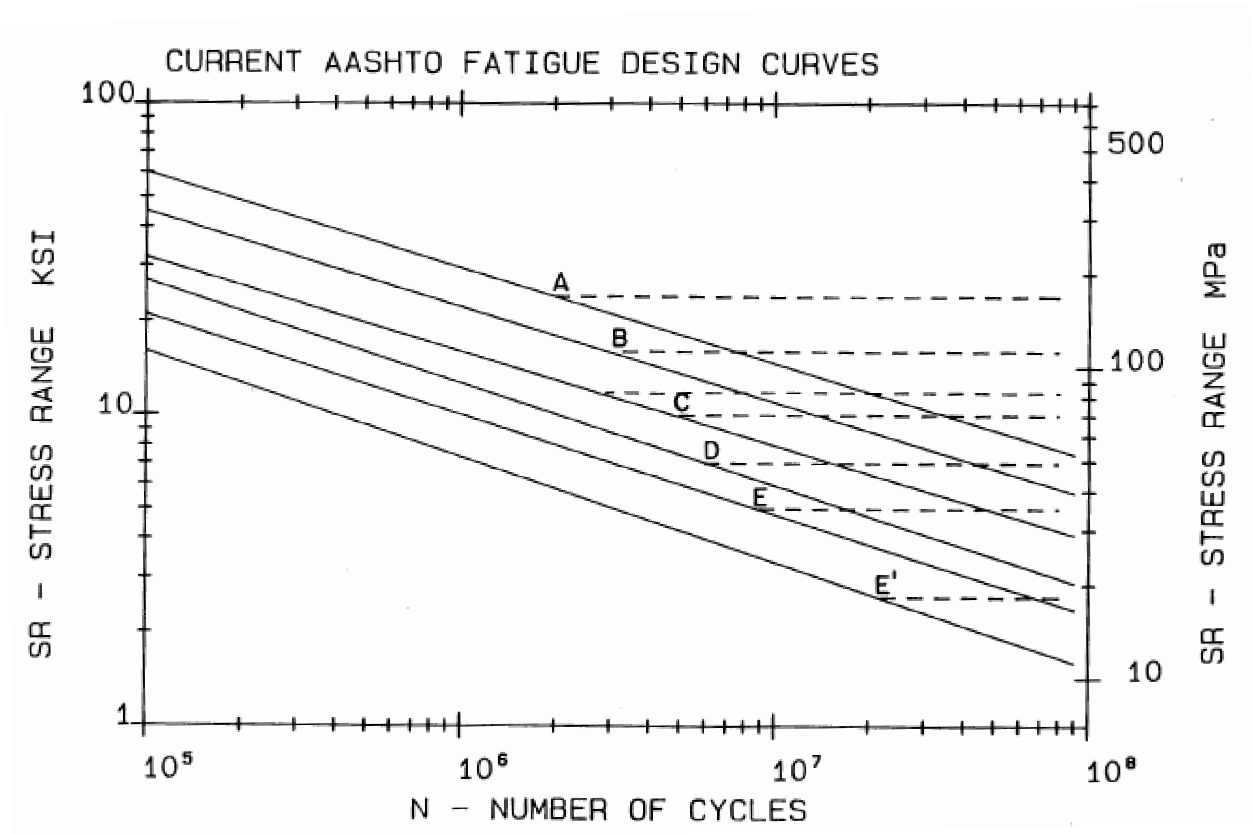

Figure 2.17. AASHTO fatigue design curves (NCHRP report 286 by Keating and Fisher, 1986).

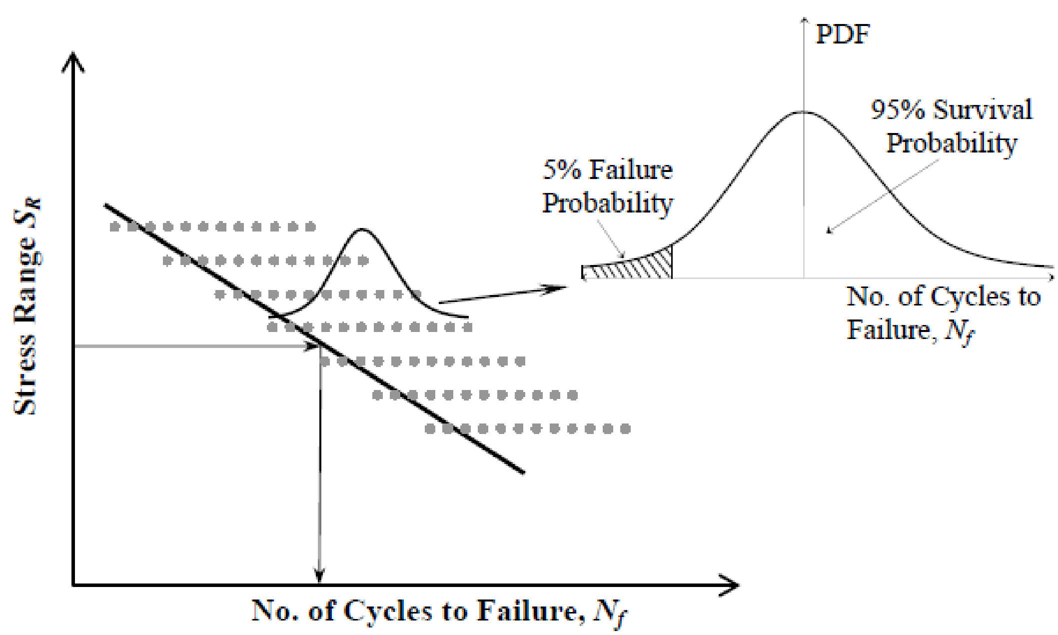

Figure 2.18. Schematic S-N curve for a typical AASHTO category (Chung, 2004)

2.5. Bridge Fatigue Reliability

AASHTO fatigue design curves (S-N curves) represent the resistance side of the reliability assessment, while the long-term load data (field monitoring data) typically represent the load/stress side. The AASHTO Design Specifications (AASHTO, 2018) provide a set of procedures for calculating the stress range and the number of cycles based on a standard truck load. Field monitoring data typically include variable amplitude stresses, which must be first converted into equivalent constant-amplitude stresses. Several cycle-counting methods such as the rain-flow method have been developed to convert variable-amplitude stress data into equivalent constant-amplitude stress cycles (Meggiolaro and de Castro, 2012; Bisping et al., 2014; Marsh et al., 2016). Uncertainties associated with load/stress ranges, material properties, and environmental exposure should be considered in probabilistic assessment of fatigue failure.

In a bridge fatigue reliability assessment, a load versus resistance limit state function is commonly used, and probability density functions (such as normal, lognormal and Weibull) are assigned to each random variable. As discussed earlier, the fatigue reliability assessment has been investigated through limit state functions applied on Miner's cumulative damage rules. In this section we review literature on fatigue reliability assessment incorporating AASHTO S-N curves.

Incorporating the equations of S-N curves into the Miner's rule (Eq 2.1) with variable amplitude stress, we have (Zhao 1991; Zhao et al., 1994):

$$D = \sum_{i=1}^{n} \Delta D_i = \sum_{i=1}^{n} \frac{n_i}{N_i} = \frac{N_C}{A} E(S_r^B) \qquad \text{Equation 2.20}$$

Where A is fatigue strength coefficient and B is exponent of S-N curve. $E(S_r^B)$ is the expected value or mean of S_r^B, while, S_r is the stress range (as a covariate).

The reliability approach is intended to be implicitly embedded in the AASHTO S-N curves (Yang et al., 2011) and other design codes to ensure a consistent level of reliability (of fatigue strength) in members and details of structures (Albrecht, 1983). To evaluate fatigue reliability of steel bridge components, commonly used statistical distributions (such as lognormal and Weibull) have been frequently used to define the basic random variables such as A, B, and S_r in the limit state equations (Equation 2.21). Combining the Miner's rule with AASHTO S-N curve, the limit state function, g, can be written as (Zhao et al., 1994):

$$g = \Delta - D \leq 0 \quad or$$

$$g = \Delta - \left[\frac{N}{A} E(S_r^B)\right] \leq 0 \qquad \text{Equation 2.21}$$

Chung (2004) reported on the application of Rayleigh, Weibull, Beta, Polynomial, and lognormal distributions for calculating an equivalent stress range in fatigue analysis. Pourzeynali and Datta (2005) used lognormal and Weibull distributions to estimate fatigue reliability of suspension bridges. They reported that the choice of stress range distribution plays a significant role in fatigue reliability calculations.

Kwon and Frangopol (2010) utilized the reliability index approach to evaluate bridge fatigue reliability. The authors used field monitoring data to calculate equivalent stress range and cumulative number of cycles. Stress range (S_r) and fatigue detail coefficient (A) were considered as load and resistance random variable, respectively. The authors employed lognormal, Weibull, and gamma distributions as assumed PDFs for stress range.

Yang et al. (2011) developed a reliability index approach for assessment of fatigue life of bridge welded details, based on long-term load monitoring data. They included the number of cycles as a random variable in addition to the equivalent stress range. They studied the effect of traffic (load) variations and traffic growth on the reliability of bridge details with respect to fatigue. Results of their study indicated that traffic growth had a significant effect on reducing the reliability of welded details in bridges.

Although crack size and crack growth are important factors in assessment of fatigue failure and fatigue cumulative damage, they are not explicitly considered in the AASHTO fatigue equations (AASHTO, 2018). To establish an alternative fatigue reliability analysis including crack growth, Zhao et al. (1994) combined a linear elastic fracture mechanics theory (LEFM) with the Miner's rule to develop a probability function for fatigue failure of steel bridge members. The corresponding limit state function was defined based on crack size at N number of cycles (α_N) and critical crack size (α_C) (Equation 2.23). The Weibull distribution was used to represent the variable amplitude stress in the limit states function covering uncertainties associated with loading.

$$g = \alpha_C - \alpha_N \leq 0 \qquad \text{Equation 2.22}$$

Albrecht (1983) studied the probability of fatigue failure in highway bridges under variable amplitude loads. The author used a normal distribution for both stress range (as load) and number of cycles to failure (as resistance) and calculated a reliability index for fatigue of highway bridges. He also calculated an equivalent stress range (constant stress range) using data recorded on bridges. Comparing the results from reliability-based analyses and AASHTO design specifications, he showed inconsistencies in fatigue reliability of typical bridge details.

Chapter 3. Survival Analysis

3.1. Background

Survival analyses has been extensively used in medical research. There are three general categories of survival analysis: non-parametric, semi-parametric, and parametric. The parametric survival analysis is the most comprehensive approach, as it can provide the most detailed probabilistic answers. When conducting a parametric survival analysis, an assumption must be made about the distribution function. The chosen distribution would affect the survival and hazard functions. The best fit model to the data can be chosen based on the shape of the hazard functions or comparing different models according to Akaike Information Criteria (AIC).

When a medical study reports that one in four persons would die from cancer during their lifetime, the results were likely obtained from a non-parametric Kaplan-Meier (K-M) analysis of cancer data. Non-parametric analyses cannot address the effect of influential covariates on the outcome. On the other hand, semi-parametric survival analysis (also known as Cox regression) involve an important assumption of proportionality of hazards (which may not be true under many circumstances) (Tabatabai et al., 2011). Furthermore, the semi-parametric models do not make any assumptions or representations regarding the underlying statistical distributions. Although the semi-parametric analysis is simpler to use (when the assumption of proportionality of hazards is satisfied), the parametric approach provides the most complete and detailed information and is the preferred approach. If a set of "time-to-event" data along with observation data on various covariates corresponding to the event is available, a parametric survival analysis can be performed. There are two terms commonly used in survival analyses that may not be commonly used in conventional engineering reliability analyses:

1. Survival (or reliability in engineering terms) refers to the probability of not failing (or 1 – the probability of failure) at any given time. The survival function, *S*, represents the values of survival at various times.
2. Hazard is the conditional failure rate at any given time, assuming survival up to that time. The shape of the hazard function with time is an important characteristic of the problem at hand. The time to failure of different products may have different characteristic hazard shapes. For example, electronic components may have "bathtub" hazard shape when failure rates are higher at both early and advanced ages. Other hazard shapes may be monotonically increasing or decreasing with upward or downward concavity or have unimodal or multi-modal shapes.

Most statistical distributions can represent only a very limited number of hazard shapes (Tabatabai et al., 2011); therefore, one statistical distribution may not be applicable to all fatigue reliability cases (or to all diseases). Finally, the probability density function (pdf) and cumulative density function (CDF) are defined in a similar manner to those in conventional statistics and reliability theory.

3.2. Survival Functions

Three distinct functions commonly used in survival analysis are: 1) survival function, (*S(t)*, 2) probability density function, (*f(t)*, and 3) hazard function (*h(t)* (Tabatabai et al., 2016):

$$S(t) = P(T > t) = 1 - F(t) \quad \text{Equation 3.1}$$

$$f(t) = \lim_{\Delta t \to 0} P(t < T < t + \Delta t)/\Delta t \quad \text{Equation 3.2}$$

$$h(t) = \lim_{\Delta t \to 0} p(t < T < t + \Delta t | T > t)/\Delta t \quad \text{Equation 3.3}$$

where T indicates the survival time as a random variable, t is the time, and $F(t)$ denotes the cumulative probability of failure at various times. $S(t) = 1$ at $t = 0$ and $S(t) \rightarrow 0$ as $t \rightarrow \infty$.

In survival analysis, the study time may not cover the entire survival time. For instance, a patient may leave the clinical investigation early and the researchers are unable to follow up and determine the actual survival time. In other cases, reasons unrelated to the study may lead to the end of survival. These kinds of observations are called "censored". Censoring corresponds to missing data within the observation time. When survival extends beyond the observation period, this is referred to as right censored data. When a component fails before the observation interval begins, the associated data is called "left censored". The right censored data are more common (Sobanjo et al. 2010).

In parametric survival analyses, the baseline statistical distribution must be determined for specific types of data at hand; therefore, the appropriate distribution cannot be assumed upfront without first finding the best fit model. Statistical distributions used in survival analyses, including weibull, lognormal, log-logistic, and hypertabastic, can represent specific hazard shapes, and thus it is important that the correct hazard shape be represented using the appropriate distribution function. Typically, the Akaike Information Criterion (AIC) and the chi-squared goodness-of-fit test are used to find the best-fit baseline distribution function, as well as the parameters associated with each covariate, using the method of maximum likelihood.

There are several types of parametric survival models, the most common of which are the Proportional Hazard model (PH) and the Accelerated Failure Time (AFT) model. If the proportionality of hazards is established (generally through an initial non-parametric K-M evaluation), then the PH model can be used. When the covariates act multiplicatively on the time scale, the AFT model is commonly used. The proportional hazard model has a hazard function, which represents the instantaneous failure rate at time *t*, given survival up to time *t*, of the form:

$$h(t|x,\theta) = h_0(t)g(x|\theta) \qquad \text{Equation 3.4}$$

Where, θ is a vector of unknown parameters and x is a p-dimensional vector of covariates. For categorical parameters, x can take values of either 0 or 1. When a categorical parameter has more than two possible outcomes, additional binary parameters (x_1, x_2, …) can be used to represent the various outcomes. For example, for a categorical parameter with three outcomes, three binary parameters (x_1, x_2, and x_3) can be used.

Outcome 1: $x_1 = 1$; $x_2 = 0$; and $x_3 = 0$

Outcome 2: $x_1 = 0$; $x_2 = 1$; and $x_3 = 0$

Outcome 3: $x_1 = 0$; $x_2 = 0$; and $x_3 = 1$

$g(x|\theta)$ is a non-negative function of *x*, satisfying the condition that $g(0|\theta) = 1$, and $g(x|\theta) = e^{\sum_{k=1}^{p}\theta_k x_k}$.

Let $h_0(t)$ be the baseline hazard function. For the PH model, the survival function $S(t|x,\theta)$ is defined as:

$$S(t|x,\theta) = [S_0(t)]^{g(x|\theta)} \qquad \text{Equation 3.5}$$

The probability density function for the PH model is defined as:

$$f(t|x,\theta) = f_0(t)[S_0(t)]^{g(x|\theta)-1} g(x|\theta) \qquad \text{Equation 3.6}$$

The AFT model uses a hazard function $h(t|x,\theta)$ of the form:

$$h(t|x,\theta) = h_0(tg(x|\theta))g(x|\theta) \qquad \text{Equation 3.7}$$

For the AFT model, the survival function is defined as:

$$S(t|x,\theta) = S_0(tg(x|\theta)) \qquad \text{Equation 3.8}$$

The probability density function for the AFT model is:

$$f(t|x,\theta) = f_0(tg(x|\theta))g(x|\theta) \qquad \text{Equation 3.9}$$

The data collected from observations are used to determine the model parameters using the maximum likelihood estimation. This is accomplished by maximizing the likelihood functions (described below). The effect of censored data (such as runout data in fatigue) is considered in the likelihood functions.

In the absence of censoring, the log-likelihood function is:

$$LL(\theta : x) = \sum_{i=1}^{n} \ln\left[f(t_i|x_i,\theta)\right] \qquad \text{Equation 3.10}$$

Where n is the total number of observations. For right-censored data, the log-likelihood function is:

$$LL(\theta : x) = \sum_{i=1}^{n} \left(\delta_i \ln\left[h(t_i|x_i,\theta)\right] + \ln\left[S(t_i|x_i,\theta)\right]\right) \qquad \text{Equation 3.11}$$

where $\delta_i = 0$ if the i^{th} observation is right-censored; and $\delta_i = 1$ if otherwise. Tabatabai et al (2011) report the log-likelihood functions for data with other types of censoring. The chi-squared test and the AIC criterion are typically used to find the best fit models for the specific data at hand.

In this study, lognormal, log-logistic, Weibull, and hypertabastic distributions were considered for the analysis of fatigue data for bridge, and the AIC was the criterion used to determine the best fit distribution (Tabatabai et al., 2011). Also, the K-M nonparametric method was used to determine if PH or AFT models should be used. In the following sections, the basic equations for the K-M estimation are presented. Also, the distribution functions considered for the fatigue survival analyses are briefly discussed.

3.3 Nonparametric Survival Models - The Kaplan-Meier (K-M) or Product Limit Method

The K-M method is one of the most common methods used to estimate the empirical distribution of survival time. This method is non-parametric because the influence of potential parameters contributing to the outcomes are not explicitly considered. In this method, the observation time is divided into a series of time intervals such that only one failure occurs at the beginning of each time interval. In other words, the survival times are first sorted, and then ranked from lowest to highest. The probability of survival at time t, $\hat{S}(t)$, can be estimated using the Kaplan-Meier method as follows (Lee and Go, 1997):

$$\hat{S}(t) = \prod_{t_i<t}[\frac{n-r_i}{n-r_i+1}]^{\delta_i}, \qquad t \le t_{(n)} \qquad \text{Equation 3.12}$$

Where t_i represents the ith survival time (can be censored or uncensored), δ_i is a parameter taken as 0 for censored data and 1 for uncensored data, r_i is the rank of t_i, n is the total number of observation intervals, and $t_{(n)}$ indicates the longest survival time (Lee and Go, 1997).

K-M survival estimates performed on different categorical data sets can be used to establish whether the appropriate survival model should be PH or AFT. If the survival curves for different categories intersect each other, then the AFT model should be used in the survival analysis. In contrast, parallel K-M survival curves indicates proportionality of the hazard function.

In fatigue survival analysis, K-M survival curves of each fatigue category, category A through E′, were developed and according to the results, AFT model was selected for further survival analysis, as will be discussed in detail in Chapter 4.

3.4. Lognormal Distribution

A random variable is lognormally distributed if the logarithm of the random variable follows the normal distribution. The lognormal distribution has been commonly used to model the fatigue failure modes. The baseline lognormal probability density function is defined as:

$$f(t) = \frac{1}{t.\sigma\sqrt{2\pi}} exp\left\{\frac{-(ln(t)\,/\mu))^2}{2\sigma^2}\right\}; t > 0 \qquad \text{Equation 3.13}$$

where parameters μ and σ are the mean and the standard deviation of the random variable, respectively. The baseline lognormal survival function and cumulative distribution functions are given in Eqs. 3.14 and 15, respectively.

$$S(t) = \frac{1}{2} - \frac{1}{2} er\,f\left[\frac{ln(t) - \mu}{\sqrt{2}\sigma}\right] \qquad \text{Equation 3.14}$$

$$F(t) = 1 - S(t) = \frac{1}{2} + \frac{1}{2} er\,f\left[\frac{ln(t) - \mu}{\sqrt{2}\sigma}\right] \qquad \text{Equation 3.15}$$

where *erf* is the Error function. The baseline lognormal hazard function *h(t)* can be calculated using:

$$h(t) = \frac{f(t)}{S(t)} = -\sqrt{2}e^{-\frac{(ln(t)-\mu)^2}{2\sigma^2}}\frac{1}{\sqrt{\pi}}t^{-1}\sigma^{-1}\left\{-1 + erf\left[\frac{\sqrt{2}(ln(t)-\mu)}{2\sigma}\right]\right\}^{-1}; t > 0 \qquad \text{Equation 3.16}$$

The lognormal hazard function increases with time until it reaches a maximum point and then decreases (unimodal function).

As described earlier, in proportional hazard models, it is assumed that the hazard functions for groups of risk factors are proportional within the observation time, which means that hazard function curves are not intersecting over time (Breslow, 1975). AFT hazard functions, as opposed to proportional hazard models, are introduced when the effects of covariates on the failure time is multiplicative with time. When using right censored data, the log-likelihood function for the lognormal AFT model can be written as:

$$LL(\theta,\alpha,\beta : t) = \sum_{i=1}^{n}\left(\delta_i \ln(\, h\,(t_g)).\, t_i g(x_i|\theta) + ln[S(t_g)]\right)$$

$$LL(\theta,\alpha,\beta : t) = \sum_{i=1}^{n}(\ln\left(\frac{1}{2} - \frac{1}{2}.\,\text{erf}\left(\frac{\ln(t_g)-\alpha}{\sqrt{2}.\,\beta}\right)\right)$$
$$+ \delta_i[t_i g(x_i|\theta).\,[\frac{1}{\beta.\,t_g.\sqrt{2\pi}}.\exp(-\frac{1}{2}(\frac{(\ln(t_g-\alpha)^2}{\beta}))]$$
$$- \ln\left(\frac{1}{2}\right.$$
$$\left.- \frac{1}{2}.\,\text{erf}\left(\frac{\ln(t_g)-\alpha}{\sqrt{2}.\,\beta}\right)\right)]) \qquad \text{Equation 3.17}$$

Where,t_i is the ith survival time, and t_g and δ_i are defined as following:

$t_g = t_i g(x_i|\theta)$

$$\delta_i = \begin{cases} 0 & \text{if } t_i \text{ is a right censored observation} \\ 1 & \text{otherwise} \end{cases}$$

3.5. Log-logistic Distribution

Log-logistic distribution is a continuous probability function of non-negative random variables. This distribution is used in different applications (lifetime or service time) such as survival analyses of cancer patients, hydrology, and economics.

When a random variable is represented with a log-logistic distribution function, the logarithm of the variable follows logistic distribution. A log-logistic random variable (t) with parameters α and β has the following probability density function:

$$f(t) = \frac{(\beta/\alpha)(t/\alpha)^{\beta-1}}{(1+(t/\alpha)^{\beta})^2} \qquad \text{Equation 3.18}$$

Where α and β are both positive and define the scale and shape parameters, respectively. The cumulative distribution function is given as shown below:

$$F(t) = \frac{1}{1+(t/\alpha)^{-\beta}} \qquad \text{Equation 3.19}$$

The log-logistic survival function is defined as below:

$$S(t) = \frac{1}{1+(t/\alpha)^{\beta}} \qquad \text{Equation 3.20}$$

The log-logistic hazard rate and cumulative hazard functions are shown in Eqs. 3.21 and 3.22, respectively. The shape of the log logistic hazard function can be either monotonically decreasing or have a single-mode shape.

$$h(t) = \frac{(\beta/\alpha)(t/\alpha)^{\beta-1}}{1 + (t/\alpha)^{\beta}} \qquad \text{Equation 3.21}$$

$$H(t) = -\ln(S) = \ln(1 + \left(t/\alpha)^{\beta}\right) \qquad \text{Equation 3.22}$$

When right censored data are present (such as fatigue run-out data), the log-likelihood function for log-logistic AFT model can be defined as:

$$LL(\theta, \alpha, \beta: t) = \sum_{i=1}^{n} \left(\delta_i \ln(\, h\,(t_g)).\, t_i g(x_i|\theta) + ln[S\left(t_g\right)]\right)$$

$$LL(\theta, \alpha, \beta: t) = \sum_{i=1}^{n} (\delta_i\, ln\left(\frac{(\beta/\alpha)(t_g/\alpha)^{\beta-1}}{1 + (t_g/\alpha)^{\beta}} t_i g(x_i|\theta)\right) - ln(1 + \left(t_g/\alpha)^{\beta}\right) \qquad \text{Equation 3.23}$$

The t_g and δ_i are defined in section 3.4.

3.6. Weibull Distribution

Weibull is a continuous distribution also called type III extreme value distribution. Probability density function of a random variable (t) following Weibull distribution is shown as:

$$f(t) = \frac{\gamma}{\theta}\left(\frac{t}{\theta}\right)^{\gamma-1} exp\left(-\frac{t}{\theta}\right)^{\gamma} \qquad \text{Equation 3.24}$$

Where parameters θ and γ represent scale and shape factors, respectively. Eqs. 3.25 through 3.27 define survival, hazard rate, and cumulative hazard functions for Weibull distribution. Failure rate of a Weibull distribution can follow a constant, monotonically decreasing, or monotonically increasing pattern.

$$S(t) = exp\left(-\frac{t}{\theta}\right)^{\gamma} \quad \text{Equation 3.25}$$

$$h(t) = \frac{\gamma}{\theta}\left(\frac{t}{\theta}\right)^{\gamma-1} \quad \text{Equation 3.26}$$

$$H(t) = \left(\frac{t}{\theta}\right)^{\gamma} \qquad t \geq 0 \; and \; \gamma \geq 0 \quad \text{Equation 3.27}$$

The log-likelihood function for Weibull AFT model for right-censored data is shown in Equation 3.28.

$$LL(\theta, \alpha, \beta : t) = \sum_{i=1}^{n}\left(\delta_i \ln(h\,(t_g)).\, t_i g(x_i|\theta) + ln[S(t_g)]\right)$$

$$LL(\theta, \alpha, \beta : t) = \sum_{i=1}^{n}\left(\delta_i ln\left(\frac{\gamma}{\theta}\left(\frac{t}{\theta}\right)^{\gamma-1} .\, t_i g(x_i|\theta)\right) + \left(\frac{t_g}{\theta}\right)^{\gamma}\right) \quad \text{Equation 3.28}$$

The t_g and δ_i are defined in section 3.4.

3.7. Hypertabastic Distribution

The hypertabastic distribution is a relatively new type of distribution, which was introduced by Tabatabai et al. (2007). It has been used in several applications including studying the effect of covariates on the survival time of cancer patients and engineering applications (Tabatabai et al., 2007; Tran, 2014; Nikulin and Wu, 2016; Tahir et al., 2017). The most prominent feature of the hypertabastic survival function is its capability to represent a variety of different hazard shapes (Tabatabai et al., 2007).

Considering the continuous random variable t (representing time to an event or waiting time for the occurrence of the event), the hypertabastic cumulative distribution function could be represented as follows (Tabatabai, 2011):

$$F(t) = \begin{cases} 1 - sech\{W(t)\} & for\ t > 0 \\ 0 & for\ t \leq 0 \end{cases} \qquad \text{Equation 3.29}$$

Where, $W(t) = \alpha\left[1 - t^{\beta}\coth(t^{\beta})\right]/\beta$. The parameters α and β are both positive and *sech*[] and *coth*[] are hyperbolic secant and hyperbolic cotangent functions, respectively. The probability density function of hypertabastic distribution is given as (Tabatabai, 2011):

$$f(t) = \begin{cases} sech[W(t)]\left[\alpha t^{2\beta-1}\operatorname{csch}^2\left(t^{\beta}\right) - \alpha t^{\beta-1}\, coth\left(t^{\beta}\right)\right]tanh[W(t)] & for\ t > 0 \\ 0 & for\ t \leq 0 \end{cases}$$

Equation 3.30

Where *csch*[] is hyperbolic cosecant.

The hypertabastic survival function is defined as (Tabatabai, 2011):

$$S(t) = sec\,h[W(t)] \qquad \text{Equation 3.31}$$

The hypertabastic hazard function, *h(t)*, is defined as (Tabatabai, 2011):

$$h(t) = \alpha\left[t^{2\beta-1}\operatorname{csch}^2\left(t^{\beta}\right) - t^{\beta-1}\, coth\left(t^{\beta}\right)\right]tanh[W(t)] \qquad \text{Equation 3.32}$$

And the cumulative hazard function *H(t)* is defined as:

$$H(t) = -\ln(Sech[W(t)]) \qquad \text{Equation 3.33}$$

When right censored data is used, the log-likelihood function for the hypertabastic AFT model is defined in Equation 3.34 (Tabatabai et al., 2011).

$$LL(\theta,\alpha,\beta:x)=\sum_{i=1}^{n}(\ln[\mathrm{Sech}(\frac{\alpha(1-[t_g^{\beta}Coth\left(t_g^{\beta}\right))}{\beta})]+\delta_i\ln[t_i((\alpha[t_g]^{-1+2\beta}Csch\left([t_g]^{\beta}\right)^2$$
$$-\alpha[t_g]^{-1+\beta}Coth\left([t_g]^{\beta}\right))$$
$$*\tanh(\frac{\alpha\left[1-[t_g]^{\beta}Coth\left([t_g]^{\beta}\right)\right]}{\beta}))g(x_i|\theta)] \qquad \text{Equation 3.34}$$

The t_g and δ_i are defined in section 3.4.

3.7. Conditional Survival

Conditional Survival (*CS*) analyses have recently (last 10-15 years) found more widespread applications and use in medical research (Merrill and Hunter, 2010; Zabor et al., 2013; Hieke et al., 2015). Survival estimates, as discussed here up to this point, are based on information available at the initial time or time of prognosis (t = 0). For example, a patient (or a fatigue-prone component) may be given 10% chance of survival 10 years (or 1000,000 stress cycles) after diagnosis (or start of stress applications). As time passes by (stress cycles accumulate), additional information (knowledge) is gathered that can improve future survival forecasts. The knowledge, that the additional evidence provides, can be used for updated estimates of survival as time progresses. For example, after five years (or 500,000 cycles), the fact that the patient (or the component) has survived (not failed) alters the 10-year (1000,000 cycle) probability of survival from 10% to a higher number. This conditional survival estimate depends on the shape of the original (overall) survival function. The original (*OS*) and conditional (*CS*) survival can also be considered as “static” and “dynamic” estimates of the survival function, respectively. Based on the conditional probability theory, the probability of survival at time *t*, given that the patient (component) has already survived t_s years can be calculated using the following equation:

$$CS(t,t_s) = \begin{cases} 1 \; when & 0 \le t \le t_s \\ \dfrac{S(t)}{S(t_s)} & when \; t > t_s \end{cases} \qquad \text{Equation 3.35}$$

The above equations indicate that, given the fact that survival has been achieved up to time t_s, the conditional probability of survival would be equal to 1 (100%) at or before time t_s. The originally estimated survival probabilities are then adjusted using Equation 3.35. The change in the probability of survival at times greater than t_s (as reflected in Equation 3.35) also changes the expected life beyond time t_s.

This relationship is graphically illustrated in Figure 3.1. The original (static) survival curve is shown on the left (solid curve), while the CS curve (dynamic survival) associated with known survival at time t_s is shown on the right (dashed line curve). Since survival was achieved at time t_s, the conditional reliability jumps to 1.0 (100%) at time t_s. The rest of the response is in accordance with Equation 3.35.

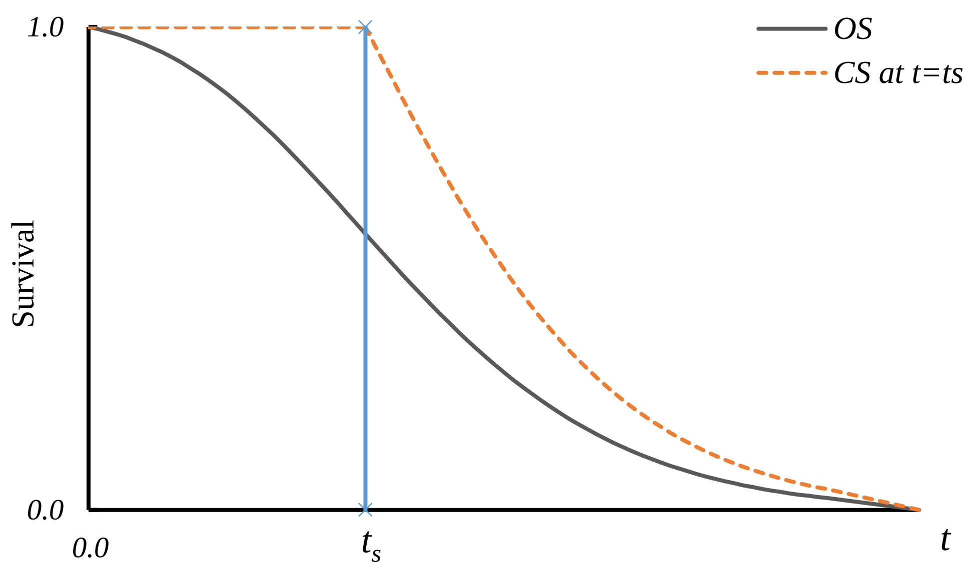

Figure 3.1. Original and conditional survival functions.

3.8. NCHRP Fatigue Data

The AASHTO bridge design specifications include specific provisions for the fatigue design of steel bridges. These specifications are defined based on fatigue resistance curves (S-N curves) for different categories of bridge details. The AASHTO fatigue provisions were primarily based on results of research sponsored by the National Cooperative Highway Research Program (NCHRP) in the 1970s (NCHRP Report 102 by Fisher et al., 1970 and NCHRP Report 147 by Fisher et al., 1974). These research reports included discussions of tests on full-scale beams as well as welded test specimens that provided a significant dataset of fatigue test results. Several subsequent fatigue studies (also sponsored by NCHRP) were also conducted that expanded the available fatigue data to a wider range of details and sizes (NCHRP Report 181 by Barsom and Novak, 1977; NCHRP Report 188 by Schilling et al., 1978; NCHRP Report 206 by Fisher et al., 1979; NCHRP Report 227 by Fisher et al., 1980; NCHRP Report 267 by Fisher et al., 1983).

The initial NCHRP projects (NCHRP Report 102 by Fisher et al., 1970; NCHRP Report 147 by Fisher et al., 1974) conducted experimental tests on 530 test specimens. The experiments were designed to provide data for evaluation of contributing factors and their significance on fatigue life of steel beams and girders. The primary design variables considered in the tests included the type of weld detail, stress conditions, and type of steel. However, the combined influence (interaction) of these variables was not evaluated. Other factors that could affect the fatigue strength including rate of loading, temperature, surface condition, and corrosion were not considered (NCHRP Report 102 by Fisher et al., 1970).

The main emphasis of the two initial NCHRP studies was on cover-plated beams, web and flange attachments, and stiffeners. Weld details included longitudinal and transverse fillet welds. Plain rolled and welded beams were also tested to evaluate the fatigue strength without cover-plate and flange splice. All these tests were limited to constant-amplitude cyclic loading.

Controlled stress variables included the minimum stress, maximum stress, and the stress range. The point of maximum moment for plain rolled beams and the point of maximum flexural stress at the tension flange of base metal in the welded detail were considered as the points for stress range measurements. Three different steel types (A36, A441, and A514) were used, which covered yield strengths ranging from 36 to 100 ksi (248 to 690 MPa) (NCHRP Report 102 by Fisher et al., 1970).

The major general findings of these reports included the following:

1. Stress range was the prominent stress variable (among all controlled stress variables) in all specimens including those with different weld details and steel types.
2. Type of the steel was not a significant factor affecting the fatigue life.
3. the type of detail significantly influenced the fatigue strength of welded elements.
4. The log of the number of cycles to failure at different stress ranges showed nearly normal distributions.
5. The empirical exponential model relating the number of cycles to the stress range (shown below) fit to the test data in all specimens:

   $$N = A.S_r^{-B}$$

   Where, N_C is number of cycles and S_r is stress range.

   The relationship between the stress range and the number of cycles to failure can be represented as a straight line (constant slope) on a log-log plot in nearly all detail types:

   $$\log N = \log A - B.\log S_r$$

Where, log A is the intercept and B is the slope of the S-N line.

6. Linear regression analyses of test data showed that all curves (related to different detail categories) had a slope of approximately -3.0.

The fatigue test data related to plain rolled beams (obtained from various NCHRP studies) were grouped together to develop the detail category A (data points are shown in Figure 3.2) (NCHRP Report 286 by Keating and Fisher, 1986). Category B data grouped the fatigue test data on longitudinal welds and flange splices. The individual Category B data points areas shown in Figure 3.3. Transverse stiffeners and short (2-in) attachments were used to define category C (Figure 3.4). Intermediate attachments were considered in the development of Category D, (Figure 3.5). Category E included cover-plated beams and long attachments (Figure 3.6). Later, the NCHRP report 206 (Fisher et al., 1979) resulted in an expansion of the cover-plated beam data, and therefore a new category E′ was proposed. Figure 3.7 shows the fatigue data for the coverplated beams in both E and E′ categories. Appendix A lists the numerical fatigue test data associated with each fatigue category. These data form the basis for the current AASHTO bridge design specifications (NCHRP Report 286 by Keating and Fisher, 1986).

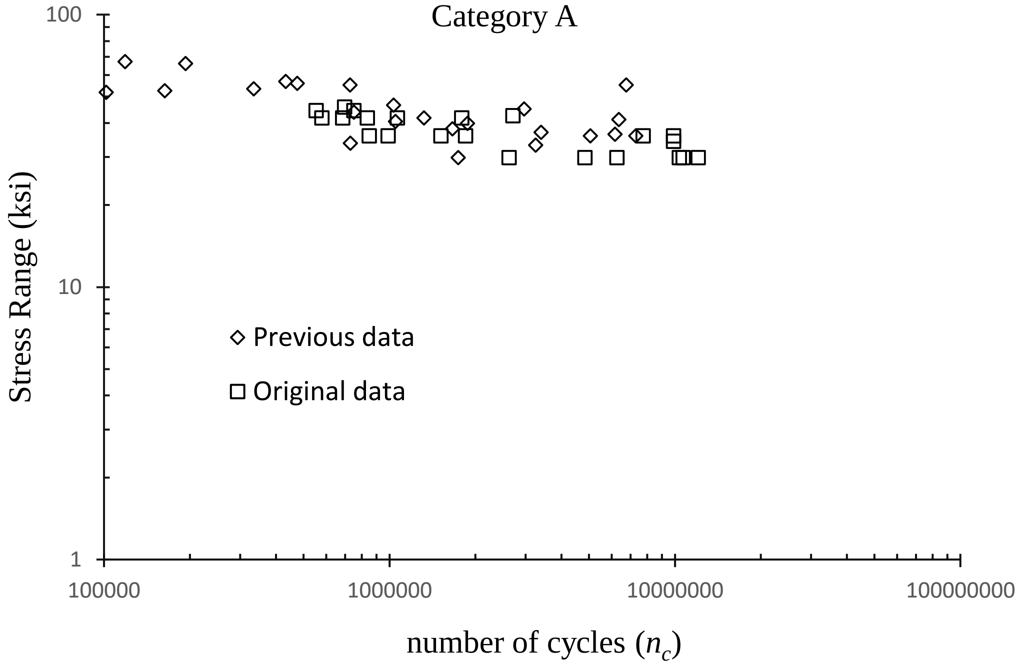

Figure 3.2. Fatigue data of category A, original database (NCHRP Report 286 by Keating and Fisher, 1986)

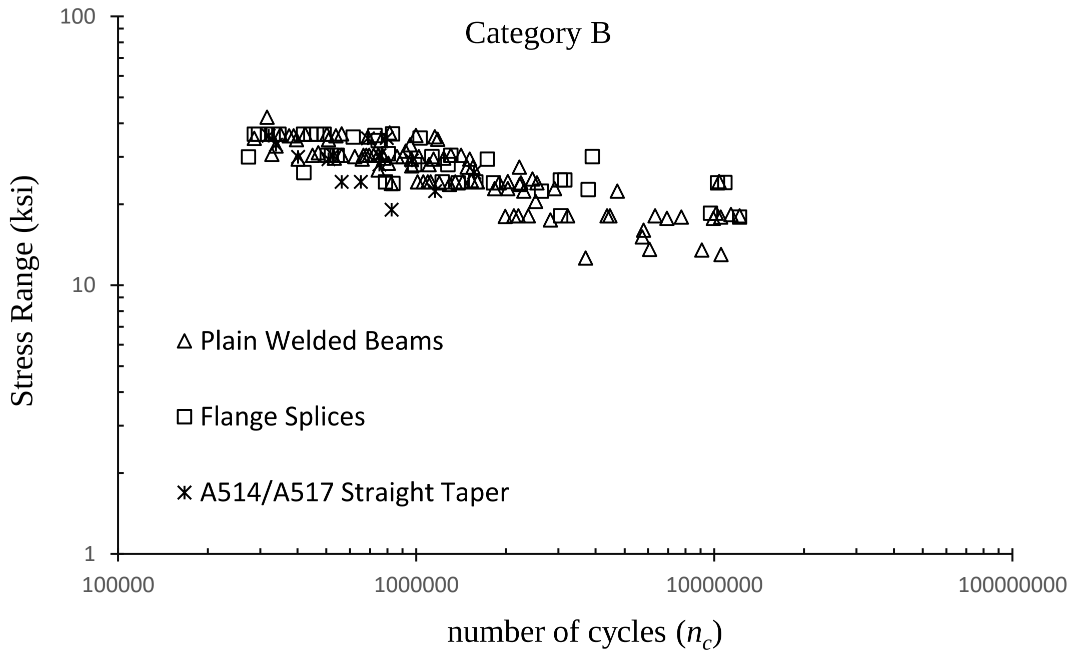

Figure 3.3. Fatigue data of category B, original database (NCHRP Report 286 by Keating and Fisher, 1986)

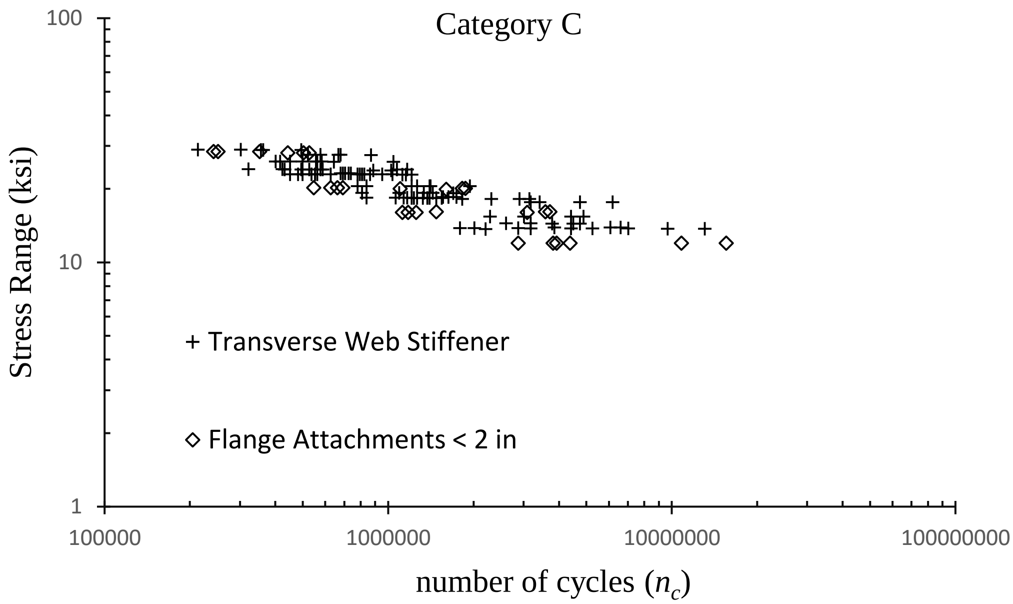

Figure 3.4. Fatigue data of category C, original database (NCHRP Report 286 by Keating and Fisher, 1986)

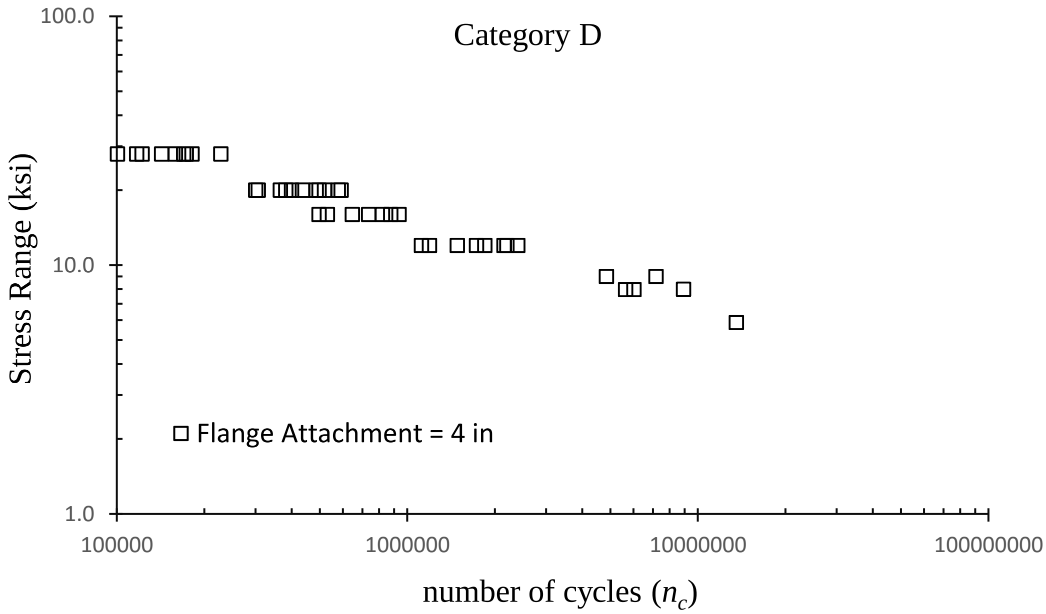

Figure 3.5. Fatigue data of category D, original database (NCHRP Report 286 by Keating and Fisher, 1986)

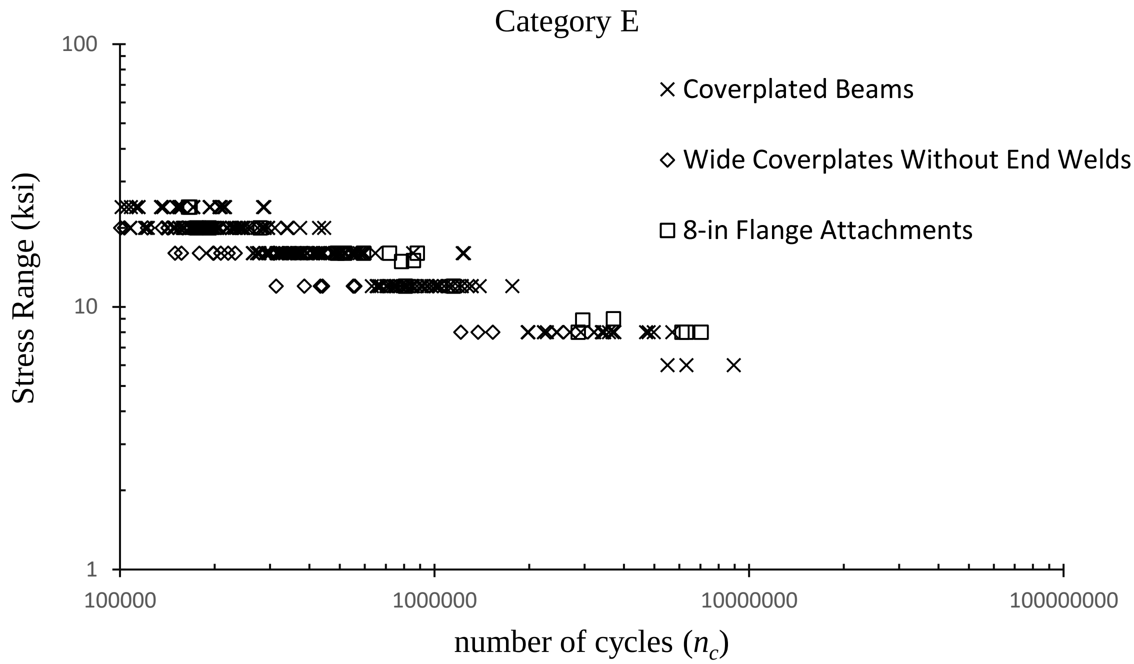

Figure 3.6. Fatigue data of category E, original database (NCHRP Report 286 by Keating and Fisher, 1986)

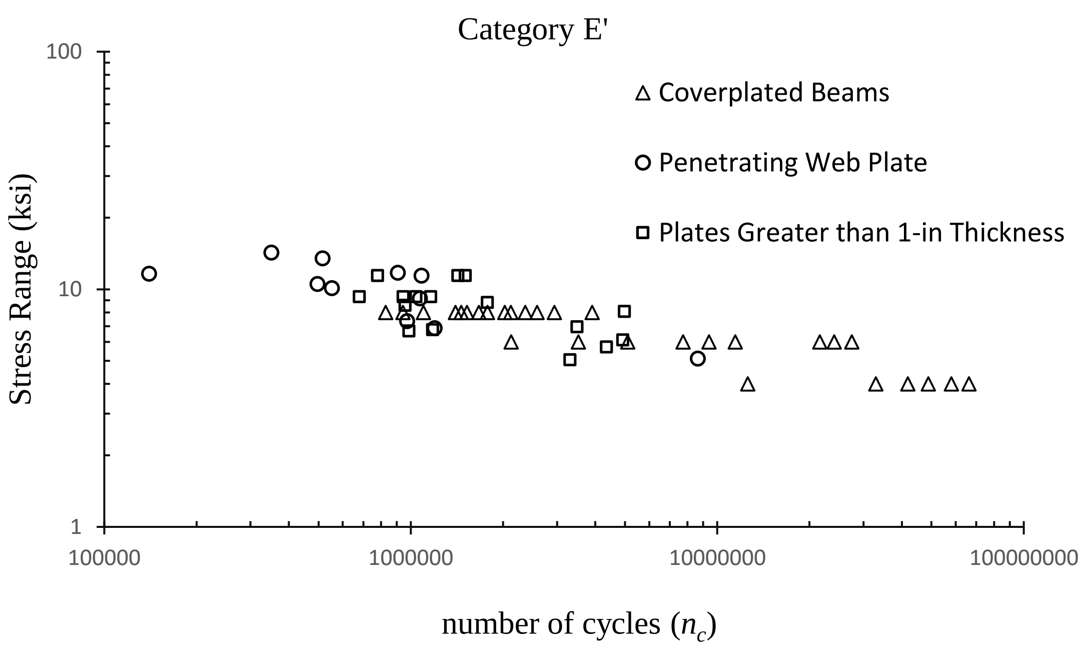

Figure 3.7. Fatigue data of category E′, NCHRP Reports 206 and 227(NCHRP Report 286 by Keating and Fisher, 1986)

Table 3.1 shows the intercept and slope values for all S-N curves that were fitted to the fatigue test data through linear regression analyses for each category according to the results of NCHRP Report 286 (Keating and Fisher, 1986). The fifth column in Table 3.1 includes the lower (horizontal) intercept of fatigue data calculated two standard deviations from the mean of data assuming lognormally distributed. Figure 3.8 shows the 1986 AASHTO fatigue curves, according to regression results listed in Table 3.1 (NCHRP Report 286 by Keating and Fisher, 1986).

Table 3.1. Regression Analysis results for 1986 AASHTO curves from NCHRP 286 (Keating and Fisher, 1986)

Category	Slope	Intercept (mean)	Standard Deviation	Intercept (lower)
A	3.178	11.121	0.221	10.688
B	3.372	10.87	0.147	10.582
C	3.250	10.038	0.063	9.915
D	3.071	9.664	0.108	9.453
E	3.095	9.292	0.101	9.094
E′	3.000			8.61

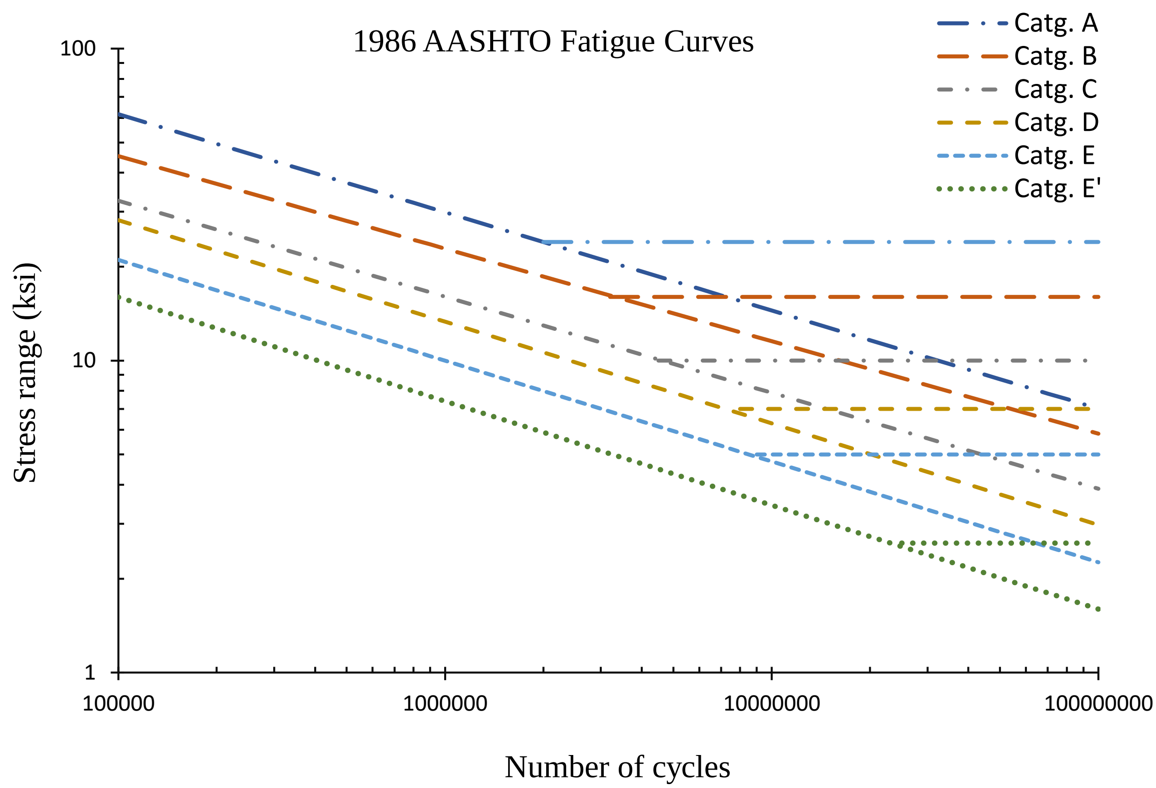

Figure 3.8. Fatigue design curves in the 1986 AASHTO specifications (NCHRP Report 286 by Keating and Fisher, 1986)

Following to the original NCHRP reports 102 and 147, other NCHRP studies (including NCHRP Reports 181, 188, 206, 227, and 267) reported on full scale and welded steel specimens to investigate different aspects of fatigue in the design of bridges and to expand the range of detail types and sizes included in AASHTO fatigue curves.

NCHRP Report 286 (Keating and Fisher, 1986) reviewed and compared fatigue test data from all prior NCHRP reports as well as data from fatigue tests conducted in Japan and Europe to assess the adequacy of AASHTO provisions on fatigue design criteria for bridge welded details. This study proposed a few adjustments to the fatigue design curves of the AASHTO 1986 provisions, which were originally developed based on the data in NCHRP Reports 102 and 147. The adjustment included addition of new categories B′, C′, and E′ to cover other detail types. Based on a linear regression analysis of the data (from prior works) for each fatigue category, the authors proposed that a constant slope of - 3 would best fit data from all categories (Equation 3.31), resulting in parallel fatigue curves (with different intercepts) for all categories. The values proposed for constant A are shown in Table 3.2. The modified fatigue design curves, as current AASHTO fatigue curves, based on the proposed values of slope and constants A are shown in Figure 3.9.

$$N = A.S_r^{-3} \qquad \text{Equation 3.31}$$

Table 3.2. Coefficient A for fatigue design curves (NCHRP Report 286 by Keating and Fisher, 1986)

Category	Constant A
A	2.500E+10
B	1.191E+10
C	4.446E+09
D	2.185E+09
E	1.072E+09
E′	3.908E+08

A comparison of the allowable stress ranges for different load cycles of 1986 AASHTO and the proposed values as a result of NCHRP Report 286 (Keating and Fisher, 1986) is given in Table 3.3. The values outside the parentheses show 1986 AAHTO values and the values in the parentheses show proposed values from NCHRP Report 286.

Table 3.3. Comparison of allowable stress ranges obtained from the 1986 AASHTO provisions and the values proposed in NCHRP report 286 (NCHRP Report 286 by Keating and Fisher, 1986).

Allowable Stress Range, ksi				
Category	100,000 cycles	500,000 cycles*	2,000,000 cycles*	Above 2,000,000 cycles*
A	60 (63)	---(37)	24 (24)	24 (24)
B	45 (49)	---(29)	18 (18)	16 (16)
C	32 (35.5)	---(21)	13 (13)	10 (10)
D	27 (28)	---(16)	10 (10)	7 (7)
E	21 (22)	---(13)	8 (8)	5 (4.5)
E′	16 (16)	---(9.2)	5.8 (5.8)	2.6 (2.6)

* The values outside the parentheses show 1986 AASHTO values and the values in the parentheses show proposed values from NCHRP report 286.

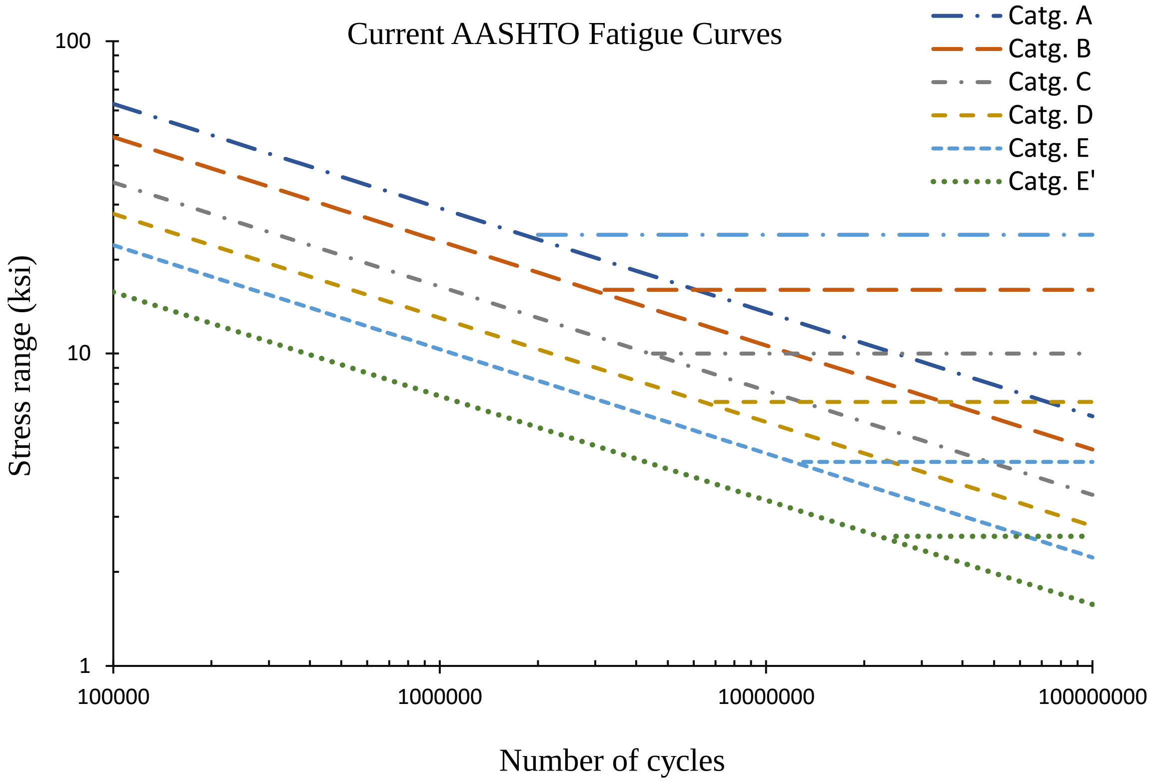

Figure 3.9. Current AASHTO fatigue curves (AASHTO, 2018)

In this study, to apply the survival analysis to fatigue data to each category, an attempt was made to extract the numerical data for different categories from the original fatigue studies (i.e. NCHRP Reports 102, 147, as shown in Figures 3.2 to 3.7). However, not all the data points that are shown on the graphs were listed in tabular form in NCHRP Reports 102 and 147. More than 80% of the data shown graphically matched the tabular data. Attempts to obtain a complete list of numerical data from the authors and the sponsor were unsuccessful. Therefore, the remaining (missing) data were recovered by digitizing the plots included in NCHRP Report 286. The entire dataset for categories A through E′ are listed in Table A.1 through A.6 of Appendix A.

Chapter 4. Application of Survival Analysis to Fatigue Test Data

In this chapter, survival analysis of fatigue data is studied, considering the effect of different contributing factors (covariates) on the reliability of fatigue resistance and the corresponding failure rates (hazard). The fatigue data used in these analyses (listed in Appendix A) were obtained in the 1970's (add references) and are the basis for the current design codes for steel buildings and bridges (reference AISC and AASHTO). The covariates considered here are the stress range (numerical parameter) and the fatigue detail category (categorical parameter). Four different baseline survival distributions (Weibull, log-logistic, lognormal, Hypertabastic) were considered and the model parameters were determined using maximum likelihood estimation. The best -fit distribution (among the four evaluated) was then selected based on the AIC criterion. A description of the data analysis methods and the survival models are given in the following sections of this chapter.

4.1. Nonparametric Survival Analysis of Fatigue Data

The K-M nonparametric analysis was first performed to the fatigue data (listed in Appendix A). Figures 4.1 and 4.2. show the K-M survival and cumulative failure curves for different fatigue categories based on the original NCHRP fatigue data (NCHRP Report 102 by Fisher et al., 1970; NCHRP Report 147 by Fisher et al., 1974). The reliability curves for different categories in K-M plot intersect each other in several points, which is an indication that the AFT model should be used in lieu of the PH model.

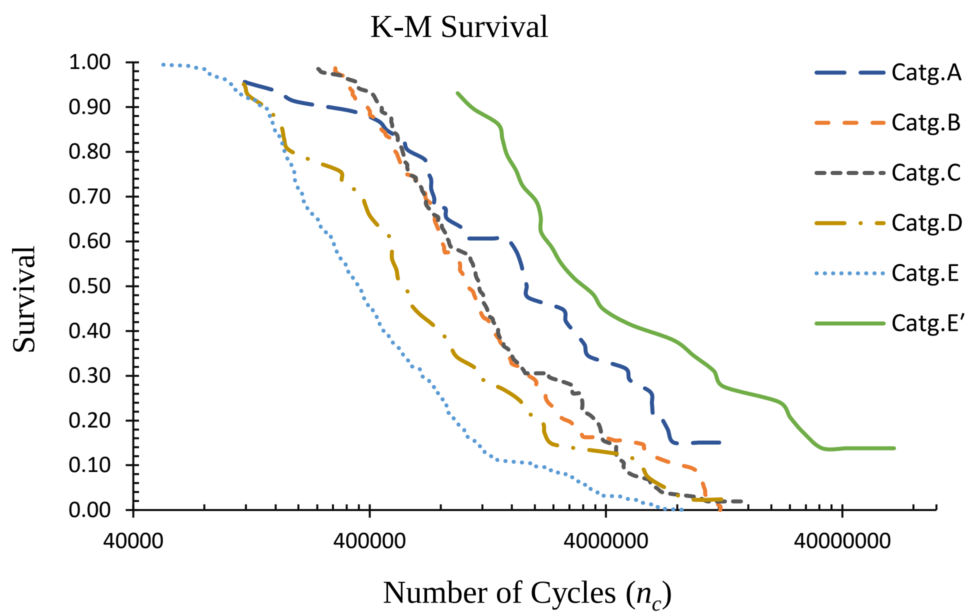

Figure 4.1. K-M survival curves for different detail categories of fatigue data

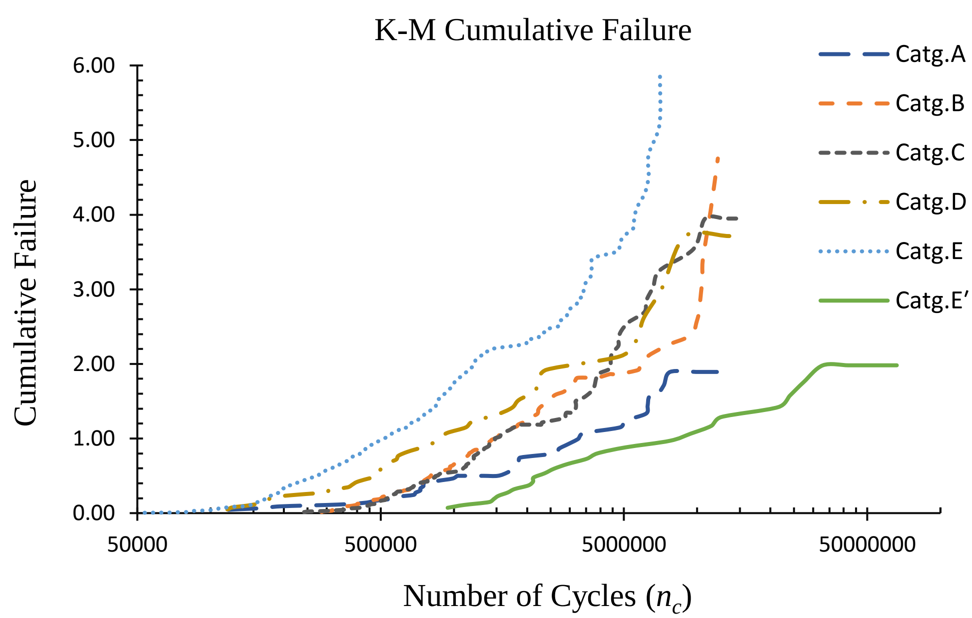

Figure 4.2. K-M cumulative failure for different categories of AASHTO fatigue data

4.2. Parametric Survival Analysis of Fatigue Data

As described in Chapter 3, the parametric survival analysis models need assumption of a baseline distribution function. Various criteria, including goodness-of-fit tests, can be used to find the best-fit baseline distribution function. The maximum likelihood estimation (maximizing the log-likelihood function was used to find the model parameters for each of the four evaluated baseline distribution functions. The AIC criterion was used to find the most suitable distribution function for the survival analysis of bridge fatigue data. The Mathematica® and SAS/STAT® software programs were used to perform the maximum likelihood estimation and to determine various model parameters and AIC values. Appendix B includes the SAS and Mathematica codes used for the survival analyses in this study.

Table 4.1 shows the results of maximum likelihood estimation and the AIC values for log-logistic, lognormal, Hypertabastic, and Weibull distributions. Based on the AIC results, the log-logistic distribution was selected as the best-fit distribution for the bridge fatigue data. Equation 4.1 shows the log-likelihood function for the parametric AFT model using the log-logistic distribution.

$$LL(\theta,\alpha,\beta : t) = \sum_{i=1}^{n}(\delta_i \, ln\left(\frac{(\beta/\alpha)(Z(t_i)/\alpha)^{\beta-1}}{1+(Z(t_i)/\alpha)^{\beta}} t_i g(X_i|\theta)\right) - ln(1 + \left(Z(t_i)/\alpha)^{\beta}\right) \qquad \text{Equation 4.1}$$

$$\delta_i = \begin{cases} 0 & if\ t_i\ is\ a\ right\ censored\ observation \\ 1 & otherwise \end{cases}$$

$$Z(t_i) = t_i g(X_i|\theta)$$

The survival time for the i^{th} data set (out of a total of n sets) is t_i. The α and β are positive constants representing the scale and shape parameters, respectively. X is a vector containing p covariates, and θ defines a vector of p constant multipliers for the different covariates. The constants α, β, $\theta_1, \theta_2, \dots, \theta_7$ need to be determined during the maximum likelihood estimation.

In fatigue survival analysis, the number of cycles applied (n_c) replaces the time to event parameter t discussed in Chapter 3 (Equation 4.2). There are two covariates (stress range and detail category) in the fatigue analyses presented here. When a categorical parameter is binary (two outcomes), one parameter can be used and the corresponding covariates can take a value of either 0 or 1. When the categorical parameter contains more than two possible outcomes, additional binary parameters and coefficients are introduced. For example, for a categorical parameter with five possible outcomes, five parameters and five coefficients are introduced with each parameter having two possible outcomes of 0 or 1. This approach is illustrated in Table 4.2.

The log-likelihood function for the AFT log-logistic model can be represented as follows:

$$LL(\theta,\alpha,\beta\colon n_c) = \sum_{i=1}^{n} (\delta_i \, ln\left(t_i \frac{(\beta/\alpha)(Z(n_{ci})/\alpha)^{\beta-1}}{1+(Z(n_{ci})/\alpha)^{\beta}} g(X_i|\theta) \right) - ln(1 + \left(Z(n_{ci})/\alpha)^{\beta}\right)$$

Equation 4.2

The function $g(x|\theta)$ for the fatigue analysis described here is defined as:

$$g(x|\theta) = \exp(S_r.\theta_1 + C_A.\theta_2 + C_B.\theta_3 + C_C.\theta_4 + C_D.\theta_5 + C_E.\theta_6 + C_{E'}.\theta_7)$$

Where S_r is the stress range. C_A, C_B, C_C, C_D, C_E, and $C_{E'}$ represent categorical parameters corresponding to fatigue detail categories A through E′, respectively. For each categorical parameter, a value of 1 is assigned to the coefficient associated with the applicable category while 0 is assigned to all other categories. For example, the covariate "C_A", for the fatigue detail category A, would have a value equal to 1 for the data belonging to category A and 0 for the fatigue data associated with other categories. Parameters θ_1 through θ_7 are the constants that must be determined using the maximum likelihood estimation.

Table 4.1. Akaike Information Criteria (AIC) for different distribution functions

Model Distribution	-2 log-likelihood	AIC
Log-logistic	-676.007	-686.007
Lognormal	-707.582	-717.582
Hypertabastic	-717.189	-727.189
Weibull	-811.709	-821.709

Table 4.2. Binary covariates for categorical data

Category	C_A	C_B	C_C	C_D	C_E	$C_{E'}$
A	1	0	0	0	0	0
B	0	1	0	0	0	0
C	0	0	1	0	0	0
D	0	0	0	1	0	0
E	0	0	0	0	1	0
E′	0	0	0	0	0	1

4.3. Log-logistic AFT Model for Fatigue

Based on the results of analyses discussed in the previous section, the parametric log-logistic AFT model was selected for the survival analysis of the fatigue data related to structural steel. The probability of survival (*S*), probability of failure (*F*), probability density function (*f*), hazard rate (*h*), and cumulative hazard (*H*) functions for the log-logistic AFT model for fatigue data are given in Eqs. 4.3 through 4.7.

$$S(n_{cg}) = \frac{1}{1 + (n_{cg}/\alpha)^{\beta}}$$ Equation 4.3

$$F(n_{cg}) = 1 - S(n_{cg}) = \frac{1}{1 + (n_{cg}/\alpha)^{-\beta}}$$ Equation 4.4

$$f(n_{cg}) = \frac{1}{1000}\frac{(\beta/\alpha)(n_{cg}/\alpha)^{\beta-1}}{\left(1+(n_{cg}/\alpha)^{\beta}\right)^2}g(x|\theta) \qquad \text{Equation 4.5}$$

$$h(n_{cg}) = \frac{1}{1000}\frac{(\beta/\alpha)(n_{cg}/\alpha)^{\beta-1}}{1+(n_{cg}/\alpha)^{\beta}}g(x|\theta) \qquad \text{Equation 4.6}$$

$$H(n_{cg}) = -\ln\left(S(n_{cg})\right) = -\ln\left(\frac{1}{1+(n_{cg}/\alpha)^{\beta}}\right) \qquad \text{Equation 4.7}$$

Where n_{cg} and $g(x|\theta)$ are defined as:

$$n_{cg} = \frac{n_c}{1000}.\exp(S_r.\theta_1 + C_A.\theta_2 + C_B.\theta_3 + C_C.\theta_4 + C_D.\theta_5 + C_E.\theta_6 + C_{E'}.\theta_7) \qquad Eq.4.8$$

$$g(x|\theta) = \exp(S_r.\theta_1 + C_A.\theta_2 + C_B.\theta_3 + C_C.\theta_4 + C_D.\theta_5 + C_E.\theta_6 + C_{E'}.\theta_7) \qquad Eq.4.9$$

As mentioned in the previous sections, parameters α, β, θ_1, θ_2,…, and θ_7 are determined using the maximum likelihood method. Table 4.2. lists the calculated parameters when the entire dataset is analyzed together (herein referred to as “Global Analyses”). A second form of analysis when datasets associated with individual categories are analyzed separately (“Category Analyses”) is discussed later.

Table 4.3. Parameter and Standard Error Estimation for Log-logistic AFT Model (Global Analysis)

All Categories				
Parameter	Estimate	Standard Error	t value	P-value
α	7.161	135.209	0.053	9.578E-01
β	3.150	0.098	32.248	1.184E-145
θ_1	0.163	0.004	41.267	2.597E-198
θ_2	-12.168	18.882	-0.644	5.195E-01
θ_3	-9.626	18.882	-0.510	6.103E-01
θ_4	-8.497	18.882	-0.450	6.528E-01
θ_5	-7.507	18.882	-0.398	6.910E-01
θ_6	-6.757	18.882	-0.358	7.206E-01
θ_7	-7.503	18.882	-0.397	6.912E-01

4.4. Comparison of Global Fatigue Survival Functions with K-M Results

The developed global log-logistic AFT model (Eqs. 4.3 through 4.8) can estimate the reliability (with respect to fatigue resistance) and hazard rate as a function of number of cycles (n_c), stress range (S_r), and fatigue category (C_A through $C_{E'}$). Figures 4.3 through 4.8 show survival curves for different fatigue categories using the global log-logistic AFT model. Survival curves for each fatigue category are shown for the stress ranges that were predominant in the experimental data. In other words, the plots shown are associated with the discrete stress ranges for the actual data points in each category as reported in the fatigue test data. For comparison, the K-M survival curves are also plotted for each stress range in Figures 4.3 through 4.8. A comparison of the K-M survival curves (nonparametric model) with the log-logistic AFT model (parametric model) can be used to assess the overall accuracy of the predicted model in comparison with the actual test data. The consistency observed between the K-M and global AFT model curves shows that the model parameters represented the fatigue data reasonably well for the most part. Some stress ranges in different categories had very limited number of data points. Therefore, the K-M comparison may not be ideal in such cases.

Figure 4.3 shows survival curves using the global log-logistic AFT and K-M models for category A and S_r values of 30, 36, 42, and 57 ksi. For most stress ranges, the survival curves show acceptable agreement with the K-M curves. However, the survival curve at S_r = 30 ksi was not compatible with the corresponding K-M curve with limited data points (Figure 4.3).

Figure 4.4 shows the survival curves for category B data for S_r values of 18, 24, 30, and 36 ksi. The survival curves for S_r values of 18, 24, and 30 show very close agreement with the corresponding K-M curves. The estimated survival curve S_r of 36 ksi follows the slope of the corresponding K-M curve, but there is a shift between the two survival curves.

Figures 4.5 and 4.6 show survival curves for category C and D, respectively. Survival curves in these figures for all stress range are very close to the K-M curves, indicating that the global log-logistic AFT model is a good representative of survival times of fatigue data in these categories. Survival curves for category E is presented for S_r values of 8, 12, 16, 20, and 24 ksi in Figure 4.7. The survival curves for most stress ranges are consistent with the corresponding K-M curves except for the curve at S_r = 8 ksi, which shows deviation from the corresponding K-M curve at that stress range.

Figure 4.8 displays the survival curves for category E′. The number of data points for each stress range in this category was very limited and many were censored (run-out) data. Therefore, the K-M results could not be properly estimated for comparison with the model results.

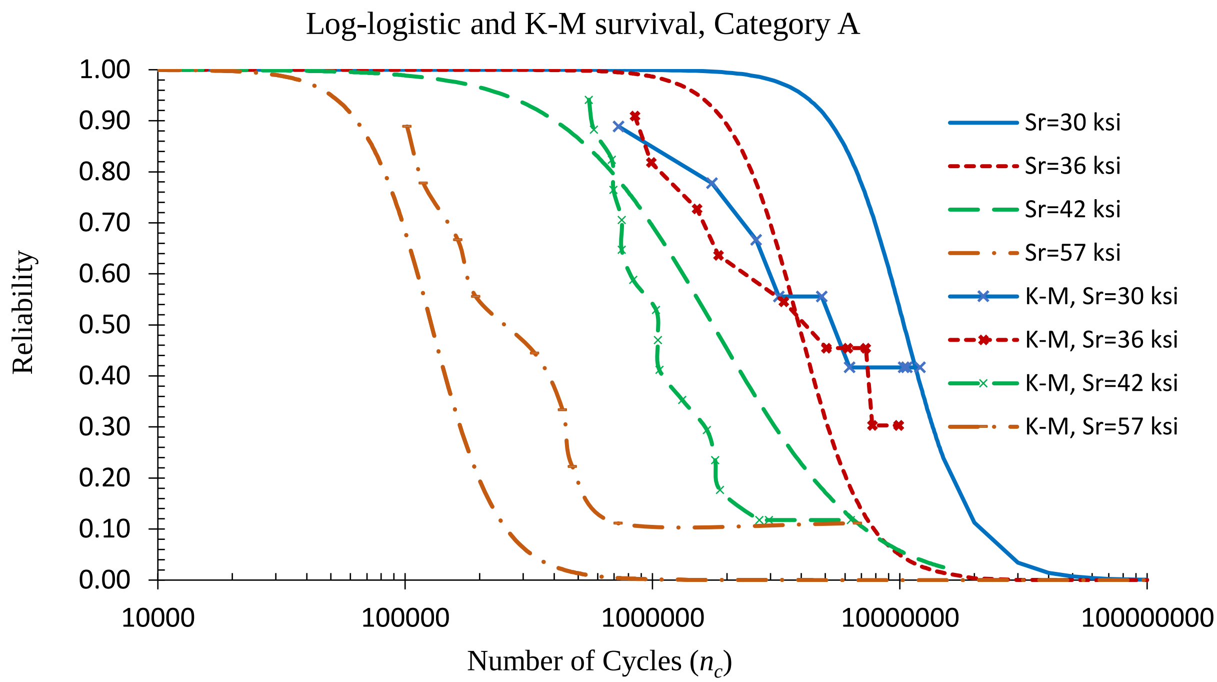

Figure 4.3. Global Log-logistic AFT survival curves versus K-M survival curves for Category A

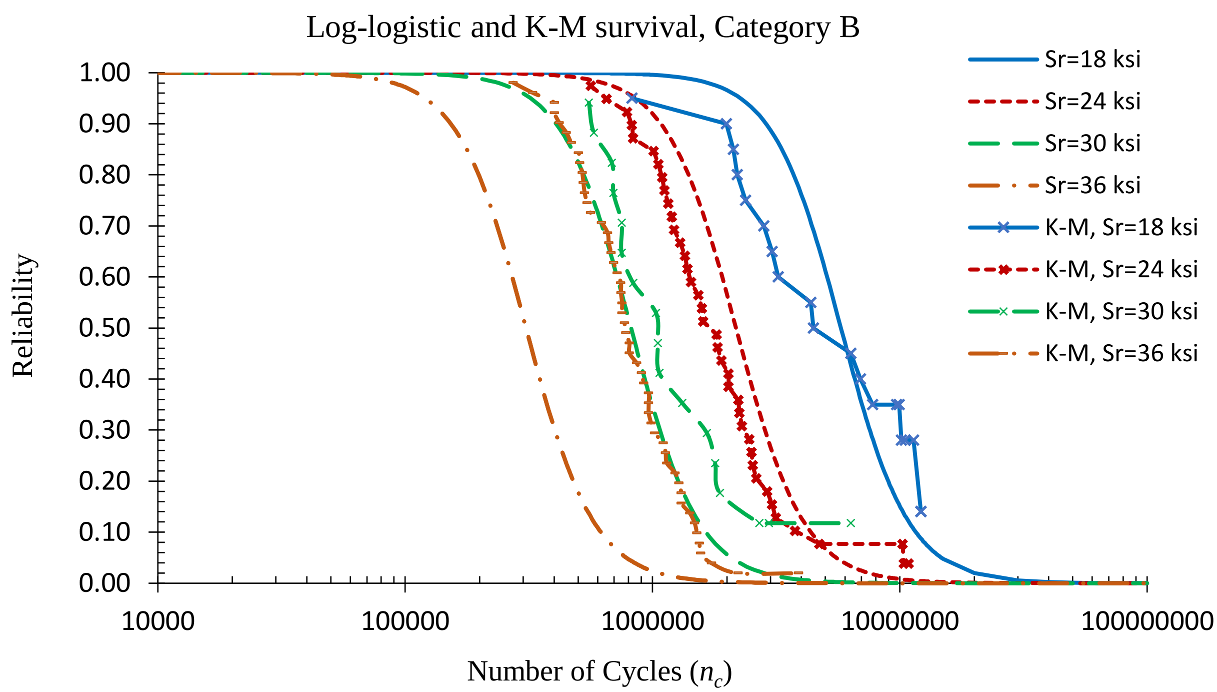

Figure 4.4. Global Log-logistic AFT survival curves versus K-M survival curves for Category B

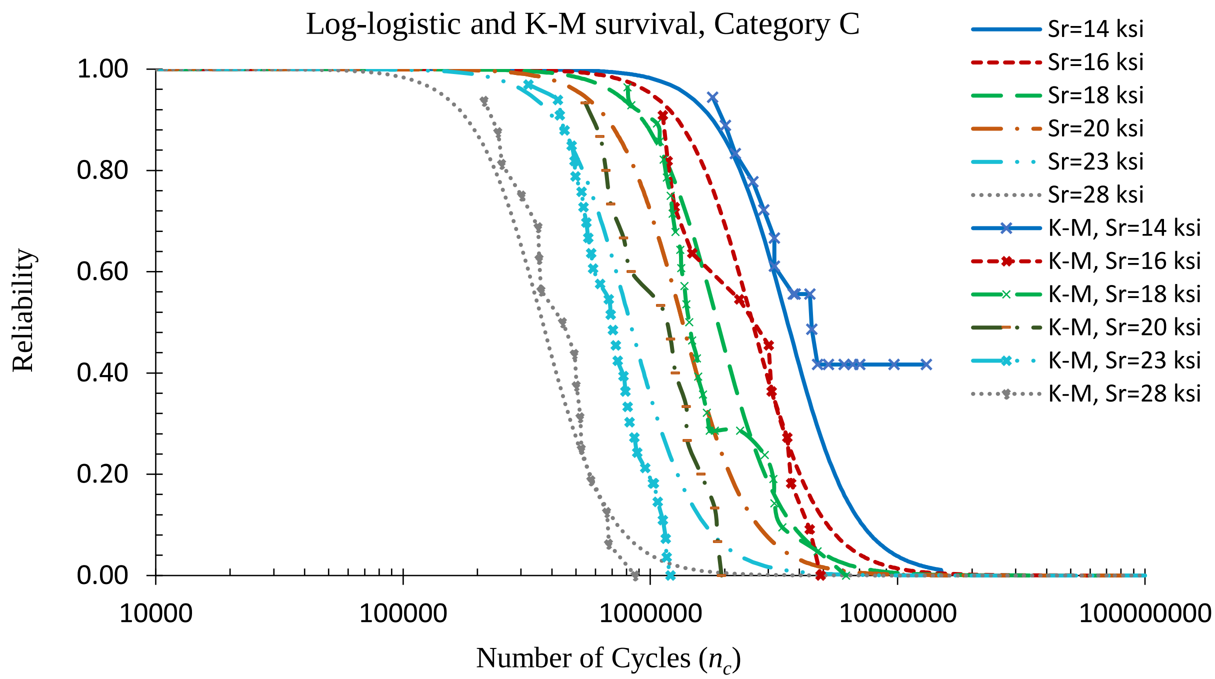

Figure 4.5. Global Log-logistic AFT survival curves versus K-M survival curves for Category C

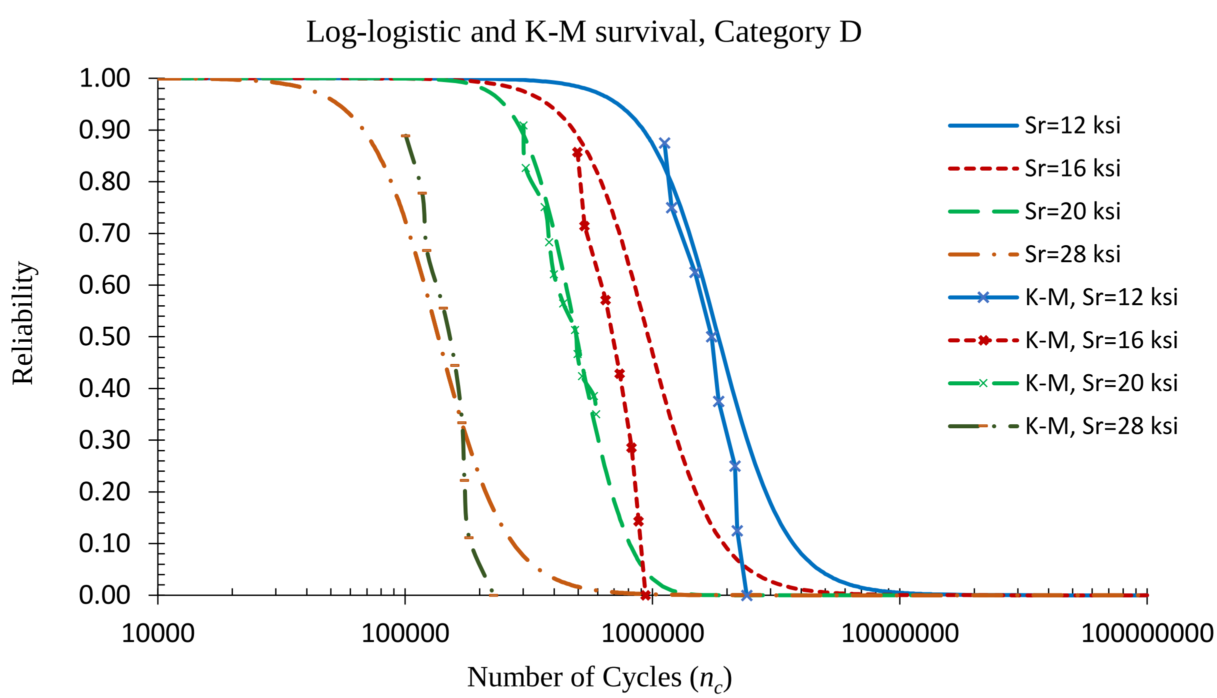

Figure 4.6. Global Log-logistic AFT survival curves versus K-M survival curves for Category D

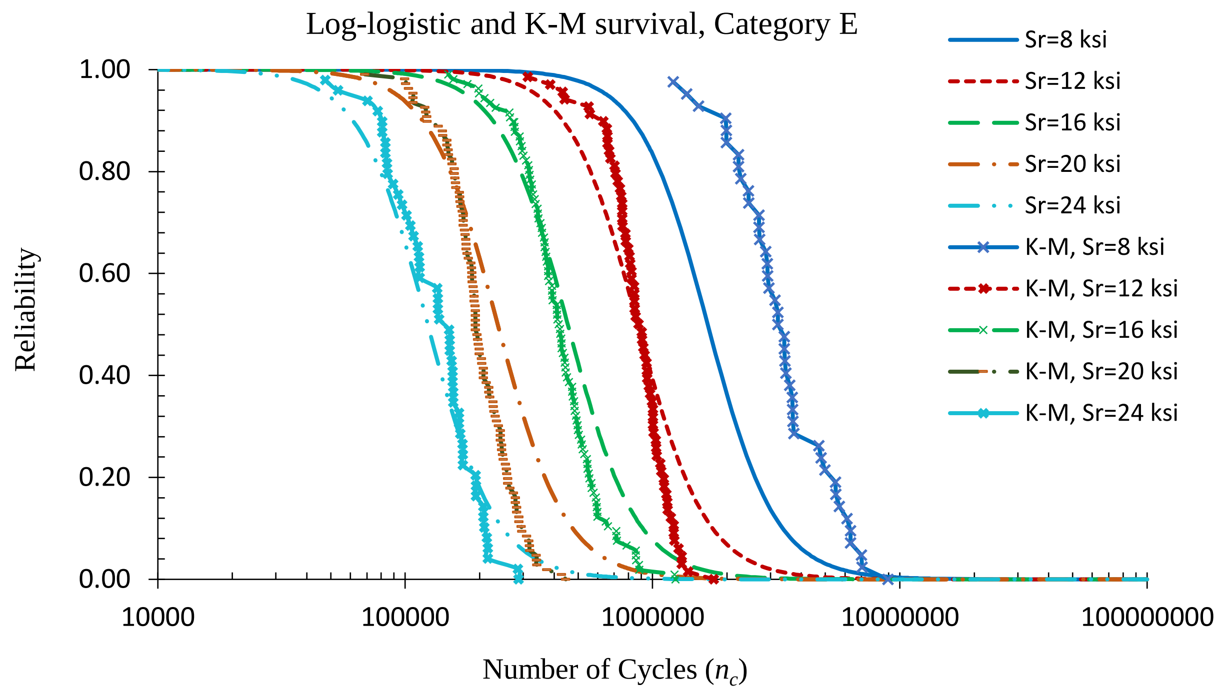

Figure 4.7. Global Log-logistic AFT survival curves versus K-M survival curves for Category E

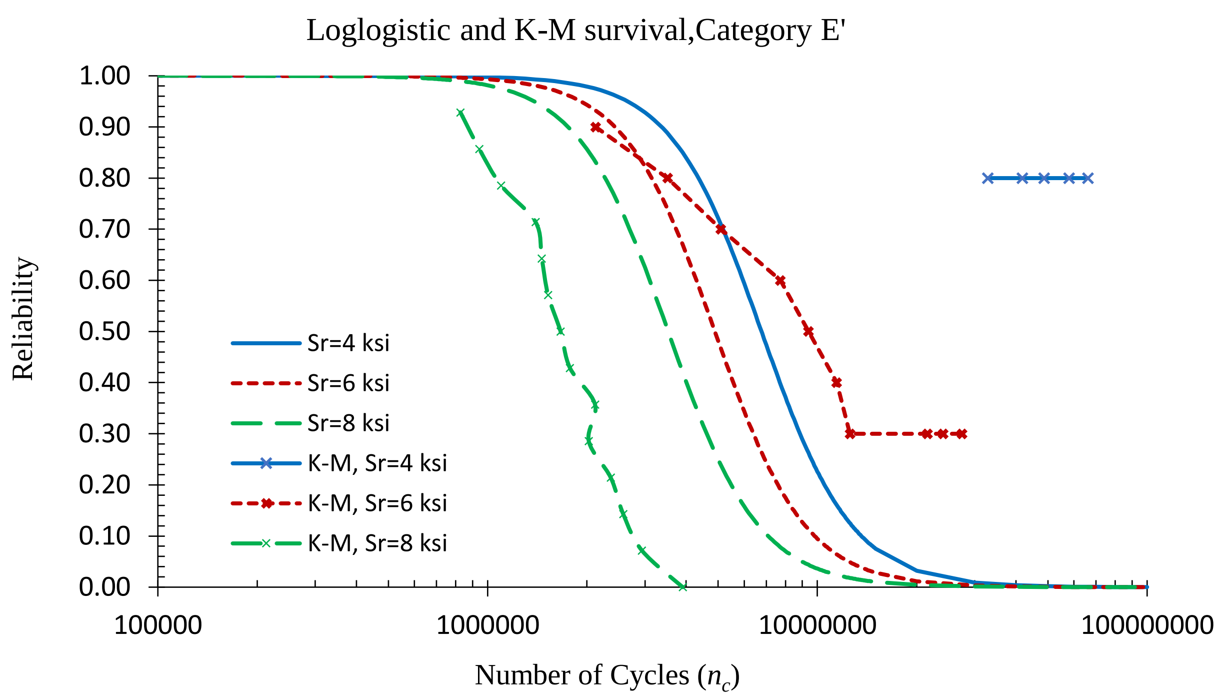

Figure 4.8. Global Log-logistic AFT survival curves versus K-M survival curves for Category E′

Based on comparison of the global AFT log-logistic model with K-M results, it was concluded that, although there was good overall agreement between the model and K-M results, the global survival model was not in full agreement with the K-M results for all stress ranges and detail categories. Therefore, to further improve the compatibility of the model results with the non-parametric results, the survival analyses were performed separately on the fatigue data for each category. These are referred to as "category-based analyses". A set of new model parameters were calculated using the category-based analyses. Tables 4.4 through 4.9 list the calculated parameters along with standard error and P-values for the category analyses.

The initial category E' (NCHRP Report 286) was developed using data for coverplated beams from NCHRP Report 102 and 147 that fell below category E. However, later NCHRP Report 227 conducted test on different fatigue details including coverplates thicker than 1-in that showed strength less than category E. These data were used to expand the available data for category E'. In this research, the category E' data was considered from original data base (NCHRP Reports 102 AND 147).

Table 4.11 provides a summary of parameters estimates for different categories. The equations for n_{cg} and $g(x|\theta)$ to be used within Equation 4.4 through 4.9 are restated as shown below:

$$n_{cg} = \frac{n_c}{1000}.\exp(S_r.\theta_1 + \theta_2) \qquad \text{Equation 4.10}$$

$$g(x|\theta) = \exp(S_r.\theta_1 + \theta_2) \qquad \text{Equation 4.11}$$

Where $\theta_1$and θ_2 are the applicable constants for stress range and categorical data, respectively. Since, the separated data for each category is used in the category-based analyses, θ_2 has a multiplier equal to 1.

Table 4.4. Parameter and Standard Error Estimation for Category A using Log-logistic AFT Model

Category A				
Parameter	Estimate	Standard Error	t Value	P-value
α	9.918E+00	7.299E-02	1.359E+02	1.448E-61
β	1.611E+00	2.285E-01	7.051E+00	7.640E-09
θ_1	1.089E-01	1.674E-02	6.507E+00	5.021E-08
θ_2	-9.670E+00	7.239E-01	-1.336E+01	1.919E-17

Table 4.5. Parameter and Standard Error Estimation for Category B using Log-logistic AFT Model

Category B				
Parameter	Estimate	Standard Error	t Value	P-value
α	5.097	0.040	127.848	2.023E-157
β	2.975	0.207	14.396	3.002E-30
θ_1	0.121	0.007	16.447	1.197E-35
θ_2	-8.788	0.203	-43.246	1.103E-87

Table 4.6. Parameter and Standard Error Estimation for Category C using Log-logistic AFT Model

Category C				
Parameter	Estimate	Standard Error	t Value	P-value
α	3.880	0.047	82.107	9.410E-118
β	3.692	0.275	13.449	9.443E-27
θ_1	0.168	0.009	18.541	4.733E-39
θ_2	-9.215	0.183	-50.269	1.002E-89

Table 4.7. Parameter and Standard Error Estimation for Category D using Log-logistic AFT Model

Category D				
Parameter	Estimate	Standard Error	t Value	P-value
α	7.479	0.025	297.819	5.235E-70
β	4.471	0.587	7.622	2.210E-09
θ_1	0.176	0.010	18.060	3.976E-21
θ_2	-7.696	0.188	-40.980	6.757E-35

Table 4.8. Parameter and Standard Error Estimation for Category E using Log-logistic AFT Model

Category E				
Parameter	Estimate	Standard Error	t Value	P-value
α	2.299	0.029	79.249	2.582E-236
β	4.364	0.189	23.039	8.278E-74
θ_1	0.195	0.005	42.195	1.777E-144
θ_2	-8.419	0.067	-126.190	0.000E+00

Table 4.9. Parameter and Standard Error Estimation for Category E′ using Log-logistic AFT Model

Category E′				
Parameter	Estimate	Standard Error	t Value	P-value
α	9.322	0.074	125.652	3.053E-41
β	2.329	0.421	5.532	5.784E-06
θ_1	0.893	0.098	9.108	5.259E-10
θ_2	-12.370	0.692	-17.887	3.308E-17

Table 4.10. Parameter and Standard Error Estimation for Category E′ using Log-logistic AFT Model

Category E′ with Additional Data				
Parameter	Estimate	Standard Error	t Value	P-value
α	5.572	0.084	66.348	6.334E-55
β	1.877	0.222	8.445	1.438E-11
θ_1	0.470	0.059	8.001	7.696E-11
θ_2	-9.820	0.468	-20.983	3.311E-28

Table 4.11. Summary of Parameter Estimation for Category A through E′ using Log-logistic AFT Model

Category	α	β	θ_1	θ_2
A	9.918	1.611	0.109	-9.670
B	5.097	2.975	0.121	-8.788
C	3.880	3.692	0.168	-9.215
D	7.479	4.471	0.176	-7.696
E	2.299	4.364	0.195	-8.419
E′	9.322	2.329	0.893	-12.370

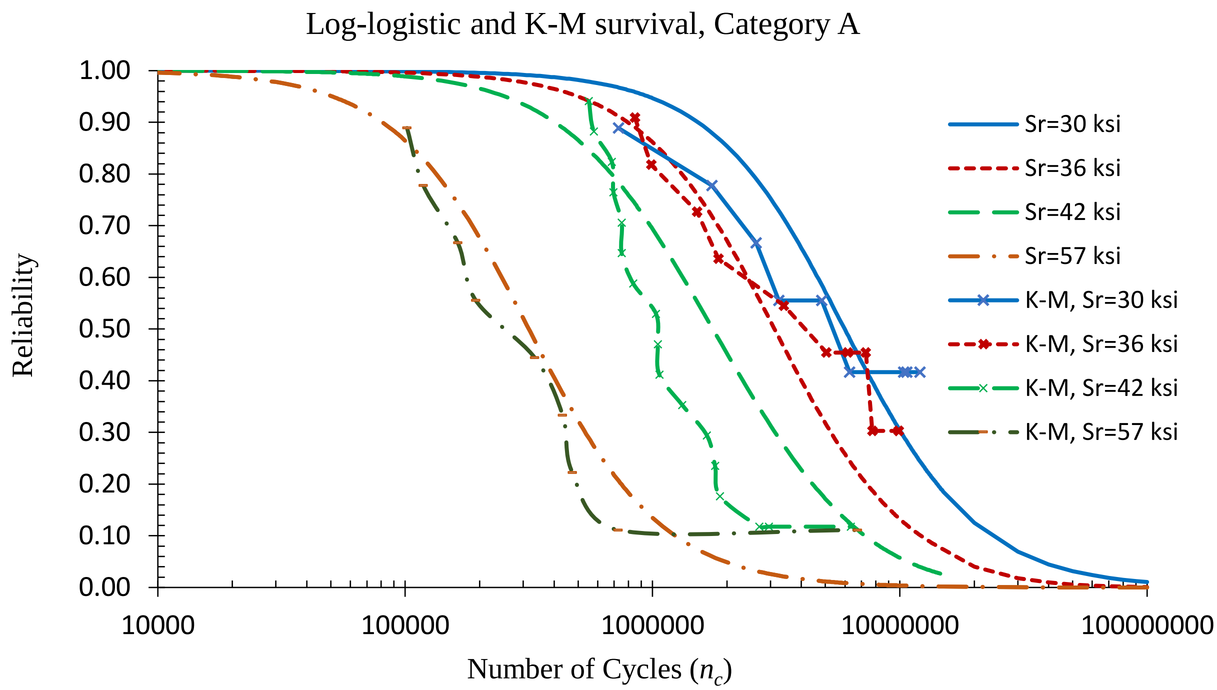

Figure 4.9. Log-logistic AFT survival curves versus K-M survival curves for Category A, analyzed separately

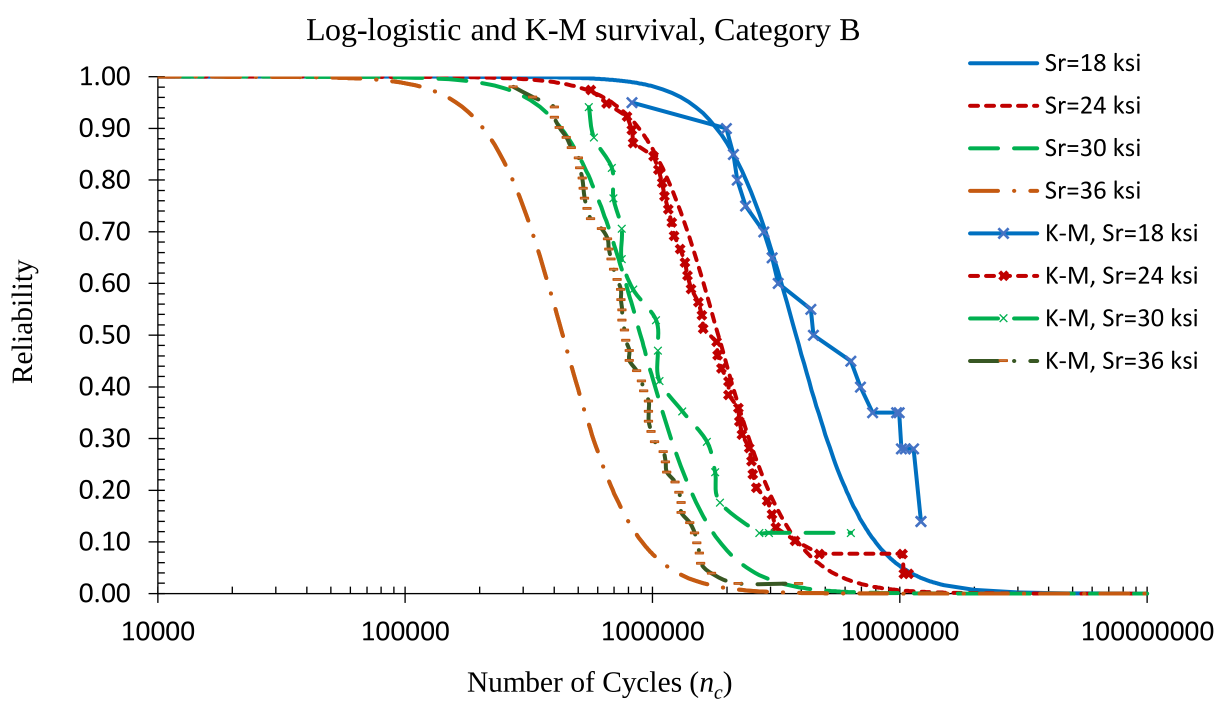

Figure 4.10. Log-logistic AFT survival curves versus K-M survival curves for Category B, analyzed separately

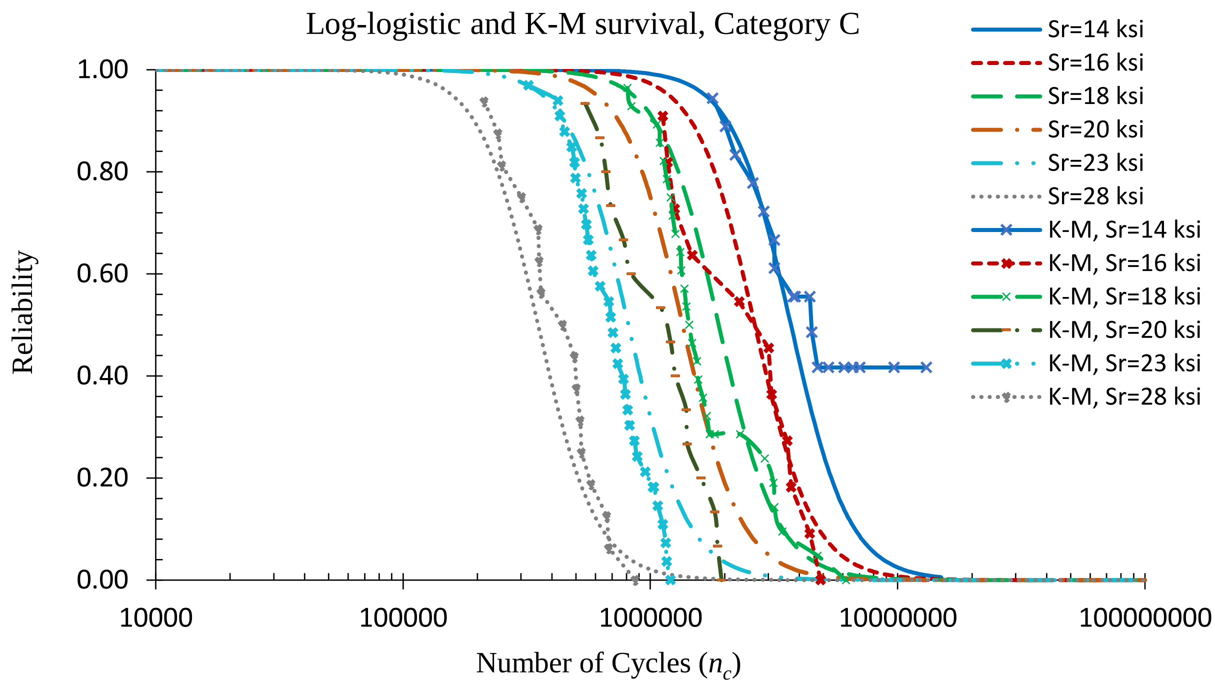

Figure 4.11. Log-logistic AFT survival curves versus K-M survival curves for Category C, analyzed separately

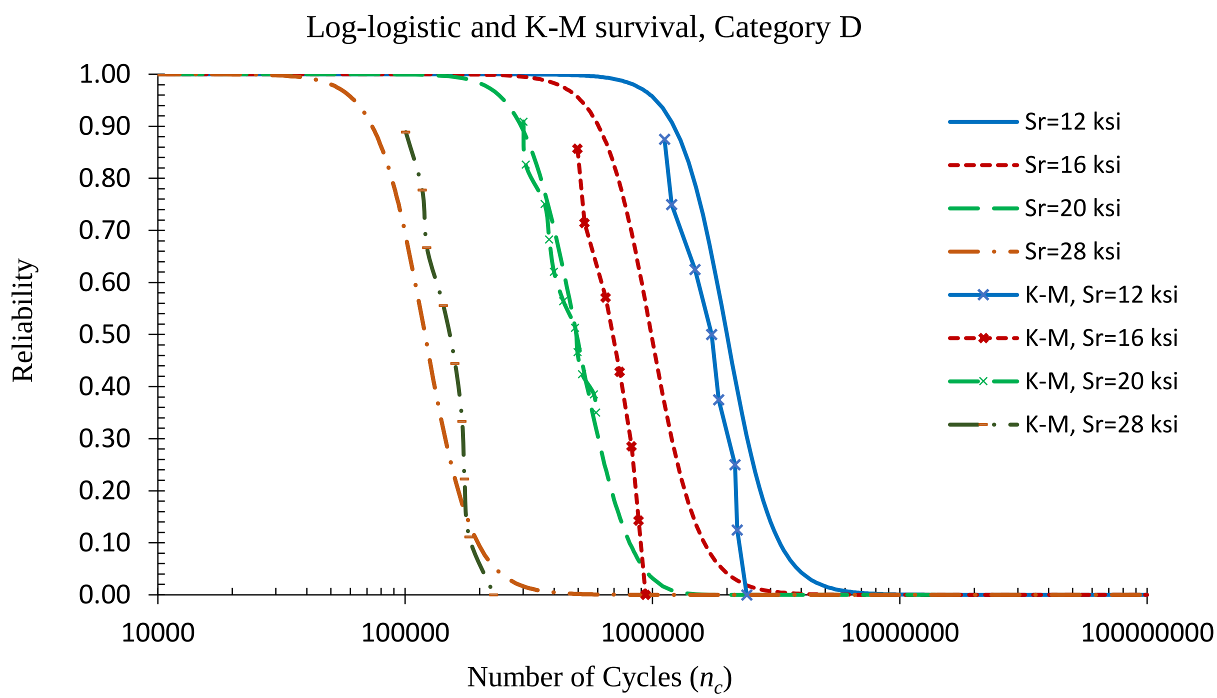

Figure 4.12. Log-logistic AFT survival curves versus K-M survival curves for Category D, analyzed separately

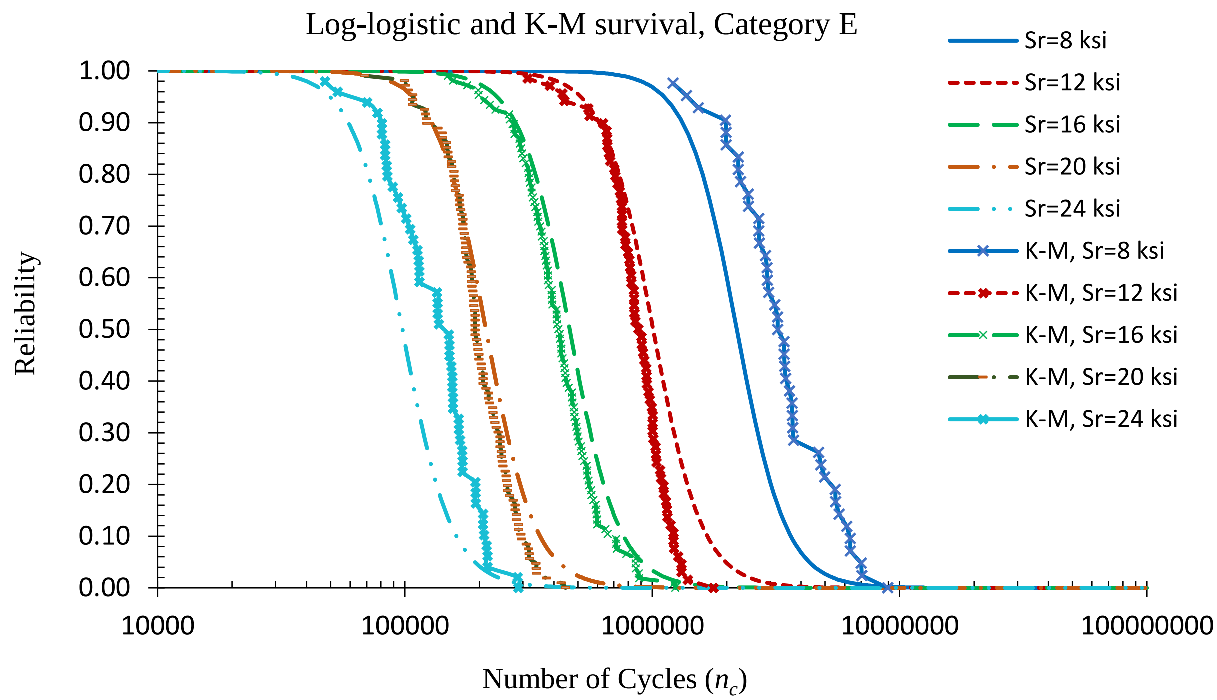

Figure 4.13. Log-logistic AFT survival curves versus K-M survival curves for Category E, analyzed separately

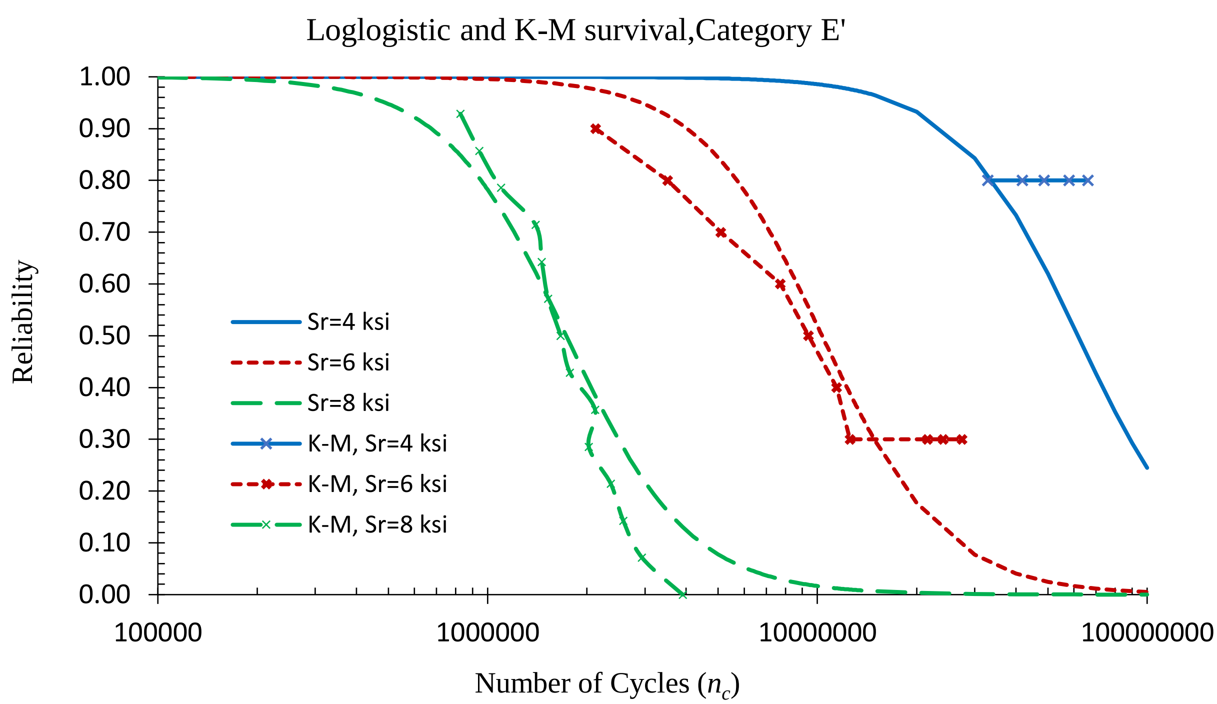

Figure 4.14. Log-logistic AFT survival curves versus K-M survival curves for Category E′, analyzed separately

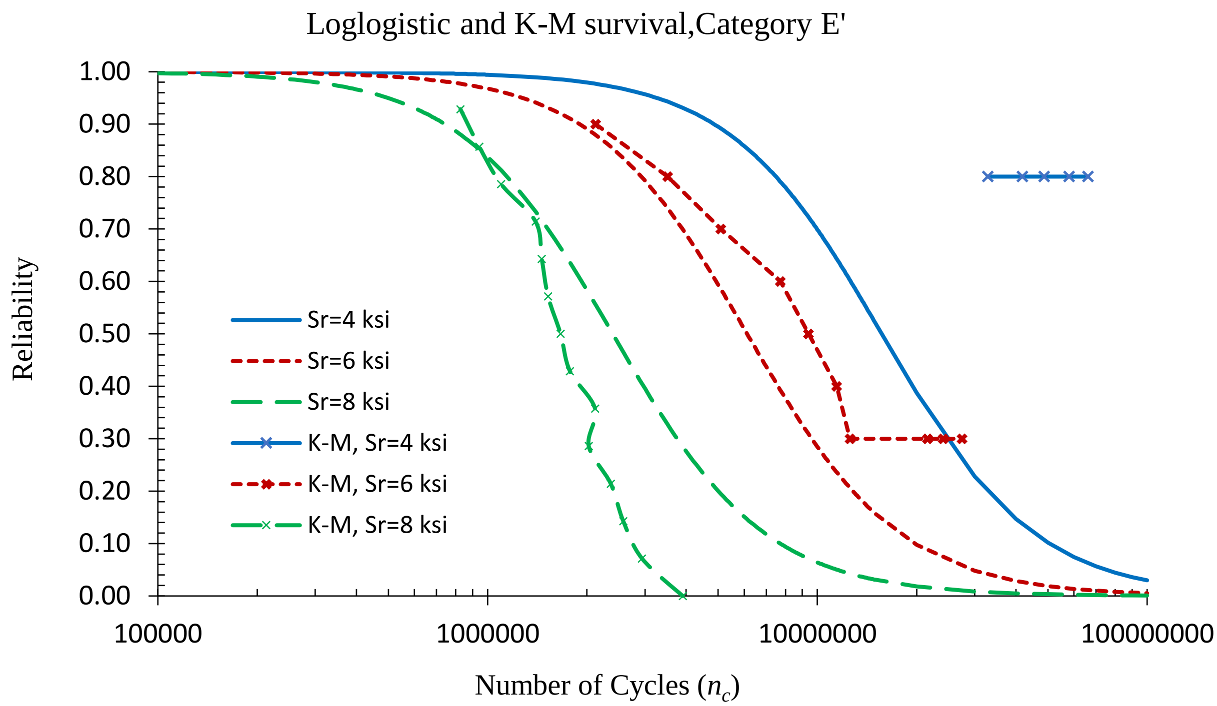

Figure 4.15. Log-logistic AFT survival curves versus K-M survival curves for Category E′, analyzed separately

The results of the category-based analysis models are shown in Figures 4.9 through 4.14 indicate that the survival curves developed using separate analyses for different categories show very close agreement with the corresponding K-M curves for various stress ranges and detail categories. Therefore, the parameters shown in Table 4.11 and Eqs. 4.10 and 4.11 are recommended for use in survival models for fatigue resistance of various detail categories in steel structures.

In the K- M (non-parametric) approach, the probability of survival is only a function of the number of cycles. As mentioned earlier, the effects of other covariates such as stress range or detail type (considered as different fatigue categories) is not explicitly considered in the non-parametric survival function. However, the effect of all covariates are implicitly included in the fatigue test data. In the log-logistic AFT model, the probability of survival (or failure) is calculated considering the influence of the covariates on the survival functions. Therefore, the good agreement observed between the non-parametric K-M curves (at different stress ranges and categories) and the parametric survival curves shows that the effects of covariates are properly simulated, and the developed log-logistic AFT model can be used for survival assessments for various fatigue categories and stress ranges.

Figures 4.15 through 4.20 show the probability density functions for the various fatigue categories at different stress ranges using the developed category-based log-logistic AFT model. As expected, with an increase in the stress range, higher peaks of probability of failure appear at fewer number of cycles. Table 4.12 shows the maximum probability of failure with corresponding number of cycles at different stress ranges for category A. At a constant number of cycles, the probabilities of failure increase as stress range increases. For example, at 10^5 cycles, the probabilities of failure for S_r values of 30, 36, 42, and 57 ksi are 2.2E-8, 6.28E-8, 1.77E-7, and 1.89E-6, respectively.

Table 4.12. Maximum PDF and corresponding number of cycles for category A

S_r *(ksi)*	N_C	Max PDF
30	2400000	1.02E-07
36	1250000	1.96E-07
42	660000	3.77E-07
57	125000	1.93E-06

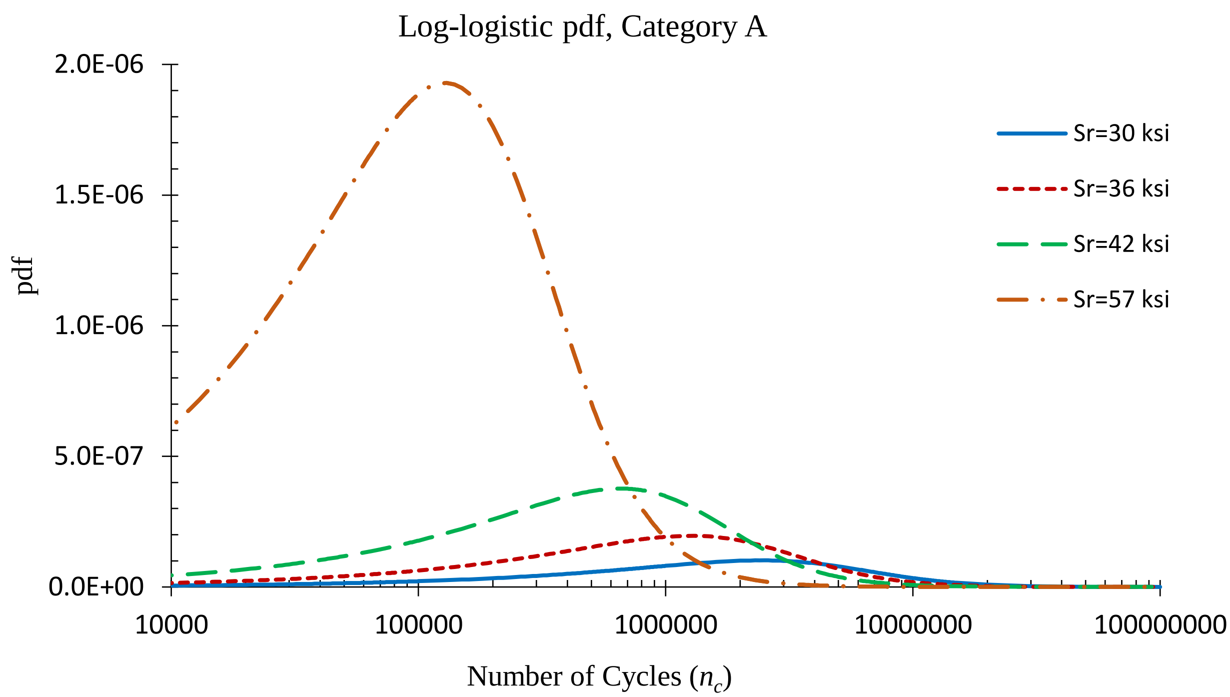

Figure 4.16. Category-based log-logistic AFT probability density functions

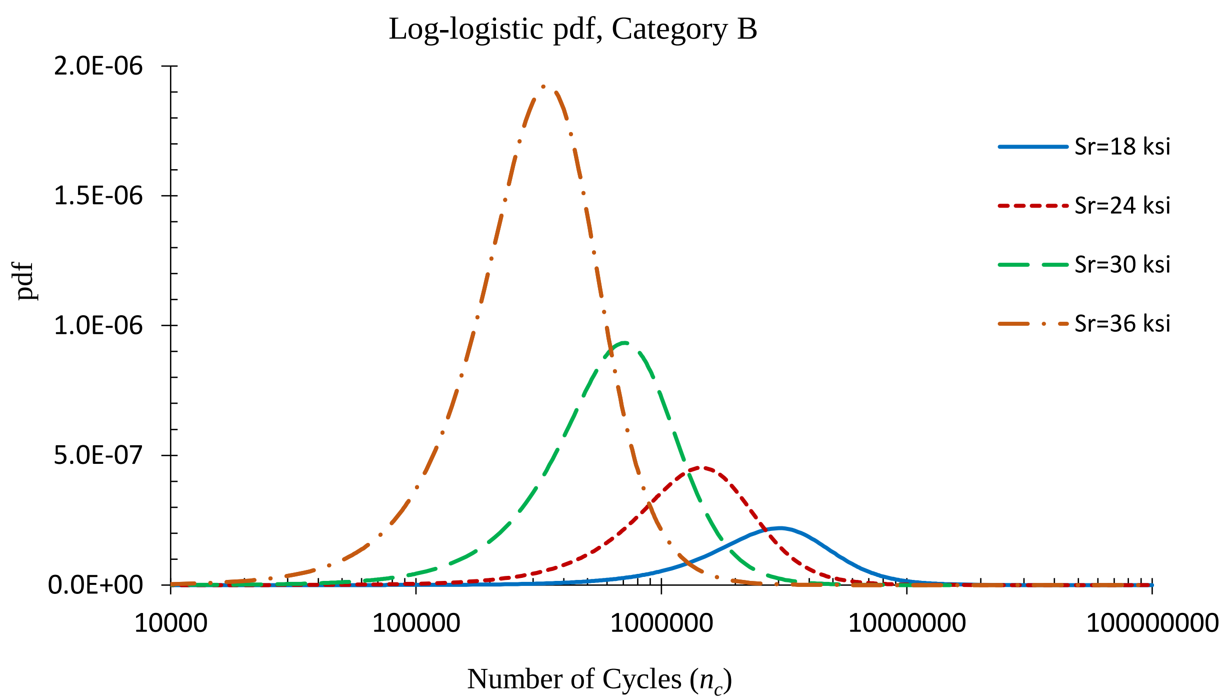

Figure 4.17. Log-logistic AFT pdf curves, for Category B analyzed separately

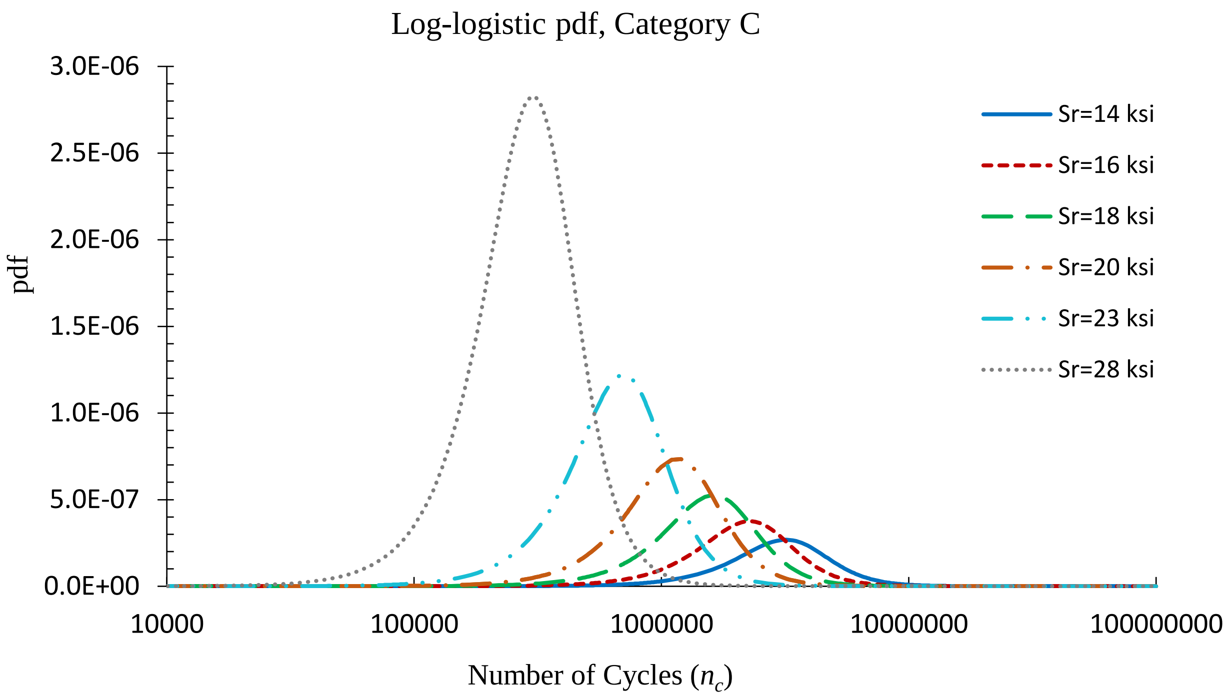

Figure 4.18. Log-logistic AFT pdf curves, for Category C analyzed separately

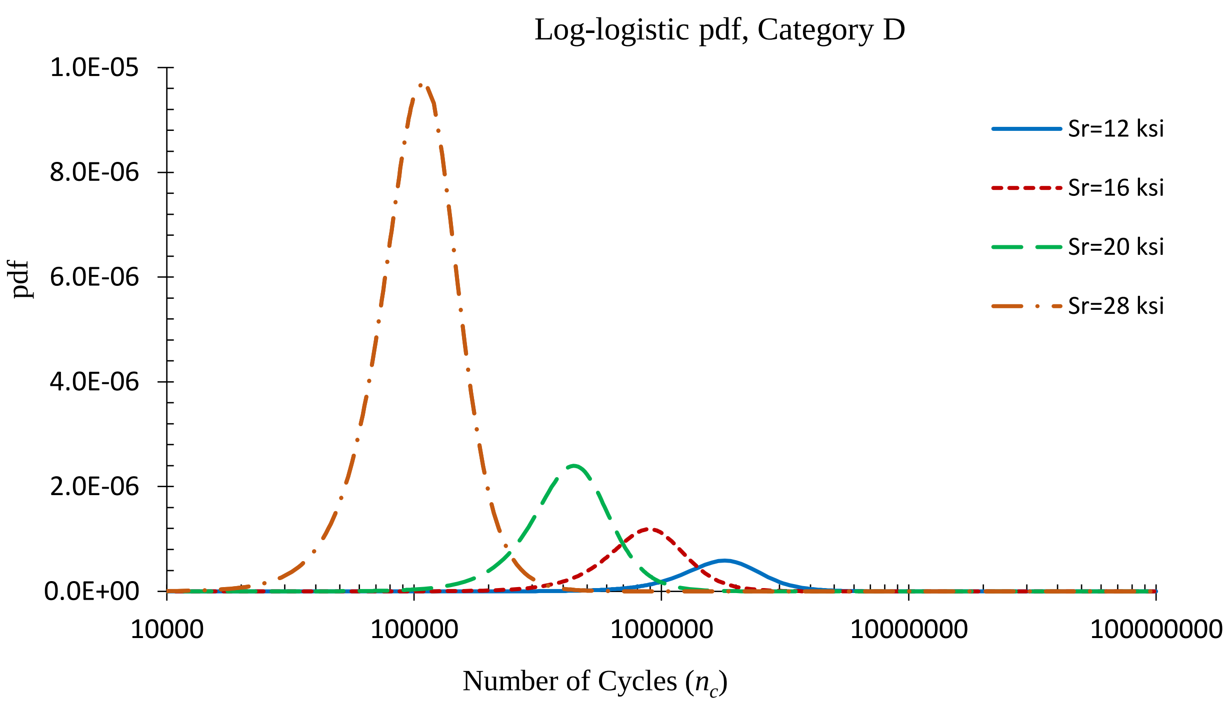

Figure 4.19. Log-logistic AFT pdf curves, for Category D analyzed separately

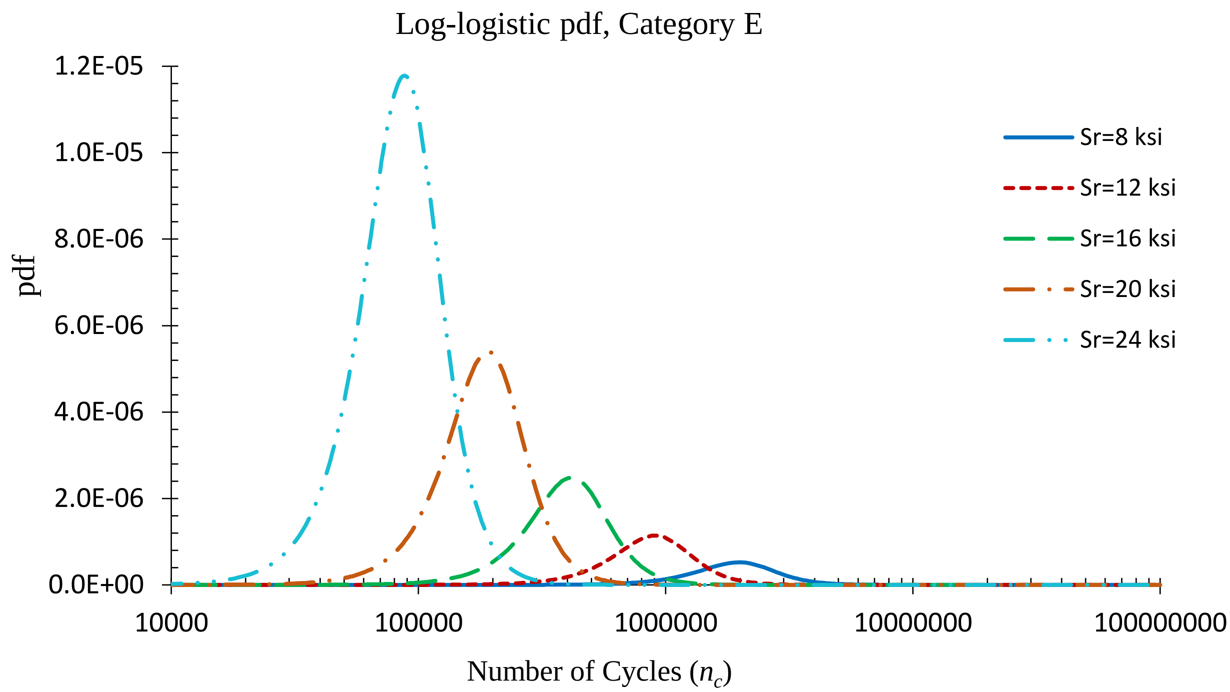

Figure 4.20. Log-logistic AFT pdf curves, for Category E analyzed separately

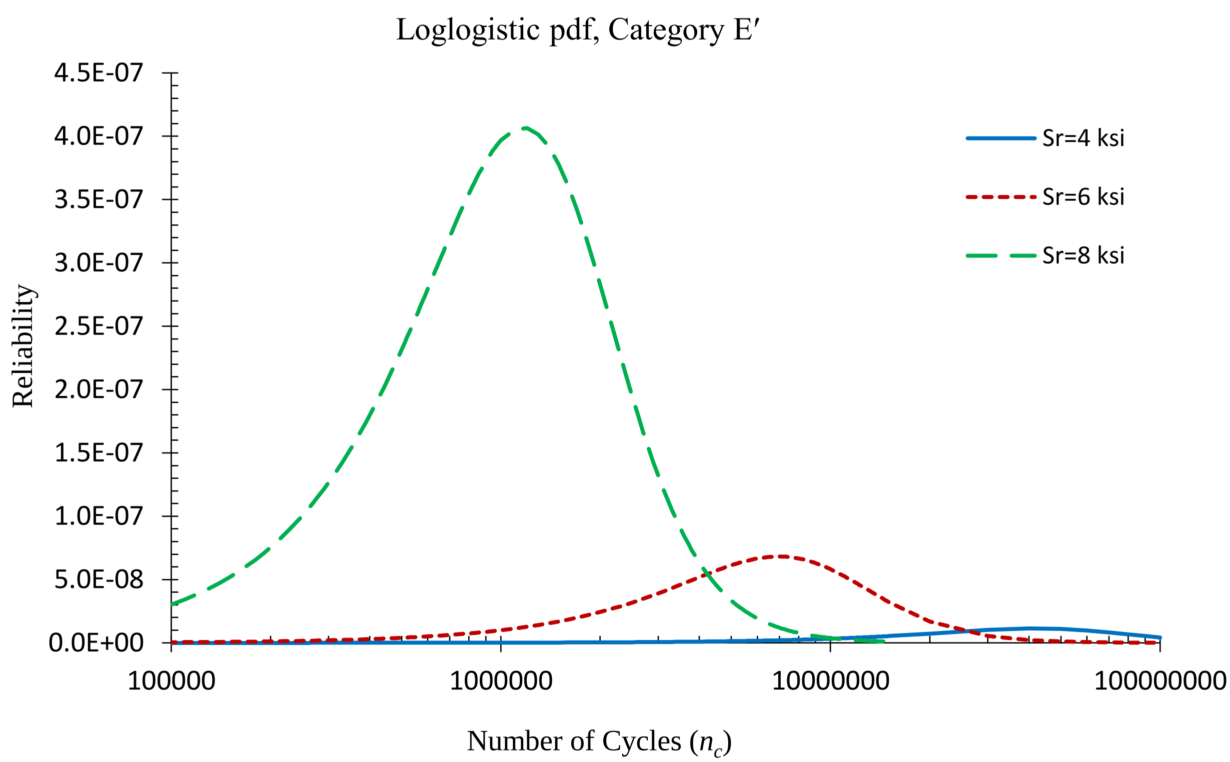

Figure 4.21. Log-logistic AFT pdf curves for Category E′, analyzed separately

Figures 4.21 through 4.26 show the characteristic hazard shapes for fatigue categories A through E′. As it is evident in these figures, the peak hazard rates corresponding to higher stress ranges occur at fewer number of cycles for all fatigue categories. Therefore, at higher stress ranges, fewer number of cycles are needed to reach the peak hazard rate. For example, for fatigue category A, the peak hazard rates for stress ranges 30, 36, 42, and 57 ksi are 1.39E-7, 2.66E-7, 5.12E-7, and 2.62E-6, respectively, and the corresponding number of cycles are 4,400,000, 2,300,000, 1,200,000, and 230,000, respectively. Similarly, at a constant number of cycles, the hazard rates increase as stress range increases. For instance, in category A, the hazard rates for S_r values of 30, 36, 42, and 57 ksi are 2.21E-8, 6.31E-8, 1.79E- 8, and 2.18E-6, respectively.

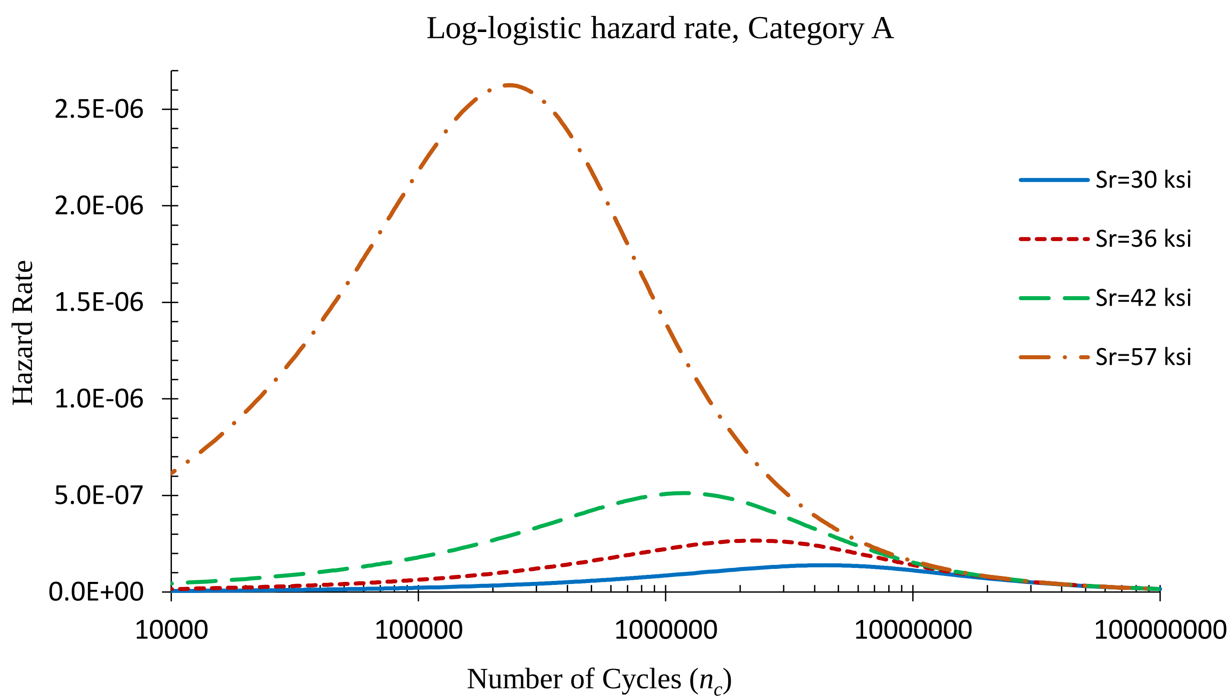

Figure 4.22. Log-logistic AFT hazard rates for Category A analyzed separately

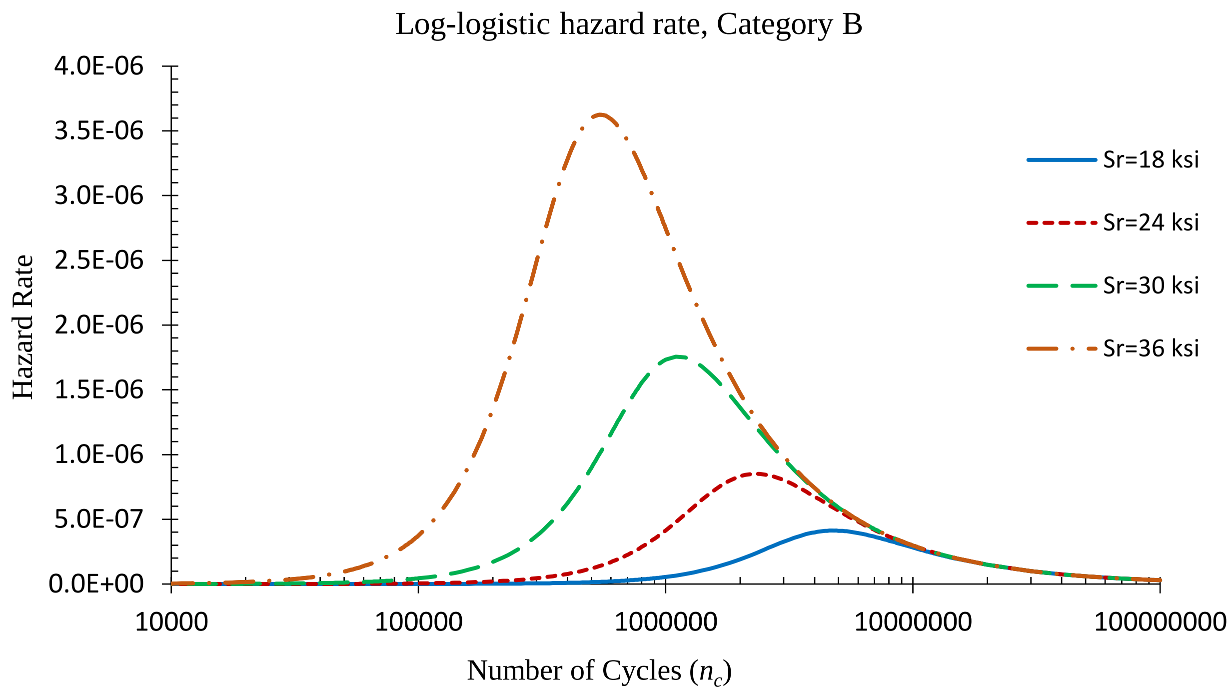

Figure 4.23. Log-logistic AFT hazard rates for Category B analyzed separately

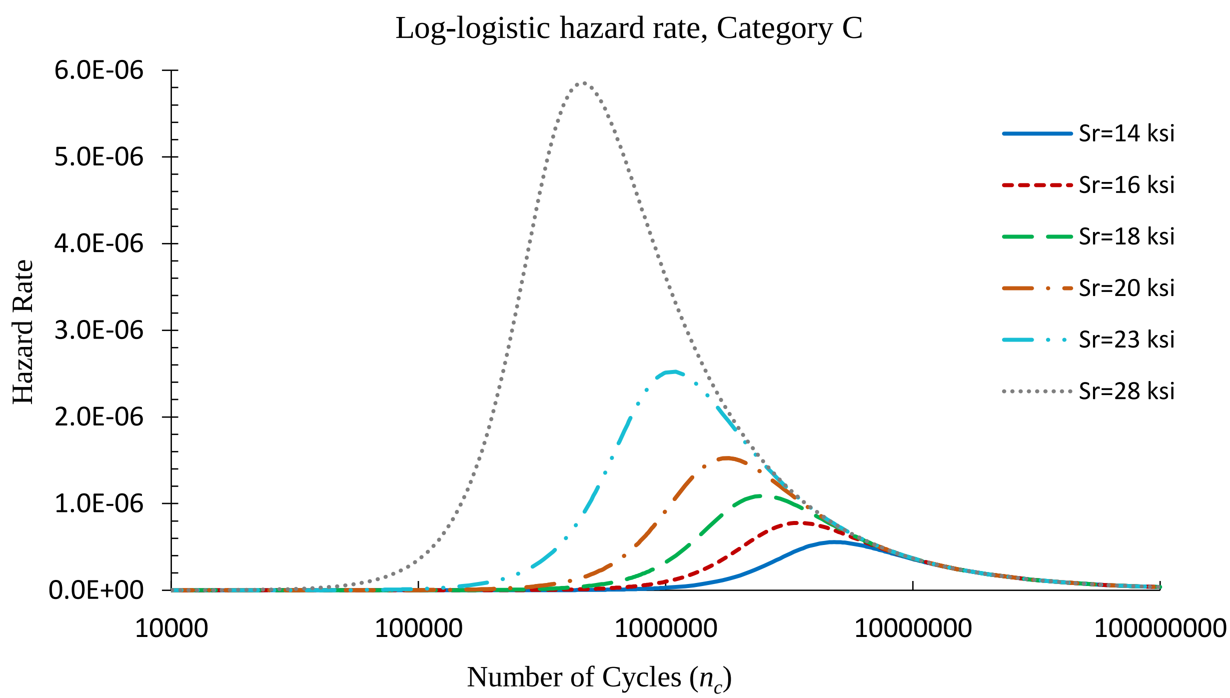

Figure 4.24. Log-logistic AFT hazard rates for Category C analyzed separately

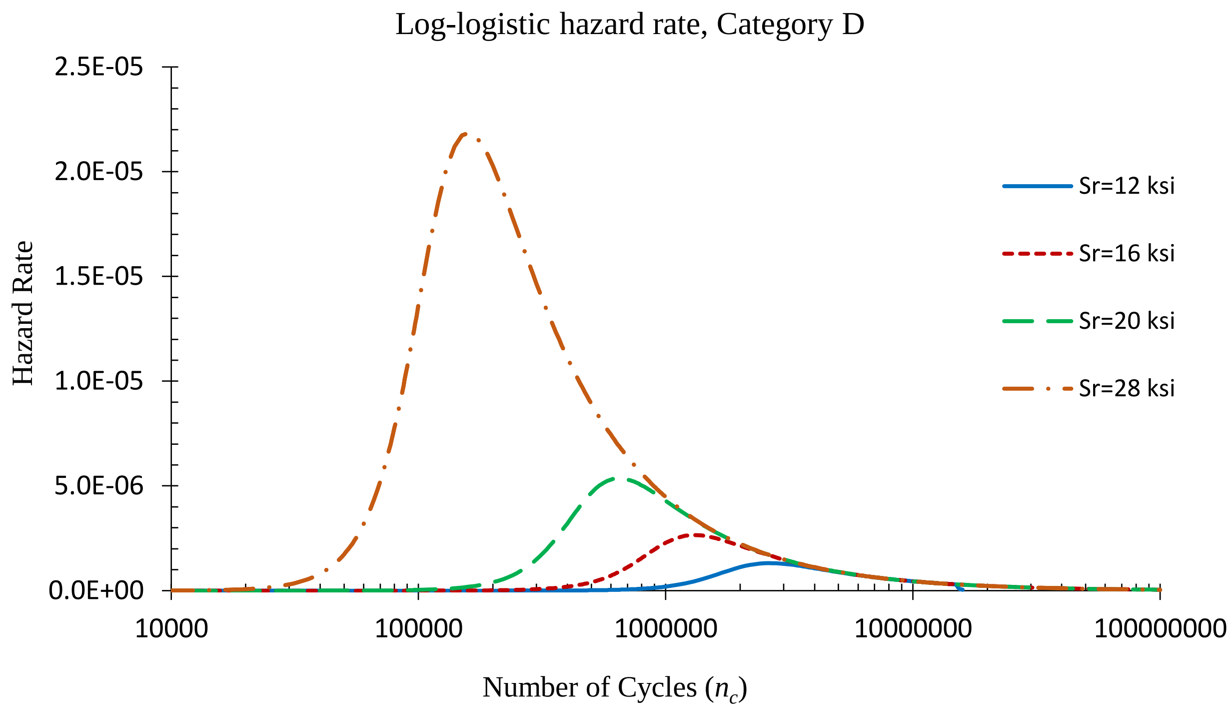

Figure 4.25. Log-logistic AFT hazard rates for Category D analyzed separately

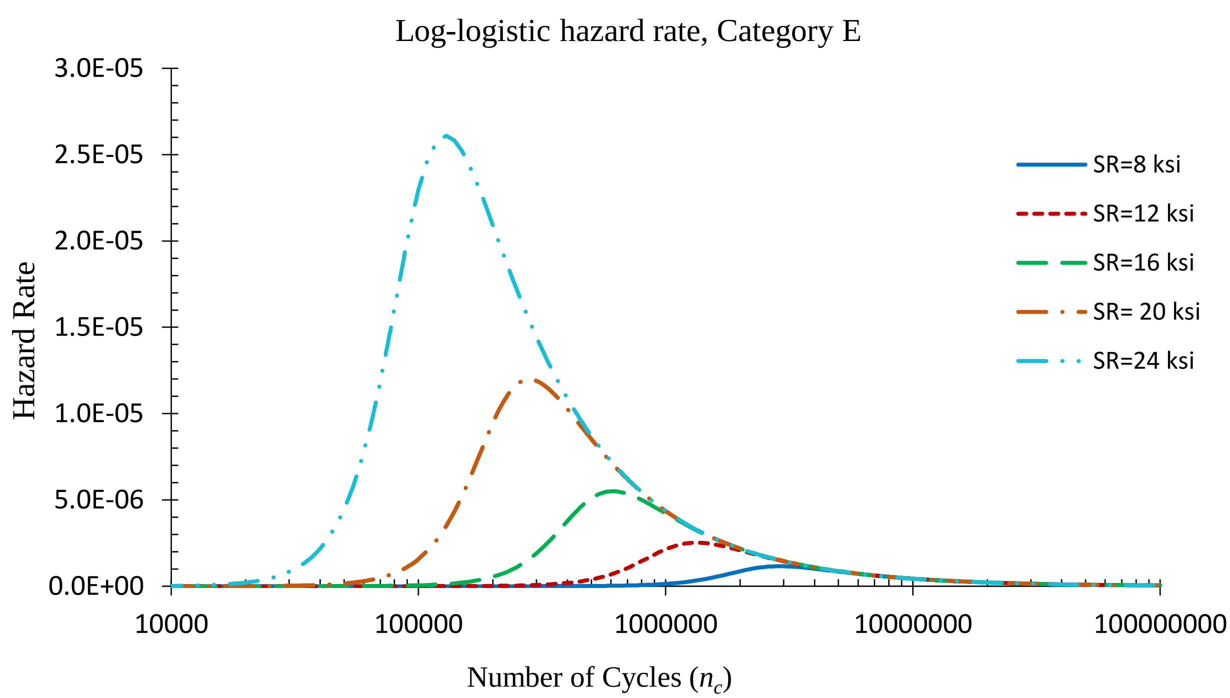

Figure 4.26. Log-logistic AFT hazard rates for Category E analyzed separately

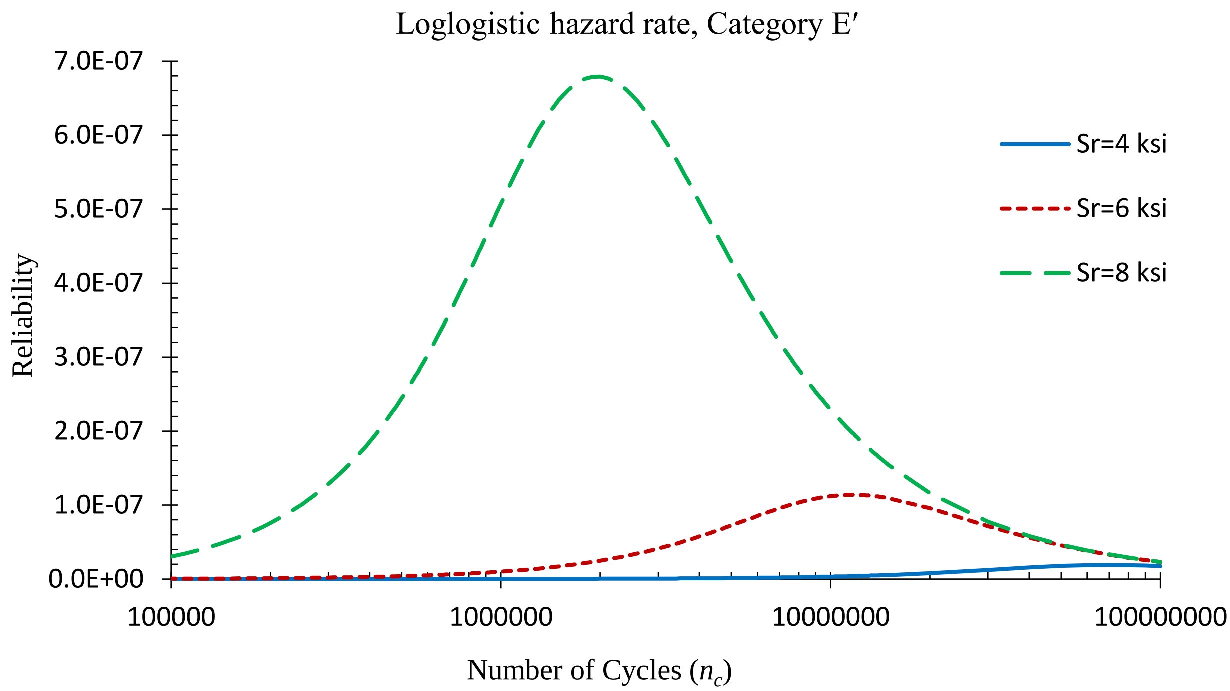

Figure 4.27. Log-logistic AFT hazard rates for Category E′, analyzed separately

Figures 4.27 through 4.32 show the cumulative hazard for different fatigue categories using the K-M and log-logistic AFT models. The cumulative hazard plots are shown at different stress ranges for each fatigue category. As it is evident from these figures, the estimated cumulative hazard using the log-logistic AFT model follows the non-parametric K-M cumulative hazard with good agreement.

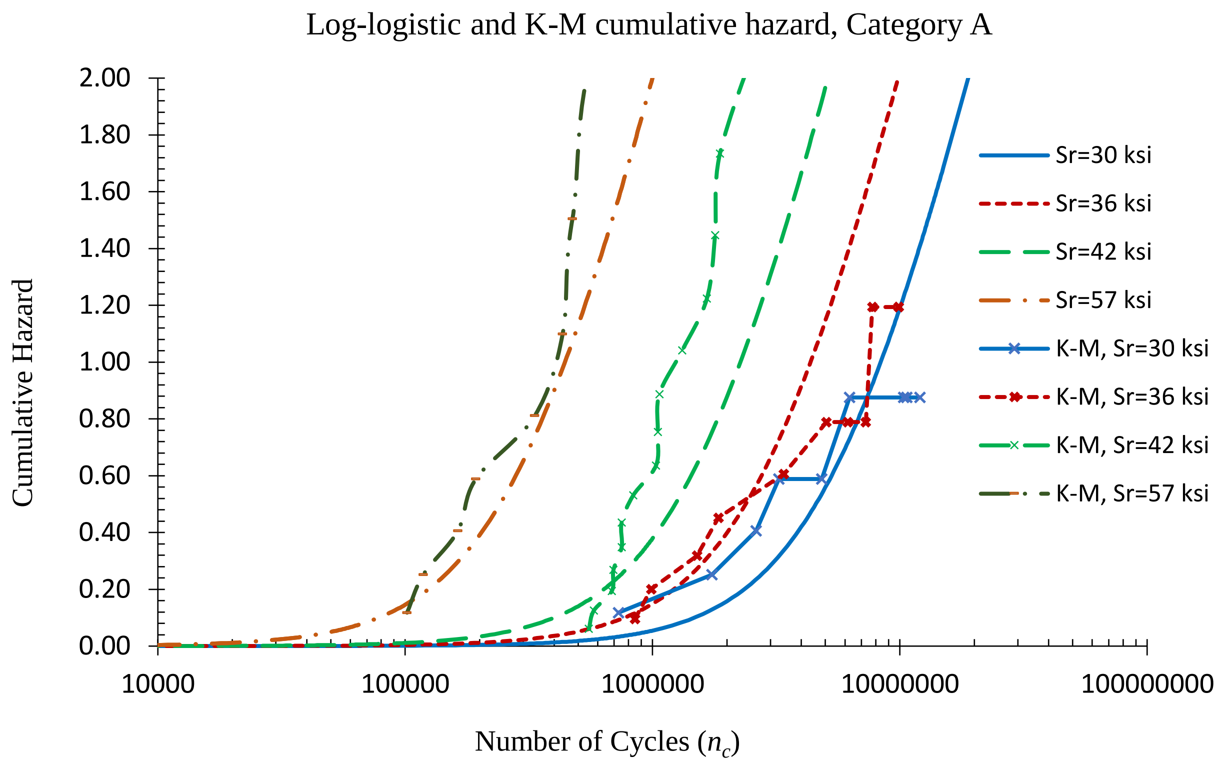

Figure 4.28. Log-logistic AFT and K-M cumulative hazard for Category A analyzed separately

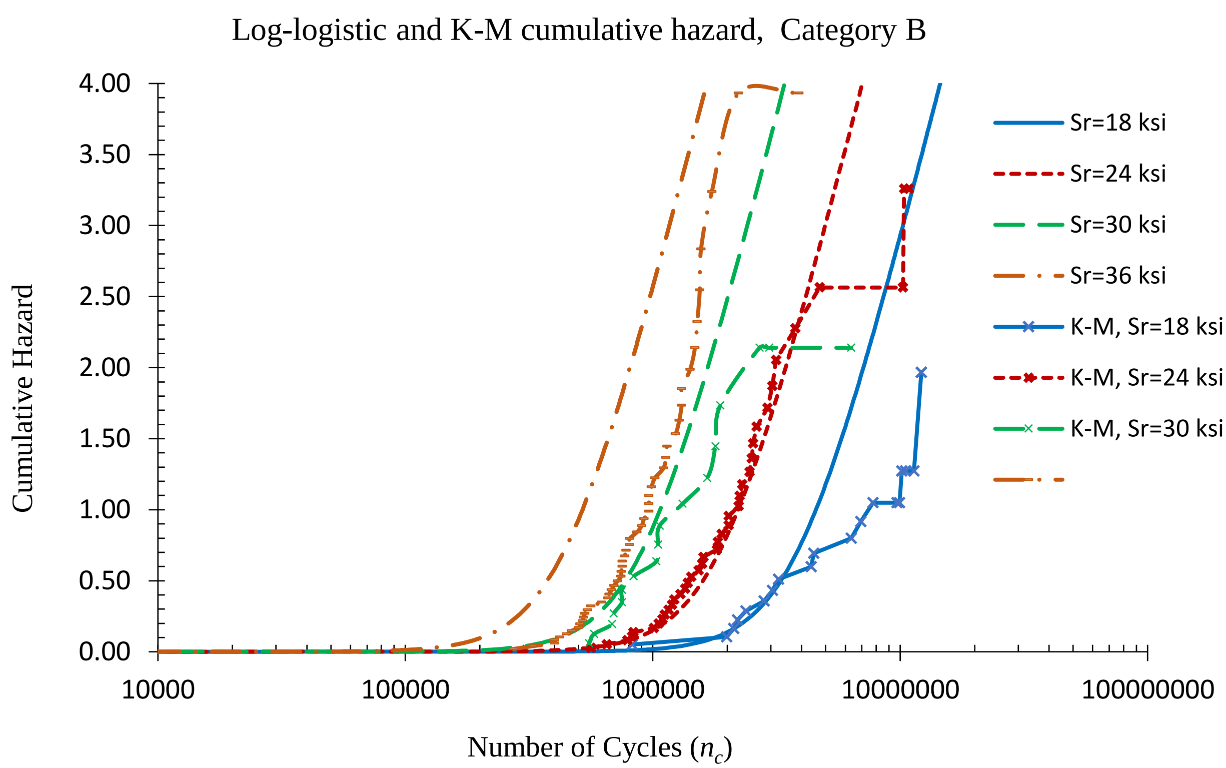

Figure 4.29. Log-logistic AFT and K-M cumulative hazard for Category B analyzed separately

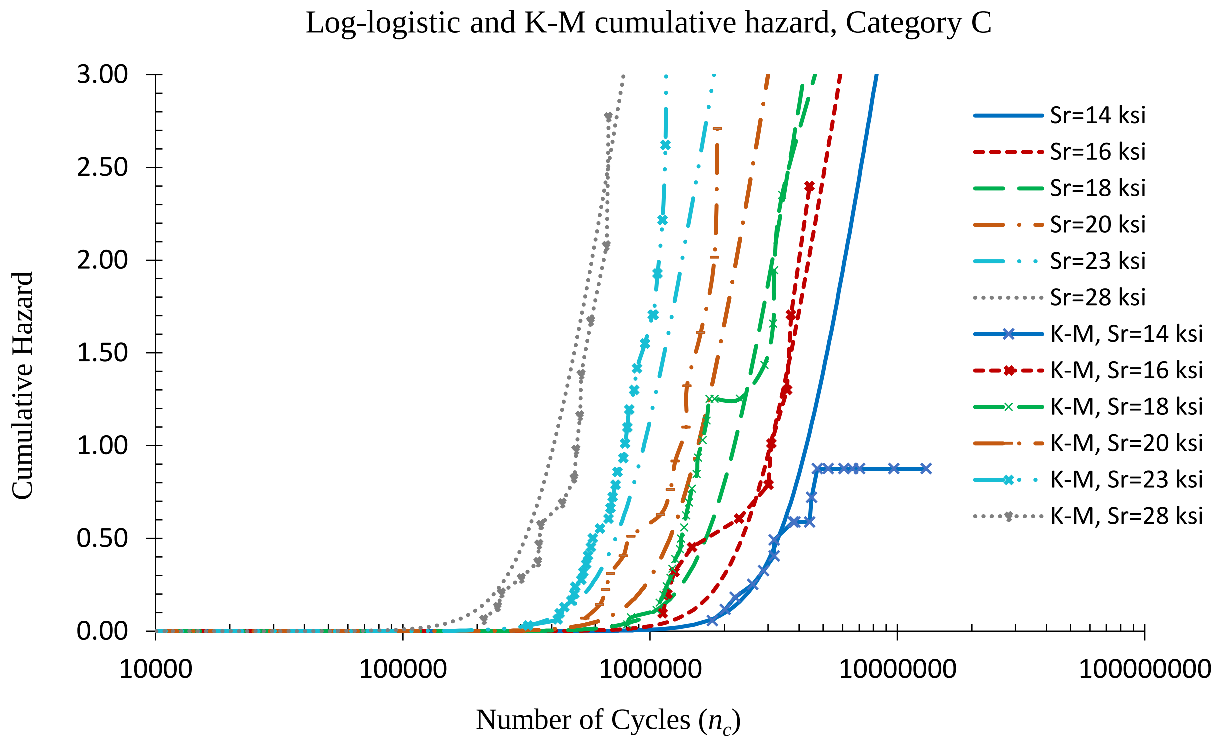

Figure 4.30. Log-logistic AFT and K-M cumulative hazard for Category C analyzed separately

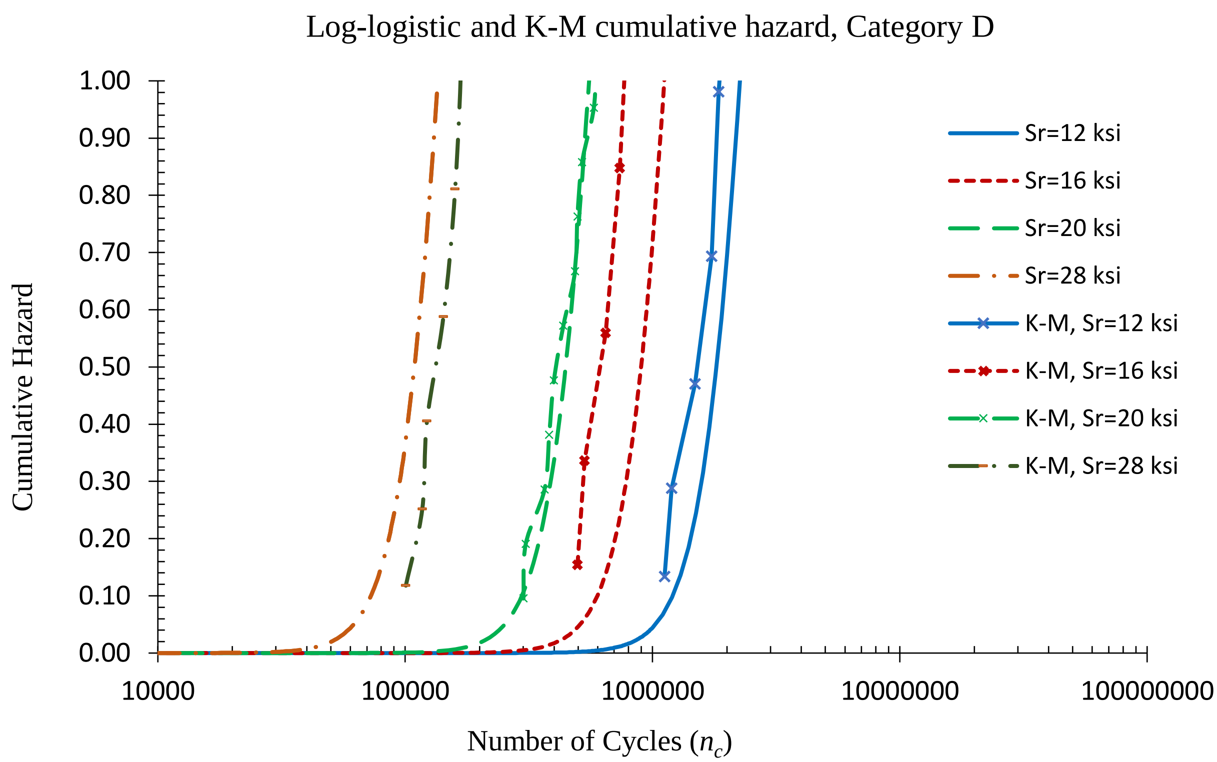

Figure 4.31. Log-logistic AFT and K-M cumulative hazard for Category D analyzed separately

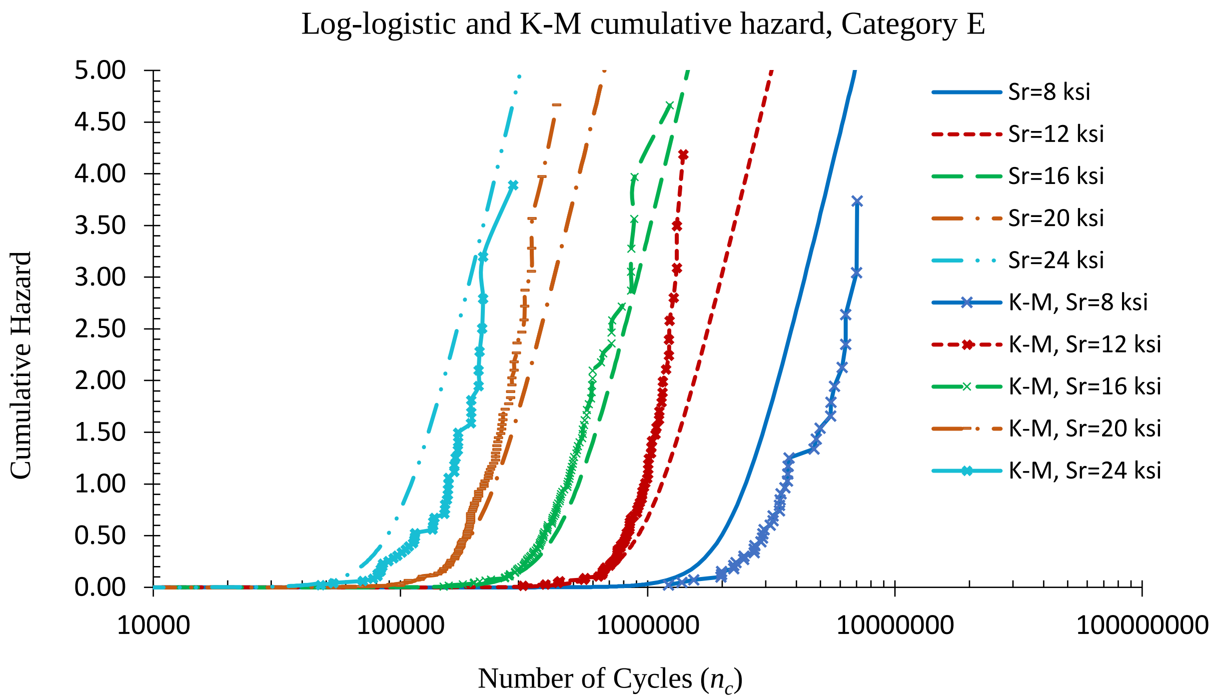

Figure 4.32. Log-logistic AFT and K-M cumulative hazard for Category E analyzed separately

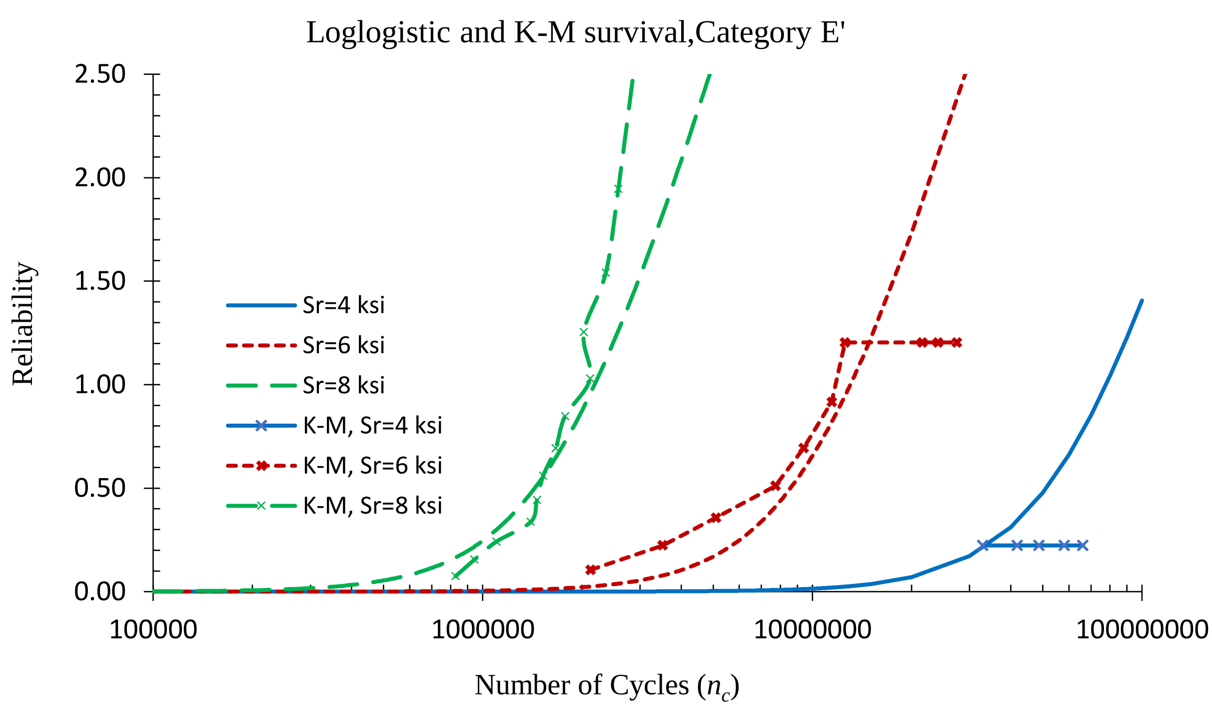

Figure 4.33. Log-logistic AFT and K-M cumulative hazard for Category E′ analyzed separately

4.5. Conditional Survival (*CS*) Analyses for Fatigue

The concept of conditional survival is based on the conditional probability theory. The probability of survival changes as time goes on without failure. The knowledge gained by the fact that failure has not occurred at a particular time changes the probability of survival in the future. The CS concept has experienced significant development and use in the medical field in recent years (Merrill et al., 1999; Kato et al., 2001; Harshman et al., 2001; Wang et al., 2007; Fuller et al., 2007; Chang et al., 2009; Janssen-Heijnen et al., 2010; Xing et al., 2010; Merrill and Hunter, 2010; Zamboni et al., 2010; Parsons et al., 2011; Baade et al., 2011; Yu et al., 2012; Zabor et al., 2013; Hieke et al., 2015). This important concept has generally been neglected in probabilistic remaining service analysis of bridges subjected to fatigue. The *CS* approach can be a powerful tool in probabilistic assessments of the remaining fatigue service life of bridge components after they have been subjected to a history of stress applications without failure. Furthermore, the *CS* approach can provide an important platform for reliability assessments due to cumulative damage (of different stress ranges) including their sequence.

If a component has sustained n_{c1} cycles at a stress range of S_{r1}, what is the probability that it would survive n_{c2} additional cycles at the same stress range (or a different stress range)? After surviving n_{c1} cycles, the information gained from the fact that must be updated to reflect the new knowledge gained. Conditional survival (Equation 3.35) can be used as a measure to estimate remaining number of cycles (n_{c2}) for a given level of reliability (survival), when the component has already survived a specific number of cycles (n_{c1}).

Conditional survival is calculated using Equation 3.35:

$$CS(t, t_s) = \begin{cases} 1\, when & 0 \le t \le t_s \\ \dfrac{S(t)}{S(t_s)} & when\ t > t_s \end{cases}$$

In the example provided above, the *CS* equation for fatigue can be written as:

$$CS(n_c, n_{c1}) = \begin{cases} 1\, when & 0 \le n_c \le n_{c1} \\ \dfrac{S(n_{c1} + n_{c2})}{S(n_{c1})} & when\ n_c > n_{c1} \end{cases}$$

The nc_1 indicates the number of cycles that a component from a particular fatigue category has already survived at a specific stress range. The n_{c2} is the number of cycles that the fatigue prone component can survive (after surviving n_{c1} number of cycles) to achieve a particular survival (probability of failure). The terms $S(n_{c1} + n_{c2})$ and $S(n_{c1})$ can be calculated using Equation 4.3.

A series of *CS* estimates for fatigue categories A, C, and E are calculated and shown in Figs 4.33 through 4.47. These *CS* curves are calculated for different stress ranges and n_{c1} of 10^6, $5X10^5$, and $5X10^5$ cycles for categories A , C and E, respectively. Tables 4.9 through 4.11 list the survival probabilities associated with additional n_{c2} cycles calculated at different stress ranges, for categories A, C, and E, respectively. These tables provide a comparison between the results associated with unconditional/original (*OS*) and conditional (*CS*) survival estimates.

As noted earlier, any additional information obtained from continued survival with future stress applications would alter the conditional survival curves and provide a broader and more accurate perspective of the remaining fatigue life. According to Figures 4.33 through 4.47, the probability of survival (or failure) on updated curves increases (or decreases) as a component survives a specific number of cycles, n_{c1}. For example, *OS* and *CS* survival for fatigue category A at n_{c1} =

$2x10^6$ and S_r = 36 ksi are 0.671 and 0.779, respectively. The "survival dividend" (better prognosis or difference between OS and CS) resulting from continued survival is more noticeable at higher stress ranges. As stress ranges increase, the survival dividend increases. The estimates of such a difference for category A at S_r of 30, 36, 42, and 57 ksi (n_c = $2x10^6$) are 0.048, 0.108, 0.191, and 0.311, respectively. However, at lower stress ranges, the difference between *OS* and *CS* curves would still exist but would not be as significant.

Table 4.13. Unconditional and conditional survival values for category A for different n_c and S_r values

Catg. A	S_r= 30 ksi		S_r = 36 ksi		S_r = 42 ksi		S_r =57 ksi	
n_C	*OS*	*CS*	*OS*	*CS*	*OS*	*CS*	*OS*	*CS*
$2x10^6$	0.854	0.902	0.671	0.779	0.416	0.607	0.049	0.360
$3x10^6$	0.753	0.795	0.515	0.598	0.270	0.395	0.026	0.192
$4x10^6$	0.657	0.694	0.400	0.465	0.189	0.276	0.016	0.122
$5x10^6$	0.572	0.604	0.318	0.369	0.140	0.204	0.012	0.086
$6x10^6$	0.499	0.527	0.258	0.299	0.108	0.158	0.009	0.064
$7x10^6$	0.437	0.462	0.213	0.248	0.086	0.126	0.007	0.050
$8x10^6$	0.385	0.407	0.179	0.208	0.071	0.103	0.005	0.040
$9x10^6$	0.341	0.360	0.153	0.178	0.059	0.087	0.005	0.033
10^7	0.304	0.321	0.132	0.154	0.051	0.074	0.004	0.028

Table 4.14. Unconditional and conditional survival values for category C at different n_c and S_r values

Catg. C	S_r = 14 ksi		S_r = 18 ksi		S_r = 23 ksi		S_r = 28 ksi	
N_C	*OS*	*CS*	*OS*	*CS*	*OS*	*CS*	*OS*	*CS*
$6x10^5$	0.999	0.999	0.986	0.993	0.756	0.880	0.122	0.570
$7x10^5$	0.998	0.998	0.975	0.982	0.637	0.742	0.073	0.341
$8x10^5$	0.997	0.997	0.960	0.967	0.517	0.602	0.046	0.214
$9x10^5$	0.995	0.995	0.939	0.946	0.410	0.477	0.030	0.141
10^6	0.992	0.993	0.913	0.920	0.320	0.372	0.021	0.096

Table 4.15. Unconditional and conditional survival values for category E at different n_c and S_r values

Catg. E	S_r = 8 ksi		S_r = 12 ksi		S_r = 16 ksi		S_r = 20 ksi		S_r = 24 ksi	
N_C	*OS*	*CS*	*OS*	*CS*	*OS*	*CS*	*OS*	*CS*	*OS*	*CS*
$6x10^5$	0.998	0.998	0.906	0.948	0.244	0.585	0.011	0.457	0.0004	0.451
$7x10^5$	0.993	0.995	0.831	0.870	0.141	0.339	0.005	0.235	0.0002	0.230
$8x10^5$	0.988	0.990	0.733	0.767	0.084	0.202	0.003	0.131	0.0001	0.129
$9x10^5$	0.980	0.982	0.622	0.651	0.052	0.125	0.0018	0.079	0.0001	0.077
10^6	0.969	0.970	0.509	0.533	0.034	0.080	0.001	0.050	0.0000	0.049

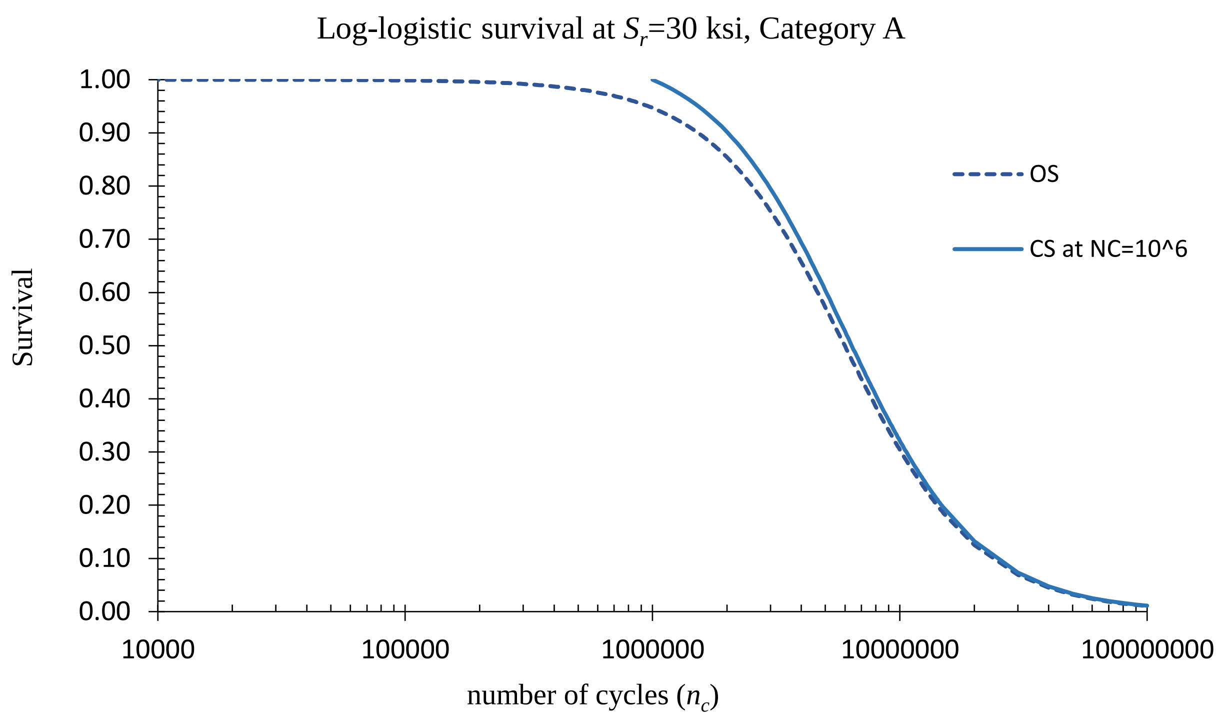

Figure 4.34. Log-logistic unconditional survival (*OS*) versus conditional survival (*CS*) of fatigue category A at S_r=30 ksi

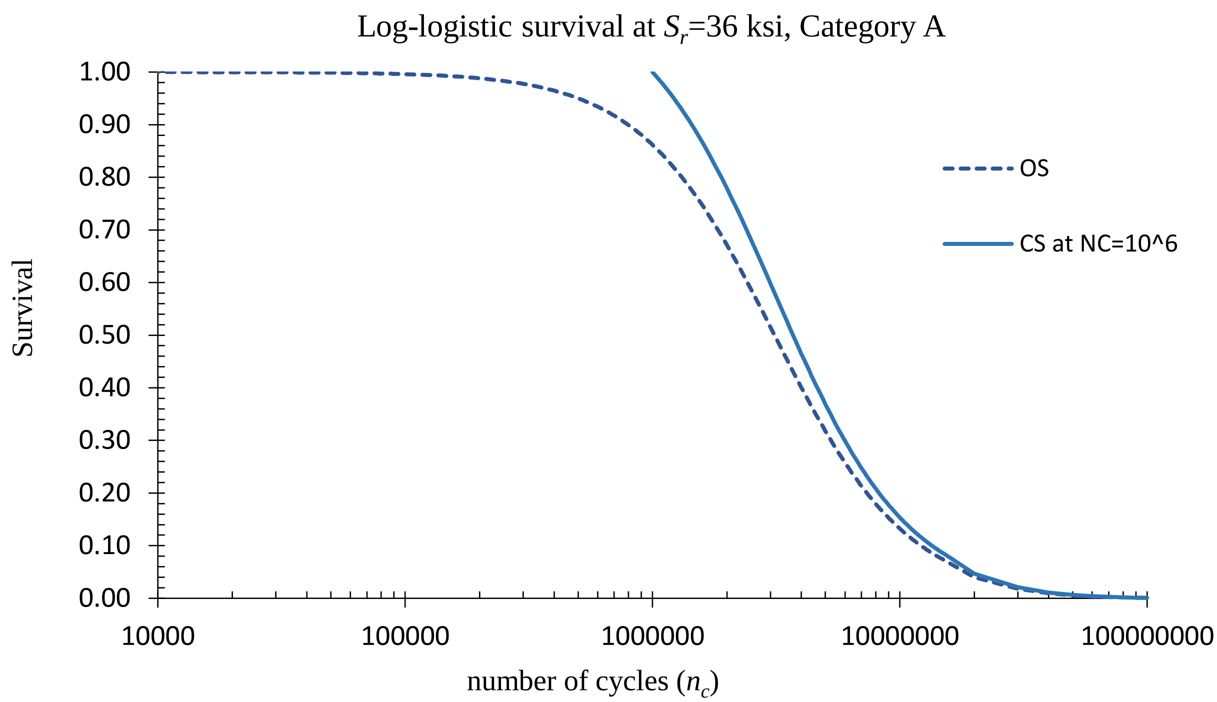

Figure 4.35. Log-logistic unconditional survival (OS) versus conditional survival (CS) of fatigue category A at Sr=36 ksi

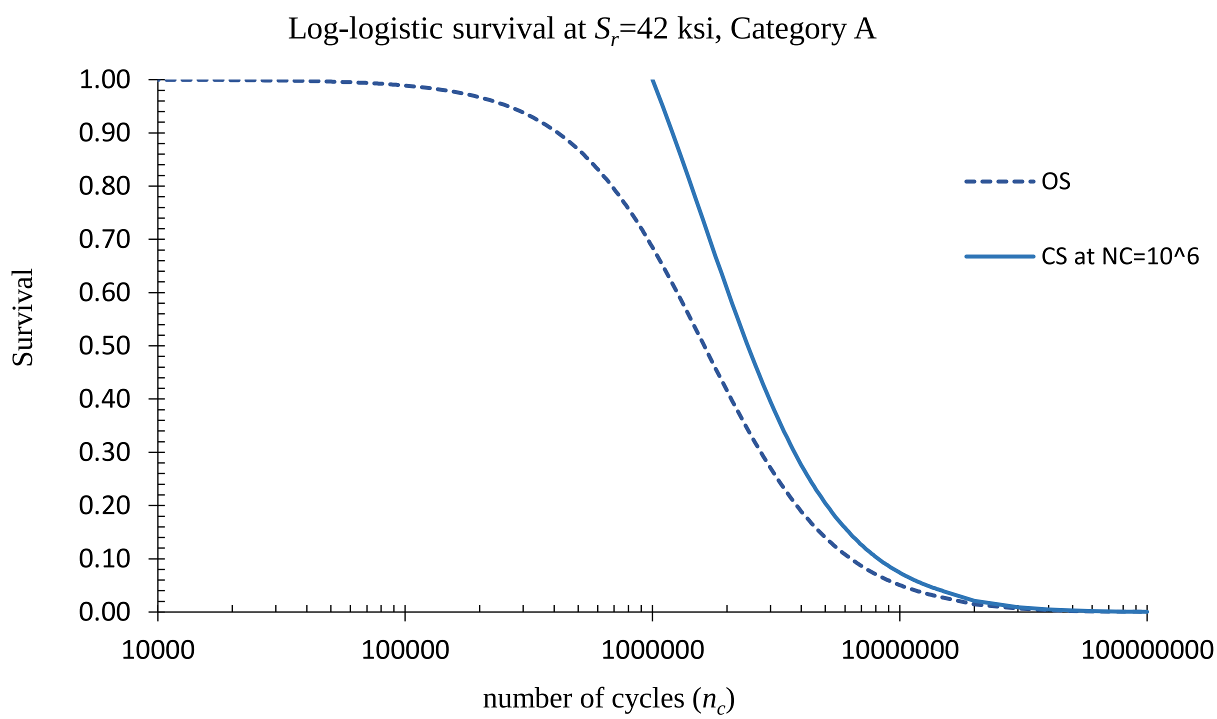

Figure 4.36. Log-logistic unconditional survival (*OS*) versus conditional survival (*CS*) of fatigue category A at S_r=42ksi

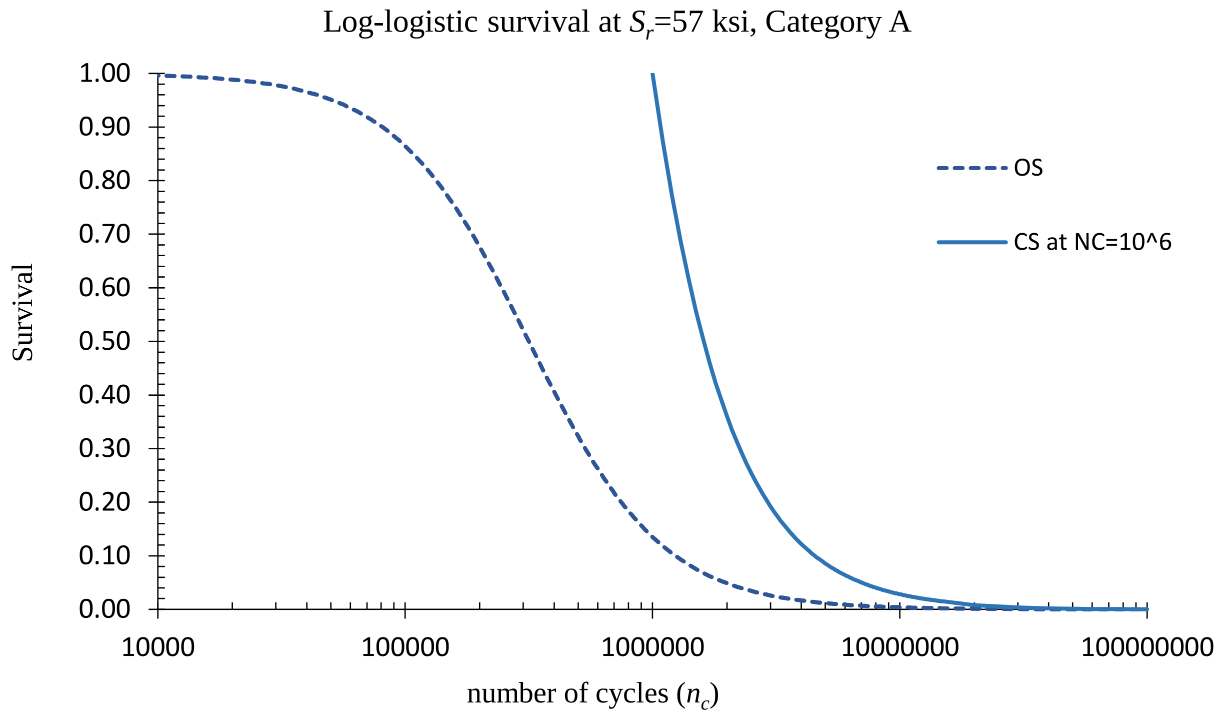

Figure 4.37. Log-logistic unconditional survival (OS) versus conditional survival (CS) of fatigue category A at S_r=57 ksi

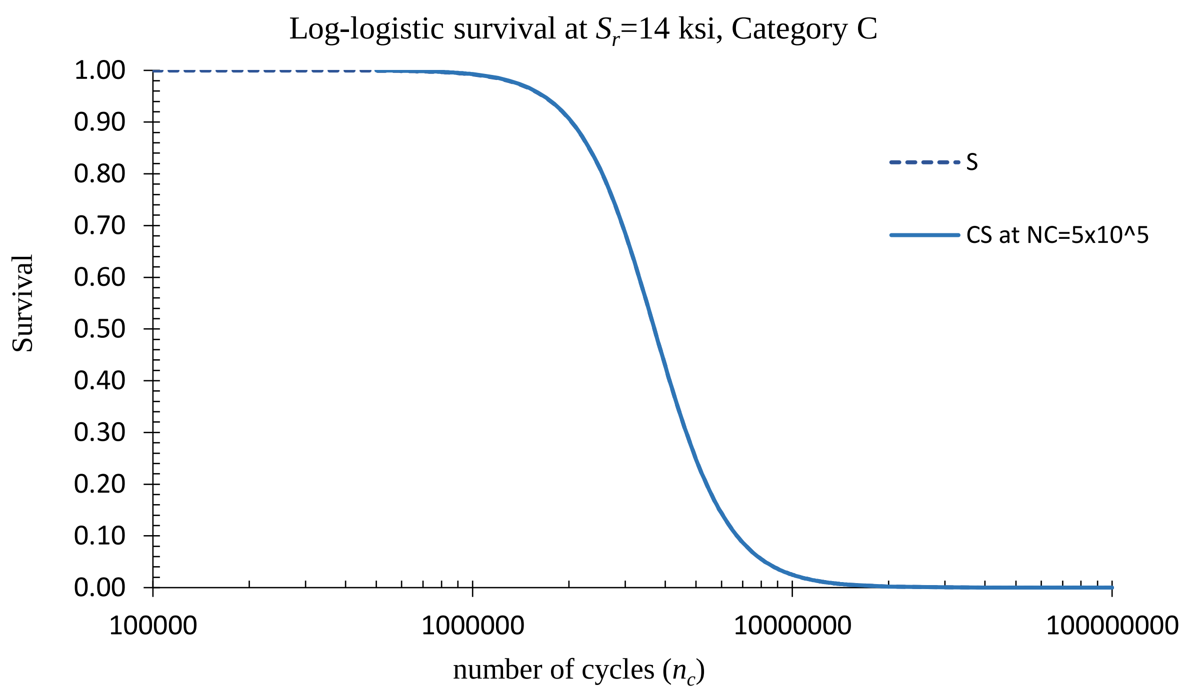

Figure 4.38. Log-logistic unconditional survival (OS) versus conditional survival (CS) of fatigue category C, at S_r=14 ksi

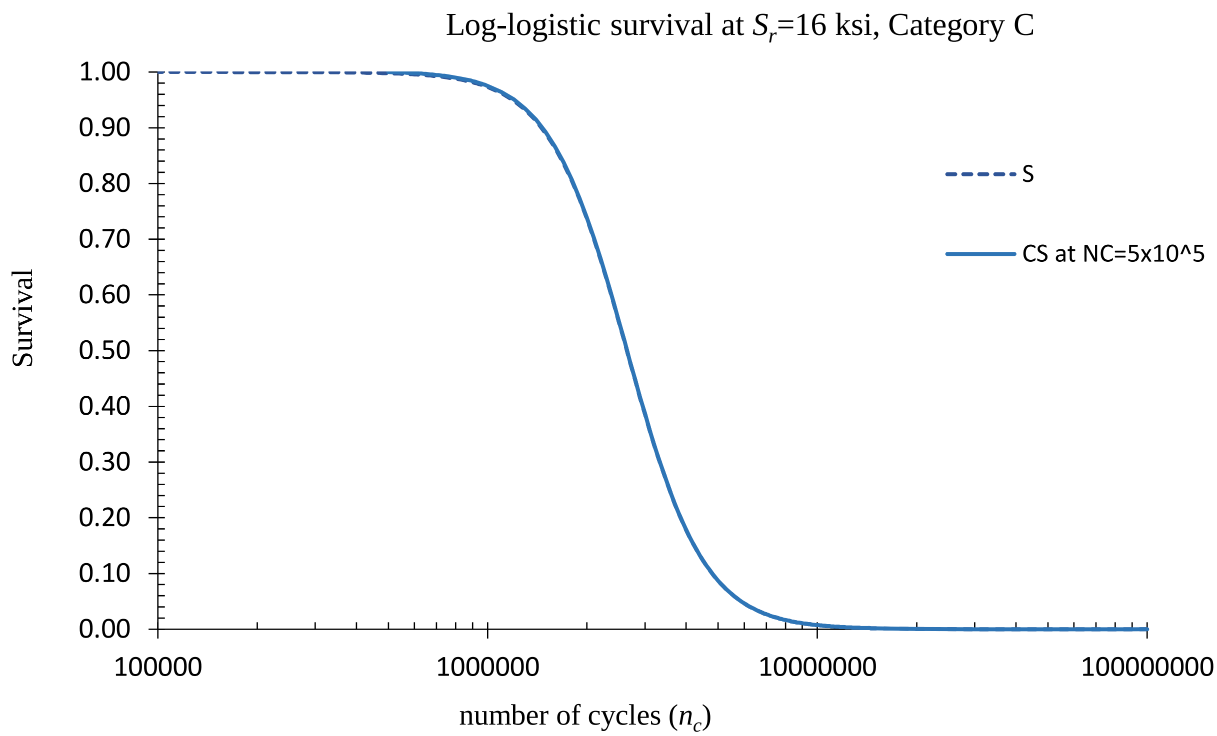

Figure 4.39. Log-logistic unconditional survival (OS) versus conditional survival (CS) of fatigue category C, at S_r=16 ksi

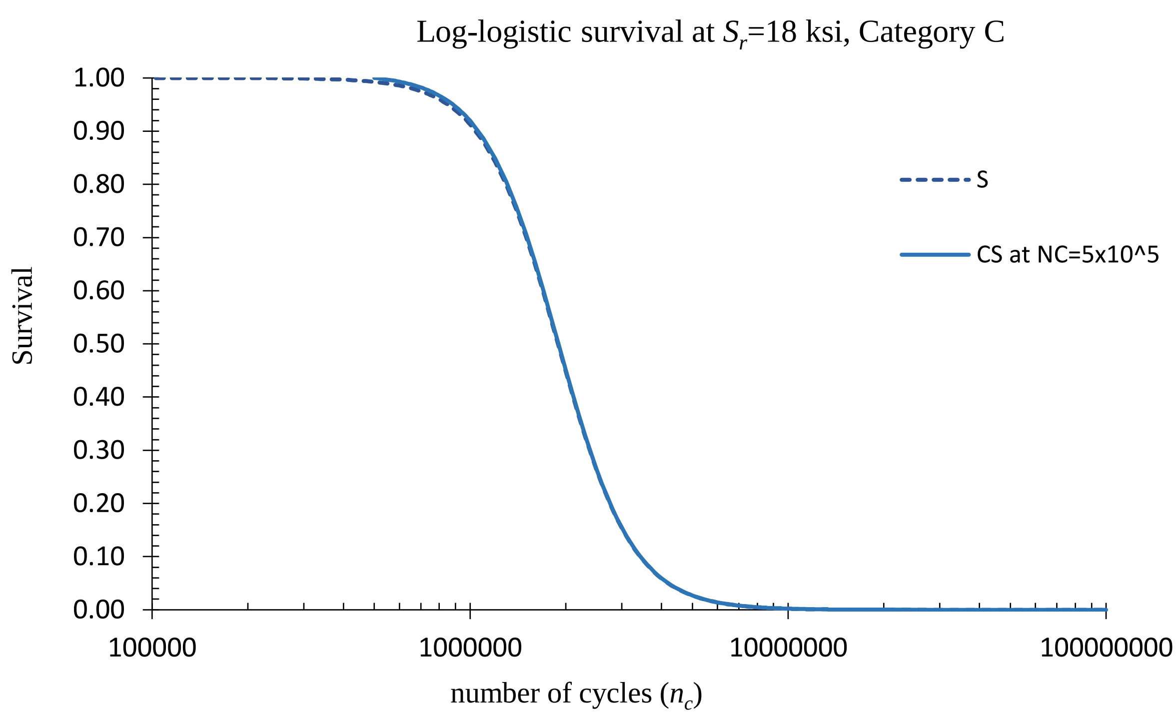

Figure 4.40. Log-logistic unconditional survival (OS) versus conditional survival (CS) of fatigue category C, at S_r=18 ksi

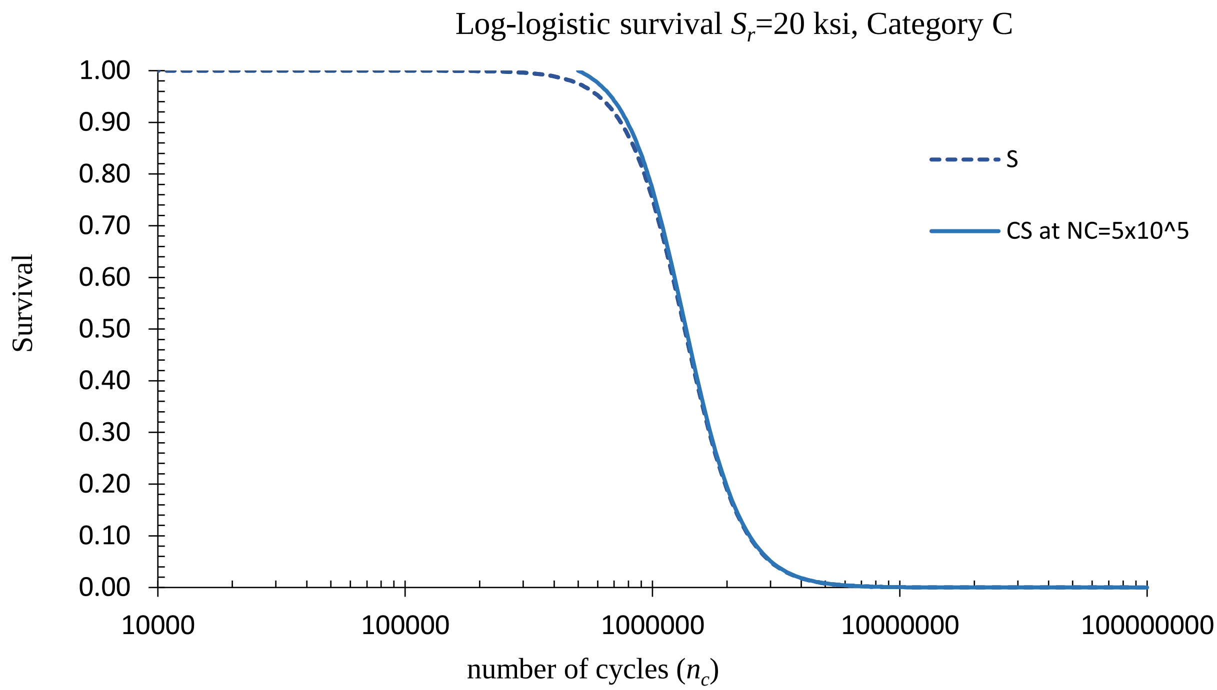

Figure 4.41. Log-logistic unconditional survival (S) versus conditional survival (CS) of fatigue category C, at S_r=20 ksi

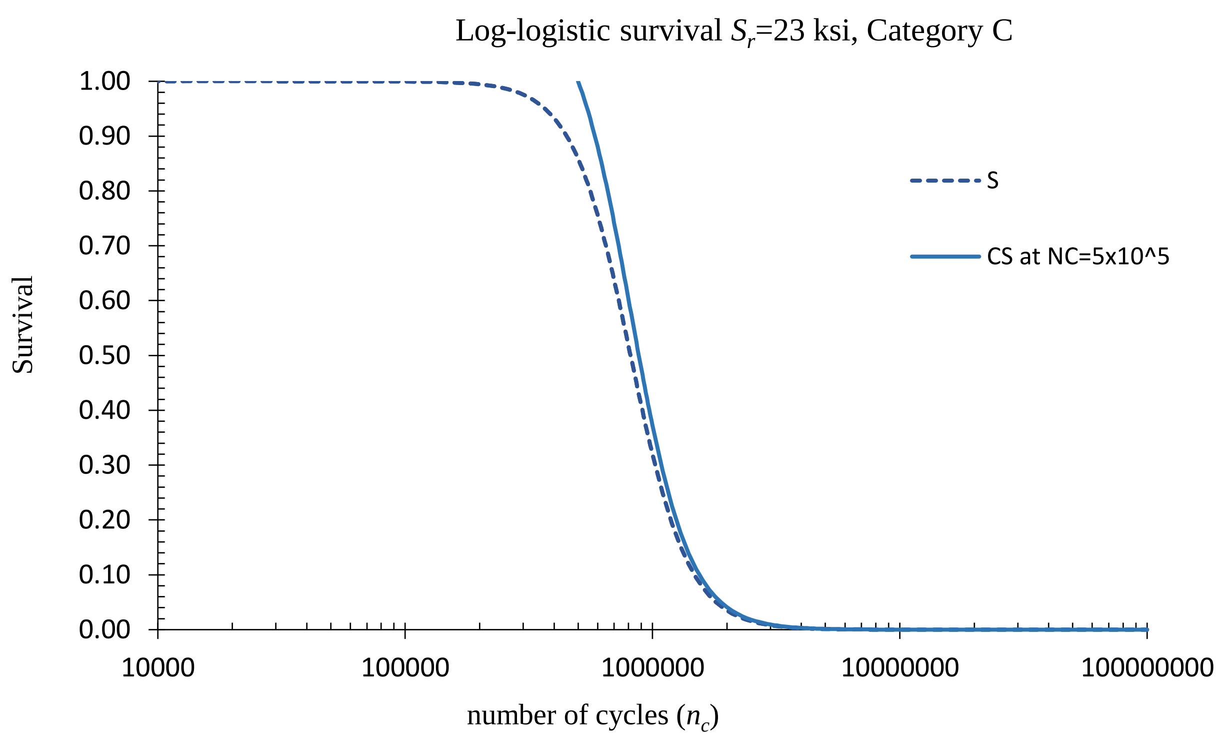

Figure 4.42. Log-logistic unconditional survival (S) versus conditional survival (CS) of fatigue category C, at S_r=23 ksi

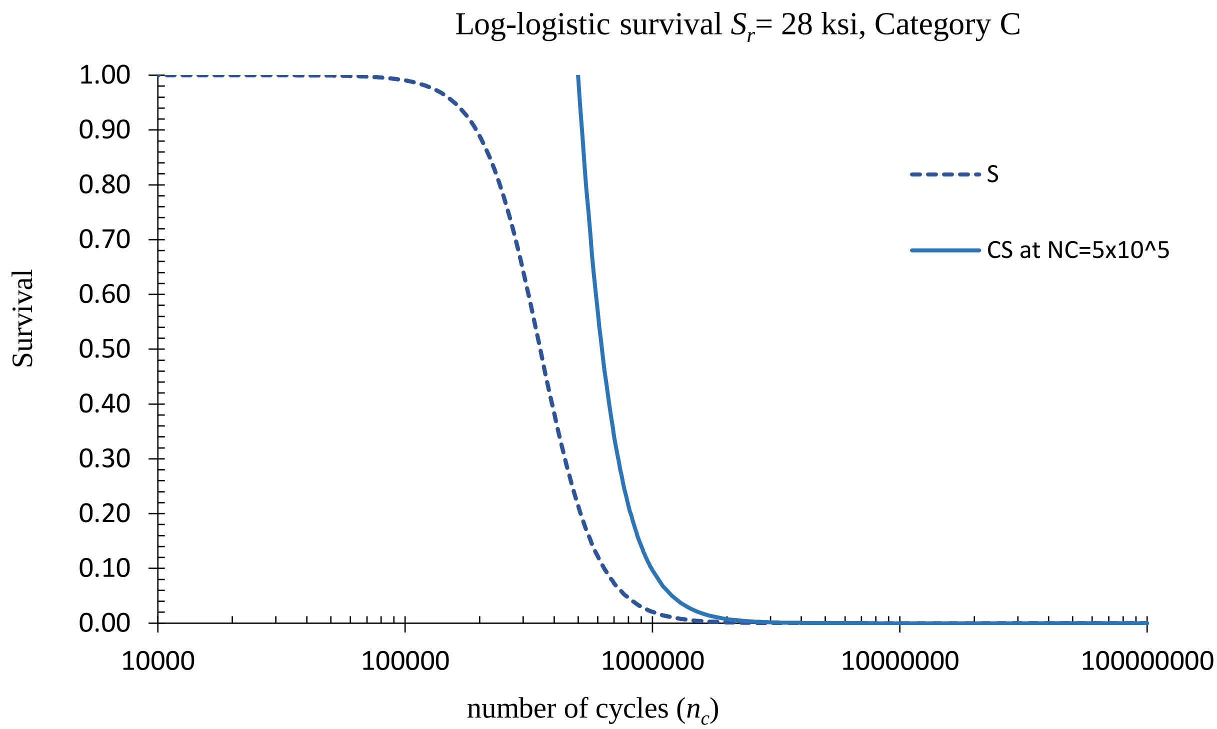

Figure 4.43. Log-logistic unconditional survival (S) versus conditional survival (CS) of fatigue category C, at S_r=28 ksi

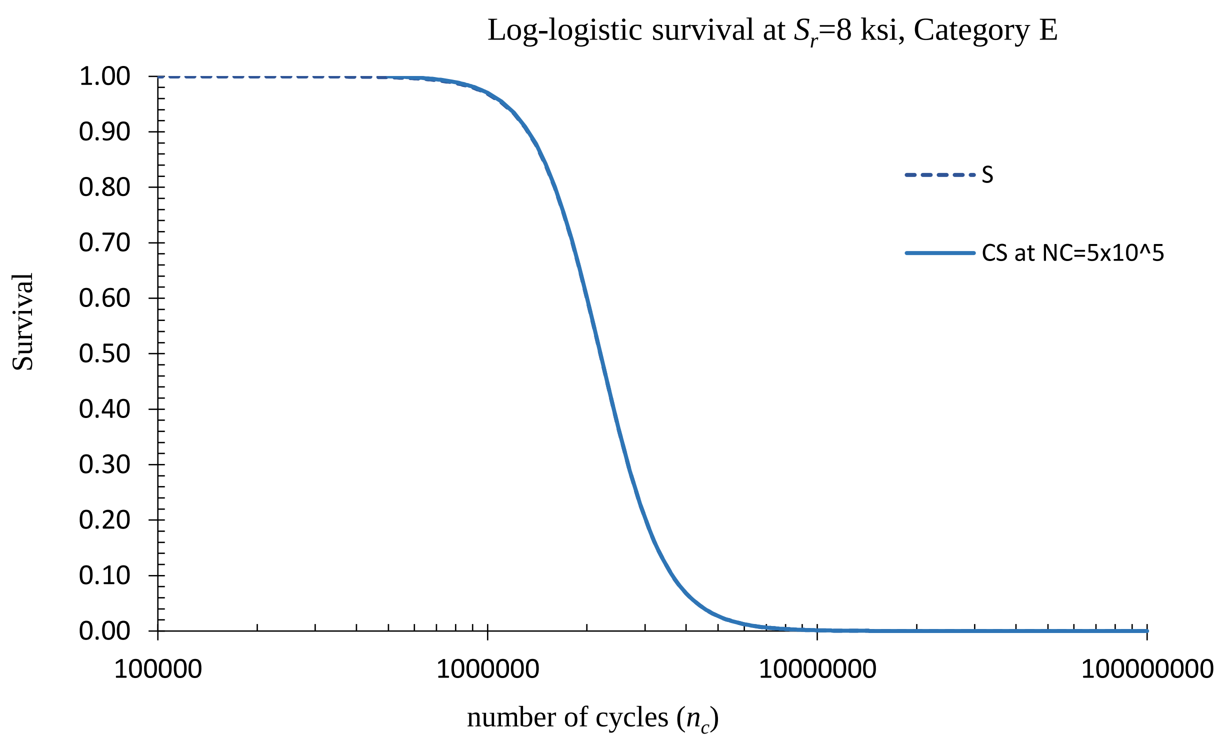

Figure 4.44. Log-logistic unconditional survival (S) versus conditional survival (CS) of fatigue category E, at S_r=8 ksi

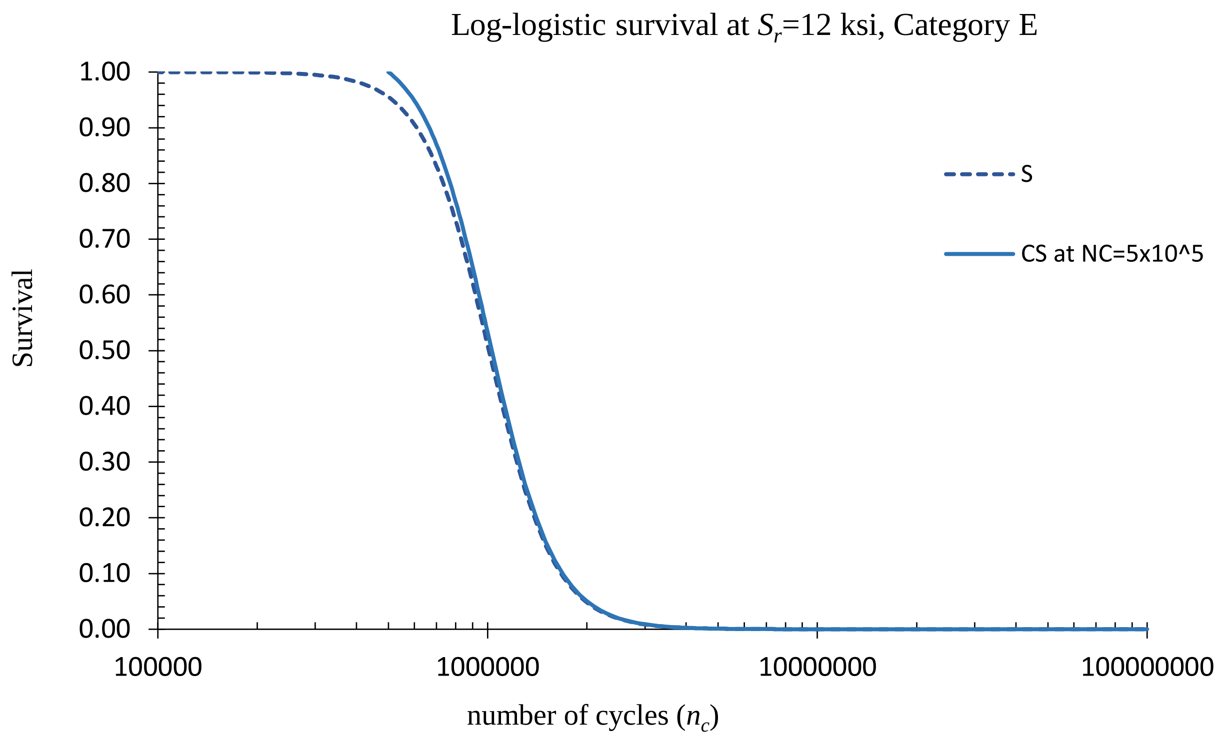

Figure 4.45. Log-logistic unconditional survival (S) versus conditional survival (CS) of fatigue category E, at S_r=12 ksi

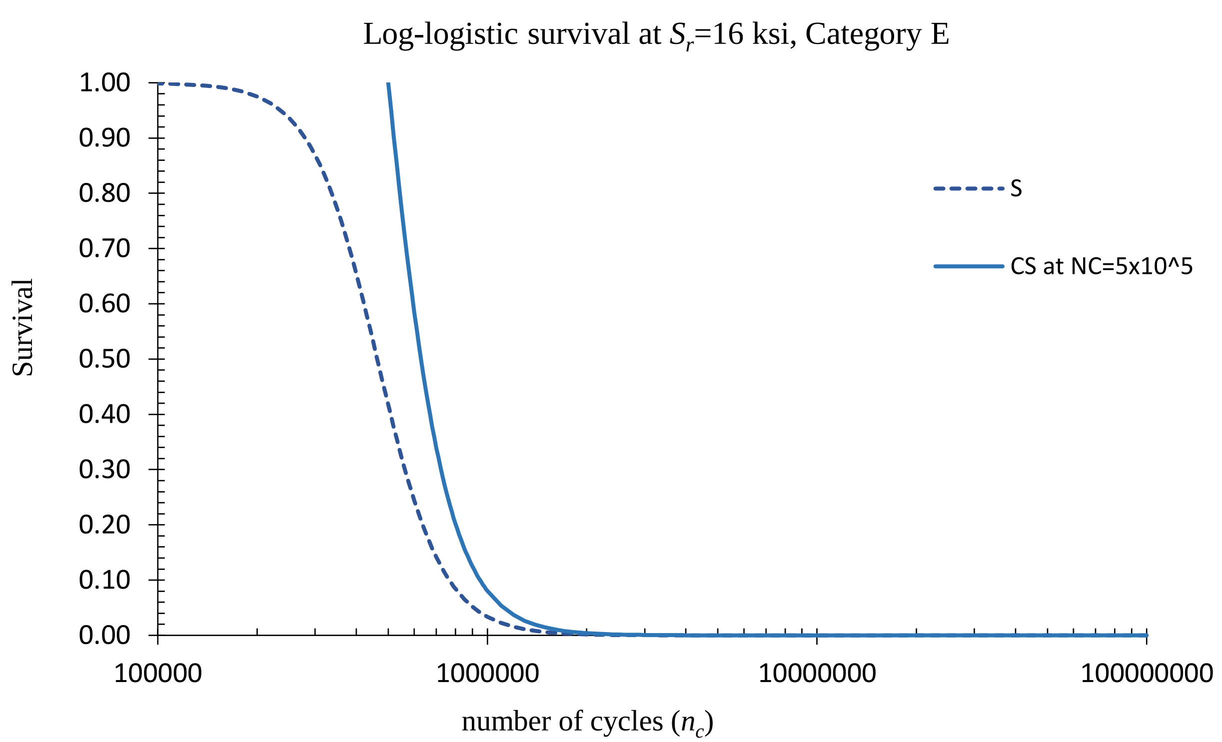

Figure 4.46. Log-logistic unconditional survival (S) versus conditional survival (CS) of fatigue category E, at S_r=16 ksi

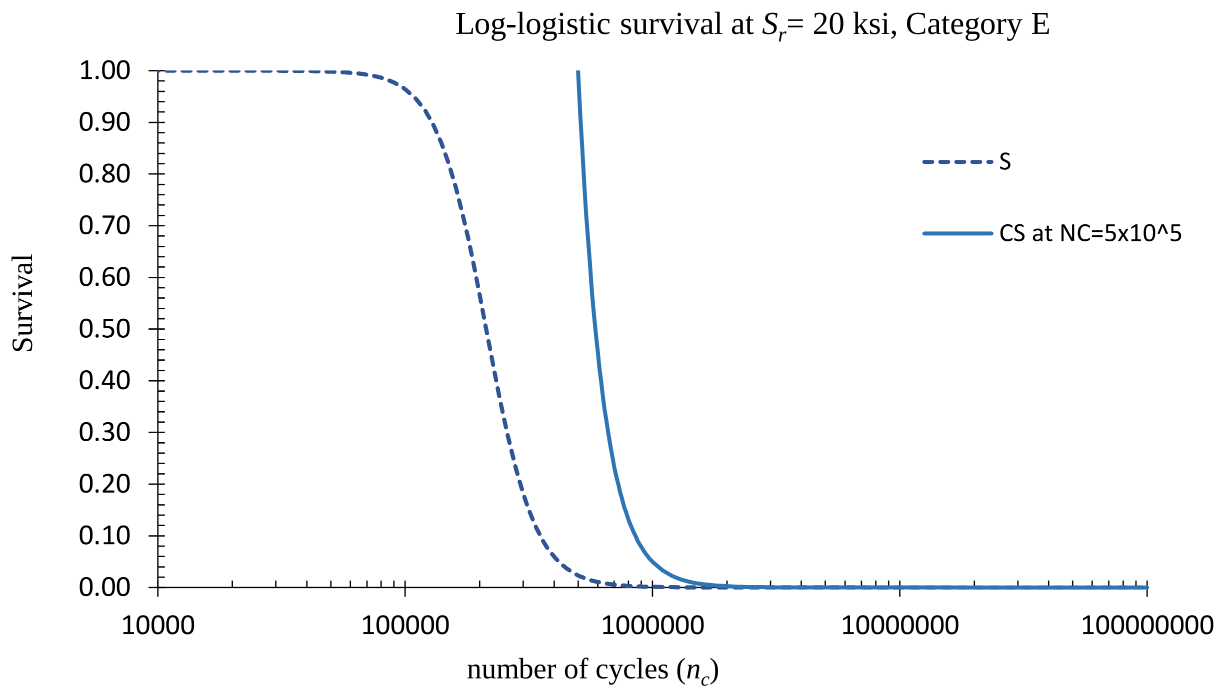

Figure 4.47. Log-logistic unconditional survival (S) versus conditional survival (CS) of fatigue category E, at S_r=20 ksi

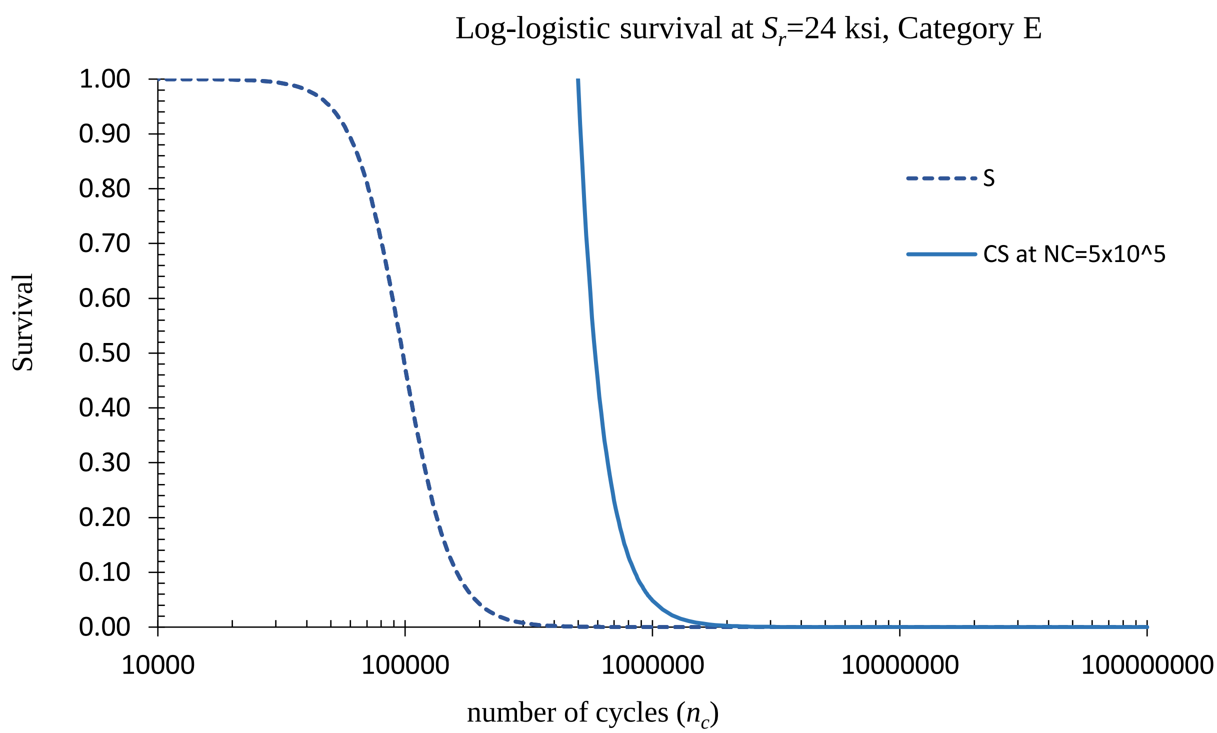

Figure 4.48. Log-logistic unconditional survival (S) versus conditional survival (CS) of fatigue category E, at S_r=24 ksi

4.5.1. Example:

Consider a bridge connection detail (category C) under tension and compressive stresses of 20 ksi (±20 ksi). Determine the following:

a) probability of survival (reliability) at $0.5X10^6$ number of cycles?

b) probability of (unconditional) survival at 10^6 number of cycles?

c) Assuming the bridge connection already survived $0.5X10^6$ number of cycles, determine the probability of surviving (conditional survival) another $0.5X10^6$ number of cycles?

d) Estimate the survival dividend, the difference between unconditional and conditional survival, at 10^6 number of cycles?

Solution:

a) According to Eqs. 4.3 and using calculated parameters for fatigue category C, shown in Table 4.4:

α= 3.87952 β= 3.69204 θ_1= 0.16813 θ_2= -9.21465

<u>Probability of survival at S_r= 20 ksi and $n_c = 0.5X10^6$:</u>

$$n_{cg} = \frac{n_c}{1000}.\exp(S_r.\theta_1 + \theta_2) = \frac{0.5 * 10^6}{1000}\exp(20 * 0.16813 + -9.21465) = 1.437$$

$$S(n_{cg}) = \frac{1}{1 + (n_{cg}/\alpha)^\beta} = \frac{1}{1 + \left({1.437}/{3.87952}\right)^{3.69204}} = 0.975$$

Therefore, the probability of survival at $5X10^6$ is 97.5%.

b) Similarly, probability of survival at S_r= 20 ksi and $n_c = 10^6$ would be calculated as:

$$n_{cg} = \frac{n_c}{1000}.\exp(S_r.\theta_1 + \theta_2) = \frac{10^6}{1000}\exp(20 * 0.16813 + -9.21465) = 2.874$$

$$S(n_{cg}) = \frac{1}{1+(n_{cg}/\alpha)^{\beta}} = \frac{1}{1+\left({}^{2.874}/_{3.87952}\right)^{3.69204}} = 0.751$$

c) The conditional survival can be calculated through Equation 3.35, as following:

$$CS(n_c, n_{c1}) = \begin{cases} 1\ when & 0 \le n_c \le n_{c1} \\ \dfrac{S(n_{c1}+n_{c2})}{S(n_{c1})} & when\ n_c > n_{c1} \end{cases}$$

$$CS(10^6, 5X10^6) = \frac{S(0.5X10^6 + 0.5X10^6)}{S(0.5X10^6)} = \frac{0.751}{0.975} = 0.770$$

Chapter 5. Proposed Fatigue Reliability Equations and Their Application to AASHTO Fatigue Curves

This Chapter includes a proposed set of survival equations developed for probabilistic reliability assessments of fatigue resistance in steel structures considering various detail categories and stress ranges. These equations are based on a log-logistic AFT survival model that was derived using the same fatigue test data that is the basis of the current AASHTO bridge design specifications. Furthermore, using these survival models, the level of reliability (probability of survival) associated with the various points located on the current AASHTO fatigue design curves are assessed for all fatigue categories. This is meant to assess the consistency of probability of survival (or failure) associated with the design fatigue curves for each category as well as across all different categories. In addition, a set of equations are derived (based on the developed log-logistic survival model) to determine the number of cycles needed to reach any level of reliability (of fatigue resistance) for any specific stress range. Similarly, an equation is proposed to determine the stress range that would result in a particular level of reliability for any given number of stress cycles.

5.1. Proposed Equation for Consistent Fatigue Reliability

Survival functions for log-logistic AFT model were introduced in section 4.3 of this study. Equation 4.3 computes the probability of survival (reliability with respect to fatigue resistance) as a function of the number of cycles applied. An equation for calculating the fatigue life at any particular level of reliability and any stress range is derived in this section based on the developed survival model. The proposed equation can be used to generate a fatigue design curve that would result in a uniform level of reliability for different values of n_c and S_r. The proposed equation is derived as a function of the number of cycles, S_r, and the required level of reliability (S_{req}) using the following steps:

$$S(n_{cg}) = \frac{1}{1 + (n_{cg}/\alpha)^{\beta}} \qquad \text{Equation 4.4}$$

If $S(n_{cg})$ is kept at a constant level of reliability, S_{req}, then:

$$S_{req}.(1 + (n_{cg}/\alpha)^{\beta}) = 1 \qquad \text{Equation 5.1}$$

Multiplying both sides by α^{β}:

$$S_{req}.\alpha^{\beta} + S_{req}.n_{cg}^{\beta} = \alpha^{\beta} \qquad \text{Equation 5.2}$$

Solving Equation 5.2 for n_{cg}^{β} results in:

$$n_{cg}^{\beta} = \frac{\alpha^{\beta}(1 - S_{req})}{S_{req}} \qquad \text{Equation 5.3}$$

Or,

$$n_{cg} = \left(\frac{\alpha^{\beta}(1 - S_{req})}{S_{req}}\right)^{1/\beta} \qquad \text{Equation 5.4}$$

Substituting for $n_{cg} = \frac{n_c}{1000}.exp(S_r.\theta_1 + \theta_2)$ in Equation 5.4, the number of cycles associated with a specific level of reliability and stress range can be calculated as:

$$n_c(S_{req}, S_r) = 1000\left(\frac{\alpha^{\beta}(1 - S_{req})}{S_{req}}\right)^{1/\beta} e^{-(S_r.\theta_1 + \theta_2)} \qquad \text{Equation 5.5}$$

Similarly, Equation 5.5 can be rewritten to determine S_r as a function of the probability of survival (S_{req}) and number of cycles (n_c) in the following form:

$$S_r(S_{req}, n_c) = \left[\ln \left(\frac{\left(\frac{\alpha^\beta (1 - S_{req})}{S_{req}} \right)^{1/\beta}}{0.001 n_c} \right) - \theta_2 \right] / \theta_1 \qquad \text{Equation 5.6}$$

The S_{req} is a chosen probability of survival. The parameters α, β, θ_1, and θ_2 were calculated using maximum log-likelihood estimation, as discussed in previous chapters and summarized in Table 4.11. Eqs. 5.5 and 5.6 can be developed for different categories using their corresponding parameters.

5.2. Reliability Assessment for AASHTO Fatigue Equations

The governing structural design codes for both buildings and bridges in the U.S. have incorporated reliability-based design approaches to ensure consistent and quantifiable levels of reliability within the structures. As discussed in Chapter 2, most of these reliability approaches use the concept of reliability index by assessing a limit state function that incorporates the estimated variabilities on both the load and resistance sides of the limit state function to assess the overall reliability. The current AASHTO specifications do not explicitly associate the fatigue design curves (for the various categories) with any particular level of reliability. However, the early literature that presented the fatigue data (and curves) indicate that the intended level of reliability for the design curves was 97.5% (or 2.5% probability of failure).

Albrecht (1983) investigated reliability of AASHTO fatigue design curves using the reliability index approach. The linear (log-log) form of the S-N fatigue equation was used for reliability index calculations. Then, the reliability index, as a measure of probability of failure, was estimated for different fatigue details. Albrecht (1983) reported that the probability of failure could vary widely from 9.2×10^{-2} to 2.1×10^{-22} across different categories.

In this chapter, the probability of survival associated with the various points on the AASHTO fatigue curves are assessed using the proposed log-logistic AFT survival model. Using this approach, the probability of survival is calculated considering number of stress cycles and stress range as independent variables affecting the probability of survival. These calculations address the fatigue resistance side only and are calculated for each n_c and S_r pairs for the applicable fatigue detail category. These calculations do not consider the variability of load (variations in stress range).

Reliability contours for AASHTO fatigue design curves are calculated using the proposed log-logistic AFT model and plotted in Figures 5.1 through 5.6. The parameters used for survival calculations are those calculated in section 4.4 and summarized in Table 4.11 of this study.

Figures 5.1 shows the reliability contour for fatigue category A. As shown in the figure, reliabilities associated with points on the AASHTO fatigue design curve for category A vary between 0.70 to 0.95 (or probability of failure of 0.30 to 0.05) along the sloped line in the AASHTO fatigue curve. Since the available fatigue test data had very limited number of points below the threshold levels (infinite life zone), the estimates are not extended into that zone, and are only applicable to the finite life area (sloped line). The ranges of reliabilities (or probability of failures) are different for different detail categories. The variation in the reliabilities for categories A, B, C, D, E, and E′ are shown in Table 5.1.

Table 5.1. Range of reliability for different categories of AASHTO fatigue curves based on the log-logistic AFT survival model

Category	Range of reliability
A	0.7 to 0.95
B	0.4 to 0.9
C	0.6 to 0.96
D	0.2 to 0.94
E	0.1 to 0.99
E′	0.1 to 0.99

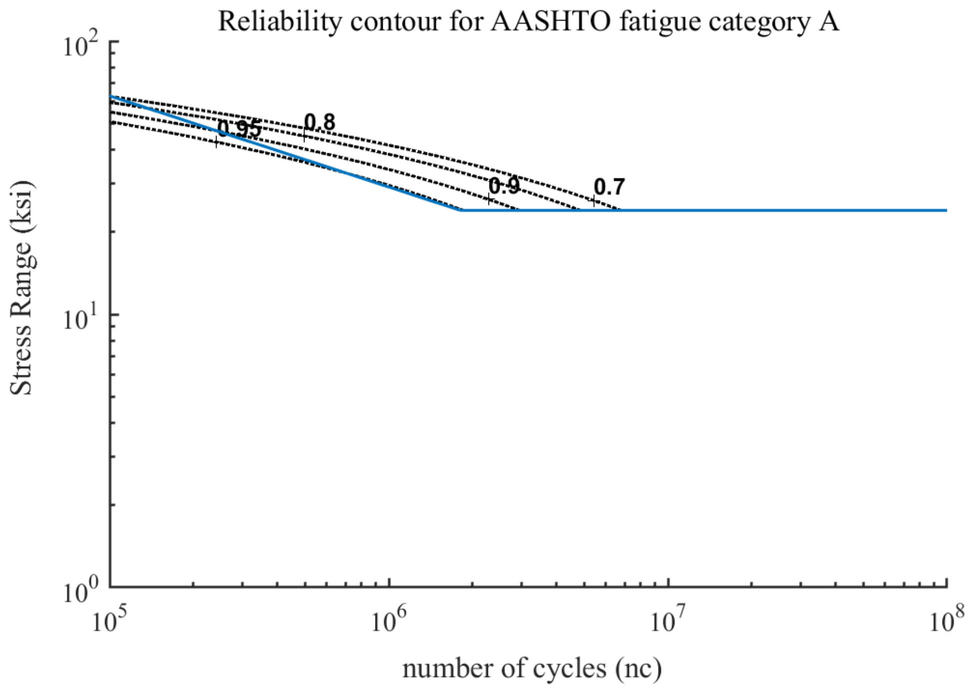

(a)

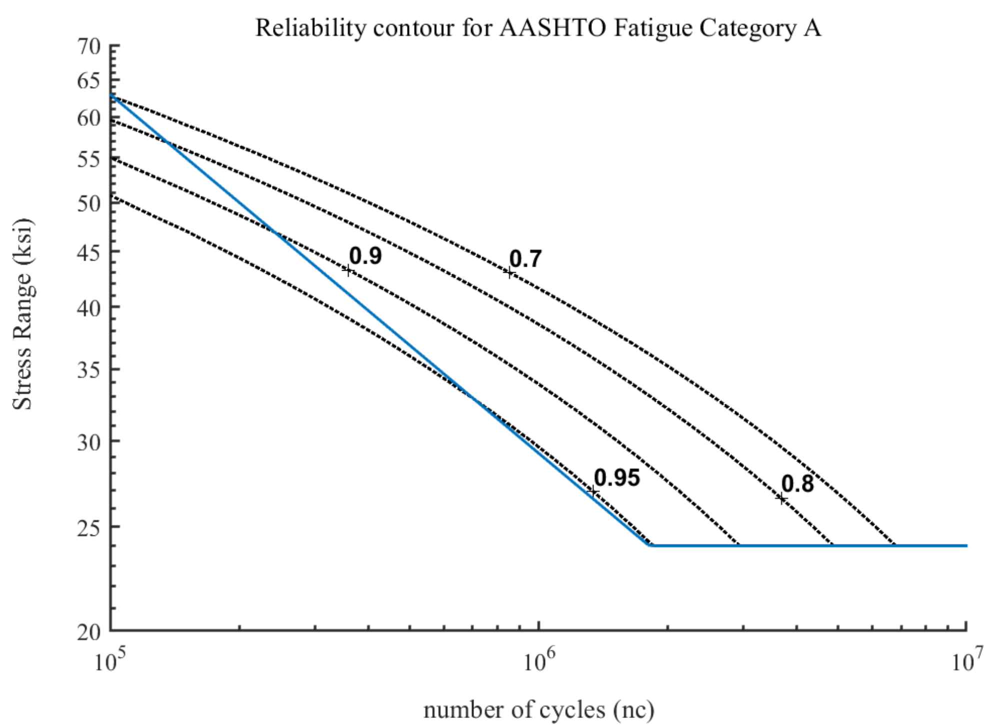

(b)

Figure 5.1. (a) Reliability contours - AASHTO fatigue category A, (b) close look at the reliability contours-AASHTO fatigue category A

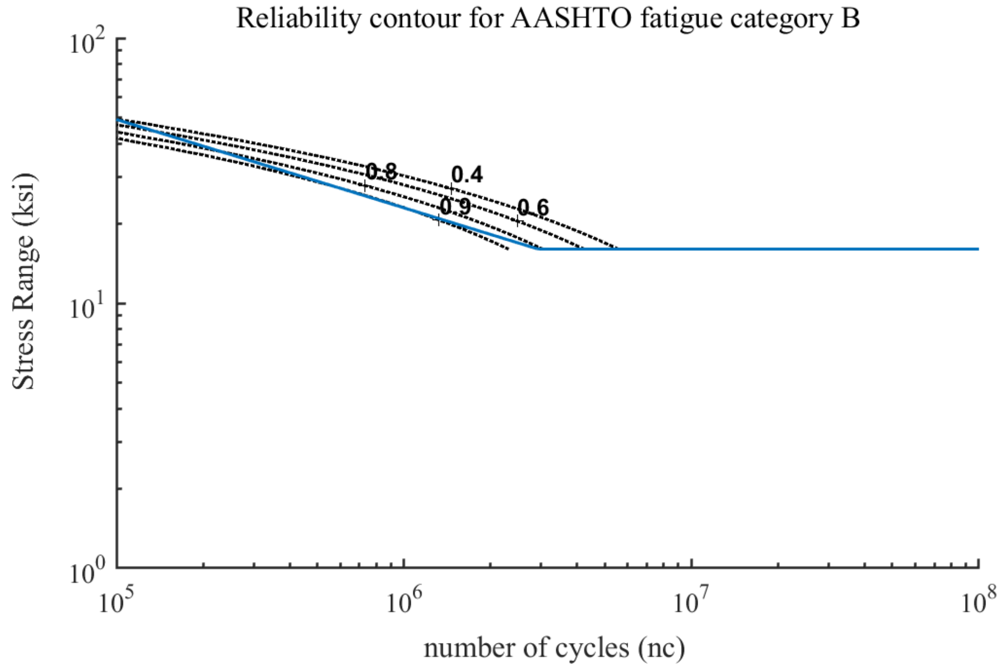

(a)

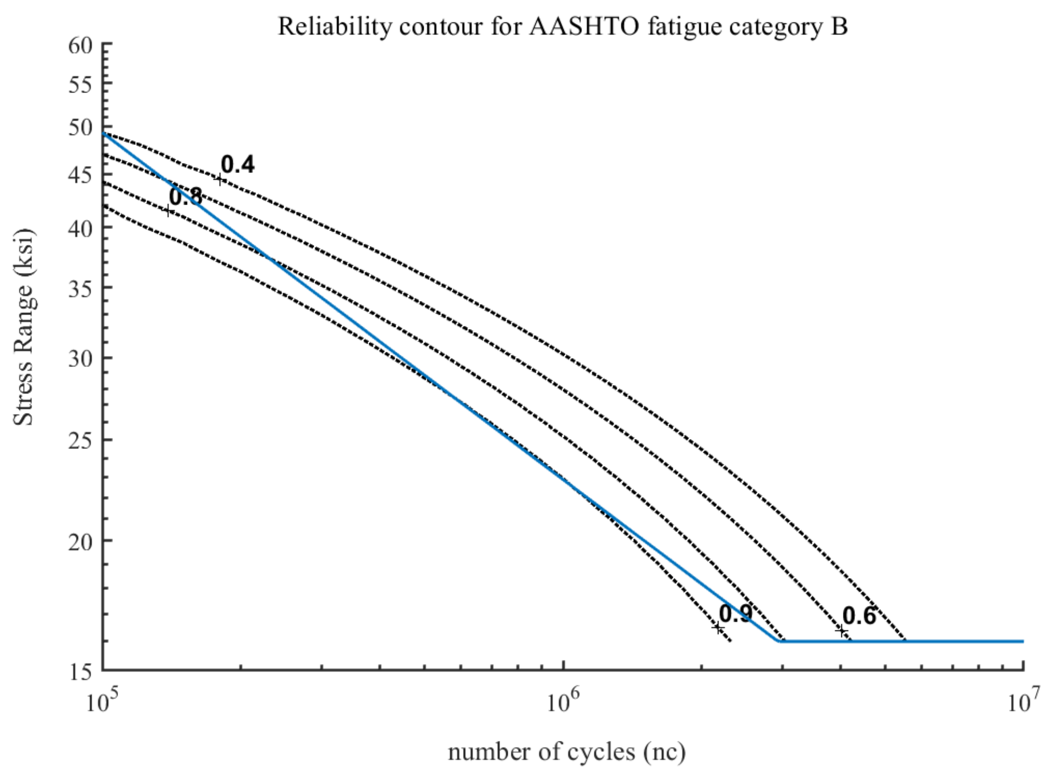

(b)

Figure 5.2. (a) Reliability contours - AASHTO fatigue category B, (b) close look at the reliability contours-AASHTO fatigue category B

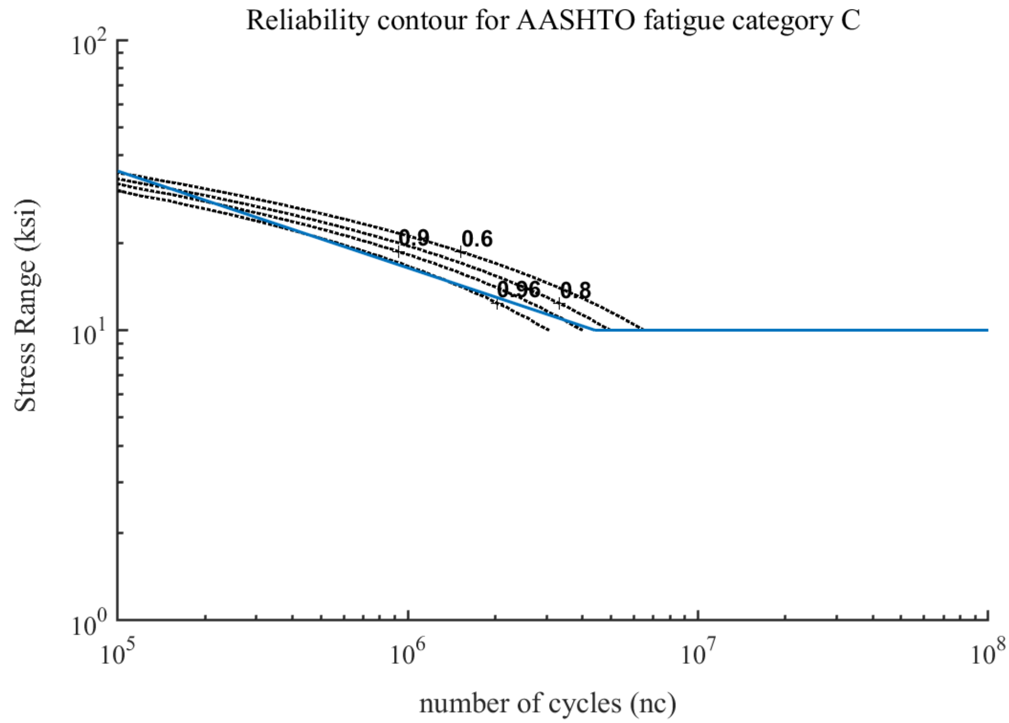

(a)

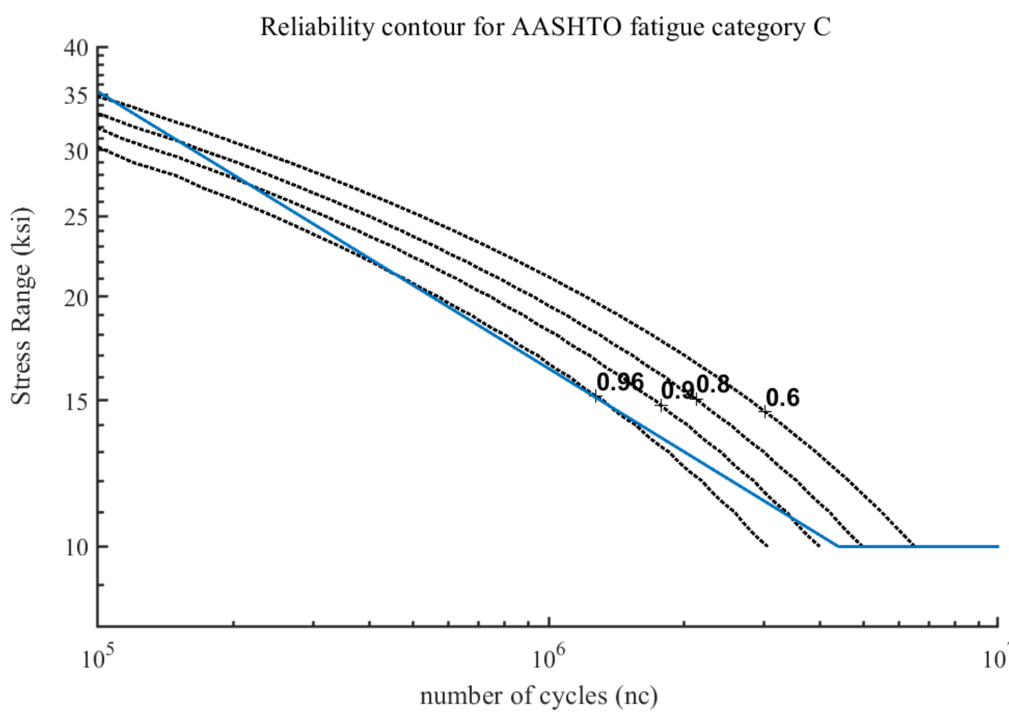

(b)

Figure 5.3. (a) Reliability contours - AASHTO fatigue category C, (b) close look at the reliability contours-AASHTO fatigue category C

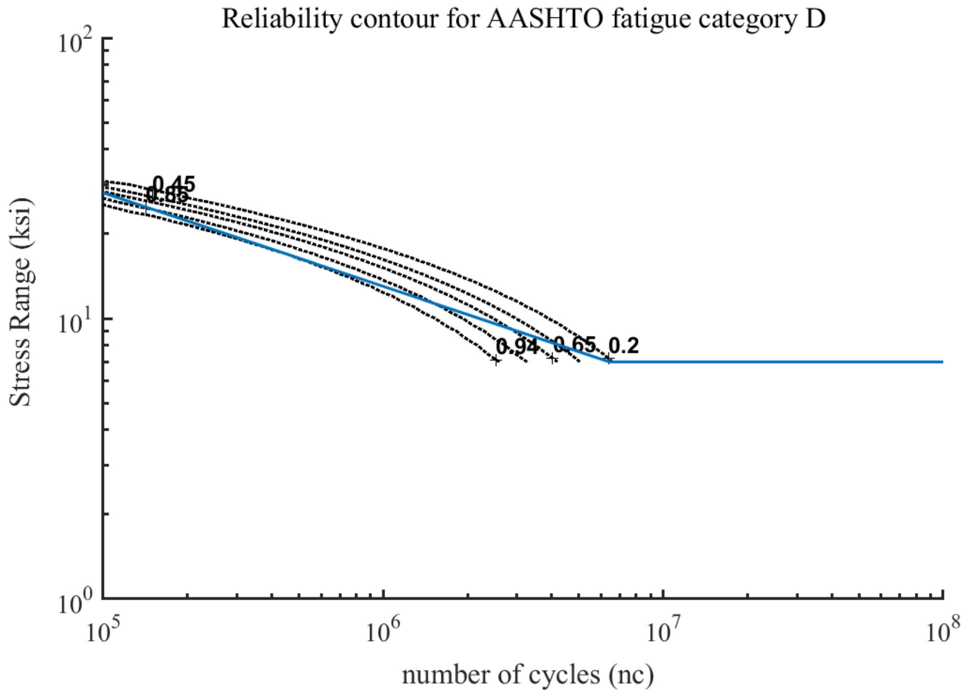

(a)

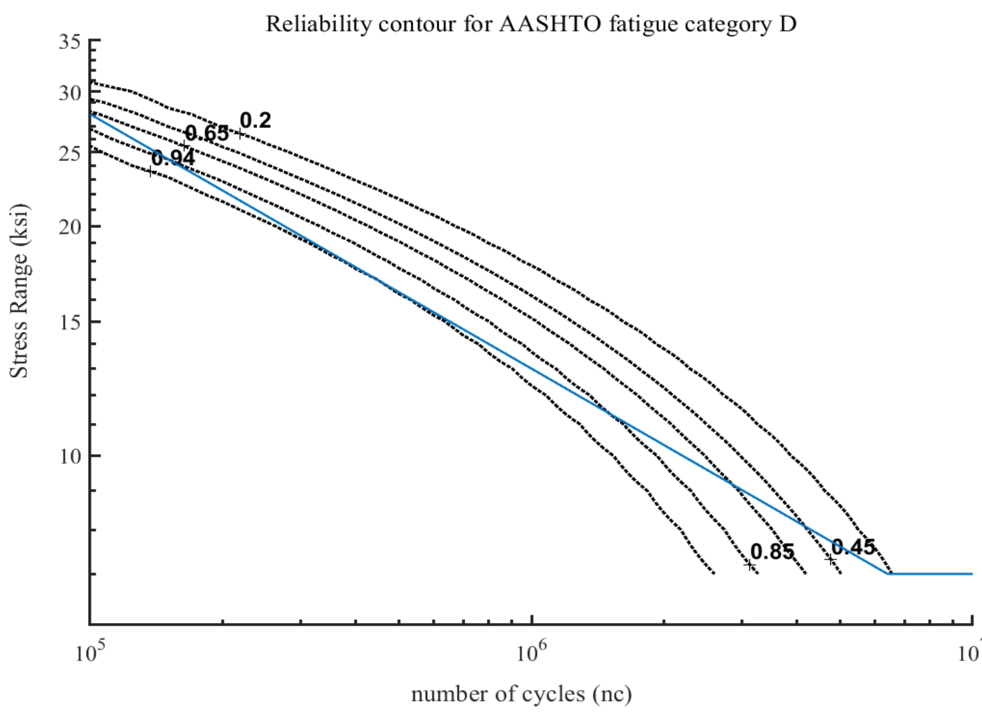

(b)

Figure 5.4. (a) Reliability contours - AASHTO fatigue category D, (b) close look at the reliability contours-AASHTO fatigue category D

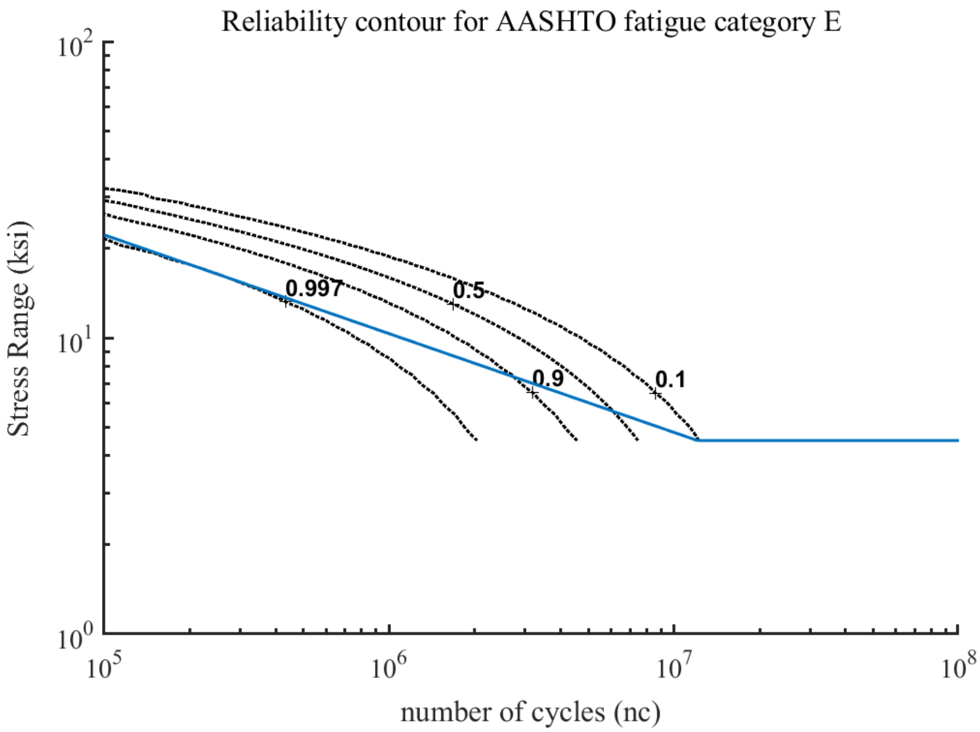

(a)

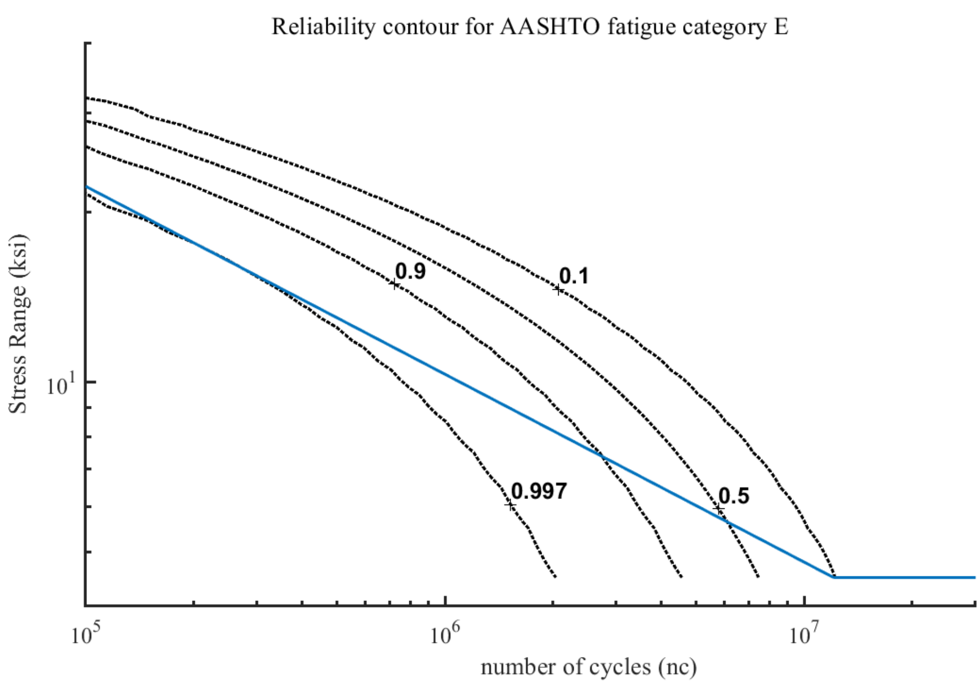

(b)

Figure 5.5. (a) Reliability contours - AASHTO fatigue category E, (b) close look at the reliability contours-AASHTO fatigue category E

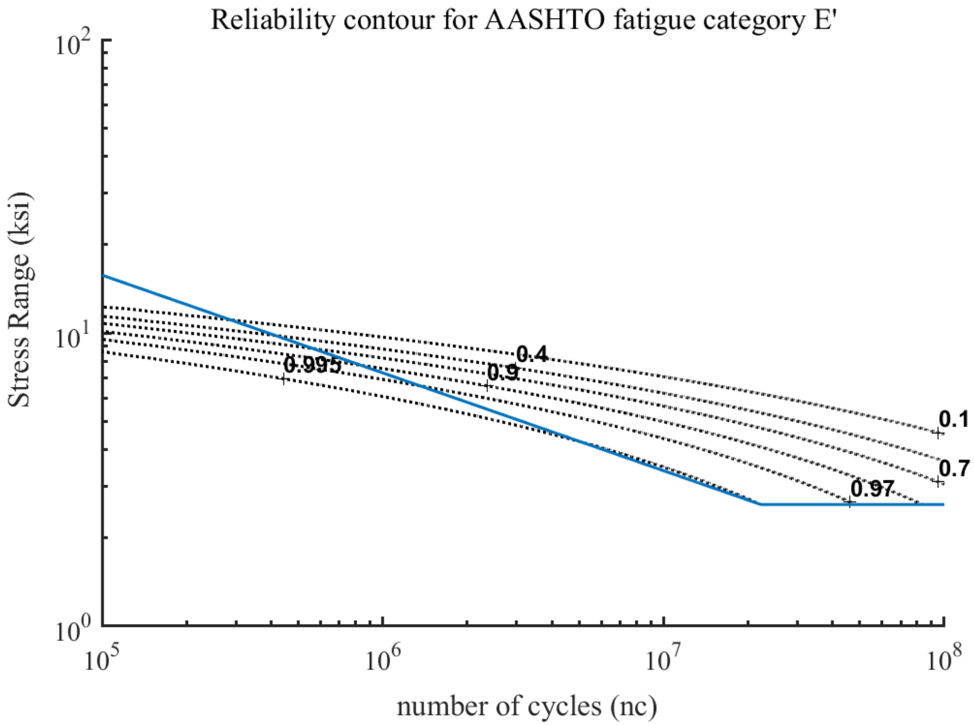

(a)

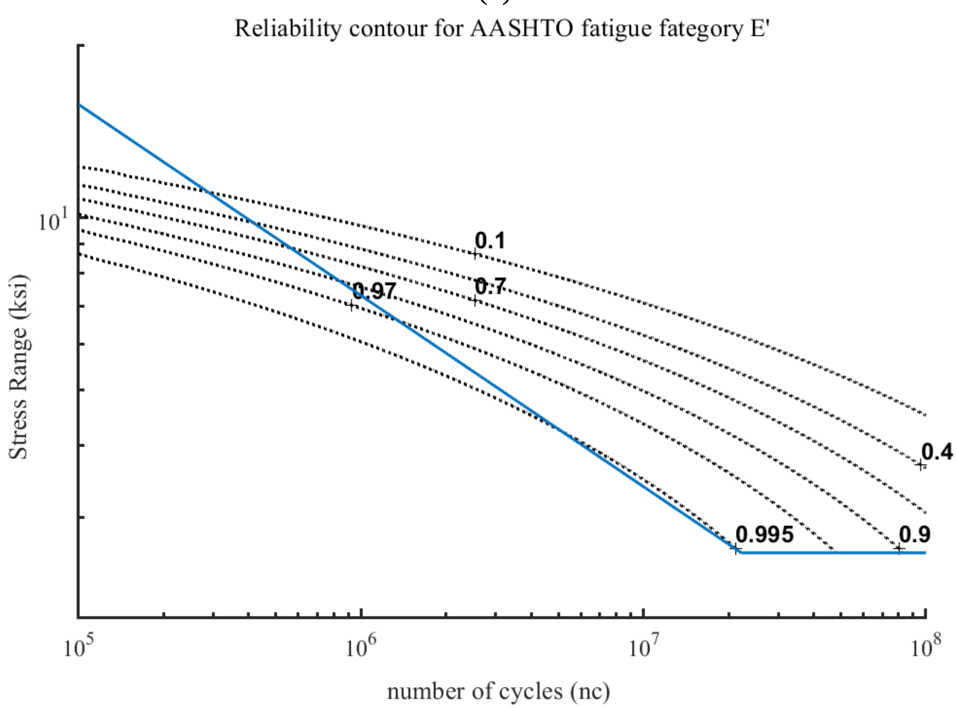

(b)

Figure 5.6. (a) Reliability contours - AASHTO fatigue category E′, (b) close look at the reliability contours-AASHTO fatigue category E′

Table 5.2 lists the means and standard deviations for the estimated probabilities of survival and failure for AASHTO fatigue categories (finite life zone) using the proposed log-logistic AFT survival model. The estimated survival probabilities are calculated for ten points along the finite life section of the AASHTO fatigue curve. The mean, standard deviation (St.Dev), and coefficient of variation (CV) values reported in Table 5.2 are calculated for those ten selected points. The estimated mean survival rate ranges between 0.882 and 0.923 and the standard deviation varies between 0.078 and 0.293 across all different categories. The reliability variations within each fatigue detail category cover a much wider range.

Table 5.2. Average probabilities of survival and failure for different AASHTO fatigue categories using the log-logistic AFT model

Category	Probability of survival	Probability of failure	St.Dev	CV (%)
A	0.923	0.077	0.078	102.06
B	0.914	0.086	0.218	255.46
C	0.913	0.087	0.254	291.70
D	0.915	0.085	0.248	291.70
E	0.909	0.091	0.246	270.48
E′	0.882	0.118	0.293	248.23

Using Equation 5.5, the uniform-reliability survival curves associated with S_{req}= 0.80, 0.85, 0.90, and 0.95 for different fatigue categories are shown in Figures 5.7 through 5.10, respectively. In these figures, the AASHTO fatigue curves are shown through dotted gray lines on the background.

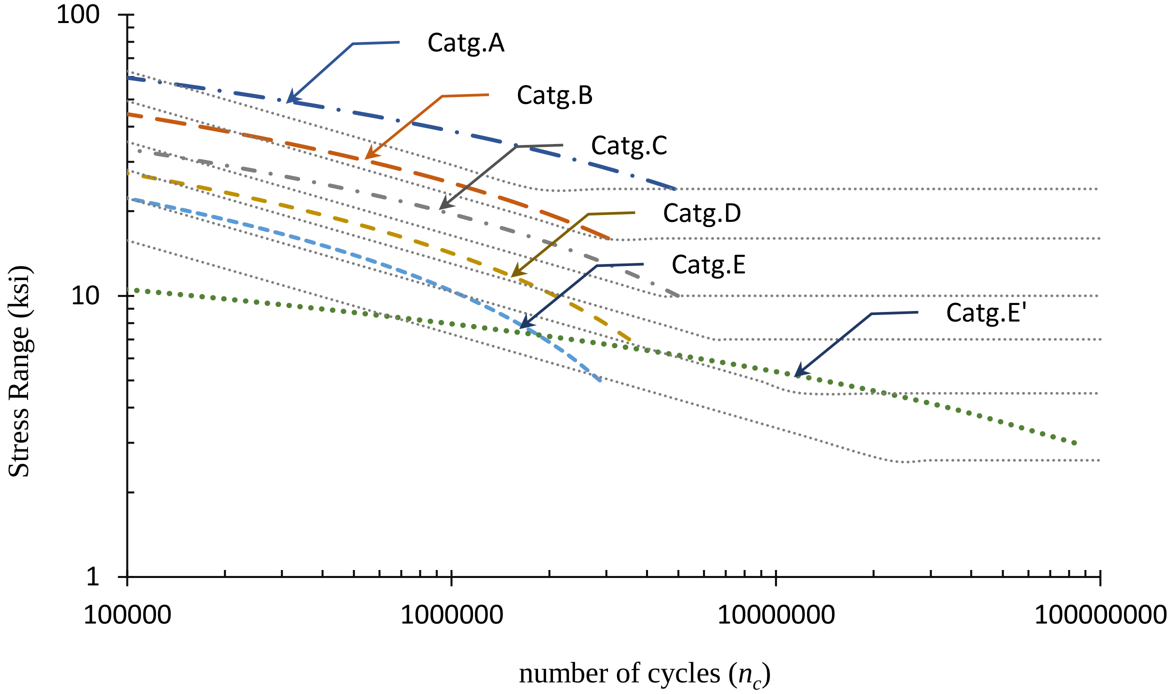

Figure 5.7. Proposed uniform-reliability design curves at S_{req}= 0.80 for fatigue categories A through E′

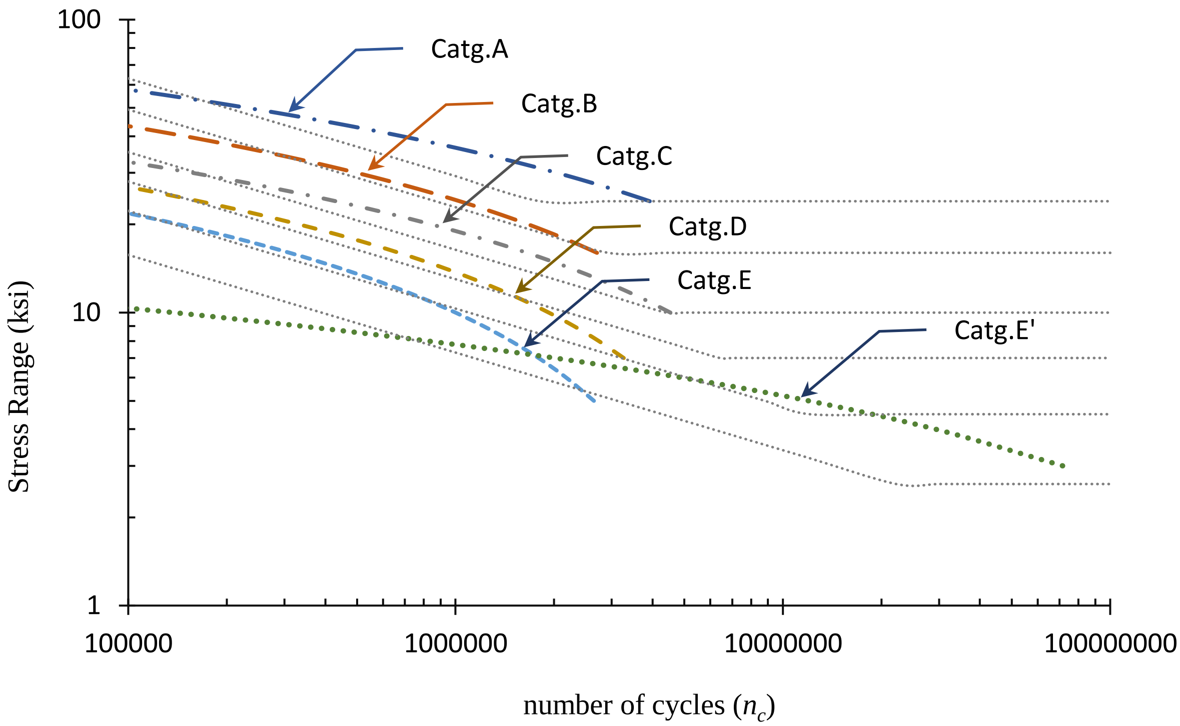

Figure 5.8. Uniform proposed reliability curves at S_{req}= 0.85 for fatigue categories A through E′

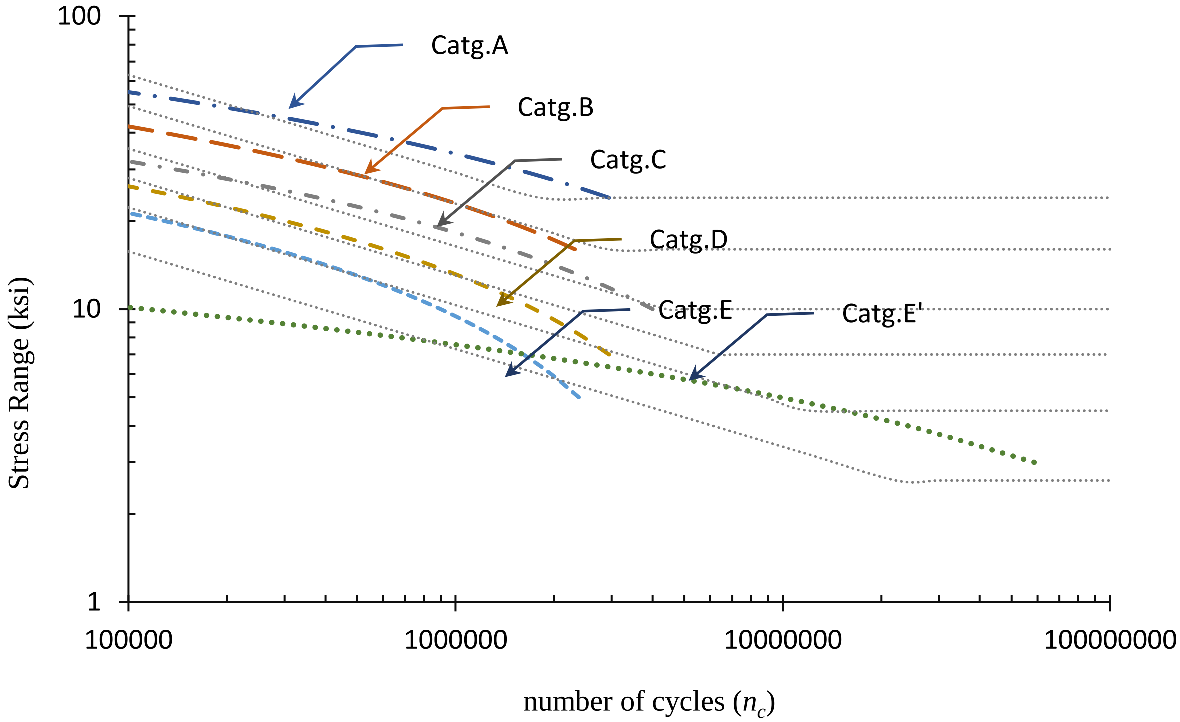

Figure 5.9. Uniform proposed reliability curves at S_{req}= 0.90 for fatigue categories A through E′

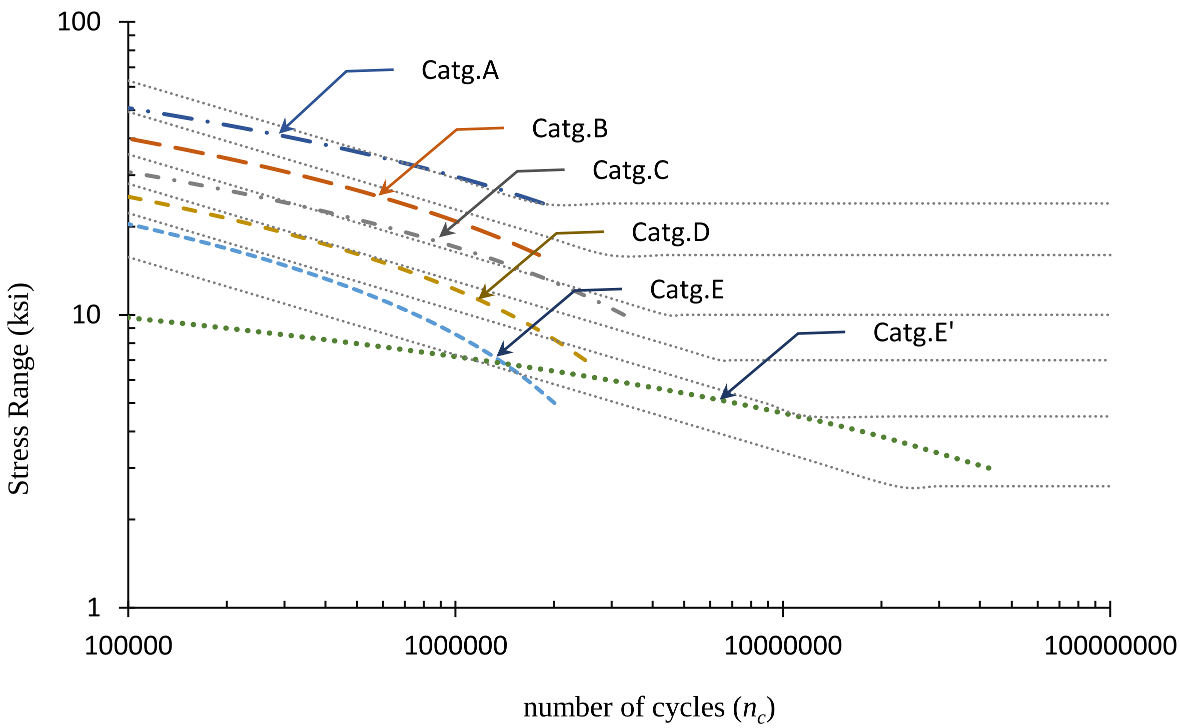

Figure 5.10. Uniform proposed reliability curves at S_{req}= 0.95 for fatigue categories A through E′

Chapter 6. Summary and Conclusions

Different parameters can influence fatigue life of engineering systems. The uncertainties inherent in these parameters make the nature of fatigue life stochastic. These parameters include materials, loading conditions, loading sequence, environmental conditions, and geometry details.

This research studied fatigue reliability and remaining number of cycles to failure in bridges including affecting parameters. An advanced statistical method called survival analysis has been employed and developed for fatigue details tested for AASHTO fatigue curves. The data used for the survival analyses were extracted from NCHRP reports (NCHRP Report 102 by Fisher et al., 1970; NCHRP Report 147 by Fisher et al., 1974; NCHRP Report 226 by Keating and Fisher, 1986). AASHTO fatigue curves include different categories with different connection and weld details. Different fatigue categories and stress range are considered covariates as influencing factors in this analysis.

Parametric survival analysis is the method used for the reliability assessment of fatigue in bridges. In parametric survival analysis, a baseline distribution which best fit the data is considered for the analysis. Lognormal distribution has been the most commonly used distribution in fatigue reliability analyses in the literature. In this study, lognormal, loglogistic, hypertabastic, and Weibull distributions were tested to find the best fit distribution for the AASHTO fatigue data. Using AIC method, loglogistic was selected as the best fit distribution for the available fatigue data. According to intersecting K-M survival curves for different AASHTO fatigue categories, AFT model was selected for further analyses.

The fatigue data were analyzed in two approaches. First, data of all categories were analyzed combined and constant parameters for covariate were calculated. Second, the data of each category were analyzed separately, and the corresponding parameters were calculated, consequently.

The K-M survival curves were plotted versus AFT loglogistic survival curves for comparison in both approaches. The results from analyses of separate data showed a better agreement with K-M curves. Therefore, the calculated parameters from the latter analyses were considered for the rest of the analyses.

The survival, hazard rate, pdf, and cumulative hazard curves were developed for different categories. According to survival curves, as stress ranges increase the probability of survival decreases and reversely the probability of failures increases. The results for pdf showed that larger probability of failures happen at smaller number of cycles and higher stress ranges, for all detail categories. Similarly, larger hazard rates occur at smaller number of cycles and higher stress ranges. The loglogistic AFT reliability contours were developed for all categories. According to the reliability contour results, the reliability of AASHTO fatigue curves are not consistent and vary in different ranges for different categories. The average reliability of ten random points on each AASHTO fatigue curve were calculated, showing a range of variation between 0.882 and 0.923 over all categories.

Conditional survival analysis was used as mean to account for updated information on survival curves. Results for CS showed that probability of survival increases as a fatigue component survives a specific number of cycles under a stress range.

At the end, a set of equations were proposed for calculating number of cycles corresponding to a specific reliability at a certain stress range. Similarly, a set of equations were proposed to calculate stress range corresponding to a specific level of reliability at a specific number of cycles.

References

ASCE Committee on Fatigue and Fracture Reliability of the Committee on Structural Safety and Reliability of the Structural Division. (1982). "Fatigue reliability 1-4." J. Struct. Eng., ASCE, 108(1), 3-88.

American Association of State Highway and Transportation Officials (AASHTO). (2018). Standard specifications for highway bridges. L.R.F.D. Washington, DC.

Albrecht, P. (1983). S-N fatigue reliability analysis of highway bridges. In: Probabilistic Fracture Mechanics and Fatigue Methods: Applications for Structural Design and Maintenance. ASTM International.

ASTM E739-10 (2015). Standard Practice for Statistical Analysis of Linear or Linearized Stress-Life (S-N) and Strain-Life (ε-N) Fatigue Data. ASTM International, West Conshohocken, PA, 2015, www.astm.org

Baade, P.D., Youlden, D.R. and Chambers, S.K. (2011). When do I know I am cured? Using conditional estimates to provide better information about cancer survival prospects. Medical Journal of Australia, 194(2), p.73.

Berger, C., Pyttel, B. and Trossmann, T. (2006). Very high cycle fatigue tests with smooth and notched specimens and screws made of light metal alloys. International journal of fatigue, 28(11), pp.1640-1646.

Bilir, O. (1991). Experimental investigation of fatigue damage accumulation in 1100 Al alloy. International Journal of Fatigue, 13(1), pp. 3-6.

Bisping, J.R., Peterwerth, B., Bleicher, C., Wagener, R. and Melz, T. (2014). Fatigue life assessment for large components based on rainflow counted local strains using the damage domain. International Journal of Fatigue, 68, pp.150-158.

Breslow, N.E. (1975). Analysis of survival data under the proportional hazards model. International Statistical Review/Revue Internationale de Statistique, pp.45-57.

Bursac, Z., Tabatabai, M., Williams, D.K. and Singh, K. (2008). A simulation study of performance of hypertabastic and hyperbolastic survival models in comparison with classic survival models. Proc. 2008 American statistical assoc. Biometrics section (CD-ROM), pp.617-622.

Castillo, E. and Fernandez-Canteli, A. (2009). A unified statistical methodology for modeling fatigue damage. Springer Science & Business Media.

Chang, G.J., Hu, C.Y., Eng, C., Skibber, J.M. and Rodriguez-Bigas, M.A. (2009). Practical application of a calculator for conditional survival in colon cancer. Journal of Clinical Oncology, 27(35), pp.5938-5943.

Chung, H.Y. (2004). Fatigue reliability and optimal inspection strategies for steel bridges. Doctoral dissertation, Civil and Environmental Engineering Department, The University of Texas at Austin, Austin, TX.

Corten, H. and Dolan, T. (1956). Cumulative fatigue damage. In: Proceedings of the International Conference on Fatigue of Metals. Vol. 1. Institution of Mechanical Engineering and American Society of Mechanical Engineers.

Cui, W. (2002). A state-of-the-art review on fatigue life prediction methods for metal structures. Journal of Marine Science and Technology, 7(1), pp 43–56.

Deng, Y., Ding, Y., Li, A. and Zhou, G. (2011). Fatigue reliability assessment for bridge welded details using long-term monitoring data. Science China Technological Sciences, 54(12), pp.3371-3381.

Fatemi, A. and Yang, L. (1998). Cumulative fatigue damage and life prediction theories: a survey of the state of the art for homogeneous materials. International journal of fatigue, 20(1), pp.9-34.

Fisher, J.W., Frank, K.H., Hirt, M.A., and McNamee, B.M. (1970). Effects of Weldments on the Fatigue Strength of Steel Beams. NCHRP Report 102, National Cooperative Highway Research Program.

Fisher, J.W., Albrecht, P.A., Yen, B.T., Klingerman, D.J., and McNamee,B.M. (1974). Fatigue Strength of Steel Beams with Welded Stiffeners and Attachments. NCHRP Report 147, National Cooperative Highway Research Program.

Freudenthal, A.M. and Heller, R.A. (1959). On stress interaction in fatigue and a cumulative damage rule. Journal of the Aerospace Sciences, 26(7), pp.431-442.

Forsyth, P. (1969). The physical basis of metal fatigue. New York: American Elsevier Publishing.

Frangopol, D.M., 1999. Bridge safety and reliability.

Fuller, C. D., Wang, S. J., Thomas Jr, C. R., Hoffman, H. T., Weber, R. S., & Rosenthal, D. I. (2007). Conditional survival in head and neck squamous cell carcinoma: results from the

SEER dataset 1973–1998. Cancer: Interdisciplinary International Journal of the American Cancer Society, 109(7), 1331-1343.

Gao, H., Huang, H.Z., Zhu, S.P., Li, Y.F. and Yuan, R. (2014). A modified nonlinear damage accumulation model for fatigue life prediction considering load interaction effects. The Scientific World Journal.

Gratts. R. (1961). Trans. ASME, Journal of Basic Engineering, 83(12), pp. 529.

Grover, H. (1960). ASTM, STP274. Symposium on Fatigue of Aircraft Structures. pp. 120.

Henry, D.L. (1953). A theory of fatigue damage accumulation in steel (Doctoral dissertation, Ohio State University).

Henry, D., and Johnson, J. (2004). Fatigue Failure through Bending Experiment. Lab report.

Hieke, S., Kleber, M., König, C., Engelhardt, M. and Schumacher, M. (2015). Conditional survival: a useful concept to provide information on how prognosis evolves over time. Clinical Cancer Research, 21(7), pp.1530-1536.

Hosmer, D.W., Lemeshow, S. and May, S. (2008). Model development. Applied Survival Analysis: Regression Modeling of Time-to-Event Data, Second Edition, pp.132-168.

Kaechele, L. (1963). Review and Analysis of Cumulative-fatigue-damage Theories. Report No. RAND-RM-3650-PR. Santa Monica, CA: Rand Corporation

Janssen-Heijnen, M.L., Gondos, A., Bray, F., Hakulinen, T., Brewster, D.H., Brenner, H. and Coebergh, J.W.W. (2010). Clinical relevance of conditional survival of cancer patients in

Europe: age-specific analyses of 13 cancers. Journal of clinical oncology, 28(15), pp.2520-2528.

Kato, I., Severson, R.K. and Schwartz, A.G. (2001). Conditional median survival of patients with advanced carcinoma: surveillance, epidemiology, and end results data. Cancer, 92(8), pp.2211-2219.

Keating, P.B. and Fisher, J.W. (1986). Review of fatigue tests and design criteria on welded details, Final Report, July 1986, 180p. NCHRP Report 286, Publication 86-21.

Kibbey, D.R., 1949. Cumulative Damage in Fatigue in Steel, (Doctoral dissertation, Ohio State University).

Kordijazi, A. (2014). Electrochemical Characteristics of an Optimized Ni-P-Zn Electroless Composite Coating. In Advanced Materials Research (Vol. 1043, pp. 124-128). Trans Tech Publications.

Kordijazi, A. (2019). Optimization of Ni-P-Zn electroless bath and investigation of corrosion resistance of as-plated coatings. Materials Research Express.

Kwon, K. and Frangopol, D.M. (2010). Bridge fatigue reliability assessment using probability density functions of equivalent stress range based on field monitoring data. International Journal of Fatigue, 32(8), pp.1221-1232.

Langer, B. (1937). Fatigue failure stress cycles of varying amplitude. Transactions of the ASME, 59, pp. A-160.

Levy, J. C. (1955). Cumulative damage in fatigue. Engineering, 179, pp. 724-726.

Lee, E. T., & Go, O. T. (1997). Survival analysis in public health research. Annual review of public health, 18(1), 105-134.

Liu, X. (2012). Survival analysis: models and applications. John Wiley & Sons.

Manson, S. (1966). Interfaces between fatigue, creep, and fracture. International Journal of Fracture Mechanics, 2(1), pp. 327-363.

Manson, S., Freche J. and Ensign, C. (1967), Application of a Double Linear Damage Rule to Cumulative Fatigue. Washington, D.C.: NASA.

Manson, S. and Halford, G. (1981). Practical implementation of the double linear damage rule and damage curve approach for treating cumulative fatigue damage. International Journal of Fracture, 17(2), pp. 169-192.

Manson, S. and Hirschberg, M. (1966). Prediction of Fatigue of Notched Specimens by Consideration of Crack Initiation and Propagation. NASA TN D-3146.

Manson, S., Nachtigall, A. and Freche, J. (1961). A proposed new relation for cumulative fatigue damage in bending. ASTM Proceedings, 61, pp. 679-703.

Manson, S.S. and Halford, G.R. (1981). Practical implementation of the double linear damage rule and damage curve approach for treating cumulative fatigue damage. International journal of fracture, 17(2), pp.169-192.

Marco, S. and Starkey, W. (1954). A Concept of fatigue damage. Transaction of the ASME, 76, pp. 627-632.

Marsh, G., Wignall, C., Thies, P.R., Barltrop, N., Incecik, A., Venugopal, V. and Johanning, L. (2016). Review and application of Rainflow residue processing techniques for accurate fatigue damage estimation. International Journal of Fatigue, 82, pp.757-765.

Meggiolaro, M.A. and de Castro, J.T.P. (2012). An improved multiaxial rainflow algorithm for non-proportional stress or strain histories–Part I: Enclosing surface methods. International Journal of Fatigue, 42, pp.217-226.

Merrill, R.M. and Hunter, B.D. (2010). Conditional survival among cancer patients in the United States. The oncologist, 15(8), pp.873-882.

Merrill, R.M., Henson, D.E. and Barnes, M. (1999). Conditional survival among patients with carcinoma of the lung. Chest, 116(3), pp.697-703.

a Miller, K. (1987). The behavior of short fatigue cracks and their initiation. Part I - A review of two recent books. Fatigue and Fracture of Engineering Materials and Structures, 10, pp. 75–91.

b Miller, K. (1987). The behavior of short fatigue cracks and their initiation. Part II - A general summary. Fatigue and Fracture of Engineering Materials and Structures, 10, pp. 93–113.

Miner, M. (1945). Cumulative damage in fatigue. Journal of Applied Mechanics. 12(3), pp. A159-A164.

Munse, W.H., Wilbur, T.W., Tellalian, M.L., Nicoll, K. and Wilson, K. (1983). Fatigue characterization of fabricated ship details for design. Washington, D.C.: Ship Structure Committee.

Nabizadeh, A., Tabatabai, H., Tabatabai, M. A., (2019). Conditional survival analysis for concrete bridge decks. Life Cycle Reliability and Safety Engineering, Springer.

Nabizadeh, A., Tabatabai, H., & Tabatabai, M. (2018). Survival analysis of bridge superstructures in wisconsin. Applied Sciences, 8(11), 2079.

Parsons, H.M., Habermann, E.B., Tuttle, T.M. and Al-Refaie, W.B. (2011). Conditional survival of extremity soft-tissue sarcoma: results beyond the staging system. Cancer, 117(5), pp.1055-1060.

Pourzeynali, S. and Datta, T.K. (2005). Reliability analysis of suspension bridges against fatigue failure from the gusting of wind. Journal of Bridge Engineering, 10(3), pp.262-271.

Pyttel, B., Schwerdt, D. and Berger, C. (2011). Very high cycle fatigue–Is there a fatigue limit?. International Journal of fatigue, 33(1), pp.49-58.

Pyttel, B., Canteli, A.F. and Ripoll, A.A. (2016). Comparison of different statistical models for description of fatigue including very high cycle fatigue. International Journal of Fatigue, 93, pp.435-442.

Rathod, V., Yadav, O.P., Rathore, A. and Jain, R. (2011). Probabilistic modeling of fatigue damage accumulation for reliability prediction. International Journal of Quality, Statistics, and Reliability.

Ritchie, R. (1986). Small fatigue cracks: a statement of the problem and potential solutions. Materials Science and Engineering, 84, pp. 11–16.

Safarian, P. (2014). Fatigue and Damage Tolerance Requirements of Civil Aviation. MAE Colloquium, Aeronautics and Astronautics, University of Washington, Seattle, WA. Conference Presentation.

SAS software. Copyright © (2017) SAS Institute Inc., Cary, NC, USA.

Scharton, T. and Crandall, S. (1966). Fatigue failure under complex stress histories. Journal of Basic Engineering, 88(1), pp. 247-251.

Schijve, J. (1967). Significance of fatigue cracks in micro-range and macro-range. ASTM STP, 415, pp. 415–459.

Shang, D., Yao, W. and Wang, D. (1998). A new approach to the determination of fatigue crack initiation size. International Journal of Fatigue, 20, pp. 683–687.

Shanley, F. (1952). A Theory of Fatigue Based on Unbonding During Reversed Slip. Report P-350. Santa Monica: The Rand Corporation.

Shen, H., Lin, J. and Mu, E. (2000). Probabilistic model on stochastic fatigue damage. International Journal of Fatigue, 22(7), pp. 569–572.

Shimokawa, T. and Tanaka, S. (1980). A statistical consideration of Miner's rule. International Journal of Fatigue, 2(4), pp.165-170.

Sobanjo, J., Mtenga, P., & Rambo-Roddenberry, M. (2010). Reliability-based modeling of bridge deterioration hazards. Journal of Bridge Engineering, 15(6), 671-683. Sobczyk, K. and Spencer Jr, B. (1992). Random fatigue: from data to theory. San Diego, CA: Academic Press, Inc.

Soliman, M., Frangopol, D.M. and Kown, K. (2012). Fatigue assessment and service life prediction of existing steel bridges by integrating SHM into a probabilistic bilinear S-N approach. Journal of Structural Engineering, 139(10), pp.1728-1740.

Stallmeyer, J.E. and Walker, W.H. (1968). Cumulative damage theories and application. Journal of the Structural Division.

a Valluri, S. (1961). A Theory of Cumulative Damage in Fatigue. Report No. ARL 182. Aeronautical Research Laboratory, Office of Aerospace Research, United States Air Force.

b Valluri, S. (1961). A unified engineering theory of high stress level fatigue. Aerospace Engineering, 20, pp. 18-19.

Yu, X.Q., Baade, P.D. and O'Connell, D.L. (2012). Conditional survival of cancer patients: an Australian perspective. BMC cancer, 12(1), p.460.

Wang, S.J., Emery, R., Fuller, C.D., Kim, J.S., Sittig, D.F. and Thomas, C.R. (2007). Conditional survival in gastric cancer: a SEER database analysis. Gastric Cancer, 10(3), pp.153-158.

Wheatley-Price, P., Hutton, B., & Clemons, M. (2012). The Mayan Doomsday's effect on survival outcomes in clinical trials. CMAJ, 184(18), 2021-2022.

Wirsching, P.H. (1984). Fatigue reliability for offshore structures. Journal of Structural Engineering, 110(10), pp.2340-2356.

Wirsching, P.H. and Chen, Y.N. (1988). Considerations of probability-based fatigue design for marine structures. Marine Structures, 1(1), pp. 23-45.

Wolfram Research, Inc. (2017). Mathematica, Version 11.2, Champaign, IL.

Wu, W.F., Liou, H.Y. and Tse, H.C. (1997). Estimation of fatigue damage and fatigue life of components under random loading. International Journal of Pressure Vessels and Piping, 72(3), pp. 243-249.

Xing, Y., Chang, G.J., Hu, C.Y., Askew, R.L., Ross, M.I., Gershenwald, J.E., Lee, J.E., Mansfield, P.F., Lucci, A. and Cormier, J.N. (2010). Conditional survival estimates improve over time for patients with advanced melanoma: Results from a population-based analysis. Cancer, 116(9), pp.2234-2241.

Zabor, E.C., Gonen, M., Chapman, P.B. and Panageas, K.S. (2013). Dynamic prognostication using conditional survival estimates. Cancer, 119(20), pp.3589-3592.

Zaccone, M.A. (2001). Failure analysis of helical suspension springs under compressor start/stop conditions. Journal of Failure Analysis and Prevention, 1(3), pp. 51-62.

Zamboni, B.A., Yothers, G., Choi, M., Fuller, C.D., Dignam, J.J., Raich, P.C., Thomas Jr, C.R., O'Connell, M.J., Wolmark, N. and Wang, S.J. (2010). Conditional survival and the choice of conditioning set for patients with colon cancer: an analysis of NSABP trials C-03 through C-07. Journal of Clinical Oncology, 28(15), p.2544.

Zhao, Z., Haldar, A. and Breen Jr, F.L. (1994). Fatigue-reliability evaluation of steel bridges. Journal of structural engineering, 120(5), pp.1608-1623.

Zhao, Z. (1991). Reliability-based fatigue analysis under random loading through NDT considering modeling updating for steel bridges (Doctoral dissertation, MS thesis, University of Arizona, Tucson, Arizona).

ZHU, S.P. and HUANG, H.Z. (2010). A generalized frequency separation–strain energy damage function model for low cycle fatigue–creep life prediction. Fatigue & Fracture of Engineering Materials & Structures, 33(4), pp.227-237.

Zhu, S.P., Huang, H.Z., Ontiveros, V., He, L.P. and Modarres, M. (2012). Probabilistic low cycle fatigue life prediction using an energy-based damage parameter and accounting for model uncertainty. International Journal of Damage Mechanics, 21(8), pp.1128-1153.

Zhu, S.P., Huang, H.Z., Liu, Y., He, L.P. and Liao, Q. (2012). A practical method for determining the Corten-Dolan exponent and its application to fatigue life prediction. Int. J. Turbo Jet-Engines, 29(2), pp.79-87.

Tabatabai, H., Tabatabai, M. and Lee, C.W. (2011). Reliability of bridge decks in Wisconsin. Journal of Bridge Engineering, 16(1), pp.53-62.

Tabatabai, H., Lee, C.W. and Tabatabai, M.A. (2015). Reliability of bridge decks in the United States. Bridge Structures, 11(3), pp.75-85.

Tabatabai, H., Lee, C.W. and Tabatabai, M.A. (2016). Survival Analyses for Bridge Decks in Northern United States.

Tanaka, S. and Akita, S. (1975). On the miner's damage hypothesis in notched specimens with emphasis on scatter of fatigue life. Engineering Fracture Mechanics, 7(3), pp.473-480.

Tanaka, S., Ichikawa, M. and Akita, S. (1980). Statistical aspects of the fatigue life of nickel-silver wire under two-level loading. International Journal of Fatigue, 2(4), pp.159-163.

Tabatabai, M.A., Bursac, Z., Williams, D.K. and Singh, K.P. (2007). Hypertabastic survival model. Theoretical Biology and Medical Modelling, 4(1), p.40.

Theil, N. (2016). Fatigue life prediction method for the practical engineering use taking in account the effect of the overload blocks. International Journal of Fatigue, 90, pp.23-35.

Tran, X.Q. (2014). Dynamic regression models and their applications in survival and reliability analysis (Doctoral dissertation, Université de Bordeaux).

Appendix A

Table A-1: Fatigue data of category A, original database (NCHRP Report 286 by Keating and Fisher, 1986)

	Previous data		
	N_c	S_r (ksi)	Status
1	101758	51.8	1
2	118419	67.2	1
3	192913	66.2	1
4	163247	52.6	1
5	334257	53.4	1
6	433088	56.8	1
8	474606	55.9	1
8	727420	55.1	1
9	728600	33.7	1
10	1033582	46.5	1
11	1049943	40.5	1
12	1319652	41.8	1
13	1659316	38.1	1
14	1738396	29.9	1
15	1874318	39.9	1
16	2960348	45.1	0
17	3247266	33.2	1
18	3398063	37	1
19	5051971	35.9	1
20	6740198	55.1	0
21	6347469	41.2	0
22	6159303	36.4	0
23	7284526	35.9	0
24	750517	43.8	1

	Original data		
	N_c	S_r (ksi)	Status
1	553207	44.4	1
2	579220	41.8	1
3	685001	41.8	1
4	695315	45.8	1
5	750479	44.4	1
6	835187	41.8	1
7	848450	35.9	1
8	988215	35.9	1
9	1065968	41.8	1
10	1514545	35.9	1
11	1790234	41.8	1
12	1846608	35.9	1
13	2623957	29.9	1
14	2702064	42.5	1
15	4829002	29.9	0
16	6258066	29.9	1
17	7742680	35.9	1
18	9882154	35.9	0
19	9883656	34.3	0
20	10351021	29.9	0
21	10671567	29.9	0
22	12056141	29.9	0

Table A-2: Fatigue data of category B, original database (NCHRP Report 286 by Keating and Fisher, 1986)

Plain Welded Beams			
	N_C	S_r (ksi)	Status
1	316374	42.2	1
2	286163	35.2	1
3	327744	30.7	1
4	374825	36.0	1
5	387691	36.0	1
6	396580	34.8	1
7	561951	36.5	1
8	997485	36.1	1
9	953962	33.3	1
10	1154643	35.7	1
11	1181049	34.9	1
12	1105123	28.1	1
13	401401	29.4	1
14	449123	30.4	1
15	469744	31.1	1
16	562451	30.4	1
17	622418	30.1	1
18	658507	29.4	1
19	665846	30.4	1
20	745588	26.8	1
21	806454	28.4	1
22	1021090	30.1	1
23	1414923	30.4	1
24	1513982	29.4	1
25	1480791	27.5	1
26	1294720	23.7	1
27	1118434	24.2	1
28	1010733	24.2	1
29	1057257	24.2	1
30	1093549	24.2	1
31	1603101	24.2	1
32	2220179	27.5	1
33	761623	34.5	1
34	814537	36.9	1
35	688167	35.6	1

Plain Welded Beams (continued)			
	N_C	S_r (ksi)	Status
36	779517	29.7	1
37	862531	30.1	1
38	825493	23.9	1
39	1548950	27.5	1
40	2030890	22.9	1
41	1835324	22.9	1
42	1897904	24.0	1
43	2030326	24.3	1
44	2246795	24.0	1
45	2457982	24.8	1
46	2542781	24.0	1
47	2910965	22.9	1
48	4722601	22.4	1
49	4468996	18.1	1
50	4369563	18.1	1
51	3224907	18.1	1
52	2818112	17.5	1
53	2380107	18.1	1
54	2199859	18.1	1
55	2126850	18.1	1
56	1988022	18.0	1
57	3697607	12.6	1
58	6063647	13.6	1
59	5729107	15.1	1
60	5792316	16.0	1
61	6333948	18.1	1
62	6931231	17.7	1
63	7756143	17.9	1
64	9091852	13.5	1
65	10525486	13.0	1
66	9934841	17.7	0
67	11368940	18.3	0
68	10158657	18.5	1
69	2516291	20.5	1
70	2298689	22.4	1

Table A-2 (continued).

Plain Welded Beams (continued)			
	N_C	S_r (ksi)	Status
71	1532473	24.5	1
72	1354165	24.2	1
73	350339	36.4	1
74	424179	36.4	1
75	507950	34.8	1
76	502156	36.4	1
77	680998	30.4	1
78	696494	30.4	1
79	720403	30.4	1
80	745132	30.4	1
81	770710	30.4	1
82	902233	30.1	1
83	965345	29.4	1
84	922559	31.5	1
85	537253	36.0	1
86	531744	29.7	1
87	1307769	30.4	1
88	1236373	29.7	1
89	10375981	24.3	1
90	10509125	17.9	0
91	12163536	18.1	1
92	2221783	23.7	1
93	1142805	29.4	1
94	338881	32.9	1
95	1196603	24.0	1
96	1432522	24.2	1
97	965613	27.8	1

Flange Splices			
	N_C	S_r (ksi)	Status
1	286115	36.4	1
2	295937	36.4	1
3	316603	36.4	1
4	331176	36.4	1
5	346420	36.4	1
6	419434	36.4	1
7	443704	36.4	1
8	464127	36.4	1
9	490984	36.4	1
10	502603	30.4	1
11	519856	30.4	1
12	543784	30.4	1
13	727947	36.1	1
14	833119	36.5	1
15	744677	34.5	1
16	1031840	35.3	1
17	806141	30.8	1
18	1129894	30.1	1
19	1307769	30.4	1
20	1279169	28.1	1
21	1732815	29.4	1
22	1223765	24.2	1
23	1814389	24.0	1
24	1385057	24.0	1
25	789125	24.2	1
26	834833	23.9	1
27	987532	28.1	1
28	1585166	24.2	1
29	2630944	22.4	1
30	3043940	24.6	1
31	3148429	24.6	1
32	3770839	22.7	1
33	3894868	30.1	0
34	10260472	24.0	0
35	10854182	24.1	0

Table A-2 (continued).

Flange Splices (continued)			
36	3048509	18.1	1
37	9711638	18.5	0
38	12164212	17.9	0
39	614942	35.6	1
40	420110	26.2	1
41	273784	30.0	1

A514/517 Straight Taper			
	N_C	S_r	Status
1	338863	33.3	1
2	320203	36.0	1
3	688205	35.2	1
4	796591	35.3	1
5	401356	30.0	1
6	508374	29.4	1
7	525737	30.4	1
8	753563	30.4	1
9	753856	28.1	1
10	1566823	26.3	1
11	1157276	22.4	1
12	826411	19.1	1
13	651755	24.2	1
14	563076	24.2	1
15	965399	29.1	1

Table A-3: Fatigue data of category C, original database (NCHRP Report 286 by Keating and Fisher, 1986)

Transverse Web Stiffener			
	N_C	S_r (ksi)	Status
1	213270	28.92669	1
2	301665	28.90006	1
3	355516	28.88746	1
4	362063	28.88606	1
5	576631	27.55695	1
6	679567	27.54493	1
7	667277	27.54627	1
8	493773	28.86226	1
9	521561	27.5643	1
10	400293	25.86805	1
11	415174	25.86555	1
12	450710	25.8599	1
13	498299	25.85301	1
14	555963	25.84549	1
15	561060	25.84487	1
16	581917	25.84236	1
17	643361	25.83547	1
18	321563	24.05159	1
19	422820	24.03411	1
20	430608	24.03295	1
21	493773	24.02421	1
22	526342	24.02014	1
23	576631	24.01431	1
24	587252	24.01315	1
25	1043504	25.80231	1
26	869428	27.52691	1
27	885441	23.76793	1
28	1024632	23.75872	1
29	1072465	23.97477	1
30	1164261	23.96954	1
31	450710	22.95272	1
32	480439	22.94882	1

Transverse Web Stiffener (Continued)			
	N_C	S_r (ksi)	Status
33	498299	22.9466	1
34	536036	22.94215	1
35	550913	22.94048	1
36	561060	22.93937	1
37	625987	22.9327	1
38	679567	23.13899	1
39	692084	23.13787	1
40	704830	23.13675	1
41	724392	23.13507	1
42	737734	23.13395	1
43	779252	22.91936	1
44	793604	22.91825	1
45	808220	22.91714	1
46	823106	22.91603	1
47	861531	22.91325	1
48	952498	22.90714	1
49	1034025	22.90215	0
50	1122531	22.89715	1
51	1153685	22.89549	1
52	1207542	22.89271	1
53	779252	20.53023	1
54	838266	20.52625	1
55	1207542	20.50636	1
56	1263913	20.50387	1
57	1397367	20.49841	1
58	1410176	20.49791	1
59	1940791	20.48053	1
60	2308214	18.16972	0
61	1820697	18.18118	0
62	1739493	18.52008	1
63	1631855	18.52322	1
64	1476007	18.35896	1

Table A-3 (continued).

Transverse Web Stiffener (Continue)			
	N_C	S_r (ksi)	Status
65	1559073	18.52546	1
66	1544911	18.35674	1
67	808220	19.25144	1
68	838266	18.38657	1
69	1092217	19.23605	1
70	1062723	18.37499	1
71	1132821	18.37187	1
72	1164261	18.37054	1
73	1207542	18.36876	1
74	1229782	18.36787	1
75	1263913	18.36653	1
76	1322916	18.3643	1
77	1335043	19.22579	1
78	1372096	18.36252	1
79	1397367	18.36163	1
80	1436149	19.22207	1
81	1692520	19.21368	1
82	2899689	18.15872	1
83	3147882	18.15476	1
84	3176739	17.66151	1
85	3417320	17.65808	1
86	4746287	17.64268	1
87	6184169	17.63029	1
88	2287247	15.40443	1
89	3007485	15.39324	1
90	2598934	14.44142	1
91	3176739	14.43372	1
92	3778146	14.42708	1
93	4493409	14.42043	1
94	4746287	14.41834	1
95	4878014	15.37348	1
96	4412147	15.37757	1
97	3847731	13.9066	0
98	4412147	13.7746	0
99	5247436	13.76826	0
100	6072330	13.88976	0
101	6592080	13.88673	0

Transverse Web Stiffener (Continued)			
	N_C	S_r (ksi)	Status
102	7026896	13.75759	0
103	3176739	13.78663	1
104	2873349	13.7903	1
105	2205266	13.67398	1
106	2012940	13.80334	1
107	1787770	13.80769	1
108	9670900	13.746	0
109	13069000	13.746	0

Table A-3 (continued).

Flange Attachments < 2 in			
	N_C	S_r (ksi)	Status
1	242333	28.4	1
2	251342	28.4	1
3	352286	28.4	1
4	442559	28.1	1
5	526342	28.1	1
6	502867	28.1	1
7	545909	20.2	1
8	625987	20.2	1
9	661216	20.2	1
10	692084	20.2	1
11	1102230	20	1
12	1602344	19.9	1
13	1820697	20.1	1
14	1871229	20.1	1
15	1122531	16	1
16	1174933	16	1
17	1252432	16	1
18	1476007	16.1	1
19	3090954	16	1
20	3576849	16.1	1
21	3709819	16.1	1
22	2873349	12	1
23	4372068	12	1
24	10790091	12	1
25	15543384	12	1
26	3812780	12	0
27	3918599	12	0

Table A-4: Fatigue data of category D, original database (NCHRP Report 286 by Keating and Fisher, 1986)

Flange Attachments L = 4 in			
	N_C	S_r (ksi)	Status
1	100608	28.0	1
2	117243	28.0	1
3	122483	28.0	1
4	142734	28.0	1
5	159219	28.0	1
6	173768	28.0	1
7	170010	28.0	1
8	181533	28.0	1
9	228381	28.0	1
10	300629	20.0	1
11	307273	20.0	1
12	365991	20.0	1
13	382347	20.0	1
14	399433	20.0	1
15	435931	20.0	1
16	486278	20.0	1
17	497025	20.0	1
18	519236	20.0	1
19	592005	20.0	1
20	579205	20.0	1
21	497545	16.0	1
22	531267	16.0	1
23	646775	16.0	1
24	737417	16.0	1
25	822584	16.0	1
26	878336	16.0	1
27	937866	16.0	1
28	1118609	12.0	1
29	1194424	12.0	1
30	1486251	12.0	1
31	1731992	12.0	1
32	1849379	12.0	1
33	2155161	12.0	1
34	2203020	12.0	1
35	2404067	12.0	1
36	4845859	9.0	1

Flange Attachments L = 4 in (continued)			
	N_C	S_r (ksi)	Status
37	5650041	8.0	1
38	6032978	8.0	1
39	7182104	9.0	1
40	8941547	8.0	1
41	13565096	5.9	0

Table A-5: Fatigue data of category E, original database (NCHRP Report 286 by Keating and Fisher, 1986)

Coverplated Beams			
	N_C	S_r (ksi)	Status
1	392500	16	1
2	393300	16	1
3	336700	16	1
4	192200	20	1
5	168100	20	1
6	288200	20	1
7	176100	20	1
8	114400	24	1
9	93700	24	1
10	85000	24	1
11	797700	12	1
12	654500	12	1
13	724300	12	1
14	276900	16	1
15	316500	16	1
16	328600	16	1
17	325000	16	1
18	197700	20	1
19	159000	20	1
20	147800	20	1
21	2227400	8	1
22	2693100	8	1
23	2453200	8	1
24	675600	12	1
25	777600	12	1
26	657800	12	1
27	738600	12	1
28	300700	16	1
29	344100	16	1
30	297200	16	1
31	107700	20	1
32	180300	20	1
33	172000	20	1
34	166000	20	1

Coverplated Beams (continued)			
	N_C	S_r (ksi)	Status
35	418100	16	1
36	356300	16	1
37	289900	16	1
38	186600	20	1
39	154200	20	1
40	170500	20	1
41	231400	20	1
42	108200	24	1
43	842300	12	1
44	667100	12	1
45	708600	12	1
46	366400	16	1
47	264100	16	1
48	317900	16	1
49	369000	16	1
50	176700	20	1
51	172000	20	1
52	149400	20	1
53	83100	24	1
54	6317000	6	1
55	2443000	8	1
56	1976500	8	1
57	2277900	8	1
58	702200	12	1
59	757100	12	1
60	747100	12	1
61	657700	12	1
62	272700	16	1
63	314300	16	1
64	295400	16	1
65	178000	20	1
66	203900	20	1
67	159900	20	1
68	199700	20	1

Table A-5 (continued).

Coverplated Beams (continued)			
	N_C	S_r (ksi)	Status
69	394700	16	1
70	482800	16	1
71	546600	16	1
72	242700	20	1
73	295000	20	1
74	254300	20	1
75	282300	20	1
76	156600	24	1
77	137400	24	1
78	170700	24	1
79	843700	12	1
80	848300	12	1
81	1310900	12	1
82	428500	16	1
83	382100	16	1
84	498000	16	1
85	378200	16	1
86	192300	20	1
87	242800	20	1
88	260000	20	1
89	154100	24	1
90	1988900	8	1
91	3409200	8	1
92	821700	12	1
93	1004700	12	1
94	1220000	12	1
95	755200	12	1
96	324800	16	1
97	378000	16	1
98	440800	16	1
99	196400	20	1
100	245400	20	1
101	220300	20	1
102	174000	20	1

Coverplated Beams (continued)			
	N_C	S_r (ksi)	Status
103	555000	16	1
104	552500	16	1
105	484200	16	1
106	192200	20	1
107	227500	20	1
108	288200	20	1
109	242900	20	1
110	114400	24	1
111	134900	24	1
112	209100	24	1
113	1073800	12	1
114	1272400	12	1
115	1392100	12	1
116	364100	16	1
117	565600	16	1
118	647800	16	1
119	546100	16	1
120	247700	20	1
121	245700	20	1
122	310400	20	1
123	2227400	8	1
124	2693100	8	1
125	3428100	8	1
126	844500	12	1
127	945400	12	1
128	1039300	12	1
129	811600	12	1
130	378800	16	1
131	441400	16	1
132	409700	16	1
133	107700	20	1
134	207400	20	1
135	195500	20	1
136	192600	20	1

Table A-5 (continued).

Coverplated Beams (continued)			
	N_C	S_r (ksi)	Status
137	660300	16	1
138	567700	16	1
139	529500	16	1
140	186600	20	0
141	318100	20	1
142	319700	20	1
143	316600	20	1
144	150500	24	1
145	1004800	12	1
146	667100	12	0
147	1150700	12	1
148	366400	16	1
149	475300	16	1
150	423500	16	1
151	256800	20	1
152	249100	20	1
153	257600	20	1
154	113600	24	1
155	5488400	6	1
156	2713600	8	1
157	3132200	8	1
158	2919800	8	1
159	965900	12	1
160	1085800	12	1
161	993900	12	1
162	930500	12	1
163	446400	16	1
164	459200	16	1
165	450800	16	1
166	228500	20	1
167	265700	20	1
168	217800	20	1
169	199700	20	1

Coverplated Beams (continued)			
	N_C	S_r (ksi)	Status
170	514800	16	1
171	1227800	16	1
172	854900	16	1
173	341300	20	1
174	429100	20	1
175	445900	20	1
176	282300	20	1
177	156600	24	1
178	213800	24	1
179	285200	24	1
180	1031100	12	1
181	848300	12	0
182	1310900	12	1
183	428500	16	1
184	542200	16	1
185	598500	16	1
186	492900	16	1
187	192300	20	1
188	339500	20	1
189	260000	20	1
190	192500	24	1
191	1988900	8	1
192	2916200	8	1
193	3409200	8	1
194	821700	12	1
195	1004700	12	1
196	1220000	12	1
197	755200	12	1
198	412500	16	1
199	589600	16	1
200	578000	16	1
201	238800	20	1
202	374000	20	1
203	296000	20	1
204	207000	20	1

Table A-5 (continued).

Coverplated Beams (continued)			
	N_C	S_r (ksi)	Status
205	427400	16	1
206	411800	16	1
207	592600	16	1
208	150000	20	1
209	190000	20	1
210	217900	20	1
211	112300	24	1
212	80800	24	1
213	101200	24	1
214	904300	12	1
215	1033700	12	1
216	755100	12	1
217	373800	16	1
218	345700	16	1
219	481100	16	1
220	166400	20	1
221	185700	20	1
222	188400	20	1
223	84500	24	1
224	8946200	6	1
225	3211100	8	1
226	4979000	8	1
227	4798200	8	1
228	778500	12	1
229	632100	12	1
230	919200	12	1
231	423100	16	1
232	503200	16	1
233	371400	16	1
234	189600	20	1

Coverplated Beams (continued)			
	N_C	S_r (ksi)	Status
235	352500	16	1
236	275700	16	0
237	291300	16	1
238	186300	20	1
239	158200	20	1
240	204000	20	1
241	89300	24	1
242	97000	24	1
243	70500	24	1
244	1768900	12	1
245	1139100	12	1
246	1109400	12	1
247	499500	16	1
248	444200	16	1
249	410400	16	1
250	207500	20	1
251	176300	20	1
252	155000	20	1
253	3588700	8	1
254	3460700	8	1
255	4706800	8	1
256	1113300	12	1
257	878700	12	1
258	907500	12	1
259	277600	16	1
260	472600	16	1
261	522600	16	1
262	120000	20	1
263	147600	20	1
264	233900	20	1

Table A-5 (continued).

Coverplated Beams (continued)			
	N_C	S_r (ksi)	Status
265	6111000	8	1
266	6317000	8	1
267	2866000	8	1
268	7004000	8	1
269	2960000	9	1
270	3681000	9	1
271	808000	12	1
272	1147000	12	1
273	1225000	12	1
274	595000	16	1
275	714000	16	1
276	491000	16	1
277	885000	16	1
278	518000	16	1
279	714000	16	1
280	279000	20	1
281	279000	20	1
282	192000	20	1
283	213000	20	1
284	786000	15	1
285	855000	15	1
286	175000	20	1
287	190000	20	1
288	165000	24	1
289	165000	24	1
290	167000	24	1

Coverplated Beams (continued)			
	N_C	S_r (ksi)	Status
291	320100	16	1
292	391900	16	1
293	265500	16	1
294	160300	20	1
295	121200	20	1
296	122600	20	1
297	80700	24	1
298	105000	24	1
299	83300	24	1
300	949400	12	1
301	951100	12	1
302	976900	12	1
303	342700	16	1
304	357800	16	1
305	472500	16	1
306	172000	20	1
307	166800	20	1
308	226400	20	1
309	3728600	8	1
310	3679300	8	1
311	3217900	8	1
312	1011000	12	1
313	855700	12	1
314	1186400	12	1
315	334100	16	1
316	598400	16	1
317	433400	16	1
318	184600	20	1
319	141400	20	1
320	273900	20	1

Table A-5 (continued).

Coverplated Beams (continued)			
	N_C	S_r (ksi)	Status
321	135599	24.0	1
322	151247	24.0	1
323	155434	24.0	1
324	171020	24.0	1
325	193378	24.0	1
326	207038	24.0	1
327	215693	24.0	1
328	107571	20.0	1
329	287316	24.0	1
330	5505186	6.0	1
331	1239579	16.0	1
332	338638	20.0	1
333	135599	24.0	1
334	151247	24.0	1
335	155434	24.0	1
336	171020	24.0	1
337	193378	24.0	1
338	207038	24.0	1
339	215693	24.0	1

8 in Flange Attachments			
	N_C	S_r (ksi)	Status
1	3701033	9.0	1
2	7032651	8.0	1
3	717965.8	16.0	1
4	857564.6	15.0	1
5	881121.9	16	1

Wide Coverplates without End Welds			
	N_C	S_r (ksi)	Status
1	308200	16.0	1
2	156700	16.0	1
3	198600	16.0	1
4	186300	20.0	1
5	158200	20.0	1
6	122400	20.0	1
7	77400	24.0	1
8	47500	24.0	1
9	53600	24.0	1
10	557600	12.0	1
11	432900	12.0	1
12	440600	12.0	1
13	232400	16.0	1
14	178700	16.0	1
15	197600	16.0	1
16	99700	20.0	1
17	103200	20.0	1
18	142200	20.0	1
19	1533600	8.0	1
20	1211800	8.0	1
21	1374000	8.0	1
22	385500	12.0	1
23	313300	12.0	1
24	551400	12.0	1
25	149500	16.0	1
26	208900	16.0	1
27	220700	16	1
28	68700	20	1
29	100500	20	1
30	136300	20	1

Table A-6: Fatigue data of category E′, original database (NCHRP Report 286 by Keating and Fisher, 1986)

Coverplated Beams			
	N_C	S_r (ksi)	Status
1	827065	8.0	1
2	942955.8	8.0	1
3	1098841	8.0	1
4	1397482	8.0	1
5	1459924	8.0	1
6	1525156	8.0	1
7	1664493	8.0	1
8	1777288	8.0	1
9	2116866	8.0	1
10	2026327	8.0	1
11	2362051	8.0	1
12	2577847	8.0	1
13	2939062	8.0	1
14	3904848	8.0	1
15	2126184	6.0	1
16	3514921	6.0	1
17	5096578	6.0	1
18	7720148	6.0	1
19	9398384	6.0	1
20	11445030	6.0	1
21	12561375	4.0	1
22	21571650	6.0	0
23	24062631	6.0	0
24	27434357	6.0	0
25	32861154	4.0	1
26	41805216	4.0	0
27	48716277	4.0	0
28	58024267	4.0	0
29	66154797	4.0	0

Data from Figure 14 Report 286 Penetrating Web Plate			
	N_C	S_r (ksi)	Status
1	139935	11.6	1
2	350966	14.3	1
3	515626	13.5	1
4	495181	10.5	1
5	552753	10.1	1
6	905832	11.7	1
7	1082976	11.4	1
8	1068908	9.2	1
9	1194069	6.9	1
10	971575	7.4	1
11	8634881	5.1	1

Data from Figure 14 Report 286 Greater than 1 in Thickness			
	N_C	S_r (ksi)	Status
1	679363	9.3	1
2	778891	11.4	1
3	944592	9.3	1
4	1160668	9.3	1
5	1039906	9.3	1
6	985293	6.7	1
7	1177831	6.8	1
8	1776933	8.8	1
9	1425292	11.4	1
10	1505778	11.4	1
11	957890	8.6	1
12	3485162	6.9	1
13	4978483	8.1	1
14	4914620	6.1	1
15	4344112	5.7	1
16	3301997	5.1	1

Appendix B

This appendix includes the SAS and Mathematica codes used for data analysis in this study. These codes were used to find the maximum log-likelihood values and the parameters for Weibull, Lognormal, log-logistic, and hypertabastic distributions.

B.1 SAS Code for Weibull Distribution

```
Proc nlp data=Mylib.Fatiguedata tech=quanew cov=2 vardef=n pcov phes
maxiter=250;
/*Weibull Accelerated Failure Model*/
title1 'Fatigue-Wribull Accelerated Failure Model-Log time';  /*fit model 1*/
max logf;
parms alpha=0.01, beta=0.1, c1=0.01, c2=0, c3=0, c4=0, c5=0, c6=0, c7=0;
Bounds alpha>0;
Bounds beta>0;
t=NC/1000;
Eg = exp(c1*SR + c2*A + c3*B+c4*C+c5*D+c6*E+c7*EP);
tg = t*Eg;
t1 = (tg/alpha)**beta;
t2 = (tg/alpha)**(beta-1);
S1 = exp(-t1);
h = (beta/alpha)*t2;
survival = log(S1) + Status*log(t*h*Eg);
logf=survival;
run;
ods graphics off;
```

B.2 SAS Code for Lognormal Distribution

```
Proc nlp data=Mylib.Fatiguedata tech=quanew cov=2 vardef=n pcov phes
maxiter=15000;
/*Lognormal Accelerated Failure Model*/
title1 'Fatigue-Lognormal Accelerated Failure Model-Log time';  /*fit model 1*/
max logf;
parms alpha=3, beta=.01, c1=0.1, c2=0, c3=0, c4=0, c5=0, c6=0, c7=0;
Bounds alpha>0;
Bounds beta>0;
t=NC/1000;
Eg = exp(c1*SR + c2*A + c3*B+c4*C+c5*D+c6*E+c7*EP);
tg = t*Eg;
pi=constant("pi");
St = (1/2)-(1/2)*erf((log(tg)-alpha)/(beta*sqrt(2)));
h1=(-1)*sqrt(2)*exp((((-1)*(log(tg)-alpha))**2)/(2*beta**2));
h2=1/(sqrt(pi)*tg*beta);
h3=1/(erf((sqrt(2)*(log(tg)-alpha))/(2*beta))-1);
h=h1*h2*h3;
survival = log(St) + Status*log(h*t*Eg);
logf=survival ;
run;
ods graphics off;
```

B.3 SAS Code for Log-logistic Distribution

```
Proc nlp data=Mylib.Fatiguedata tech=quanew cov=2 vardef=n pcov phes
maxiter=250;
/*Loglogistic Accelerated Failure Model*/
title1 'Fatigue-Loglogistic Accelerated Failure Model-Log time';  /*fit model
1*/
max logf;
parms alpha=1, beta=3, c1=0.1, c2=0, c3=0, c4=0, c5=0, c6=0, c7=0;
Bounds alpha>0;
Bounds beta>0;
t=NC/1000;
Eg = exp(c1*SR + c2*A + c3*B+c4*C+c5*D+c6*E+c7*EP);
tg = t*Eg;
t1 = (tg/alpha)**beta;
t2 = (tg/alpha)**(beta-1);
S1 = 1/(1+(t1));
h = ((beta/alpha)*t2)/(1+t1);
survival = log(S1) + Status*log(t*h*Eg);
logf=survival;
run;
ods graphics off;
```

B.4 SAS Code for Hypertabastic Distribution

```
Proc nlp data=Mylib.Fatiguedata tech=quanew cov=2 vardef=n pcov phes
maxiter=250;
/*Hypertabastic Accelerated Failure Model*/
title1 'Fatigue-Hypertabastic Accelerated Failure Model-Log time';  /*fit model
1*/
max logf;
parms alpha=0.01, beta=0.1, c1=0.01, c2=0, c3=0, c4=0, c5=0, c6=0, c7=0;
Bounds alpha>0;
Bounds beta>0;
t=NC/1000;
Eg = exp(c1*SR + c2*A + c3*B+c4*C+c5*D+c6*E+c7*EP);
tg = t*Eg;
t1 = tg**beta;
t2 = tg**(beta-1);
t3 = tg**(2*beta-1);
W = alpha*(1-t1*(1/tanh(t1)))/beta;
S1 = 1/cosh(W);
h = alpha*(t3*(1/sinh(t1))**2-t2*(1/tanh(t1)))*tanh(W);
survival = log(S1) + Status*log(t*h*Eg);
logf=survival;
run;
ods graphics off;
```

B.5 Mathematica Code for Lognormal Distribution

```
In[ · ]:= n = 780;
t = N[
Rationalize[{1.01758, 1.184185, 1.929133, 1.632468, 3.342573, 4.330875, 4.746055, 7.2742,
7.286002, 10.335824, 10.499428, 13.196519, 16.593162, 17.383961, 18.74318, 29.60348,
32.472662, 33.980631, 50.519712, 67.401977, 63.474692, 61.593032, 72.845255, 7.505166,
5.532074, 5.792199, 6.85001, 6.953151, 7.504785, 8.351873, 8.484503, 9.882154,
10.65968, 15.145446, 17.902337, 18.466083, 26.239568, 27.020643, 48.290015,
62.580658, 77.426804, 98.821536, 98.836556, 103.510205, 106.715672, 120.561414,
3.163742, 2.86163, 3.277438, 3.748247, 3.876913, 3.965796, 5.619509, 9.974846,
9.539624, 11.54643, 11.810489, 11.051229, 4.014008, 4.491231, 4.697437, 5.624507,
6.22418, 6.585067, 6.658459, 7.455877, 8.064543, 10.210903, 14.149226, 15.139823,
14.807906, 12.947201, 11.184336, 10.107334, 10.572567, 10.935492, 16.031005,
22.201791, 7.616226, 8.145369, 6.88167, 7.795166, 8.625312, 8.254934, 15.489503,
20.308901, 18.353244, 18.979038, 20.303261, 22.467953, 24.579823, 25.427813,
29.109649, 47.22601, 44.689955, 43.69563, 32.249074, 28.181115, 23.80107, 21.998588,
21.268504, 19.880221, 36.976074, 60.636466, 57.291073, 57.923163, 63.33948, 69.312312,
77.561428, 90.918521, 105.254858, 99.34841, 113.689403, 101.586574, 25.162909,
22.986888, 15.324729, 13.541645, 3.503389, 4.241794, 5.079504, 5.021562, 6.809977,
6.964943, 7.204029, 7.451322, 7.707103, 9.022329, 9.653452, 9.225588, 5.372528,
5.317444, 13.077689, 12.36373, 103.759805, 105.091251, 121.635358, 22.217832,
11.428045, 3.388813, 11.96603, 14.325217, 9.656134, 2.861153, 2.959368, 3.166028,
3.311758, 3.464195, 4.19434, 4.43704, 4.641274, 4.909836, 5.026028, 5.198557,
5.437842, 7.279465, 8.331185, 7.446769, 10.318399, 8.061407, 11.298941, 13.077689,
12.791692, 17.328152, 12.237645, 18.143889, 13.850565, 7.891247, 8.348329, 9.875317,
15.851662, 26.309442, 30.439395, 31.484288, 37.708394, 38.948676, 102.604716,
108.541818, 30.485089, 97.116383, 121.642116, 6.149422, 4.201103, 2.737836,
3.388625, 3.202026, 6.882052, 7.965909, 4.013562, 5.083739, 5.257372, 7.535625,
7.538556, 15.66823, 11.572761, 8.264111, 6.517551, 5.63076, 9.653988, 2.13270107,
3.016646621, 3.55515592, 3.620634425, 5.766313932, 6.795673372, 6.672774875,
4.937727067, 5.215610511, 4.002928263, 4.151737193, 4.507097589, 4.982990882,
5.559634422, 5.61059922, 5.819173347, 6.433605475, 3.215625928, 4.228203472,
4.306078098, 4.937727067, 5.263421666, 5.766313932, 5.872517322, 10.43503849,
8.694283906, 8.854414354, 10.24632275, 10.72464909, 11.64260593, 4.507097589,
4.804387683, 4.982990882, 5.360362837, 5.50913257, 5.61059922, 6.259871088,
6.795673372, 6.920835401, 7.048302652, 7.243918907, 7.377336678, 7.792515504,
7.936037272, 8.082202408, 8.2310596, 8.615307952, 9.524977021, 10.34025011,
11.22530502, 11.53684841, 12.07542002, 7.792515504, 8.382658428, 12.07542002,
12.63913362, 13.97366849, 14.10176418, 19.40791422, 23.08214101, 18.20697436,
17.39493144, 16.31855269, 14.76007306, 15.5907346, 15.4491136, 8.082202408,
8.382658428, 10.9221746, 10.62722998, 11.32820664, 11.64260593, 12.07542002,
12.29782389, 12.63913362, 13.22916291, 13.35043377, 13.72095728, 13.97366849,
14.36148906, 16.92519518, 28.99688773, 31.47882361, 31.76738789, 34.17319628,
47.46287364, 61.84169348, 22.8724706, 30.07484755, 25.98933962, 31.76738789,
37.7814596, 44.93409071, 47.46287364, 48.78014251, 44.12146599, 38.47731472,
44.12146599, 52.47436114, 60.72329788, 65.92079816, 70.26896233, 31.76738789,
28.73348974, 22.05266247, 20.12940378, 17.8777046, 96.709, 130.69, 2.423328,
2.513415, 3.522862, 4.425588, 5.263422, 5.02867, 5.459089, 6.259871, 6.612162,
6.920835, 11.022297, 16.023435, 18.206974, 18.712285, 11.225305, 11.749333,
12.524324, 14.760073, 30.909535, 35.768494, 37.098189, 28.73349, 43.720681,
107.900908, 155.433839, 38.1278, 39.185986, 1.00608466, 1.172433479, 1.224827639,
1.427344027, 1.592192518, 1.737677239, 1.700104939, 1.815331231, 2.28380551,


3.006287171, 3.072726083, 3.659914284, 3.823469948, 3.99433465, 4.359312285,
4.862783097, 4.970250547, 5.192363025, 5.920049649, 5.79204551, 4.975451655,
5.312667806, 6.467748315, 7.374174525, 8.225841345, 8.783355868, 9.378656488,
```

```
11.18608703, 11.94423513, 14.86251063, 17.31991921, 18.49379385, 21.55160884,
22.03020316, 24.04067254, 48.45859322, 56.50041014, 60.32978125, 71.82104227,
89.41546755, 135.6509554, 3.925, 3.933, 3.367, 1.922, 1.681, 2.882, 1.761, 1.144,
0.937, 0.85, 7.977, 6.545, 7.243, 2.769, 3.165, 3.286, 3.25, 1.977, 1.59, 1.478,
22.274, 26.931, 24.532, 6.756, 7.776, 6.578, 7.386, 3.007, 3.441, 2.972, 1.077,
1.803, 1.72, 1.66, 4.181, 3.563, 2.899, 1.866, 1.542, 1.705, 2.314, 1.082, 8.423,
6.671, 7.086, 3.664, 2.641, 3.179, 3.69, 1.767, 1.72, 1.494, 0.831, 63.17, 24.43,
19.765, 22.779, 7.022, 7.571, 7.471, 6.577, 2.727, 3.143, 2.954, 1.78, 2.039, 1.599,
1.997, 3.947, 4.828, 5.466, 2.427, 2.95, 2.543, 2.823, 1.566, 1.374, 1.707, 8.437,
8.483, 13.109, 4.285, 3.821, 4.98, 3.782, 1.923, 2.428, 2.6, 1.541, 19.889, 56.986,
34.092, 8.217, 10.047, 12.2, 7.552, 3.248, 3.78, 4.408, 1.964, 2.454, 2.203, 1.74,
5.55, 5.525, 4.842, 1.922, 2.275, 2.882, 2.429, 1.144, 1.349, 2.091, 10.738, 12.724,
13.921, 3.641, 5.656, 6.478, 5.461, 2.477, 2.457, 3.104, 22.274, 26.931, 34.281,
8.445, 9.454, 10.393, 8.116, 3.788, 4.414, 4.097, 1.077, 2.074, 1.955, 1.926, 6.603,
5.677, 5.295, 1.866, 3.181, 3.197, 3.166, 1.505, 10.048, 6.671, 11.507, 3.664, 4.753,
4.235, 2.568, 2.491, 2.576, 1.136, 54.884, 27.136, 31.322, 29.198, 9.659, 10.858,
9.939, 9.305, 4.464, 4.592, 4.508, 2.285, 2.657, 2.178, 1.997, 5.148, 12.278, 8.549,
3.413, 4.291, 4.459, 2.823, 1.566, 2.138, 2.852, 10.311, 8.483, 13.109, 4.285, 5.422,
5.985, 4.929, 1.923, 3.395, 2.6, 1.925, 19.889, 29.162, 34.092, 8.217, 10.047,
12.2, 7.552, 4.125, 5.896, 5.78, 2.388, 3.74, 2.96, 2.07, 4.274, 4.118, 5.926, 1.5,
1.9, 2.179, 1.123, 0.808, 1.012, 9.043, 10.337, 7.551, 3.738, 3.457, 4.811, 1.664,
1.857, 1.884, 0.845, 89.462, 32.111, 49.79, 47.982, 7.785, 6.321, 9.192, 4.231,
5.032, 3.714, 1.896, 3.525, 2.757, 2.913, 1.863, 1.582, 2.04, 0.893, 0.97, 0.705,
17.689, 11.391, 11.094, 4.995, 4.442, 4.104, 2.075, 1.763, 1.55, 35.887, 34.607,
47.068, 11.133, 8.787, 9.075, 2.776, 4.726, 5.226, 1.2, 1.476, 2.339, 3.082, 1.567,
1.986, 1.863, 1.582, 1.224, 0.774, 0.475, 0.536, 5.576, 4.329, 4.406, 2.324, 1.787,
1.976, 0.997, 1.032, 1.422, 15.336, 12.118, 13.74, 3.855, 3.133, 5.514, 1.495,
2.089, 2.207, 0.687, 1.005, 1.363, 61.11, 63.17, 28.66, 70.04, 29.6, 36.81, 8.08,
11.47, 12.25, 5.95, 7.14, 4.91, 8.85, 5.18, 7.14, 2.79, 2.79, 1.92, 2.13, 7.86,
8.55, 1.75, 1.9, 1.65, 1.65, 1.67, 3.201, 3.919, 2.655, 1.603, 1.212, 1.226, 0.807,
1.05, 0.833, 9.494, 9.511, 9.769, 3.427, 3.578, 4.725, 1.72, 1.668, 2.264, 37.286,
36.793, 32.179, 10.11, 8.557, 11.864, 3.341, 5.984, 4.334, 1.846, 1.414, 2.739,
1.355991302, 1.512472385, 1.554336664, 1.710199688, 1.933776116, 2.070381059,
2.156933433, 1.075714587, 2.873158828, 55.05185855, 12.39578922, 3.386378775,
1.355991302, 1.512472385, 1.554336664, 1.710199688, 1.933776116, 2.070381059,
2.156933433, 37.0103336, 70.32651004, 7.17965761, 8.575646443, 8.8112194,
8.270650394, 9.429558098, 10.98841275, 13.97482483, 14.59924058, 15.25155614,
16.64492883, 17.77287888, 21.1686592, 20.26326661, 23.62051326, 25.77846867,
29.39062304, 39.04847643, 21.26183892, 35.14921148, 50.9657797, 77.20148442,
93.983836, 114.4502989, 125.6137499, 215.7165032, 240.6263054, 274.3435665,
328.611543, 418.0521594, 487.1627739, 580.2426722, 661.5479712}, 0], 25];
x1 =
N[Rationalize[{51.8, 67.2, 66.2, 52.6, 53.4, 56.8, 55.9, 55.1, 33.7, 46.5, 40.5, 41.8,
38.1,
29.9, 39.9, 45.1, 33.2, 37.0, 35.9, 55.1, 41.2, 36.4, 35.9, 43.8, 44.4, 41.8, 41.8, 45.8,
44.4, 41.8, 35.9, 35.9, 41.8, 35.9, 41.8, 35.9, 29.9, 42.5, 29.9, 29.9, 35.9, 35.9,
34.3, 29.9, 29.9, 29.9, 42.2, 35.2, 30.7, 36.0, 36.0, 34.8, 36.5, 36.1, 33.3, 35.7,
34.9, 28.1, 29.4, 30.4, 31.1, 30.4, 30.1, 29.4, 30.4, 26.8, 28.4, 30.1, 30.4, 29.4, 27.5,
23.7, 24.2, 24.2, 24.2, 24.2, 24.2, 27.5, 34.5, 36.9, 35.6, 29.7, 30.1, 23.9,
27.5, 22.9, 22.9, 24.0, 24.3, 24.0, 24.8, 24.0, 22.9, 22.4, 18.1, 18.1, 18.1, 17.5,
18.1, 18.1, 18.1, 18.0, 12.6, 13.6, 15.1, 16.0, 18.1, 17.7, 17.9, 13.5, 13.0, 17.7,
18.3, 18.5, 20.5, 22.4, 24.5, 24.2, 36.4, 36.4, 34.8, 36.4, 30.4, 30.4, 30.4, 30.4,
30.4, 30.1, 29.4, 31.5, 36.0, 29.7, 30.4, 29.7, 24.3, 17.9, 18.1, 23.7, 29.4, 32.9,
24.0, 24.2, 27.8, 36.4, 36.4, 36.4, 36.4, 36.4, 36.4, 36.4, 36.4, 36.4, 30.4, 30.4,
30.4, 36.1, 36.5, 34.5, 35.3, 30.8, 30.1, 30.4, 28.1, 29.4, 24.2, 24.0, 24.0, 24.2,
23.9, 28.1, 24.2, 22.4, 24.6, 24.6, 22.7, 30.1, 24.0, 24.1, 18.1, 18.5, 17.9, 35.6,
26.2, 30.0, 33.3, 36.0, 35.2, 35.3, 30.0, 29.4, 30.4, 30.4, 28.1, 26.3, 22.4, 19.1,
24.2, 24.2, 29.1, 28.9, 28.9, 28.9, 28.9, 27.6, 27.5, 27.5, 28.9, 27.6, 25.9, 25.9,
```

```
25.9, 25.9, 25.8, 25.8, 25.8, 25.8, 24.1, 24.0, 24.0, 24.0, 24.0, 24.0, 24.0, 25.8,
27.5, 23.8, 23.8, 24.0, 24.0, 23.0, 22.9, 22.9, 22.9, 22.9, 22.9, 22.9, 23.1, 23.1,
23.1, 23.1, 23.1, 22.9, 22.9, 22.9, 22.9, 22.9, 22.9, 22.9, 22.9, 22.9, 22.9, 20.5,
20.5, 20.5, 20.5, 20.5, 20.5, 20.5, 18.2, 18.2, 18.5, 18.5, 18.4, 18.5, 18.4, 19.3,
18.4, 19.2, 18.4, 18.4, 18.4, 18.4, 18.4, 18.4, 18.4, 19.2, 18.4, 18.4, 19.2, 19.2,
18.2, 18.2, 17.7, 17.7, 17.6, 17.6, 15.4, 15.4, 14.4, 14.4, 14.4, 14.4, 14.4, 15.4,
15.4, 13.9, 13.8, 13.8, 13.9, 13.9, 13.8, 13.8, 13.8, 13.7, 13.8, 13.8, 13.7, 13.7,
28.4, 28.4, 28.4, 28.1, 28.1, 28.1, 20.2, 20.2, 20.2, 20.2, 20.0, 19.9, 20.1, 20.1,
16.0, 16.0, 16.0, 16.1, 16.0, 16.1, 16.1, 12.0, 12.0, 12.0, 12.0, 12.0, 12.0, 28.0,
28.0, 28.0, 28.0, 28.0, 28.0, 28.0, 28.0, 28.0, 20.0, 20.0, 20.0, 20.0, 20.0, 20.0,
20.0, 20.0, 20.0, 20.0, 20.0, 16.0, 16.0, 16.0, 16.0, 16.0, 16.0, 16.0, 12.0, 12.0,
12.0, 12.0, 12.0, 12.0, 12.0, 12.0, 9.0, 8.0, 8.0, 9.0, 8.0, 5.9, 16.0, 16.0, 16.0,
20.0, 20.0, 20.0, 20.0, 24.0, 24.0, 24.0, 12.0, 12.0, 12.0, 16.0, 16.0, 16.0, 16.0,
20.0, 20.0, 20.0, 8.0, 8.0, 8.0, 12.0, 12.0, 12.0, 12.0, 16.0, 16.0, 16.0, 20.0, 20.0,
20.0, 20.0, 16.0, 16.0, 16.0, 20.0, 20.0, 20.0, 20.0, 24.0, 12.0, 12.0, 12.0, 16.0,
16.0, 16.0, 16.0, 20.0, 20.0, 20.0, 24.0, 6.0, 8.0, 8.0, 8.0, 12.0, 12.0, 12.0, 12.0,
16.0, 16.0, 16.0, 20.0, 20.0, 20.0, 20.0, 16.0, 16.0, 16.0, 20.0, 20.0, 20.0, 20.0,
24.0, 24.0, 24.0, 12.0, 12.0, 12.0, 16.0, 16.0, 16.0, 16.0, 20.0, 20.0, 20.0, 24.0,
8.0, 8.0, 8.0, 12.0, 12.0, 12.0, 12.0, 16.0, 16.0, 16.0, 20.0, 20.0, 20.0, 20.0, 16.0,
16.0, 16.0, 20.0, 20.0, 20.0, 20.0, 24.0, 24.0, 24.0, 12.0, 12.0, 12.0, 16.0, 16.0,
16.0, 16.0, 20.0, 20.0, 20.0, 8.0, 8.0, 8.0, 12.0, 12.0, 12.0, 12.0, 16.0, 16.0,
16.0, 20.0, 20.0, 20.0, 20.0, 16.0, 16.0, 16.0, 20.0, 20.0, 20.0, 20.0, 24.0, 12.0,
12.0, 12.0, 16.0, 16.0, 16.0, 20.0, 20.0, 20.0, 24.0, 6.0, 8.0, 8.0, 8.0, 12.0, 12.0,
12.0, 12.0, 16.0, 16.0, 16.0, 20.0, 20.0, 20.0, 20.0, 16.0, 16.0, 16.0, 20.0, 20.0,
20.0, 20.0, 24.0, 24.0, 24.0, 12.0, 12.0, 12.0, 16.0, 16.0, 16.0, 16.0, 20.0, 20.0,
20.0, 24.0, 8.0, 8.0, 8.0, 12.0, 12.0, 12.0, 12.0, 16.0, 16.0, 16.0, 20.0, 20.0,
20.0, 20.0, 16.0, 16.0, 16.0, 20.0, 20.0, 20.0, 24.0, 24.0, 24.0, 12.0, 12.0, 12.0,
16.0, 16.0, 16.0, 20.0, 20.0, 20.0, 24.0, 6.0, 8.0, 8.0, 8.0, 12.0, 12.0, 12.0, 16.0,
16.0, 16.0, 20.0, 16.0, 16.0, 16.0, 20.0, 20.0, 20.0, 24.0, 24.0, 24.0, 12.0, 12.0,
12.0, 16.0, 16.0, 16.0, 20.0, 20.0, 20.0, 8.0, 8.0, 8.0, 12.0, 12.0, 12.0, 16.0,
16.0, 16.0, 20.0, 20.0, 20.0, 16.0, 16.0, 16.0, 20.0, 20.0, 20.0, 24.0, 24.0, 24.0,
12.0, 12.0, 12.0, 16.0, 16.0, 16.0, 20.0, 20.0, 20.0, 8.0, 8.0, 8.0, 12.0, 12.0,
12.0, 16.0, 16.0, 16.0, 20.0, 20.0, 20.0, 8.0, 8.0, 8.0, 8.0, 8.9, 9.0, 12.0, 12.0,
12.0, 16.0, 16.0, 16.0, 16.0, 16.0, 16.0, 20.0, 20.0, 20.0, 20.0, 14.9, 15.0, 20.0,
20.0, 24.0, 24.0, 24.0, 16.0, 16.0, 16.0, 20.0, 20.0, 20.0, 24.0, 24.0, 24.0, 12.0,
12.0, 12.0, 16.0, 16.0, 16.0, 20.0, 20.0, 20.0, 8.0, 8.0, 8.0, 12.0, 12.0, 12.0,
16.0, 16.0, 16.0, 20.0, 20.0, 20.0, 24.0, 24.0, 24.0, 24.0, 24.0, 24.0, 24.0, 20.0,
24.0, 6.0, 16.0, 20.0, 24.0, 24.0, 24.0, 24.0, 24.0, 24.0, 24.0, 9.0, 8.0, 16.0,
15.0, 16.0, 8.0, 8.0, 8.0, 8.0, 8.0, 8.0, 8.0, 8.0, 8.0, 8.0, 8.0, 8.0, 8.0, 8.0,
6.0, 6.0, 6.0, 6.0, 6.0, 6.0, 4.0, 6.0, 6.0, 6.0, 4.0, 4.0, 4.0, 4.0, 4.0}, 0], 25];


Status ={1, 1, 1, 1, 1, 1, 1, 1, 1, 1, 1, 1, 1, 1, 1, 0, 1, 1, 1, 0, 0, 0, 0, 1, 1, 1, 1,
1, 1, 1, 1,
1, 1, 1, 1, 1, 1, 1, 0, 1, 1, 0, 0, 0, 0, 0, 1, 1, 1, 1, 1, 1, 1, 1, 1, 1, 1, 1, 1, 1,
1, 1, 1, 1, 1, 1, 1, 1, 1, 1, 1, 1, 1, 1, 1, 1, 1, 1, 1, 1, 1, 1, 1, 1, 1, 1, 1, 1, 1, 1,
1, 1, 1, 1, 1, 1, 1, 1, 1, 1, 1, 1, 1, 1, 1, 1, 1, 1, 1, 1, 0, 0, 1, 1, 1, 1, 1, 1, 1, 1,
1, 1, 1, 1, 1, 1, 1, 1, 1, 1, 1, 1, 1, 1, 0, 1, 1, 1, 1, 1, 1, 1, 1, 1, 1, 1, 1, 1, 1, 1,
1, 1, 1, 1, 1, 1, 1, 1, 1, 1, 1, 1, 1, 1, 1, 1, 1, 1, 1, 1, 1, 1, 1, 1, 0, 0, 0, 1, 0, 0,
1, 1, 1, 1, 1, 1, 1, 1, 1, 1, 1, 1, 1, 1, 1, 1, 1, 1, 1, 1, 1, 1, 1, 1, 1, 1, 1, 1, 1, 1,
1, 1, 1, 1, 1, 1, 1, 1, 1, 1, 1, 1, 1, 1, 1, 1, 1, 1, 1, 1, 1, 1, 1, 1, 1, 1, 1, 1, 1, 1,
1, 1, 1, 1, 1, 1, 0, 1, 1, 1, 1, 1, 1, 1, 1, 1, 1, 0, 0, 1, 1, 1, 1, 1, 1, 1, 1, 1, 1, 1,
1, 1, 1, 1, 1, 1, 1, 1, 1, 1, 1, 1, 1, 1, 1, 1, 1, 1, 1, 1, 1, 1, 1, 1, 0, 0, 0, 0, 0, 0,
1, 1, 1, 1, 1, 0, 0, 1, 1, 1, 1, 1, 1, 1, 1, 1, 1, 1, 1, 1, 1, 1, 1, 1, 1, 1, 1, 1, 1, 1,
1, 1, 0, 0, 1, 1, 1, 1, 1, 1, 1, 1, 1, 1, 1, 1, 1, 1, 1, 1, 1, 1, 1, 1, 1, 1, 1, 1, 1, 1,
1, 1, 1, 1, 1, 1, 1, 1, 1, 1, 1, 1, 1, 1, 0, 1, 1, 1, 1, 1, 1, 1, 1, 1, 1, 1, 1, 1, 1, 1,
1, 1, 1, 1, 1, 1, 1, 1, 1, 1, 1, 1, 1, 1, 1, 1, 1, 1, 1, 1, 1, 1, 1, 1, 1, 1, 1, 1, 1, 1,
1, 1, 1, 1, 1, 1, 1, 1, 1, 1, 1, 1, 1, 1, 1, 1, 1, 1, 1, 1, 1, 1, 1, 1, 1, 1, 1, 1, 1, 1,
```

```
1, 1, 1, 1, 1, 1, 1, 1, 1, 1, 1, 1, 1, 1, 1, 1, 1, 1, 1, 1, 1, 1, 1, 1, 1, 1, 1, 1, 1, 1,
1, 1, 1, 1, 1, 1, 1, 1, 1, 1, 1, 1, 1, 1, 1, 1, 1, 1, 1, 1, 1, 1, 1, 1, 1, 1, 1, 1, 1, 1,
1, 1, 1, 1, 1, 0, 1, 1, 1, 1, 1, 0, 1, 1, 1, 1, 1, 1, 1, 1, 1, 1, 1, 1, 1, 1, 1, 1, 1, 1,
1, 1, 1, 1, 1, 1, 1, 1, 1, 1, 1, 1, 1, 1, 1, 1, 0, 1, 1, 1, 1, 1, 1, 1, 1, 1, 1, 1, 1, 1,
1, 1, 1, 1, 1, 1, 1, 1, 1, 1, 1, 1, 1, 1, 1, 1, 1, 1, 1, 1, 1, 1, 1, 1, 1, 1, 1, 1, 1, 1,
1, 1, 1, 1, 1, 1, 1, 1, 1, 1, 1, 0, 1, 1, 1, 1, 1, 1, 1, 1, 1, 1, 1, 1, 1, 1, 1, 1, 1, 1,
1, 1, 1, 1, 1, 1, 1, 1, 1, 1, 1, 1, 1, 1, 1, 1, 1, 1, 1, 1, 1, 1, 1, 1, 1, 1, 1, 1, 1, 1,
1, 1, 1, 1, 1, 1, 1, 1, 1, 1, 1, 1, 1, 1, 1, 1, 1, 1, 1, 1, 1, 1, 1, 1, 1, 1, 1, 1, 1, 1,
1, 1, 1, 1, 1, 1, 1, 1, 1, 1, 1, 1, 1, 1, 1, 1, 1, 1, 1, 1, 1, 1, 1, 1, 1, 1, 1, 1, 1, 1,
1, 1, 1, 1, 1, 1, 1, 1, 1, 1, 1, 1, 1, 1, 1, 1, 1, 1, 1, 1, 1, 1, 1, 1, 1, 1, 1, 1, 1, 1,
1, 1, 1, 1, 1, 1, 1, 1, 1, 1, 1, 1, 1, 1, 1, 1, 1, 1, 1, 1, 1, 1, 1, 1, 1, 0, 0, 0, 0};
x2 ={1, 1, 1, 1, 1, 1, 1, 1, 1, 1, 1, 1, 1, 1, 1, 1, 1, 1, 1, 1, 1, 1, 1, 1, 1, 1, 1, 1,
1, 1, 1,
1, 1, 1, 1, 1, 1, 1, 1, 1, 1, 1, 1, 1, 1, 1, 0, 0, 0, 0, 0, 0, 0, 0, 0, 0, 0, 0, 0, 0, 0,
0, 0, 0, 0, 0, 0, 0, 0, 0, 0, 0, 0, 0, 0, 0, 0, 0, 0, 0, 0, 0, 0, 0, 0, 0, 0, 0, 0, 0, 0,
0, 0, 0, 0, 0, 0, 0, 0, 0, 0, 0, 0, 0, 0, 0, 0, 0, 0, 0, 0, 0, 0, 0, 0, 0, 0, 0, 0, 0, 0,
0, 0, 0, 0, 0, 0, 0, 0, 0, 0, 0, 0, 0, 0, 0, 0, 0, 0, 0, 0, 0, 0, 0, 0, 0, 0, 0, 0, 0, 0,
0, 0, 0, 0, 0, 0, 0, 0, 0, 0, 0, 0, 0, 0, 0, 0, 0, 0, 0, 0, 0, 0, 0, 0, 0, 0, 0, 0, 0, 0,
0, 0, 0, 0, 0, 0, 0, 0, 0, 0, 0, 0, 0, 0, 0, 0, 0, 0, 0, 0, 0, 0, 0, 0, 0, 0, 0, 0, 0, 0,
0, 0, 0, 0, 0, 0, 0, 0, 0, 0, 0, 0, 0, 0, 0, 0, 0, 0, 0, 0, 0, 0, 0, 0, 0, 0, 0, 0, 0, 0,
0, 0, 0, 0, 0, 0, 0, 0, 0, 0, 0, 0, 0, 0, 0, 0, 0, 0, 0, 0, 0, 0, 0, 0, 0, 0, 0, 0, 0, 0,
0, 0, 0, 0, 0, 0, 0, 0, 0, 0, 0, 0, 0, 0, 0, 0, 0, 0, 0, 0, 0, 0, 0, 0, 0, 0, 0, 0, 0, 0,
0, 0, 0, 0, 0, 0, 0, 0, 0, 0, 0, 0, 0, 0, 0, 0, 0, 0, 0, 0, 0, 0, 0, 0, 0, 0, 0, 0, 0, 0,
0, 0, 0, 0, 0, 0, 0, 0, 0, 0, 0, 0, 0, 0, 0, 0, 0, 0, 0, 0, 0, 0, 0, 0, 0, 0, 0, 0, 0, 0,
0, 0, 0, 0, 0, 0, 0, 0, 0, 0, 0, 0, 0, 0, 0, 0, 0, 0, 0, 0, 0, 0, 0, 0, 0, 0, 0, 0, 0, 0,
0, 0, 0, 0, 0, 0, 0, 0, 0, 0, 0, 0, 0, 0, 0, 0, 0, 0, 0, 0, 0, 0, 0, 0, 0, 0, 0, 0, 0, 0,
0, 0, 0, 0, 0, 0, 0, 0, 0, 0, 0, 0, 0, 0, 0, 0, 0, 0, 0, 0, 0, 0, 0, 0, 0, 0, 0, 0, 0, 0,
0, 0, 0, 0, 0, 0, 0, 0, 0, 0, 0, 0, 0, 0, 0, 0, 0, 0, 0, 0, 0, 0, 0, 0, 0, 0, 0, 0, 0, 0,
0, 0, 0, 0, 0, 0, 0, 0, 0, 0, 0, 0, 0, 0, 0, 0, 0, 0, 0, 0, 0, 0, 0, 0, 0, 0, 0, 0, 0, 0,
0, 0, 0, 0, 0, 0, 0, 0, 0, 0, 0, 0, 0, 0, 0, 0, 0, 0, 0, 0, 0, 0, 0, 0, 0, 0, 0, 0, 0, 0,
0, 0, 0, 0, 0, 0, 0, 0, 0, 0, 0, 0, 0, 0, 0, 0, 0, 0, 0, 0, 0, 0, 0, 0, 0, 0, 0, 0, 0, 0,
0, 0, 0, 0, 0, 0, 0, 0, 0, 0, 0, 0, 0, 0, 0, 0, 0, 0, 0, 0, 0, 0, 0, 0, 0, 0, 0, 0, 0, 0,
0, 0, 0, 0, 0, 0, 0, 0, 0, 0, 0, 0, 0, 0, 0, 0, 0, 0, 0, 0, 0, 0, 0, 0, 0, 0, 0, 0, 0, 0,
0, 0, 0, 0, 0, 0, 0, 0, 0, 0, 0, 0, 0, 0, 0, 0, 0, 0, 0, 0, 0, 0, 0, 0, 0, 0, 0, 0, 0, 0,
0, 0, 0, 0, 0, 0, 0, 0, 0, 0, 0, 0, 0, 0, 0, 0, 0, 0, 0, 0, 0, 0, 0, 0, 0, 0, 0, 0, 0, 0,
0, 0, 0, 0, 0, 0, 0, 0, 0, 0, 0, 0, 0, 0, 0, 0, 0, 0, 0, 0, 0, 0, 0, 0, 0, 0, 0, 0, 0, 0,
0, 0, 0, 0, 0, 0, 0, 0, 0, 0, 0, 0, 0, 0, 0, 0, 0, 0, 0, 0, 0, 0, 0, 0, 0, 0, 0, 0, 0, 0,


0, 0, 0, 0, 0, 0, 0, 0, 0, 0, 0, 0, 0, 0, 0, 0, 0, 0, 0, 0, 0, 0, 0, 0, 0, 0, 0, 0, 0, 0,
0, 0, 0, 0, 0, 0, 0, 0, 0, 0, 0, 0, 0, 0, 0, 0, 0, 0, 0, 0, 0, 0, 0, 0, 0, 0, 0, 0, 0};
x3 ={0, 0, 0, 0, 0, 0, 0, 0, 0, 0, 0, 0, 0, 0, 0, 0, 0, 0, 0, 0, 0, 0, 0, 0, 0, 0, 0, 0,
0, 0, 0,0, 0, 0, 0, 0, 0, 0, 0, 0, 0, 0, 0, 0, 0, 0, 1, 1, 1, 1, 1, 1, 1, 1, 1, 1, 1, 1,
1, 1, 1,1, 1, 1, 1, 1, 1, 1, 1, 1, 1, 1, 1, 1, 1, 1, 1, 1, 1, 1, 1, 1, 1, 1, 1, 1, 1, 1,
1, 1, 1,1, 1, 1, 1, 1, 1, 1, 1, 1, 1, 1, 1, 1, 1, 1, 1, 1, 1, 1, 1, 1, 1, 1, 1, 1, 1, 1,
1, 1, 1,1, 1, 1, 1, 1, 1, 1, 1, 1, 1, 1, 1, 1, 1, 1, 1, 1, 1, 1, 1, 1, 1, 1, 1, 1, 1, 1,
1, 1, 1,1, 1, 1, 1, 1, 1, 1, 1, 1, 1, 1, 1, 1, 1, 1, 1, 1, 1, 1, 1, 1, 1, 1, 1, 1, 1, 1,
1, 1, 1,1, 1, 1, 1, 1, 1, 1, 1, 1, 1, 1, 1, 1, 1, 1, 1, 1, 1, 0, 0, 0, 0, 0, 0, 0, 0, 0,
0, 0, 0,0, 0, 0, 0, 0, 0, 0, 0, 0, 0, 0, 0, 0, 0, 0, 0, 0, 0, 0, 0, 0, 0, 0, 0, 0, 0, 0,
0, 0, 0,0, 0, 0, 0, 0, 0, 0, 0, 0, 0, 0, 0, 0, 0, 0, 0, 0, 0, 0, 0, 0, 0, 0, 0, 0, 0, 0,
0, 0, 0,0, 0, 0, 0, 0, 0, 0, 0, 0, 0, 0, 0, 0, 0, 0, 0, 0, 0, 0, 0, 0, 0, 0, 0, 0, 0, 0,
0, 0, 0,0, 0, 0, 0, 0, 0, 0, 0, 0, 0, 0, 0, 0, 0, 0, 0, 0, 0, 0, 0, 0, 0, 0, 0, 0, 0, 0,
0, 0, 0,0, 0, 0, 0, 0, 0, 0, 0, 0, 0, 0, 0, 0, 0, 0, 0, 0, 0, 0, 0, 0, 0, 0, 0, 0, 0, 0,
0, 0, 0,0, 0, 0, 0, 0, 0, 0, 0, 0, 0, 0, 0, 0, 0, 0, 0, 0, 0, 0, 0, 0, 0, 0, 0, 0, 0, 0,
0, 0, 0,0, 0, 0, 0, 0, 0, 0, 0, 0, 0, 0, 0, 0, 0, 0, 0, 0, 0, 0, 0, 0, 0, 0, 0, 0, 0, 0,
0, 0, 0,0, 0, 0, 0, 0, 0, 0, 0, 0, 0, 0, 0, 0, 0, 0, 0, 0, 0, 0, 0, 0, 0, 0, 0, 0, 0, 0,
0, 0, 0,0, 0, 0, 0, 0, 0, 0, 0, 0, 0, 0, 0, 0, 0, 0, 0, 0, 0, 0, 0, 0, 0, 0, 0, 0, 0, 0,
0, 0, 0,0, 0, 0, 0, 0, 0, 0, 0, 0, 0, 0, 0, 0, 0, 0, 0, 0, 0, 0, 0, 0, 0, 0, 0, 0, 0, 0,
0, 0, 0,0, 0, 0, 0, 0, 0, 0, 0, 0, 0, 0, 0, 0, 0, 0, 0, 0, 0, 0, 0, 0, 0, 0, 0, 0, 0, 0,
0, 0, 0,0, 0, 0, 0, 0, 0, 0, 0, 0, 0, 0, 0, 0, 0, 0, 0, 0, 0, 0, 0, 0, 0, 0, 0, 0, 0, 0,
```

```
0, 0, 0,0, 0, 0, 0, 0, 0, 0, 0, 0, 0, 0, 0, 0, 0, 0, 0, 0, 0, 0, 0, 0, 0, 0, 0, 0, 0, 0,
0, 0, 0,0, 0, 0, 0, 0, 0, 0, 0, 0, 0, 0, 0, 0, 0, 0, 0, 0, 0, 0, 0, 0, 0, 0, 0, 0, 0, 0,
0, 0, 0,0, 0, 0, 0, 0, 0, 0, 0, 0, 0, 0, 0, 0, 0, 0, 0, 0, 0, 0, 0, 0, 0, 0, 0, 0, 0, 0,
0, 0, 0,0, 0, 0, 0, 0, 0, 0, 0, 0, 0, 0, 0, 0, 0, 0, 0, 0, 0, 0, 0, 0, 0, 0, 0, 0, 0, 0,
0, 0, 0,0, 0, 0, 0, 0, 0, 0, 0, 0, 0, 0, 0, 0, 0, 0, 0, 0, 0, 0, 0, 0, 0, 0, 0, 0, 0, 0,
0, 0, 0,0, 0, 0, 0, 0, 0, 0, 0, 0, 0, 0, 0, 0, 0, 0, 0, 0, 0, 0, 0, 0, 0, 0, 0, 0, 0, 0,
0, 0, 0,0, 0, 0, 0, 0, 0, 0, 0, 0, 0, 0, 0, 0, 0, 0, 0, 0, 0, 0, 0, 0, 0, 0, 0, 0, 0, 0,
0, 0, 0,0, 0, 0, 0, 0, 0, 0, 0, 0, 0, 0, 0, 0, 0, 0, 0, 0, 0, 0, 0, 0, 0, 0, 0, 0, 0, 0,
0, 0};

x4 ={0, 0, 0, 0, 0, 0, 0, 0, 0, 0, 0, 0, 0, 0, 0, 0, 0, 0, 0, 0, 0, 0, 0, 0, 0, 0, 0, 0,
0, 0, 0,0, 0, 0, 0, 0, 0, 0, 0, 0, 0, 0, 0, 0, 0, 0, 0, 0, 0, 0, 0, 0, 0, 0, 0, 0, 0, 0,
0, 0, 0,0, 0, 0, 0, 0, 0, 0, 0, 0, 0, 0, 0, 0, 0, 0, 0, 0, 0, 0, 0, 0, 0, 0, 0, 0, 0, 0,
0, 0, 0,0, 0, 0, 0, 0, 0, 0, 0, 0, 0, 0, 0, 0, 0, 0, 0, 0, 0, 0, 0, 0, 0, 0, 0, 0, 0, 0,
0, 0, 0,0, 0, 0, 0, 0, 0, 0, 0, 0, 0, 0, 0, 0, 0, 0, 0, 0, 0, 0, 0, 0, 0, 0, 0, 0, 0, 0,
0, 0, 0,0, 0, 0, 0, 0, 0, 0, 0, 0, 0, 0, 0, 0, 0, 0, 0, 0, 0, 0, 0, 0, 0, 0, 0, 0, 0, 0,
0, 0, 0,0, 0, 0, 0, 0, 0, 0, 0, 0, 0, 0, 0, 0, 0, 0, 0, 0, 0, 1, 1, 1, 1, 1, 1, 1, 1, 1,
1, 1, 1,1, 1, 1, 1, 1, 1, 1, 1, 1, 1, 1, 1, 1, 1, 1, 1, 1, 1, 1, 1, 1, 1, 1, 1, 1, 1, 1,
1, 1, 1,1, 1, 1, 1, 1, 1, 1, 1, 1, 1, 1, 1, 1, 1, 1, 1, 1, 1, 1, 1, 1, 1, 1, 1, 1, 1, 1,
1, 1, 1,1, 1, 1, 1, 1, 1, 1, 1, 1, 1, 1, 1, 1, 1, 1, 1, 1, 1, 1, 1, 1, 1, 1, 1, 1, 1, 1,
1, 1, 1,1, 1, 1, 1, 1, 1, 1, 1, 1, 1, 1, 1, 1, 1, 1, 1, 1, 1, 1, 1, 1, 1, 1, 1, 1, 1, 1,
1, 1, 1,1, 1, 1, 1, 0, 0, 0, 0, 0, 0, 0, 0, 0, 0, 0, 0, 0, 0, 0, 0, 0, 0, 0, 0, 0, 0, 0,
0, 0, 0,0, 0, 0, 0, 0, 0, 0, 0, 0, 0, 0, 0, 0, 0, 0, 0, 0, 0, 0, 0, 0, 0, 0, 0, 0, 0, 0,
0, 0, 0,0, 0, 0, 0, 0, 0, 0, 0, 0, 0, 0, 0, 0, 0, 0, 0, 0, 0, 0, 0, 0, 0, 0, 0, 0, 0, 0,
0, 0, 0,0, 0, 0, 0, 0, 0, 0, 0, 0, 0, 0, 0, 0, 0, 0, 0, 0, 0, 0, 0, 0, 0, 0, 0, 0, 0, 0,
0, 0, 0,0, 0, 0, 0, 0, 0, 0, 0, 0, 0, 0, 0, 0, 0, 0, 0, 0, 0, 0, 0, 0, 0, 0, 0, 0, 0, 0,
0, 0, 0,0, 0, 0, 0, 0, 0, 0, 0, 0, 0, 0, 0, 0, 0, 0, 0, 0, 0, 0, 0, 0, 0, 0, 0, 0, 0, 0,
0, 0, 0,0, 0, 0, 0, 0, 0, 0, 0, 0, 0, 0, 0, 0, 0, 0, 0, 0, 0, 0, 0, 0, 0, 0, 0, 0, 0, 0,
0, 0, 0,0, 0, 0, 0, 0, 0, 0, 0, 0, 0, 0, 0, 0, 0, 0, 0, 0, 0, 0, 0, 0, 0, 0, 0, 0, 0, 0,
0, 0, 0,0, 0, 0, 0, 0, 0, 0, 0, 0, 0, 0, 0, 0, 0, 0, 0, 0, 0, 0, 0, 0, 0, 0, 0, 0, 0, 0,
0, 0, 0, 0, 0, 0, 0, 0, 0, 0, 0, 0, 0, 0, 0, 0, 0, 0, 0, 0, 0, 0, 0, 0, 0, 0, 0, 0, 0, 0,
0, 0, 0,0, 0, 0, 0, 0, 0, 0, 0, 0, 0, 0, 0, 0, 0, 0, 0, 0, 0, 0, 0, 0, 0, 0, 0, 0, 0, 0,
0, 0, 0,0, 0, 0, 0, 0, 0, 0, 0, 0, 0, 0, 0, 0, 0, 0, 0, 0, 0, 0, 0, 0, 0, 0, 0, 0, 0, 0,
0, 0, 0,0, 0, 0, 0, 0, 0, 0, 0, 0, 0, 0, 0, 0, 0, 0, 0, 0, 0, 0, 0, 0, 0, 0, 0, 0, 0, 0,
0, 0, 0,0, 0, 0, 0, 0, 0, 0, 0, 0, 0, 0, 0, 0, 0, 0, 0, 0, 0, 0, 0, 0, 0, 0, 0, 0, 0, 0,
0, 0};

x5 ={0, 0, 0, 0, 0, 0, 0, 0, 0, 0, 0, 0, 0, 0, 0, 0, 0, 0, 0, 0, 0, 0, 0, 0, 0, 0, 0, 0,
0, 0, 0,
0, 0, 0, 0, 0, 0, 0, 0, 0, 0, 0, 0, 0, 0, 0, 0, 0, 0, 0, 0, 0, 0, 0, 0, 0, 0, 0, 0, 0, 0,
0, 0, 0, 0, 0, 0, 0, 0, 0, 0, 0, 0, 0, 0, 0, 0, 0, 0, 0, 0, 0, 0, 0, 0, 0, 0, 0, 0, 0, 0,
0, 0, 0, 0, 0, 0, 0, 0, 0, 0, 0, 0, 0, 0, 0, 0, 0, 0, 0, 0, 0, 0, 0, 0, 0, 0, 0, 0, 0, 0,
0, 0, 0, 0, 0, 0, 0, 0, 0, 0, 0, 0, 0, 0, 0, 0, 0, 0, 0, 0, 0, 0, 0, 0, 0, 0, 0, 0, 0, 0,
0, 0, 0, 0, 0, 0, 0, 0, 0, 0, 0, 0, 0, 0, 0, 0, 0, 0, 0, 0, 0, 0, 0, 0, 0, 0, 0, 0, 0, 0,
0, 0, 0, 0, 0, 0, 0, 0, 0, 0, 0, 0, 0, 0, 0, 0, 0, 0, 0, 0, 0, 0, 0, 0, 0, 0, 0, 0, 0, 0,
0, 0, 0, 0, 0, 0, 0, 0, 0, 0, 0, 0, 0, 0, 0, 0, 0, 0, 0, 0, 0, 0, 0, 0, 0, 0, 0, 0, 0, 0,
0, 0, 0, 0, 0, 0, 0, 0, 0, 0, 0, 0, 0, 0, 0, 0, 0, 0, 0, 0, 0, 0, 0, 0, 0, 0, 0, 0, 0, 0,
0, 0, 0, 0, 0, 0, 0, 0, 0, 0, 0, 0, 0, 0, 0, 0, 0, 0, 0, 0, 0, 0, 0, 0, 0, 0, 0, 0, 0, 0,
0, 0, 0, 0, 0, 0, 0, 0, 0, 0, 0, 0, 0, 0, 0, 0, 0, 0, 0, 0, 0, 0, 0, 0, 0, 0, 0, 0, 0, 0,
0, 0, 0, 0, 1, 1, 1, 1, 1, 1, 1, 1, 1, 1, 1, 1, 1, 1, 1, 1, 1, 1, 1, 1, 1, 1, 1, 1, 1, 1,
1, 1, 1, 1, 1, 1, 1, 1, 1, 1, 1, 1, 1, 1, 1, 0, 0, 0, 0, 0, 0, 0, 0, 0, 0, 0, 0, 0, 0, 0,
0, 0, 0, 0, 0, 0, 0, 0, 0, 0, 0, 0, 0, 0, 0, 0, 0, 0, 0, 0, 0, 0, 0, 0, 0, 0, 0, 0, 0, 0,
0, 0, 0, 0, 0, 0, 0, 0, 0, 0, 0, 0, 0, 0, 0, 0, 0, 0, 0, 0, 0, 0, 0, 0, 0, 0, 0, 0, 0, 0,
0, 0, 0, 0, 0, 0, 0, 0, 0, 0, 0, 0, 0, 0, 0, 0, 0, 0, 0, 0, 0, 0, 0, 0, 0, 0, 0, 0, 0, 0,
0, 0, 0, 0, 0, 0, 0, 0, 0, 0, 0, 0, 0, 0, 0, 0, 0, 0, 0, 0, 0, 0, 0, 0, 0, 0, 0, 0, 0, 0,
0, 0, 0, 0, 0, 0, 0, 0, 0, 0, 0, 0, 0, 0, 0, 0, 0, 0, 0, 0, 0, 0, 0, 0, 0, 0, 0, 0, 0, 0,
0, 0, 0, 0, 0, 0, 0, 0, 0, 0, 0, 0, 0, 0, 0, 0, 0, 0, 0, 0, 0, 0, 0, 0, 0, 0, 0, 0, 0, 0,
```

```
0, 0, 0, 0, 0, 0, 0, 0, 0, 0, 0, 0, 0, 0, 0, 0, 0, 0, 0, 0, 0, 0, 0, 0, 0, 0, 0, 0, 0, 0,
0, 0, 0, 0, 0, 0, 0, 0, 0, 0, 0, 0, 0, 0, 0, 0, 0, 0, 0, 0, 0, 0, 0, 0, 0, 0, 0, 0, 0, 0,
0, 0, 0, 0, 0, 0, 0, 0, 0, 0, 0, 0, 0, 0, 0, 0, 0, 0, 0, 0, 0, 0, 0, 0, 0, 0, 0, 0, 0, 0,
0, 0, 0, 0, 0, 0, 0, 0, 0, 0, 0, 0, 0, 0, 0, 0, 0, 0, 0, 0, 0, 0, 0, 0, 0, 0, 0, 0, 0, 0,
0, 0, 0, 0, 0, 0, 0, 0, 0, 0, 0, 0, 0, 0, 0, 0, 0, 0, 0, 0, 0, 0, 0, 0, 0, 0, 0, 0, 0, 0,
0, 0, 0, 0, 0, 0, 0, 0, 0, 0, 0, 0, 0, 0, 0, 0, 0, 0, 0, 0, 0, 0, 0, 0, 0, 0, 0, 0, 0, 0,
0, 0, 0, 0, 0, 0, 0, 0, 0, 0, 0, 0, 0, 0, 0, 0, 0, 0, 0, 0, 0, 0, 0, 0, 0, 0, 0, 0, 0};
x6 ={0, 0, 0, 0, 0, 0, 0, 0, 0, 0, 0, 0, 0, 0, 0, 0, 0, 0, 0, 0, 0, 0, 0, 0, 0, 0, 0, 0,
0, 0, 0,
0, 0, 0, 0, 0, 0, 0, 0, 0, 0, 0, 0, 0, 0, 0, 0, 0, 0, 0, 0, 0, 0, 0, 0, 0, 0, 0, 0, 0, 0,
0, 0, 0, 0, 0, 0, 0, 0, 0, 0, 0, 0, 0, 0, 0, 0, 0, 0, 0, 0, 0, 0, 0, 0, 0, 0, 0, 0, 0, 0,
0, 0, 0, 0, 0, 0, 0, 0, 0, 0, 0, 0, 0, 0, 0, 0, 0, 0, 0, 0, 0, 0, 0, 0, 0, 0, 0, 0, 0, 0,
0, 0, 0, 0, 0, 0, 0, 0, 0, 0, 0, 0, 0, 0, 0, 0, 0, 0, 0, 0, 0, 0, 0, 0, 0, 0, 0, 0, 0, 0,
0, 0, 0, 0, 0, 0, 0, 0, 0, 0, 0, 0, 0, 0, 0, 0, 0, 0, 0, 0, 0, 0, 0, 0, 0, 0, 0, 0, 0, 0,
0, 0, 0, 0, 0, 0, 0, 0, 0, 0, 0, 0, 0, 0, 0, 0, 0, 0, 0, 0, 0, 0, 0, 0, 0, 0, 0, 0, 0, 0,
0, 0, 0, 0, 0, 0, 0, 0, 0, 0, 0, 0, 0, 0, 0, 0, 0, 0, 0, 0, 0, 0, 0, 0, 0, 0, 0, 0, 0, 0,
0, 0, 0, 0, 0, 0, 0, 0, 0, 0, 0, 0, 0, 0, 0, 0, 0, 0, 0, 0, 0, 0, 0, 0, 0, 0, 0, 0, 0, 0,
0, 0, 0, 0, 0, 0, 0, 0, 0, 0, 0, 0, 0, 0, 0, 0, 0, 0, 0, 0, 0, 0, 0, 0, 0, 0, 0, 0, 0, 0,
0, 0, 0, 0, 0, 0, 0, 0, 0, 0, 0, 0, 0, 0, 0, 0, 0, 0, 0, 0, 0, 0, 0, 0, 0, 0, 0, 0, 0, 0,
0, 0, 0, 0, 0, 0, 0, 0, 0, 0, 0, 0, 0, 0, 0, 0, 0, 0, 0, 0, 0, 0, 0, 0, 0, 0, 0, 0, 0, 0,
0, 0, 0, 0, 0, 0, 0, 0, 0, 0, 0, 0, 0, 0, 0, 1, 1, 1, 1, 1, 1, 1, 1, 1, 1, 1, 1, 1, 1, 1,
1, 1, 1, 1, 1, 1, 1, 1, 1, 1, 1, 1, 1, 1, 1, 1, 1, 1, 1, 1, 1, 1, 1, 1, 1, 1, 1, 1, 1, 1,
1, 1, 1, 1, 1, 1, 1, 1, 1, 1, 1, 1, 1, 1, 1, 1, 1, 1, 1, 1, 1, 1, 1, 1, 1, 1, 1, 1, 1, 1,
1, 1, 1, 1, 1, 1, 1, 1, 1, 1, 1, 1, 1, 1, 1, 1, 1, 1, 1, 1, 1, 1, 1, 1, 1, 1, 1, 1, 1, 1,
1, 1, 1, 1, 1, 1, 1, 1, 1, 1, 1, 1, 1, 1, 1, 1, 1, 1, 1, 1, 1, 1, 1, 1, 1, 1, 1, 1, 1, 1,
1, 1, 1, 1, 1, 1, 1, 1, 1, 1, 1, 1, 1, 1, 1, 1, 1, 1, 1, 1, 1, 1, 1, 1, 1, 1, 1, 1, 1, 1,
1, 1, 1, 1, 1, 1, 1, 1, 1, 1, 1, 1, 1, 1, 1, 1, 1, 1, 1, 1, 1, 1, 1, 1, 1, 1, 1, 1, 1, 1,
1, 1, 1, 1, 1, 1, 1, 1, 1, 1, 1, 1, 1, 1, 1, 1, 1, 1, 1, 1, 1, 1, 1, 1, 1, 1, 1, 1, 1, 1,
1, 1, 1, 1, 1, 1, 1, 1, 1, 1, 1, 1, 1, 1, 1, 1, 1, 1, 1, 1, 1, 1, 1, 1, 1, 1, 1, 1, 1, 1,
1, 1, 1, 1, 1, 1, 1, 1, 1, 1, 1, 1, 1, 1, 1, 1, 1, 1, 1, 1, 1, 1, 1, 1, 1, 1, 1, 1, 1, 1,
1, 1, 1, 1, 1, 1, 1, 1, 1, 1, 1, 1, 1, 1, 1, 1, 1, 1, 1, 1, 1, 1, 1, 1, 1, 1, 1, 1, 1, 1,
1, 1, 1, 1, 1, 1, 1, 1, 1, 1, 1, 1, 1, 1, 1, 1, 1, 1, 1, 1, 1, 1, 1, 1, 1, 1, 1, 1, 1, 1,
1, 1, 1, 1, 1, 1, 1, 1, 1, 1, 1, 1, 1, 1, 1, 1, 1, 1, 1, 1, 1, 1, 1, 1, 1, 1, 1, 1, 1, 1,
0, 0, 0, 0, 0, 0, 0, 0, 0, 0, 0, 0, 0, 0, 0, 0, 0, 0, 0, 0, 0, 0, 0, 0, 0, 0, 0, 0, 0};
x7 ={0, 0, 0, 0, 0, 0, 0, 0, 0, 0, 0, 0, 0, 0, 0, 0, 0, 0, 0, 0, 0, 0, 0, 0, 0, 0, 0, 0,
0, 0, 0,
0, 0, 0, 0, 0, 0, 0, 0, 0, 0, 0, 0, 0, 0, 0, 0, 0, 0, 0, 0, 0, 0, 0, 0, 0, 0, 0, 0, 0, 0,
0, 0, 0, 0, 0, 0, 0, 0, 0, 0, 0, 0, 0, 0, 0, 0, 0, 0, 0, 0, 0, 0, 0, 0, 0, 0, 0, 0, 0, 0,
0, 0, 0, 0, 0, 0, 0, 0, 0, 0, 0, 0, 0, 0, 0, 0, 0, 0, 0, 0, 0, 0, 0, 0, 0, 0, 0, 0, 0, 0,
0, 0, 0, 0, 0, 0, 0, 0, 0, 0, 0, 0, 0, 0, 0, 0, 0, 0, 0, 0, 0, 0, 0, 0, 0, 0, 0, 0, 0, 0,
0, 0, 0, 0, 0, 0, 0, 0, 0, 0, 0, 0, 0, 0, 0, 0, 0, 0, 0, 0, 0, 0, 0, 0, 0, 0, 0, 0, 0, 0,
0, 0, 0, 0, 0, 0, 0, 0, 0, 0, 0, 0, 0, 0, 0, 0, 0, 0, 0, 0, 0, 0, 0, 0, 0, 0, 0, 0, 0, 0,
0, 0, 0, 0, 0, 0, 0, 0, 0, 0, 0, 0, 0, 0, 0, 0, 0, 0, 0, 0, 0, 0, 0, 0, 0, 0, 0, 0, 0, 0,
0, 0, 0, 0, 0, 0, 0, 0, 0, 0, 0, 0, 0, 0, 0, 0, 0, 0, 0, 0, 0, 0, 0, 0, 0, 0, 0, 0, 0, 0,
0, 0, 0, 0, 0, 0, 0, 0, 0, 0, 0, 0, 0, 0, 0, 0, 0, 0, 0, 0, 0, 0, 0, 0, 0, 0, 0, 0, 0, 0,
0, 0, 0, 0, 0, 0, 0, 0, 0, 0, 0, 0, 0, 0, 0, 0, 0, 0, 0, 0, 0, 0, 0, 0, 0, 0, 0, 0, 0, 0,
0, 0, 0, 0, 0, 0, 0, 0, 0, 0, 0, 0, 0, 0, 0, 0, 0, 0, 0, 0, 0, 0, 0, 0, 0, 0, 0, 0, 0, 0,
0, 0, 0, 0, 0, 0, 0, 0, 0, 0, 0, 0, 0, 0, 0, 0, 0, 0, 0, 0, 0, 0, 0, 0, 0, 0, 0, 0, 0, 0,
0, 0, 0, 0, 0, 0, 0, 0, 0, 0, 0, 0, 0, 0, 0, 0, 0, 0, 0, 0, 0, 0, 0, 0, 0, 0, 0, 0, 0, 0,
0, 0, 0, 0, 0, 0, 0, 0, 0, 0, 0, 0, 0, 0, 0, 0, 0, 0, 0, 0, 0, 0, 0, 0, 0, 0, 0, 0, 0, 0,
0, 0, 0, 0, 0, 0, 0, 0, 0, 0, 0, 0, 0, 0, 0, 0, 0, 0, 0, 0, 0, 0, 0, 0, 0, 0, 0, 0, 0, 0,
0, 0, 0, 0, 0, 0, 0, 0, 0, 0, 0, 0, 0, 0, 0, 0, 0, 0, 0, 0, 0, 0, 0, 0, 0, 0, 0, 0, 0, 0,
0, 0, 0, 0, 0, 0, 0, 0, 0, 0, 0, 0, 0, 0, 0, 0, 0, 0, 0, 0, 0, 0, 0, 0, 0, 0, 0, 0, 0, 0,
0, 0, 0, 0, 0, 0, 0, 0, 0, 0, 0, 0, 0, 0, 0, 0, 0, 0, 0, 0, 0, 0, 0, 0, 0, 0, 0, 0, 0, 0,
0, 0, 0, 0, 0, 0, 0, 0, 0, 0, 0, 0, 0, 0, 0, 0, 0, 0, 0, 0, 0, 0, 0, 0, 0, 0, 0, 0, 0, 0,
0, 0, 0, 0, 0, 0, 0, 0, 0, 0, 0, 0, 0, 0, 0, 0, 0, 0, 0, 0, 0, 0, 0, 0, 0, 0, 0, 0, 0, 0,
0, 0, 0, 0, 0, 0, 0, 0, 0, 0, 0, 0, 0, 0, 0, 0, 0, 0, 0, 0, 0, 0, 0, 0, 0, 0, 0, 0, 0, 0,
0, 0, 0, 0, 0, 0, 0, 0, 0, 0, 0, 0, 0, 0, 0, 0, 0, 0, 0, 0, 0, 0, 0, 0, 0, 0, 0, 0, 0, 0,
```

```
0, 0, 0, 0, 0, 0, 0, 0, 0, 0, 0, 0, 0, 0, 0, 0, 0, 0, 0, 0, 0, 0, 0, 0, 0, 0, 0, 0, 0, 0,
0, 0, 0, 0, 0, 0, 0, 0, 0, 0, 0, 0, 0, 0, 0, 0, 0, 0, 0, 0, 0, 0, 0, 0, 0, 0, 0, 0, 0, 0,
1, 1, 1, 1, 1, 1, 1, 1, 1, 1, 1, 1, 1, 1, 1, 1, 1, 1, 1, 1, 1, 1, 1, 1, 1, 1, 1, 1, 1, 1};
```

```
f = Sum[(Log[
     1/2 - 1/2 * Erf[(Log[t[[i]] * Exp[c * x1[[i]] + d * x2[[i]] + e * x3[[i]] + g * x4[[i]] +
             h * x5[[i]] + r * x6[[i]] + q * x7[[i]]]] - a) / (b * Sqrt[2])]] +
    Status[[i]] * (Log[t[[i]] * Exp[c * x1[[i]] + d * x2[[i]] + e * x3[[i]] +
            g * x4[[i]] + h * x5[[i]] + r * x6[[i]] + q * x7[[i]]] *
          (1/ (b * t[[i]] * Exp[c * x1[[i]] + d * x2[[i]] + e * x3[[i]] + g * x4[[i]] +
                h * x5[[i]] + r * x6[[i]] + q * x7[[i]]] * Sqrt[Pi * 2]) *
            Exp[-1/2 * ((Log[t[[i]] * Exp[c * x1[[i]] + d * x2[[i]] + e * x3[[i]] +
                       g * x4[[i]] + h * x5[[i]] + r * x6[[i]] + q * x7[[i]]]] - a) /b) ^2])] -
       Log[(1/2 - 1/2 * Erf[(Log[t[[i]] * Exp[c * x1[[i]] + d * x2[[i]] +
                       e * x3[[i]] + g * x4[[i]] + h * x5[[i]] + r * x6[[i]] +
                       q * x7[[i]]]] - a) / (b * Sqrt[2])])])), {i, 1, n}];
```

```
FindMaximum[{f, a >0, b >0}, {a, 0.1`25}, {b, 0.9`25}, {c, 0}, {d, 0}, {e, 0}, {g, 0}, {h, 0},
{r, 0}, {q, 0}, MaxIterations → 1000]
```

CURRICULUM VITAE

Azam Nabizadeh, PhD

University of Wisconsin-Milwaukee, Milwaukee, WI 53211

SUMMARY

Motivated and talented PhD dissertator inspired to peruse academic and personal excellence. Multidisciplinary industry, research and teaching experiences over 9 years. consistently strive to create a challenging and engaging learning environment in the work environment. Successful record of research with several publications.

EDUCATION

- PhD - Structural Engineering, (Minor: Mechanical Engineering), University of Wisconsin-Milwaukee, GPA: 3.8/4.0

  2015- 2019
- M.S. – Structural Engineering, University of Wisconsin-Milwaukee, GPA: 3.8/4.0

  2013-2015
- M.S. - Civil Engineering, Shahrood University of Technology, Iran, GPA: 3.85/4.0

  2006-2009
- B.S. - Civil Engineering, Shahrood University of Technology, Iran, GPA: 3.5/4.0

  2000-2005

RESEARCH ACTIVITIES

- Evaluation of Thin Polymer Overlays for Bridge Decks (Project funded by Department of Transportation of Wisconsin (WISDOT) and Wisconsin Highway Research Board (WHRP).

  An experimental research program was performed to study and compare the performance of nine different overlay systems. Reinforced concrete slab specimens were subjected to accelerated corrosion, freeze-thaw cycling, heat/ultraviolet/rain cycles, and tire wear tests (including "snow plow" application). The overlay system with an epoxy resin and flint rock aggregate provided the best overall performance based on performance indices determined for friction coefficient, corrosion mass loss, pull-out strength and surface deformation (rut) due to tire passage.

- Survival Analysis of Fatigue in Bridges, Reliability (Survival) of Bridge Decks and Superstructures

  In survival analysis, probability of failure of a system are investigated through regression analysis, considering affecting covariates. This research develops, applies, and verifies long-standing survival analysis techniques widely used in medical research to the fatigue problem in various engineering applications, in particular, bridge structures. This approach uses conditional survival analysis techniques derived from the conditional probability theory to address the cumulative fatigue damage, load sequencing, and irregular loading effects in a probabilistic manner. The survival analysis can also be applied for service life estimation of bridge decks, superstructures, and other type of structures.

- Strength and Serviceability of Damaged Prestressed Bridge Girders (Project funded by Department of Transportation of Wisconsin (WISDOT) and Wisconsin Highway Research Board (WHRP).

  The research focus is development of inspection guidelines for damaged prestressed girders; guidance to support decisions on actions to be taken when girder damage occurs; guidelines for methods to be used to accurately analyze damaged prestressed girders (including consideration of load re-distribution) and; guidelines on the appropriate repair actions to be employed to repair damaged prestressed girders.

<u>Software Development</u>

- PreBARS: A primary author of a comprehensive software program (PreBARS) to assess service stresses and strength for undamaged, damaged and repaired precast prestressed concrete bridge girders. The software can also be used for design of bridges prior to damage. The program calculates bridge loads, distribution factors, prestress losses, as well as strength and service stresses for prestressed bridge I girders and side-by-side box girders.

<u>ADVANCE LEVEL GRADUATE COURSES</u>

- Advanced Steel Design
- Mechanics of Composite Mat'ls
- Advanced Foundation, and soil mechanics
- Analysis and Design of Bridges
- Processing of Plastics
- Mech Reliability/Problstc Dsgn
- Properties of Concrete
- Advanced Finite Element Methods

- Design of Multistory Buildings
- Topics in Civil Engineering (Sustainable Engineering Materials)
- Advanced Strength of Materials
- Environmental, Fluid Mechanics, Adv Topics Civil Engineering

JOURNAL PUBLICATIONS

- Nabizadeh A., Tabatabai H., Tabatabai A. M., 2019. Conditional survival analysis for concrete bridge decks. Life Cycle Reliability and Safety Engineering, Springer.
- Lu, P., Zhuang, Y., Nabizadeh, A., and Tabatabai, H., 2019. Analytical and experimental evaluation of repairs to a continuous PC girder bridge. ASCE, Journal of Performance of Constructed Facilities.
- Dehghani, E., Zadeh, M.N. and Nabizadeh, A., 2019. Evaluation of seismic behaviour of railway bridges considering track-bridge interaction. Roads and Bridges-Drogi i Mosty, 18(1), pp.51-66.
- Nabizadeh, A., Tabatabai, H. and Tabatabai, M., 2018. Survival analysis of bridge superstructures in wisconsin. Applied Sciences, 8(11), p.2079.
- Tabatabai, H., Janbaz, M. and Nabizadeh, A., 2018. Mechanical and thermo-gravimetric properties of unsaturated polyester resin blended with FGD gypsum. Construction and Building Materials, 163, pp.438-445.
- Ellis, D.S., Tabatabai, H. and Nabizadeh, A., 2018. Residual Tensile Strength and Bond Properties of GFRP Bars after Exposure to Elevated Temperatures. Materials, 11(3), p.346.
- Gholampour, S., Nabizadeh, N., "Effect of strength reduction through damping enhancement on seismic performance of the steel structures with different elevations", Maxwell Scientific Organization, Dec. 2012.

CONFERENCE PUBLICATIONS

- Nabizadeh, A., Tabatabai, H., Tabatabai, M. 2019. Survival Analysis Approach for Fatigue Reliability Assessment in Bridge Structures. Conference: Bridge Engineering Institute (BEI), Honolulu, Hawaii
- Nabizadeh, A., Tabatabai, H. 2019. Assessment and Repair of Damaged Prestressed Girders. Conference: Bridge Engineering Institute (BEI), Honolulu, Hawaii
- Tabatabai, H., Nabizadeh, A., Tabatabai, M., 2018. Overview Of Survival Analysis Techniques For Probabilistic Assessment Of Bridge Service Life. Conference: Structural Faults and Repair at Edinburgh, UK.
- Tabatabai, H., and Nabizadeh, A., 2018. Evaluation Of Thin Polymer Overlays For Bridge Decks. Conference: Structural Faults and Repair at Edinburgh, UK.
- Khazaei, B., Nabizadeh, A., and Hamidi, S. A., 2018. An Empirical Approach to Estimate Total Suspended Sediment Using Observational Data in Fox River and Southern Green Bay, WI. World Environmental and Water Resources Congress (EWRI, 2018).
- Nabizadehdarabi, A., 2015. Reliability of bridge superstructures in Wisconsin (M.Sc dissertation, The University of Wisconsin-Milwaukee).
- Nabizadeh, A. Seismic Retrofit of Steel Structures Through Weakening and Damping Enhancement. The 1th Regional Conference on Civil Engineering, Qaemshahr, Iran, Apr, 2010.

TECHNICAL REPORT

- Tabatabai, H., and Nabizadeh, A., Strength and Serviceability of Damaged Prestressed Girders. Wisconsin Highway Research Program, 2019.

- Tabatabai, H., Sobolev, K., Ghorbanpoor, A., Nabizadeh, A., Lee, C.W. and Lind, M., 2016. Evaluation of Thin Polymer Overlays for Bridge Decks. Wisconsin Highway Research Program.

ACADEMIC AND TEACHING EXPERIENCES

- Research Assistant at the University of Wisconsin-Milwaukee (U.S. 2016-Present): Strength and Serviceability of Damaged Prestressed Girders
- Teaching Assistant at the University of Wisconsin-Milwaukee (U.S. 2013-Present): Statics, Dynamics, Structural Analysis, Design of Steel Structures
- Instructor at Azad University, Sarouye Institute, Rouzbahan Institute (Iran, 2009-2013): Fluid Mechanics, Hydraulics Strength of Materials, Dynamics, Statics, Analysis of Structural, Design of Steel Structures, Design of Concrete Structures, SAP2000 & ETABS & SAFE
- Advisor and instructor for master entrance exam in civil engineering (Iran, 2009-2013): Strength of materials, Fluid Mechanics, Hydraulics, Analysis of Structural, Steel and Concrete Structures Design

INDUSTRY WORK EXPERIENCES

- Structural/Bridge Engineer at Kiewit, CO, U.S. 2019-Now
- Evaluation of design of stays in a cable stay bridge, “Canada Hunt Club Pathway”, 2016.
- Project Engineer at J3 Engineers, Mequon, WI, U.S. Summer 2015 (Internship).
- Structural Designer (Civil Engineer) In Consultant Firm, Iran, 2005 – 2013, job involved design of steel and concrete structures including:

    - Retrofit of Masonry School Buildings for "School Rehabilitation Organization", Iran, 2009 -2011.
    - Design of Animal House (Animal Laboratory) In "Tarbyat Modares" University, Iran, 2012.
    - Design of Stadium, 3 story building, 2006.
- Structural Supervisor in Job Bureau, Iran, Jul.- Sep., 2006.

PROFESSIONAL MEMBERSHIPS

- Member of American Concrete Institute (ACI).
- Member of American Society of Civil Engineers (ASCE).
- AASHTO-T10 Committee Member
- PCI Bridge Committee Member

COMPUTER SKILLS

- Structural analysis Software: ABAQUS, ANSYS, SAP, SAFE, ETABS, Seismo-soft, and Auto-Cad.
- Programming: MATLAB, Visual Basic, Mathematica, VBA, SAS.
- Operating Systems: Windows (Seven, Vista and XP).
- Applications: Microsoft Office Package (Word, Excel, Power Point, Access).